Development, Analysis and Performance Assessment of Net Zero Energy House Systems

By

Anwar Rached Hassoun

A Thesis Submitted in Partial Fulfillment

of the Requirements for the Degree of Doctor of Philosophy

in

Mechanical Engineering

Faculty of Engineering and Applied Science,

University of Ontario Institute of Technology

Oshawa, Ontario, Canada

Abstract

Net zero energy buildings have captured the attention of many researchers and governments due to high energy consumptions by traditional buildings. The design stage of a net zero energy house is the most crucial and cost effective step to focus on. The orientation of the building, proper insulation, high-efficiency windows, natural ventilation and other techniques are used to curb down heat transfer from and to the building. These robust energy measures combined with using highly efficient domestic appliances, lighting fixtures, seasonal air-conditioning equipments with high coefficient of performance (COP) and thermal heating techniques reduce energy to the level where the remaining electricity required to power the building can be produced by renewable energy systems.

This PhD research aims at designing and assessing the performance of net zero energy house (NZEH). Three novel multigeneration energy systems are developed, where renewable energies will be the prime sources to supply electricity, fresh and hot water, seasonal heating and cooling.

In order to achieve NZEH, the study starts by choosing the right orientation of the house, selecting the building materials and fixtures that would save on energy, and then optimizing the thicknesses of the acoustical and thermal insulation materials used and followed by heat load calculations. After which, the total connected electrical load to the house is determined and the power system is optimized and selected. Moreover, thermodynamic modeling for all systems components is developed and design parameters are varied to note their effect on efficiencies. Exergoeconomic and exergoenvironmental analyses are performed to determine exergy destructions and greenhouse gas emission costs. In addition, design variables are optimized to maximize renewable energy use while reducing exergy destruction and minimizing total system cost and greenhouse gas emissions.

The ultimate goal of this study is to produce sustainable energy options for residential buildings with low noise pollution and very low level of greenhouse gases emissions. In this regard, three new systems are considered.

System I is composed of a photovoltaic (PV) system, wind turbine, diesel generator, battery bank and an electrical control system that supply power to the house, while solar panels power absorption and liquid desiccant systems which provide air-conditioning and fresh water. Hot water is produced by solar heat, photovoltaic thermal system (PV/T) and from a ground thermal storage, where hot water from solar panels passes through during the long summer months, raising the earth temperature, which is used in winter to heat the cold water circulated through. The optimization results show that system I with a net present cost (NPC) of US $56,558.00 in 2013 currency, and levelized cost of energy $0.127/kWh satisfies the connected load requirements. A power system optimization yields a 0.998 renewable energy penetration factor and 73 kg/yr of CO_2 emissions. While exergoeconomic analysis gives a total system cost of $107,000.00 and exergy analysis gives overall system exergy efficiency of 41 % and 26 % at 8.00 am and 2.00 pm respectively.

System II consists of organic Rankine cycle system (ORC) with a battery array to supply electricity to the house, while solar panels power a liquid desiccant system and absorption chiller system that provide the house with air-conditioning and fresh water. Hot water is produced by solar heat. The optimized power system with a NPC of $52,505.00 and LCE of $0.118/kWh, renewable energy fraction of 1.00 and zero kg/yr CO_2 emissions provides for the house.

The overall system exergetic efficiency varies between 44.76 %, 23.57 % and 36.22 % at 8.00 am, 2.00pm and 5.00 pm, due to solar energy changes, while the overall system efficiency varies between 60 %, 36.62 % and 53.95 % at 8.00 am, 2.00 pm and 5.00 pm. While exergoeconomic analysis gives a total system cost of $117,700.00 compared to $128,500.00 after running the multiobjective optimization.

System III consists of hydro turbine system, PV and battery systems with electrical control mechanism that supplies power to the house. A ground source heat pump integrated with a heat exchanger provides seasonal air-conditioning and part of the hot water. A heat transformer powered by solar energy combined to a distillation system provides the house with fresh and hot water. Hot water from the separation unit of the

distillation system heats earth soil in a ground thermal storage where cold water will be heated in the winter.

The power scheme is optimized to the total NPC $40,420.00 and LCE 0.091$/kWh with 1.00 renewable energy fraction and zero kg/yr CO_2 emission. The overall system exergetic efficiency varies from 50%, 37% and 51% at 8:00 am, 2:00 pm and 5:00 pm respectively, while the overall system cost is $68,192.25 compared to $74,384.00 after running the multiobjective optimization.

Acknowledgements

I attribute the success of this research to the guidance of my supervisor Professor Ibrahim Dincer whose teachings and supervision have really inspired me to do my best in the thesis research and complete this thesis in correct, complete and consistent manner. I am truly honored by having Professor Dincer as teacher and inspirational educator.

I would like to express my gratitude to the examining committee, whose names below add value to my research, for their time and efforts:

Dr. Dan Zhang

Dr. Bekir Yilbas

Dr. Mohamad Youssef

Dr. Fethi Aloui from University Nantes-France

Dr. Atef Mohany

I thank Dr. Atef Mohany once again for his teaching in the graduate course and his help with the algorithm on acoustics. I also thank the UOIT for the proper study environment that it provides.

Table of Contents

List of Tables

List of Figures

Nomenclature

A	Area (m^2)
C	Clearness index
$\dot{C}$	Heat capacity rate (kW/°C)
Co_{pwt}	Power coefficient
Cp	Specific heat at constant pressure (kJ/kg K)
e_x	Specific exergy flow (kJ/kg)
$\dot{E}x$	Exergy rate (kW)
$\dot{E}lec$	Electrical power rate (kW)
h	Specific enthalpy (kJ/kg)
$\dot{H}$	Enthalpy rate (kW)
h_c	Convective heat transfer coefficient (W/m^2K)
k	Battery rate constant (1/h)
$\dot{m}$	Mass flow rate (kg /s)
M	Molar mass (kg/kmol)
P	Pressure (kPa)
$\dot{P}$	Power rate (kW)
$\dot{Q}$	Heat rate (kW)
$\dot{q}$	Solar radiation (kW /m^2)
R	Ratio of radiation for tilted surface to horizontal surface
s	Specific entropy (kJ/kg K)
$\dot{S}$	Entropy rate (kW/K)
SPL	Sound pressure level (dB)

T	Temperature (°C)
U	Overall heat transfer coefficient
V_e	Wind velocity (m/s)
V_m	Maximum voltage of PV cell given by supplier (V)
$\dot{W}$	Work rate (kW)
x	Battery capacity ratio
$\dot{z}$	Battery energy rate (W)

Subscripts

abs	Absorber
absp	Absorption chiller
act	Actual
amb	Ambient
anem	Anemometer
at	After turbine
avg	average
b	Beam
batt	Battery
bl	Blade
blow	Blower
bt	Before turbine
capac	Capacitance
chg	Charge
comp	Compressor
con	Condenser

cinv	Capital investment
cond	Condensate
conv	Convective
d	Diffuse
deh	Dehumidifier
desal	Distillation
disch	Discharge
e	Exit
emb	Embedded
elec	Electrical
ert	Earth
eva	Evaporator
fnl	Final
g	Ground
gene	Generated
GH	Electricity at highest content of electron
hex	Heat exchanger
htrs	Heat transformer
hwt	Hot water tank
in	Index
i	Inlet
int	Initial
min	Minimum
mp	Maximum power

nom	Nominal
o	Dead state
oc	Open current
ot	Outlet
ov	Overall
pmp	Pump
r	Reflected
rec	Re-circulated
rect	Rectifier
reg	Regenerator
ref	Reference
rms	Root mean square
s	Solar
sat	Saturated
sep	Distillation system
sepv	Separation vessel
sol	Desiccant solution
sp	Speed
sun	Sun
supp	Supply
sw	Swept
tb	Thermal bank
theo	Theoretical
tot	Total

tp	Tip
trans	transmission
turb	Wind turbine
w	Water
wea,sol	Weak solution

Greek Letters

α	Solar absorbance
β	Slope of the surface
ε	Heat exchanger effectiveness
η	Energy efficiency
λ	latent heat of condensation (kJ/kg)
ζ	Concentration by mass (%)
$\boldsymbol{\psi}$	Exergy efficiency
ω	Air humidity ratio (kg water vapor/kg dry air)
$\boldsymbol{\varpi}$	Turbine rotational speed (rpm)
Δt	Unit of the time step (h)
π	Pi (3.1416)
τ	Solar transmittance
γ	Absorptivity (m^2/day)

Acronyms

COP	Coefficient of performance
EES	Engineering equation solver
FFT	Fast Fourier transforms
GSHP	Ground source heat pump

HVAC	Heating, ventilation and airconditioning
LCE	Levelized cost of energy
LDS	Liquid desiccant system
NZEH	Net zero energy house
PV	Photovoltaic
PV/T	Photovoltaic thermal system
ZEB	Zero energy building

Chapter 1: Introduction

Energy supply is crucial to world development and energy shortages are forecasted to mount due to population growth and increased industrial activities. Our dependence on fossil fuels is ending soon because, after the maximum rate of overall oil extraction is reached, a decline in the supply occurs, resulting in significant increase in oil prices and their byproducts and causing worldwide socio-economic implications. Delaying the time of peak oil, can be achieved by finding other alternatives for producing energy such as, nuclear, renewable and unconventional oil resources like oil shale and oil sands and by producing hydrogen fuel from electrolysis of water. Moreover, fossil fuels are a major contributor to pollution and global warming. Hence, reducing the usage of petroleum and most fossil fuels is important as much as achieving sustainable energy supply. Sustainability is therefore, a key to solving current societal, environmental, economic and technological issues [1]. Switching to renewable energy and reduction of carbon dioxide emissions is an ultimate global goal for sustainability [2].

Most renewable energy resources are driven directly or indirectly by the sun or from heat generated by the earth core, like the wind, hydro [3, 4], and biomass energies. Ocean energy is somehow affected by the sun while geothermal energy is independent of its influence. In short, all energy sources that are none fossil are renewable energies. Hybrid renewal energy systems are a useful tool to supply electricity on continuous basis while providing thermal needs of space heating and cooling, hot and fresh water. As important as these multigeneration systems to sustainability, efficiency of these systems stands tall in adding to the positive merit of the socio-economic standards of humans. Nothing more than exergy is substantial in addressing "energy destruction, chaos reaction, resource degradation and waste-exergy emissions and their impact on the environment" [1].

In the following sections, some of the renewable energy resources are introduced and discussed in brief:

1.1 Solar energy

Solar radiation is a short wave-length radiation in the range of 0.3 to 3μm and the planet earth absorbs about 3850 ZJ/yr (zetta Joule or 10^{21}J). Absorption of solar energy raises

the atmospheric temperature as well as the water and land regions causing evaporation and moist warm air to rise and condense when it hits lower temperatures and falls as rain. This movement of warm air and the heat released by condensation are responsible for creating winds [5]. Figure 1.1 shows many factors that affect the quantity of solar radiation that reaches us and in particular clouds and hazy conditions [6].

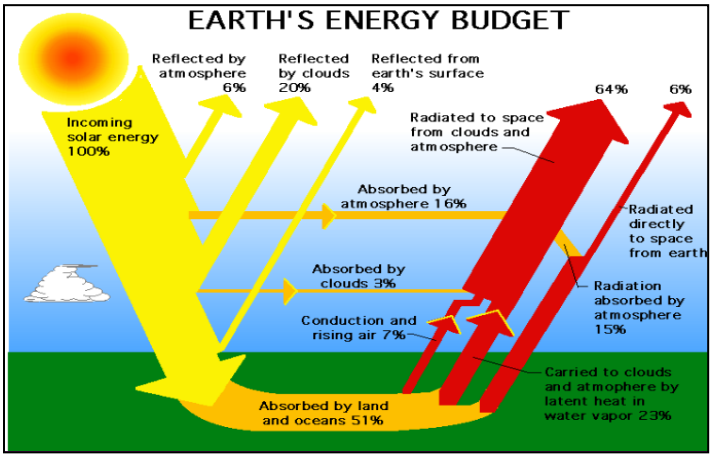

Figure 1.1: Earth's energy budget [5].

Solar energy is a clean, abundant and everlasting energy resource to humans. This energy warms our planet and powers all life. Solar energy is transformed by photosynthesis into organic matter which is the food we eat. Even fossil fuels, are actually stored solar energy. Solar energy provides our day light, shapes our weather patterns, generates solar electricity and provides heat. Solar energy maps have been developed recently to predict the solar radiation for a particular location in order to assess the feasibility of using solar to produce energy for that particular location. Further studies have evolved solar exergy maps [7] to improve the choices of locations for using solar energy to produce electricity and heat.

Solar energy is used in many aspects of our lives either passively or actively:

a. Active solar energy

Active solar energy is a most significant form of solar option, and it is essentially meaning that solar radiation is captured by a device and converted into forms of usable energies. The following are some of the usable energies produced actively:

- Electrical production

Electricity is produced from solar energy when two layers of a semi-conducting material are combined and exposed to sun light. It works when one layer has a depleted number of electrons that gets excited by absorbance of sun light photons and cause electrons to jump from one layer to the other causing electric charge. The photovoltaic material is silicon cut into very thin wafers and undergoes, contamination by doping, to create electron imbalance. These wafers are joined together to form a solar cell and many cells are connected in series and laminated between clear glazing and an encapsulating substrate.

- Water heating

Active solar heating uses mechanical equipment to convert solar energy to heat. Solar hot water systems use either flat plate or evacuated tube solar collectors to heat water. These collectors are directed toward the sun to collect as much radiation heat as possible.

- Seasonal air-conditioning

Solar energy can be used to power absorption heat pumps to cool or heat a space or by directly heating a space by circulating hot water to a radiant floor unit.

- Water treatment

Solar energy can be used to distill salt or murky water for producing fresh water or treat waste water to make it suitable by using solar nano- photocatalytic process.

- Hydrogen production

Solar concentrators can be used to separate oxygen from hydrogen at high temperatures which can be used in energy storage and other applications.

- Hybrid solar lighting

Interior illumination is caused by sunlight tracking concentrating mirrors which direct the light inside the space.

b. Passive solar energy

Solar energy is not converted into another form but rather used naturally. Some usage is listed below:

- Day lighting

Interior illumination is provided by natural lighting through proper design of windows and shades and should be integrated with decisions about the building architecture, location and exposure to sunlight, climate and lighting design controls.

- Greenhouses

Solar radiation is used directly as heat and trapped in a green house or green solarium which enables year round plantations.

- Ventilation

Solar energy can passively ventilate a space through using a solar chimney where warm air raises upward and cooler air flows downward.

1.2 Wind energy

Wind energy is renewable because it is naturally replenished, since it undergoes an endless cycle, caused by the effect of sun light, evaporation of water and pressure differences. Wind is well explained as the movement of huge amount of air with relative velocity to the forces causing this movement and the region where they happened. It is this bulk movement of air particles that create energy. Wind energy is also affected by the movement of earth around its axis.

Humans have used wind energy to power their sail ships since far back in history. The wind wheel in the first century AD was used to power a machine [8, 9] while the first windmills were used as early as the 7^{th} century in Iran [10]. Poul la Cour built wind turbines in 1890 to generate electricity, and these were used to electrolyze hydrogen and oxygen where a mixture of the two gases was stored for use as a fuel [11].

Wind power is the conversion of wind energy into useful form. Power produced from wind energy can surpass all power generated as of today from all other sources [12].

Table 1.1 shows the major producers of wind power from wind energy and the total world output.

Table 1.1: Top ten countries by name plate wind power capacity.

Country	New 2012 capacity (MW)	Wind power total capacity (MW)	Percentage of World Total Wind Power (%)
World total	44,799	282,587	100
United States	13,124	60,007	21.2
United Kingdom	1897	8,845	3
Spain	1122	22,796	8.1
Portugal	145	4,525	1.6
Italy	1273	8,144	2.9
India	2336	18,421	6.5
Germany	2145	31	11.1
France	757	7,564	2.7
China	12960	75,324	26.7
Canada	935	6,200	2.2
Rest of the World	6737	39,853	14.1

Source: [13]

Several types of wind power options are discussed briefly in the following sections:

a. Wind turbine

Electricity is produced by converting wind kinetic energy into mechanical energy to drive an electrical generator. At the end of 2009, 159.2 GW electrical powers of wind-powered generators were produced worldwide which is about 2% of global electricity usage. Several countries have achieved relatively high levels of wind power penetration. As of May 2009 eighty countries around the world were using wind power [14].

Wind turbines rotate on either horizontal axis or vertical axis. Horizontal-axis wind turbines have the main rotor shaft and electrical generator at the top of a tower while vertical-axis wind turbines have the main rotor shaft arranged vertically.

Vertical-axis wind turbines are advantageous for sites with highly variable wind direction. Wind speed is slower at a lower altitude, so less wind energy is available for a given size turbine.

b. Windmill wheel

Windmill wheel is a machine that converts wind energy into rotational energy through vanes. Windmills were among the original prime movers as a source of power. Traditionally, they were used for grinding grain and in some areas water wheels were used as land drainage and water pumping machines. Windmill use became popular in Europe from the 12^{th}century to the early 19^{th}century, but thereafter declined.

c. Wind pump

Wind pumps provide high torque through a large number of sails in low wind flow and are used mainly for irrigation purposes. A crankshaft attached at the top to a gear box and at the bottom to a pump cylinder converts the rotary motion into reciprocating strokes allowing water to flow.

Wind energy is pollutant free, inexhaustible source of fuel to power turbines. It is affordable and efficient and when coupled with other renewable energy sources like hydropower, electricity can be supplied constantly.

1.3 Geothermal energy

Geothermal energy is natural energy produced mainly from radioactive decayed minerals [15]. The earth's core temperature is about 5000℃ which tends to melt cooler rocks that pushes its way above solid matter and heats up water and rocks in the crust up to 370℃ in some places. Geothermal energy is best defined as thermal energy produced and stored in the earth. The quantity of heat within 10,000 meters of earth's surface is about 50,000 times in energy content than all fossil fuels have to offer. If these resources can be reached, they offer enormous potential for electricity production. Geothermal energy is reliable, abundant and cost effective if it finds its way close to the earth surface. It is environmentally friendly with far less greenhouse gases emissions than fossil fuels. The international geothermal association predicts that 18,500 MW of electricity will be produced in the year 2015 from geothermal energy compared to 10,715 MW in 2010[16].

The easiest way to harvest energy from geothermal resources is to capture steam from water sipping into earth crust, where it is heated and then rises to the surface naturally by hydrothermal convection. In reality, most geothermal power plants drill their own holes into the rock layer to capture steam for electricity production.

1.4 Hydro energy

Hydro energy is renewable energy. It uses the rain falling from ocean's evaporated water to replenish itself. It is considered a very reliable energy source, because, it has high kinetic energy and produces electricity day and night without any harmful emissions. It is therefore, better than all other renewable energies.

Hydropower depends on flowing water, which produces hydraulic energy as kinetic, potential and pressure energy which can be transformed into mechanical energy by driving a turbine. A hydro generator is driven by water that rotates the vanes of the turbine which in turn rotates the rotor of the generator and electricity is generated through the stator windings.

Hydro turbines are the main component of hydro energy technology and are classified as impulse or reaction machines. Impulse turbines turn the total heads available into kinetic energy through a number of nozzles, while a reaction turbine is encased in a pressure casing and submerged fully with water. The Chinese Three Gorges Dam is the world's largest hydropower plant with 22,500 MW capacities.

Another form of hydro energy that produces hydro electrical power is tidal power generator [17].Water pressure from tides in oceans and seas causes a turbine to rotate and generate electricity. Tides are caused by the rotation of the earth and the gravitational bond of the moon and sun.

1.5 Biomass energy

Biomass energy is considered renewable energy [17], because, we can grow plants if production exceeds disposed. Biomass gets its energy from the sun. Plants store energy by photosynthesis in their roots and leaves. Animals eat plants and other animals to survive thus storing solar energy. In fact, biomass is anything that is alive.

Biomass is used to generate electricity from burning trees, plants and even garbage. The estimated production of biomass is 140 billion tons per year. Biomass supplies 14% of the world's energy. It is usually solid but it can be liquid. It is formed of hydrogen, oxygen, carbon and small amounts of nitrogen and other elements. If we use biomass as a fuel to generate electricity and heat, it will emit carbon dioxide when burned. Many argue that trees and plants after being burned emit carbon dioxide, which they consumed while growing and that make them neutral to global warming. Indeed, this is the case but one can argue the designation of biomass as renewable energy when we strive to reduce greenhouse gases emissions and reproduce what we have eliminated. Biomass is a whole lot better than fossil fuels in this regard, but still it produces harmful gases. Further issues with classifying biomass as renewable energy have been raised by many. About 85 of 107 biomass plants in the U.S were fined for violating clean air laws over the years from 2007 to 2012 [18] .

Biomass is converted to energy by thermal, chemical and biochemical methods which is then used for producing biofuel and briefly discussed in the following section:

a. Thermal conversion

Thermal conversion depends mainly on heat to change biomass into another energy form.

b. Chemical conversion

Several chemical processes are used to convert biomass into an energy form as briefly outlined in the following:

- Anaerobic process produces high BTU gases like methane.
- Fermentation Process produces ethyl and other alcohols.
- Pyrolysis process produces fuels mainly syngas with high output to input ratio which makes it the most attractive process [19].

c. Biochemical conversion

Biochemical conversion breaks down biomass by using enzymes of bacteria and other micro- organisms.

Biofuel popularity is growing because of rising oil prices, but it doesn't mitigate global warming [20]. Biomass in its solid form or as biofuel in liquid form and biogas are used mainly to produce power and heat in large plants.

Biomass is abundant, inexpensive and a dependable source of energy which can be used with many other renewable resources to replace the diminishing supply of fossil fuels. Biomass is used as manure to replace chemical fertilizers for agriculture purposes. It helps in disposing of biological wastes and turns them into energy. Geographical locations affect the type of biomass produced and this might limit energy production. Methane and nitrous oxide, a product of biomass production may damage the ozone layer. In conclusion, the pros of using biomass outweigh the cons.

Renewable energies are the future of humans if a sustainable, healthy and balanced society is desired. Renewable energy will not run out and will secure our development.

Chapter 2: Literature Review

The concept of net zero energy houses is described by The U.S. department of Energy (DOE) as:

"Net-zero-energy building (ZEB) is a residential or commercial building with greatly reduced energy needs through efficiency gains such that the balance of energy needs can be supplied with renewable technologies."

Torcellini *et al*. [21] define four factors for zero energy as follows:

- Net Zero Site Energy: A site ZEB produces at least as much energy as it uses in a year, when accounted for at the site.
- Net Zero Source Energy: A source ZEB produces at least as much energy as it uses in year, when accounted for at the source. Source energy refers to the primary energy used to generate and deliver the energy to the site. To calculate a building's total source energy, imported and exported energy is multiplied by the appropriate site-to-source conversion multipliers.
- Net Zero Energy Costs: In a cost ZEB, the amount of money the utility pays the building owner for the energy the building exports to the grid is at least equal to the amount the owner pays the utility for the energy services and energy used over the year.
- Net Zero Energy Emissions: A net-zero emissions building produces at least as much emissions-free renewable energy as it uses from emissions-producing energy sources.

They present a study case which is based on using PV placed on the roof and analyze the performance of buildings, while implementing readily available energy conservation measures.

They use key energy related building parameters from a survey conducted for about 5,735 buildings in 1999 [22] and create energy models to simulate the energy performance of commercial buildings. Figure 2.1 shows the results of their analysis where:

- Standard 90.1-1999 energy use intensity (EUI) is equivalent to 956 MJ/m^2. Base scenario represents the energy use intensity (EUI) if all buildings were built to Standard 90.1-2004 which is equivalent to 564 MJ/m^2. A reduction of 41% from 1999 Standard.
- Adding a PV to the roof would reduce energy consumption by 28% to EUI of 407 MJ/m^2.
- Scenario LZEB 2005 is achieved by applying day lighting strategies through establishing a non-shaded zone from any obstacles to a distance of 4.6 m of exterior surfaces and adding overhangs to shade direct solar light, caused reduction in lighting power density by 17.5% and decreased HVAC loads, which resulted in 41.5% energy savings over the base scenario with the PV the EUI drops to 176 MJ/m^2.
- Final scenario represents a EUI -2.8 MJ/m^2 in year 2025 that results from additional technological advances for HVAC, lighting, PV efficiency improvements.

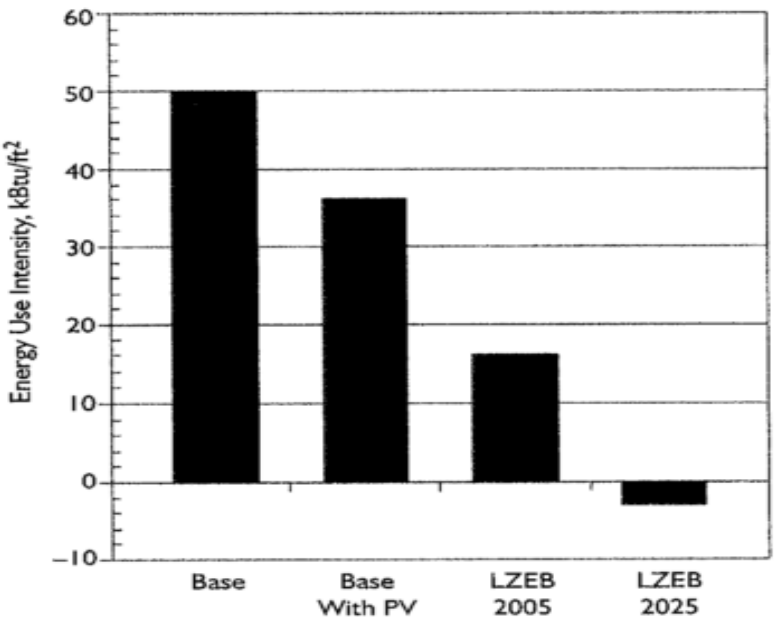

Figure 2.1: Energy use intensity for four scenarios of the commercial building stock.

The authors conclude their document by claiming that serious energy savings is achieved, by using the roof to place solar cells and using advanced technologies combined with integration and control of systems. Not only that, but also, small buildings will export electricity as shown in Figure 2.1 LZEB 2025 scenario. Moreover, Crawley *et al*. [23] go on to justify the strive toward achieving a zero energy buildings because they consume 40% of the primary energy and 71% of the total electricity in the U.S [24] which constitutes a real challenge to economic sustainability, electrical production and emissions. What makes things worse is the rapid growth of the commercial sector that requires more space every year [25]. All this means that more space implies more pressure on energy demand and hence more measures to conserve energy and work on building efficiencies to curb down energy consumption, which calls for new constructed ZEB and fixing of old buildings.

Li *et al.* [26] in their paper, define strategies used to achieve a ZEB and identify them as follows:

- EEM (energy efficient measures): Minimizing the need for energy use in buildings by undertaking energy efficient measures to curb down heat loads from internal, external sources and building services mechanisms.
- RET (renewable energy technologies): Resorting to renewable energy for power supply to meet the remaining energy needs such as photovoltaic/building-integrated systems, photovoltaic/thermal systems, wind turbines, solar water heaters, ground source heat pumps, and district heating and cooling.

They start their study by outlining the adverse effect of increased energy usage on the environment and identify China and the US as the largest primary energy consumers. China surpassed the US in 2009 in energy consumption [27, 28] and is predicted to reach 10 G tones of energy related gas emissions in 2050 [29, 30] where buildings account for a significant amount of it. They reach a conclusion, that there is a need to cut down on energy consumption, if we were to sustain our environment and economy, by resorting to achieving zero energy buildings.

Lam *et al*. [31] and Masoso *et al*. [32] concentrate their works on building envelopes for energy reduction and efficiency measures. They recommend using optimum thermal

insulation to prevent heat gains and losses, which will sharply reduce the electricity demand for heating and cooling. They assert, that careful consideration, should be taken in climates where cooling is dominant as not to over insulate to the point of thermal inflexion.

Jentsch *et al*. [33] and Artmann *et al*. [34] study the effect of thermal mass in delaying heat transfer to a building during day light where peek temperatures occur, and transfer it to night times where fewer loads are present. They claim that integrating thermal mass with mechanical ventilation would lower cooling requirements and possible passive cooling can be achieved.

Muneer *et al*. [35] and Tian *et al*. [36] concentrate their studies on windows/glazing material and types and tie all that to the day lighting. They claim that it must be harmonized properly, in order not to exceed the general rule of low, window to wall ratio, while attaining enough day light to save on electricity drawn by light fixtures.

Roussac *et al*. [37] concentrate their research on the effect of buildings internal conditions on energy reduction, especially, when it comes to indoor design conditions. They affirm that raising the setting of the temperature controller by 1℃ would reduce the cooling requirement by 6%, as reported for office building in Sydney. A 69% reduction in peak cooling demand for a residential building in Las Vegas when the thermostat is set at 26.9℃ instead of 23.9 ℃ is reported by [38]. Reducing the lighting load density by utilizing light emitting diode lighting bulbs is very important in energy reduction and sustainability [39, 40].

PV is one of the most promising systems that would achieve sustainable development as claimed by [41, 42] in their study. PV/T systems make use of thermoelectric cooling modules to reduce the solar cell temperature and takes advantage of the hot water produced by the waste heat generation [43] and would lead to higher system efficiencies as per their studies.

Wind power generation depends on wind forecast and differs from that of thermal power, but tends to complement solar power because, when solar is low, wind is high and

vice versa. As concluded by [44, 45] in their study, using solar and wind energy together could eventually help in achieving ZEB.

Shimoda *et al*. [46], in their study, claim that introducing solar water heaters for use are good solution for reduction of energy consumption and CO_2emissions.

Wang *et al.* [47] present in their research a case study for zero energy house (ZEH) in the United Kingdom. They used simulation software "Energy Plus" to muster a design through different building envelopes and layers in order to maximize energy reduction needs. They used TRNSYS [48] software to study the feasibility of using renewable energy technologies to provide electricity and achieve a ZEH. The authors performed their own simulated study on a typical house in the UK occupied by two people, where the total yearly electrical consumption was estimated at 6008.9 kWh, while the annual electricity generated with PV and wind turbine is estimated at 7305.9 kWh. They conclude that it is possible to achieve a ZEH in the UK if energy efficiency measures are taken and the right renewable technology is used. They also, listed some optimal parameters to be used in house design. They recommend using a window to wall ratio of 0.4 for the south facade and a 0.1 for all other orientations and the overall heat transfer coefficient through the external walls and roof should not exceed 0.1W/m^2 K. They conclude that 98 L/day of hot water load needs 5 square meters of solar collectors with mass flow rate 0.0056 kg/s, and hybrid system of under floor heating and heat pump reduces energy consumption better than any other electric or radiant heating systems. Two wind turbines rated at 5.0 kW in total and a 1.3 kW PV array were used for electricity generation in their case study. They recommend in their study three major design steps for achieving ZEH:

- Climate conditions analysis.
- Façade and building envelope design that achieve energy gains through efficient measures.
- Using advanced simulators to select feasible and optimal renewable energy systems.

Graça *et al*. [49, 50] conduct feasibility study on solar powered net zero energy houses (NZEH) for single family, in mild climate of southern Europe. They used

dynamic thermal simulations for two different architectural configurations powered by PV and thermal solar collectors. They recommend the following measures to be followed if an ideal NZEH is to be achieved:

- Design the house to utilize maximum natural light and ventilation with optimal passive heating and cooling.
- Use high efficient appliances.
- Adequately, size renewable energy systems.
- Properly design electrical infrastructure with flexible grid connection.

The house under study is a 110 m^2 single story two bedroom with defined parameters and heating, cooling, lighting schedules and indoor climate control systems are outlined in the study. One house is optimized for orientation, glazing and shading area and labeled as passive (*P*), while the other is not, and labeled as (*G*). The effect of building orientation on solar gains through glass is examined and results show that maximum gains occur during morning times for southeast and afternoon for southwest orientations. The two houses are heated and cooled by an electric heat pump with radiant heated/cooled floor. Simulation results show that the *G* house had higher cooling demands due to no exterior shading of the glass and higher window to glass ratio along with no proper orientation to avoid solar gains. Solar collectors are used to deliver hot water and a heat pump will deliver the extra hot water demand. PV system will supply electricity and excess power is transferred to a grid and used back when needed. The PV panels are facing south with 35° inclination to maximize electricity production. Both the PV and Solar collectors were sized to meet all annual energy needs. The total energy required by types P and G are 5074 and 8608 kWh/yr respectively. They concluded their research by claiming that it is feasible to achieve a NZEH in Portugal, but additional improvement in PV technologies that would bring the prices down, would make the domestic acceptance to such houses feasible.

Christian *et al*. [51] investigate the thermal performance of a near zero energy house, built in Tennessee USA, with structural insulated panels and powered with 2kW grid-tied photovoltaic system, while geothermal heating and cooling of the space is used. They

conclude that all five houses that cost $\$100/ft^2$ can reach zero energy status if the PV system is extended over the free area on the roof.

Most of the researchers on ZEB worked on measures to reduce energy by increasing the efficiencies of the house envelope and proper construction design and architecture along with adequate sizing of the renewable energy systems to meet the remaining electricity demand. It's worth noting, that human understanding and awareness of the need to curb energy use and sustain the environment would come beneficial to this transformation. Many have concluded their work by ascertaining that ZEB will play an important role in energy, environmental and economic sustainability. They emphasize that more work is needed on improving technologies, to enhance efficiencies, and life cycle cost analysis and social policies are to be well set and defined.

Chapter 3: Motivation and Objectives

Global energy and water shortages and Ozone depletion are the driving forces that prompted me to find solutions to electricity generation and water production with sustainable measures. These factors make the need to generate electricity by renewable energy a must. Therefore, net zero energy houses will be the main target of this research. This study is motivated by trying to achieve these goals and strive toward establishing a sustainable economic, environmental and clean habitat. After reviewing much literature and gaining an insight on how to tackle the problem, the solution to gain energy savings for the proposed house is shaped as follows:

- Selecting the location where the study is to be performed.
- Selecting the orientation of the house which allows for passive ventilation, day lighting and minimum solar gains.
- Designing the envelope of the house to curb down heat transfer in and out, with proper tightness, thermal insulation, and low window to wall ratio to avoid excessive solar gain through glass. Proper shading by introducing overhangs and fins around windows and doors to reduce solar gains.
- Avoiding shading by other houses to keep proper use of sun light.
- Selecting high efficient appliances and light fixtures which are controlled to go off whenever not used.
- Using sophisticated water fixtures that would reduce water usage like sensor type.
- Using thermal solar power to deliver hot water aided by a heat pump or thermal storage system.
- Using solar assisted equipment for seasonal cooling and heating whenever possible and a ground solar heat pump.
- Sizing the proper renewable energy systems to deliver the remaining electricity needed.

A sustainable environment is not complete if the living conditions of humans are not free of all pollutants at least reduced to non-harmful levels. Noise pollution is not

considered a nuisance anymore, but an environmental pollutant that will be considered in this study.

Driven by the need to alleviate the above mentioned problems, the work of this PhD research will aim on achieving a sustainable net zero energy houses with low noise pollution and very low level of greenhouse gases emissions.

Most researchers on NZEH tackled the measures needed to gain energy efficiencies and cut down on total electrical load. They used some renewable energy sources to supply electricity and hot water but none considered the problem of establishing a NZEH with multigeneration energy system to produce power, seasonal air-conditioning, hot and fresh water. Neither conducted a parametric analysis on the system components, to study the sensitivity and influence of each, on total system performance, nor, have they established any exergetic, exergoeconomic study to NZEH. Some researchers have carried out optimization studies, but mainly were limited to cost feasibility of the systems on hand.

This PhD research will attempt to achieve a NZEH with three novel multigeneration systems, for producing electricity, seasonal air-conditioning and supply of hot and fresh water. Reducing greenhouse gases to low level and maximizing the usage of renewable energy is of utmost importance to this study. A new dimension will be added to the research by lowering the level of noise pollution through experimental measures and optimization of the sizes of thermal and acoustic insulation to be used. After which, evaluation of the total heating and cooling load of the system and calculating the total electricity needed, which lead to sizing the renewable energy equipment. Once the design stage is finished, a comprehensive thermodynamic analysis is established and an exergetic and parametric evaluation is conducted to assess the sensitivity and improvements of the various system components.

The research is concluded by exergoeconomic exergoenvironmental analyses to evaluate the total system cost with consideration to exergy destruction and greenhouse gases emission costs. Finally, optimizing the total system cost to the overall system efficiency using genetic algorithm to obtain the optimal design or at least a set of optimal designs.

This PhD research represents originality in systems developed and applied procedures which has not been done before.

The specific objectives of this thesis are listed as follows:

a) To perform energy efficiency measures where a net zero energy house is established.

b) To evaluate the total electrical load of the house.

c) To develop three novel multi-generation systems that provides electricity, hot and fresh water and seasonal air conditioning to the NZEH.

d) To optimize the power system to the NZEH for all three novel systems.

- To minimize total NPC and CO_2 emissions.
- To maximize renewable energy fraction of the total power system used.

e) To perform thermodynamic modeling of all three systems.

f) To conduct exergy analysis of all system components.

- To establish exergy flow rate of each stream.
- To evaluate exergy destruction rate.
- To calculate overall, subsystems and individual systems components exergy efficiency.

g) To carry out parametric study on all three systems components.

- To vary parameters within acceptable range and to note any changes or improvements on individual and overall system performance.

h) To perform exergoeconomic analysis for all three systems components.

- To evaluate all streams cost.
- To calculate all streams exergy destruction cost and initial systems cost.

i) To conduct exergoenvironmental analysis of all three systems.

- To predict CO_2 emissions of the system if applicable.

j) To perform multiobjective optimization, in order, to minimize and maximize total overall system cost and exergetic efficiency respectively.

k) To conduct assessment on all three systems and select the most appropriate to the NZEH.

Chapter 4: System Description and Development

All developed systems are designed to provide electricity, hot and fresh water, heating and cooling as needed.

4.1 System I

Figure 4.1 shows the schematic of system I. Electricity is provided to the house through PV/T, wind turbine, diesel generator and battery bank systems managed by an electrical control mechanism. Excess electricity is dumped when the system is not connected to a grid to avoid over charging of the batteries.

Hot water is stored in a hot water tank that is heated by solar energy and is supplied to the house in the summer along with heated water from the PV/T system. During sunshine, hot water leaving the solar collectors at point 25 enters a three way valve and exits at point 25 to another three way valve where it exits at point 51 to release its heat to a ground storage bank and flows into another three way valve at point 52 and out at point 50 back to the solar collector where the cycle is repeated. The whole purpose of this process is to raise the temperature of the ground soil designated, as storage thermal bank, during the long sunshine summers, where it can be used during winter to supply hot water when needed.

During winter, cold water from the house passes through a three way valve at point 43 and exits at point 43 to another three way valve, where it leaves at point 52 to the hot ground thermal bank gaining heat and passing at point 51 through another three way valve, then it exits at point 45 and gets pumped to the house, where the cycle repeats itself. An auxiliary water heater is used to provide hot water during emergencies.

Absorption chiller is powered by solar collectors at point 17 where it provides cooling to a liquid desiccant system at point 13. Ambient air is cooled at the dehumidifier and is supplied to the house at point 41, while the removed moisture is condensed at point 36 and is delivered to the fresh water tank at point 37. A unitary heat pump is used to provide cooling during the night and heating during the winter. Detailed drawings and explanation of the system's subsystems are outlined below:

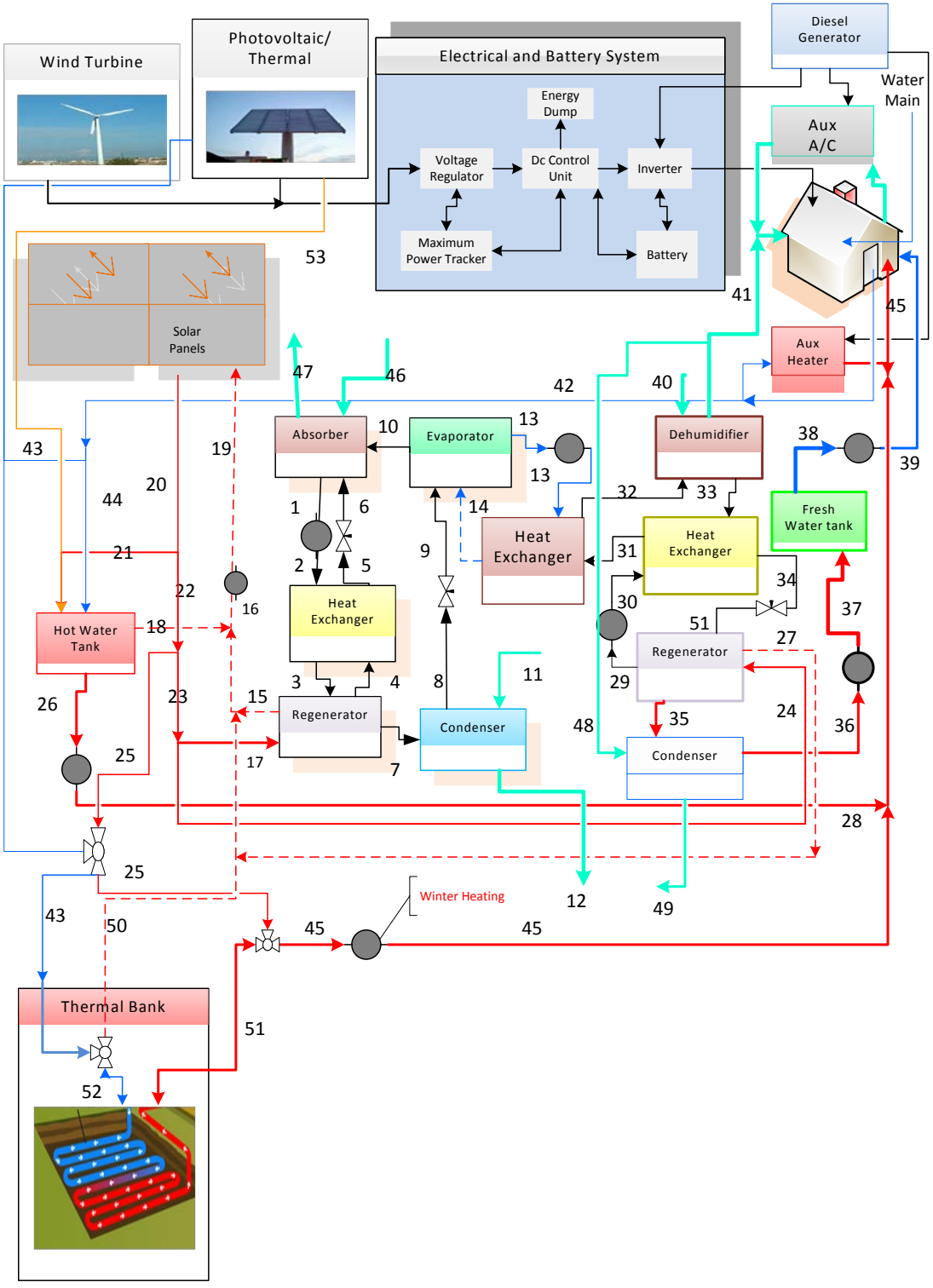

Figure 4.1: System I schematic diagram.

Figure 4.1 shows the schematic diagram of the developed system I and is composed of the following components:

4.1.1 Power system

The power system is composed of the following subsystems:

- Photovoltaic
- Wind turbine
- Battery and Electrical
- Diesel Generator

The photovoltaic and wind turbine provide *DC* current to the battery and electrical system, where it goes through a voltage regulator then to a *DC* control unit, then to an inverter that produces *AC* current which supply the house needs. The batteries get charged at the *DC* unit and through a rectifier when the diesel generator is operating because it changes *AC* current to *DC*. The electrical supply is monitored by a maximum power tracker that would cause the system to connect to a grid when access energy is available or to an energy dump when not tied to the grid. The standby generator will provide electricity when it is needed.

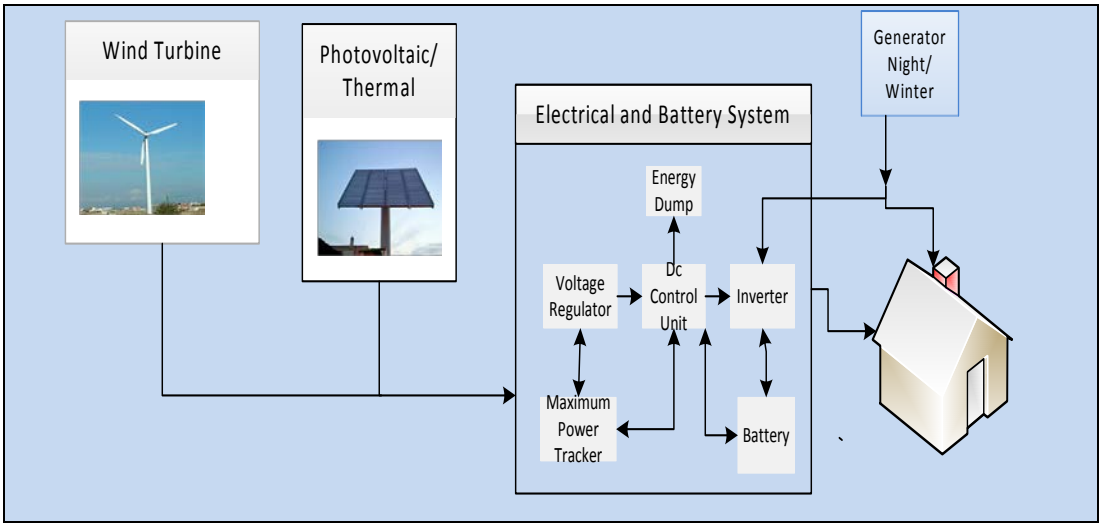

Figure 4.2: Power system schematic.

4.1.2 Solar thermal collectors system

The solar thermal collectors system has the following components:

- Solar panels
- Pump

The solar panels are made of evacuated tube collectors and solar heat is transferred to the fluid circulated through by a pump. Hot water is used to power the regenerator of the absorption chiller, liquid desiccant system, hot water storage tank and ground thermal bank. Re-circulated cold water returns back to the solar system where the cycle is repeated.

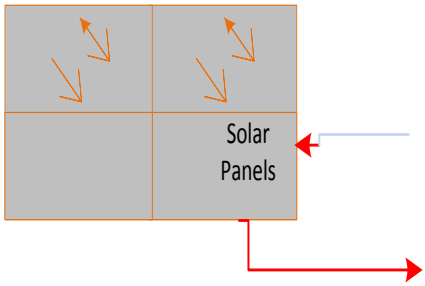

Figure 4.3: Schematic of solar panels.

4.1.3 Thermal energy storage

The thermal energy storage in this system is composed of:

- Ground storage thermal bank

Hot water is circulated through the ground storage thermal bank to heat the earth soil during the long sunny months and the same bank is used in the short winter to provide hot water when it is needed. Heat moves slowly through soil at the rate of 1℃ /m.

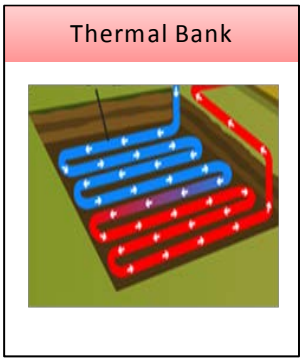

Figure 4.4: Schematic of thermal ground storage.

4.1.4 Absorption chiller

The absorption chiller is composed of the following major components:

- Absorber
- Regenerator
- Condenser
- Evaporator
- Heat Exchanger
- Expansion Valve
- Pressure Reducing valve and pump

The absorption chiller will provide cooling water at the evaporator and will operate during the long warm sunny months. The regenerator will be powered by hot water from the solar system and the condenser-absorber units will be cooled by ambient air.

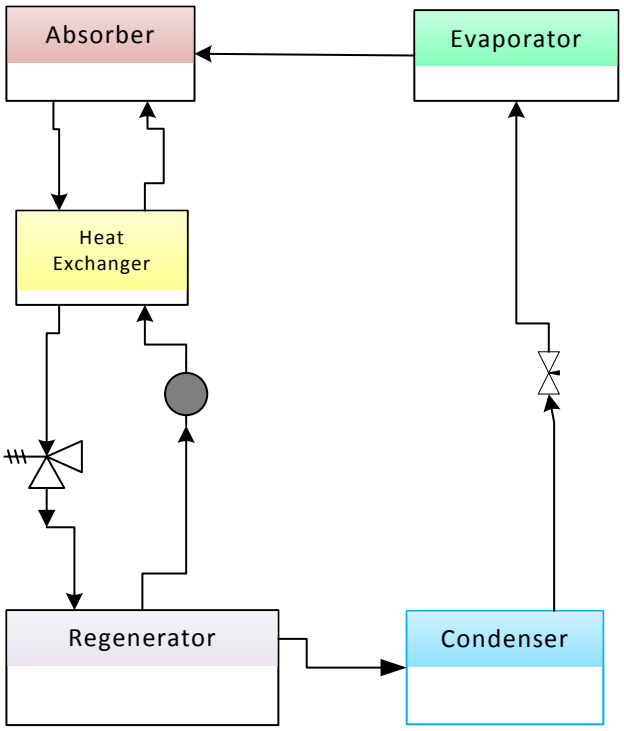

Figure 4.5: Schematic diagram of absorption chiller.

4.1.5 Liquid desiccant system

The liquid desiccant system is composed of five major components besides the piping and the working fluid of LiBr as follows:

- Dehumidifier
- Regenerator
- Heat Exchanger
- Condenser
- Pump

The LDS system is used to produce cool air and fresh water to the house by passing ambient air at the dehumidifier and condensing the absorbed water at the condenser. The system is used with the absorption chiller. The desiccant at the dehumidifier and vapor at the condenser are cooled by cold water from the evaporator of the absorption chiller.

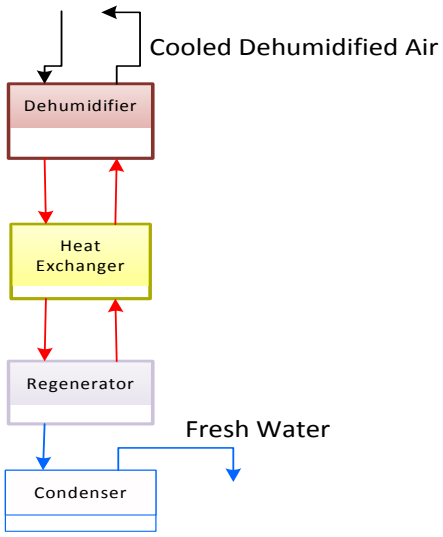

Figure 4.6: Schematic of liquid desiccant system.

4.1.6 Hot Water storage tank

The hot water storage tank is composed of:

- Well insulated thermal storage tank
- Pump

Hot water from the solar system passes through the hot water storage tank which supplies the house during the long sunny days and anytime when the water is available. The tank is properly insulated to reduce heat losses.

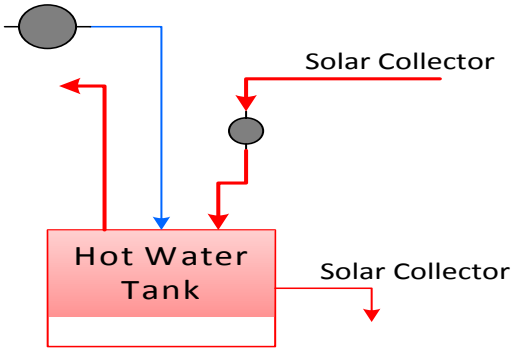

Figure 4.7: Schematic of solar tank.

4.1.7 Auxiliary water heater

The auxiliary water heater is used during the short winter season if needed and if emergency or failure of the pump occurs. It works on electricity supplied by the renewable energy power system.

4.1.8 Night and winter air-conditioning unit

A unitary unit is used to provide cooling at night and heating during winter season whenever needed. It works on electricity supplied by the renewable energy power system.

4.2 System II

Figure 4.8 shows the schematic diagram of proposed system II. Organic Rankine cycle with ammonia solution as the working fluid is the source of power to the house coupled to battery banks through electrical control system. Ammonia solution is selected because it boils at low temperature. The turbine is powered by hot solar water at point 65 and the condenser is cooled by cold water from the absorption chiller system at point 69.

During day sunshine, electricity is produced by the organic Rankine cycle (ORC) at the turbine and the surplus electricity is sold to the grid. While during night and non-sunny days, electricity is supplied by the battery banks and bought from the grid whenever needed. The proposed capacity of the ORC will offset all electrical usage. Hot water is supplied to the well sized and insulated tank by the solar collectors at point 21 during sunshine. If all the water is consumed at night and during winter non-sunny days, an auxiliary heater would replenish the house with needed hot water.

Vapor from ambient dehumidified air at the LDS condenses by blowing cold air from point 41 through the condenser at point 48 and is pumped to the fresh water tank at point 37 and then to the house at point 45.

100% ambient air passes through the dehumidifier at point 40 of the LDS system, where it exchanges heat and moisture, with the desiccant that is cooled by water from the absorption chiller at point 32. Cooled and dehumidified air is then supplied to the house. A unitary split unit is used to provide cooling during the night and heating during the winter when it is needed. Figure 4.8 shows the schematic diagram of the developed system II which is composed of the following subsystems:

4.2.1 Power system

The power system has many components as listed below in Figure 4.9:

- Organic Rankine cycle
- Evaporator
- Condenser
- Heat Exchanger
- Rectifier
- Super Heater
- Expansion Valve
- Pump
- Battery Bank
- Power Control system

The ORC is powered by solar heated water at the evaporator and cooled by water from the absorption chiller system at the condenser. Electricity is generated and connected to the house at the electrical and battery system.

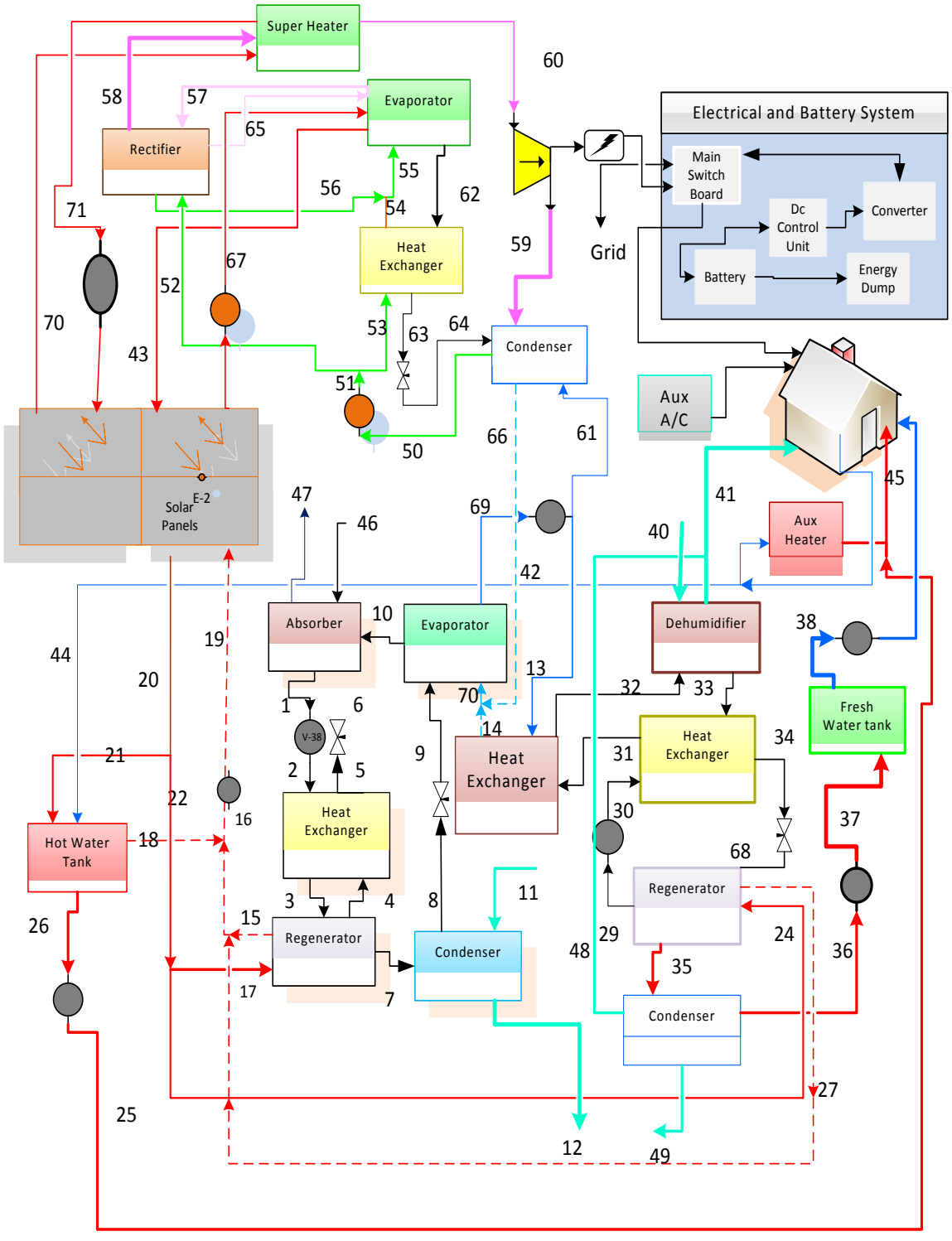

Figure 4.8: System II schematic diagram.

4.2.2 Solar thermal collectors system

The solar thermal collector's system components are:

- Solar Panels
- Pump

Solar panels are made of evacuated tube collectors and solar heat is transferred to the fluid that is circulated through by pump. Hot water is used to power the regenerators of the absorption chiller, LDS, hot water storage tank and ORC evaporator, the part of hot water that supply the super heater reach elevated temperatures to raise the ammonia/water vapor temperature entering the turbine, so it does not condense upon expansion. Re-circulated cold water returns back to the solar system where the cycle is repeated.

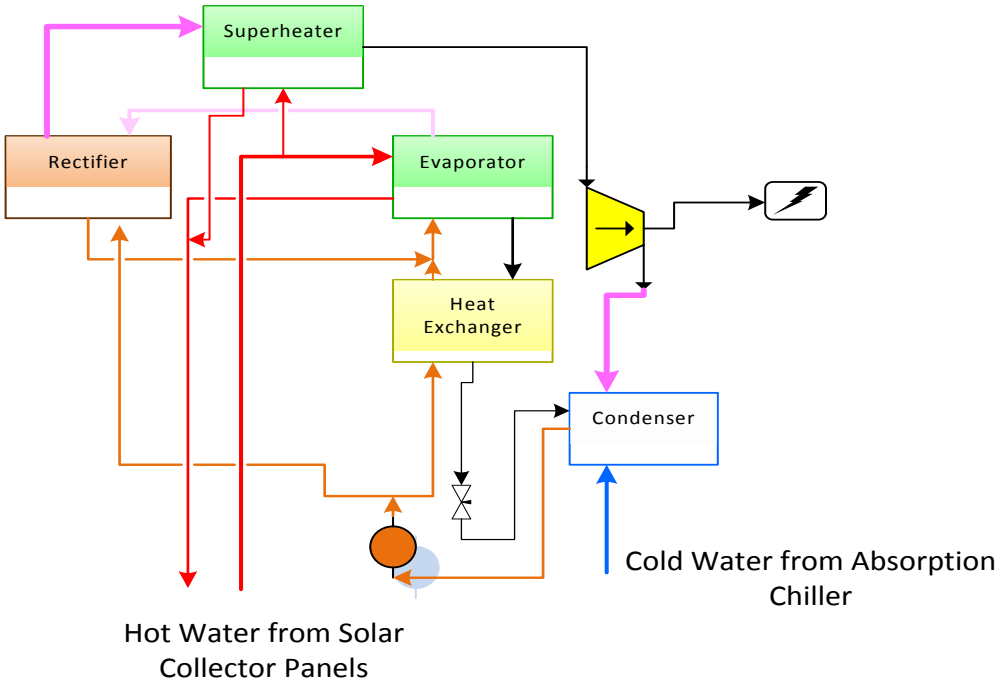

Figure 4.9: Power system.

4.2.3 Absorption chiller

The absorption chiller is composed of:

- Absorber

- Regenerator
- Condenser
- Evaporator
- Heat exchanger
- Expansion valve
- Pressure reducing valve and pump

The absorption chiller will provide cooling water at the evaporator and will operate during the long warm sunny months. The regenerator will be powered by hot water from the solar system and the condenser-absorber units will be cooled by ambient air.

4.2.4 Liquid desiccant system

The Liquid desiccant system is composed of the following subsystems:

- Dehumidifier
- Regenerator
- Heat Exchanger
- Condenser
- Pump

The LDS system is used to produce cool air and fresh water to the house by passing ambient air at the dehumidifier and condensing the absorbed water at the condenser. The system is used with the absorption chiller. The desiccant at the dehumidifier and vapor at the condenser are cooled by cold water from the evaporator of the absorption chiller.

4.2.5 Hot water storage tank

Hot water from the solar system passes through the hot water storage tank which supplies the house during the long sunny days. The tank is properly insulated to reduce heat losses to a minimum during a one day cycle.

4.2.6 Auxiliary water heater

The auxiliary water heater is used during the short winter season if needed and if emergency or failure of pumps occurs. It runs on electricity supplied to the house by the renewable energy power system.

4.2.7 Night and winter air-conditioning unit

A unitary unit is used to provide cooling at night and heating during winter season whenever needed. It runs on electricity powered by the renewable energy power system.

4.3 System III

Figure 4.10 shows the schematic diagram of system III. Hydro power turbine and PV systems are the sources of power to the house coupled to a battery bank and electrical control system. The power system is tied to grid. Batteries are used to supply power at starting stage and during emergencies to light fixtures, refrigerator and similar items. Excess electricity from the turbine is sold to the grid and bought whenever it is needed.

Solar collectors power an absorption heat transformer, at points 23 and 20 of the regenerator and evaporator respectively. At the absorber point 12, water from the river which drives the turbine at point 58 and enters the distillation heat exchanger at point 11, where it gains heat, picks up lots of heat due to heat of solution and exit at point 13 to the separator as vapor and liquid at 100 ℃. There, the vapor separates and passes through an auxiliary condenser at point 15 ,where it releases some of its heat to the water stream coming from the solar collectors, and on to the fresh water tank and part of it to the hot water tank. Hot water is also produced at the ground source heat pump, when cold water from the house passes through a heat exchanger placed at the hot gas stream exit from the compressor, at points 51 and 48.

During the long sunny days, hot water that exits the separator vessel at point 16 and loses some of its heat at the heat exchanger flows through a three way valve at point 17 and to a ground thermal storage bank at point 46, where it loses most of the heat. It then passes through another three way valve at point 43 and is pumped at point 42 to another ground thermal storage bank where it loses more heat and exits as cold water at point 40 to another three way valve. This cold water is used to cool the condenser of the

absorption heat transformer at point 28 and the condenser of the ground source heat pump at point 32.Water that leaves the absorption heat transformer's condenser at point 29 flows back to the river, while water that leaves the heat pump's condenser, exits to a three way valve at point 30 and then to the river at point 39.

During the winter non-sunny days, hot water is supplied partially from the ground source heat pump and mainly from water circulated from the hot water tank at point 37, where it is pumped through a three way valve at point 38 and exits to the heated ground thermal storage bank at point 46, where it picks up heat and leaves through a three way valve at point 43, then back to the hot water tank at point 36 and the cycle repeats itself.

Cooling of the house is achieved by circulating air from the house through the evaporator of the heat pump. The condenser is cooled by cold water from the cooling ground storage bank at point 31 as explained earlier.

Heating of the house, takes a different scheme than cooling. After hot gas is diverted to the evaporator of the ground source heat pump, cool gas goes to the condenser that needs to be heated by higher temperature medium. This is achieved, by heating cold water passing through the condenser. At point 30, water exits the condenser to a three way valve and is pumped at point 35 to the cooling ground storage bank, where it gains heat and moves out through a three way valve at point 40 and back to the condenser at point 32.

All the systems are controlled by automatic control mechanism, to switch between summer and winter operations, and all the valves are operated by electro- magnetic solenoid switches to perform the required operation.

System III is shown in Figure 4.10 and is composed of the following subsystems:

4.3.1 Power system

The power system has many subsystems as follows:

- Hydro turbine generator
- Pump
- Electrical and battery system

- Photovoltaic system

A hybrid hydro turbine generator and photovoltaic power system coupled to a battery bank and electrical panel is used to supply electricity to the house.

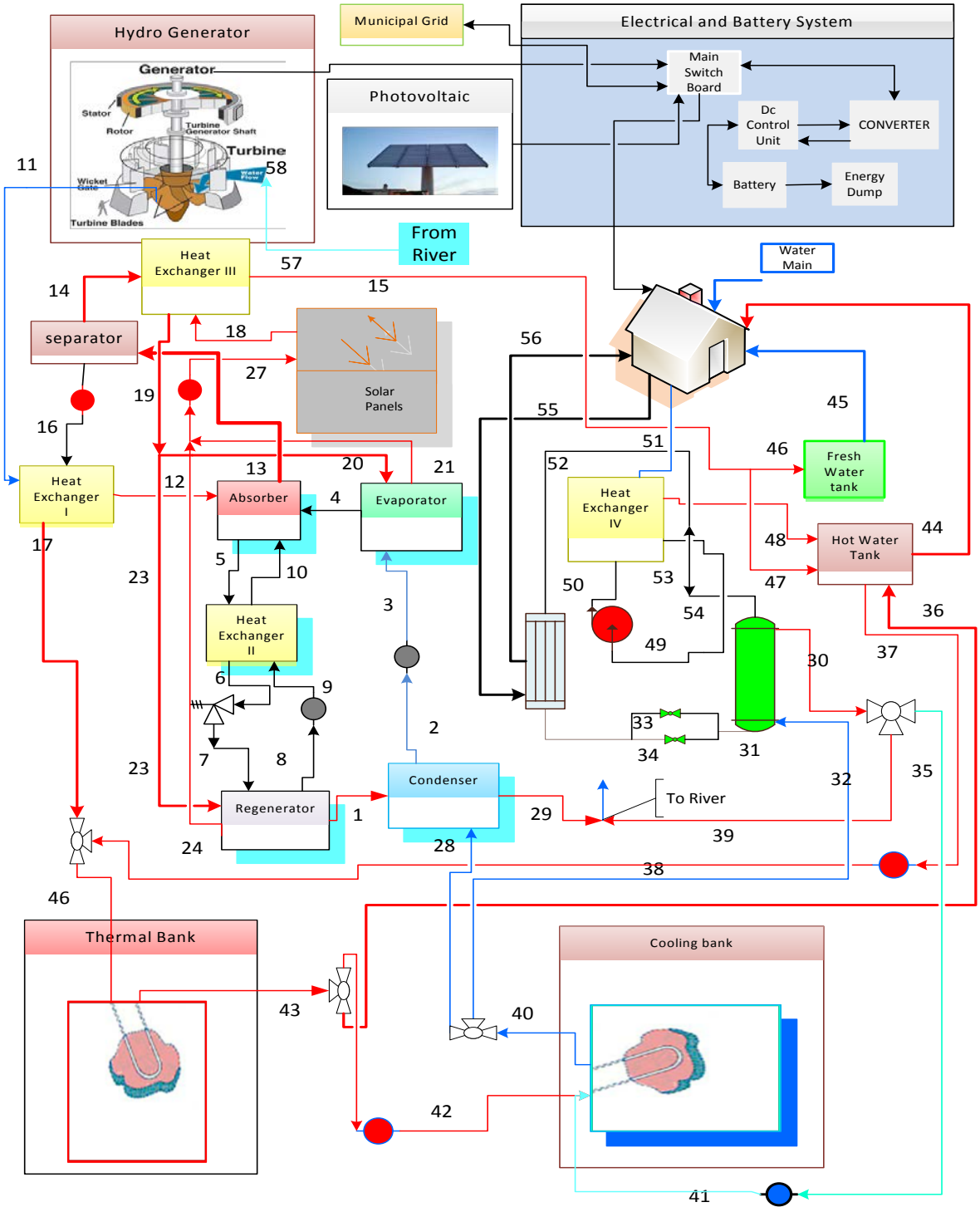

Figure 4.10: System III schematic diagram.

4.3.2 Solar thermal collectors system

The solar thermal collectors system is composed of:

- Solar panels
- Pump

The solar panels are made of evacuated tube collectors and solar heat is transferred to the fluid circulating through them by a pump. The hot water is used to power the regenerator and evaporator of the absorption chiller. Re-circulated cold water returns back to the solar system where the cycle is repeated.

4.3.3 Absorption heat transformer

The absorption heat transformer has the following components:

- Absorber
- Regenerator
- Condenser
- Evaporator
- Heat Exchanger
- Expansion Valve
- Pressure reducing valve

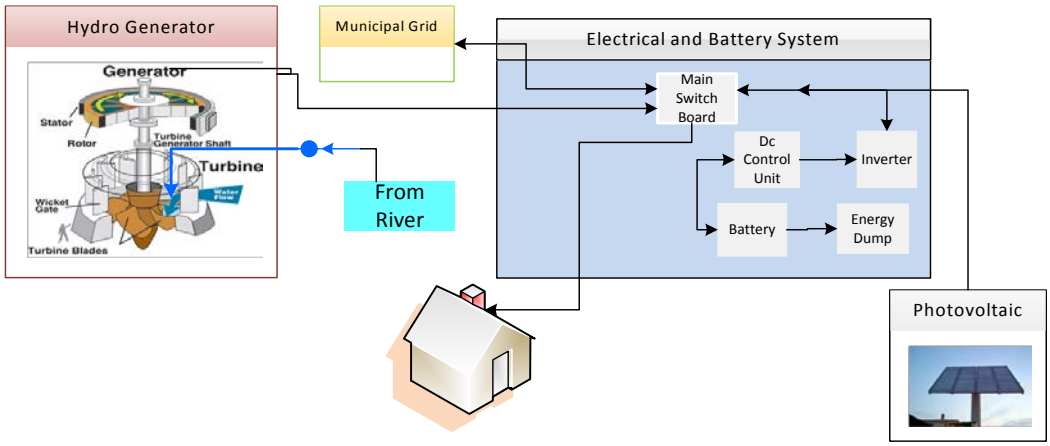

Figure 4.11: Hydro/PV power system.

Absorption heat transformer operates as a mechanical vapor compression heat pump except that the compressor is replaced by an absorbent fluid circuit.

An absorption heat transformer uses an aqueous solution of LiBr where the absorbent has a great affinity for the refrigerant. The refrigerant is absorbed by the absorbent solution in the absorber, releasing heat of solution. The weak solution is then pumped to the regenerator. In the generator, hot water is supplied to drive off the refrigerant from the absorbent solution. The refrigerant is condensed giving up its latent heat in the condenser. The strong solution is then returned to the absorber. The refrigerant from the condenser is pumped to the evaporator pressure, where hot water from the solar source causes it to evaporate. The refrigerant vapor then passes to the absorber to close the cycle. The evaporator operates at a higher temperature than the condenser.

The driving force for a heat transformer consists of heat inputs to the regenerator and the evaporator. The heat transformer then delivers part of the heat at a higher temperature from the absorber and the rest at a lower temperature from the condenser. However, the unique ability of the heat transformer to deliver heat at higher temperature than the input heat depends upon the availability of a lower temperature heat sink.

The absorber and evaporator are at the same pressures while the condenser and regenerator are at the same pressures. The absorption heat transformer is powered by hot water from the solar collectors at the evaporator and regenerator and is cooled off by cold water from the second ground thermal cooling bank at the condenser.

At the absorber, water from the river is heated into vapor and liquid. It is used to produce fresh and hot water.

4.3.4 Thermal energy storage

Thermal energy storage system uses earth as the storage medium and consists of the following:

- Ground thermal heating bank
- Ground thermal cooling bank
- Pump
- Three way valves

Hot water is circulated through the heating bank to heat the soil during the long sunny months and the same bank is used in the short winter to provide hot water when it is needed. During the summer season, hot water stores its energy in the first bank and flows to the second bank at a lower temperature to further cool off where it cools the condenser of the heat pump during cooling and the condenser of the absorption chiller. The temperature of the second bank is raised a little in the summer and is used in the winter to transfer heat to cooler water from the heat pump condenser.

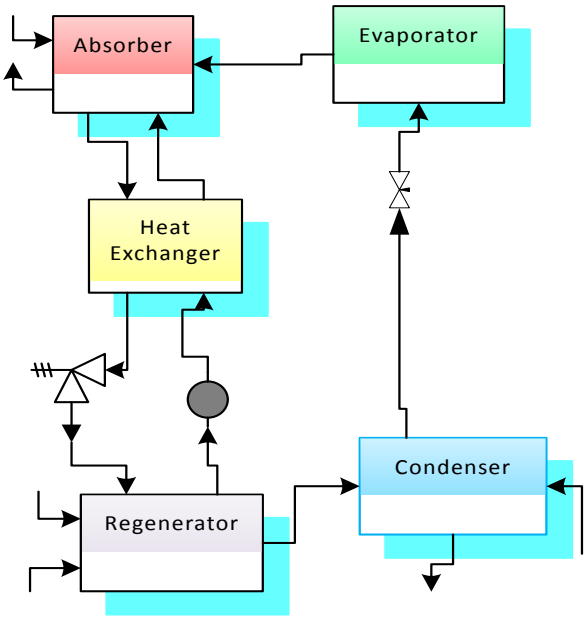

Figure 4.12: Schematic of Absorption heat transformer system.

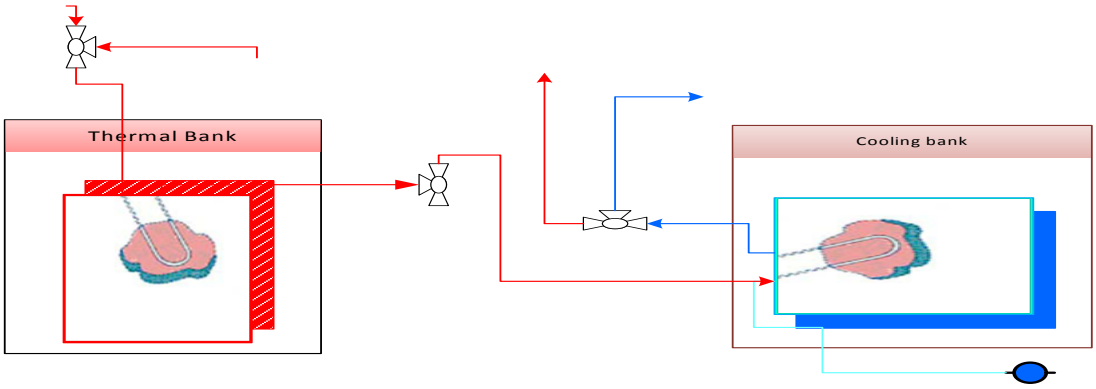

Figure 4.13: Schematic of thermal storage system.

4.3.5 Ground source heat pump coupled with heat exchanger for hot water

The GSHP system is composed of:

- Compressor
- Evaporator
- Condenser
- Pump
- Heat Exchanger
- Expansion Valve

The ground source heat pump is used to provide heating and cooling and hot water supply. The cooling ground storage bank is used for heat transfer from condenser through circulated water and hot water is produced by circulation through a heat exchanger where the compressor gas outlet passes. Cooling and heating is achieved by circulating air at the evaporator.

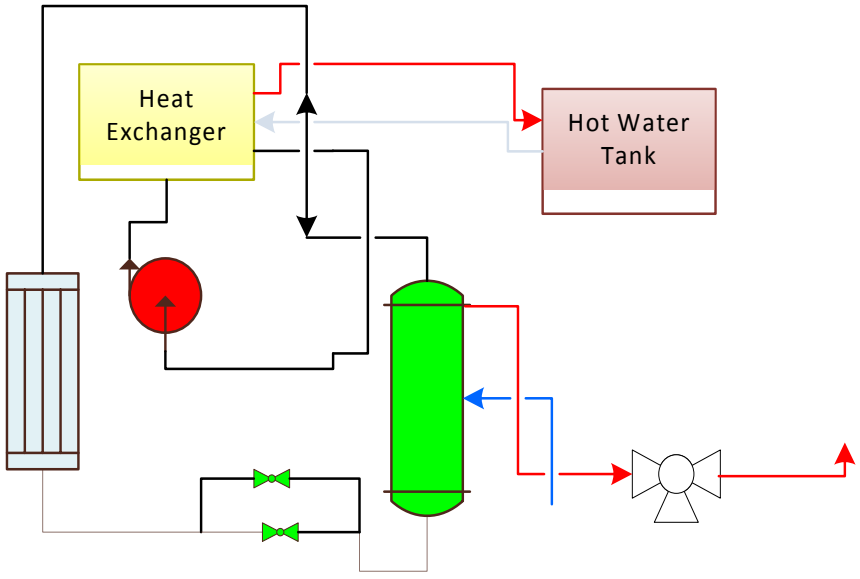

Figure 4.14: Schematic of ground source heat pump.

4.3.6 Distillation system

The distillation system has the following subsystems:

- Heat Exchanger
- Separation Unit
- Auxiliary Heat Exchanger
- Pump

The water passing through the hydro turbine is circulated through the distillation system heat- exchanger and then to the absorber after which it exits as part vapor part steam and passes through a separation unit where the distilled vapor passes through an auxiliary condenser as fresh water while the liquid passes back through the heat exchanger and to the ground storage thermal bank.

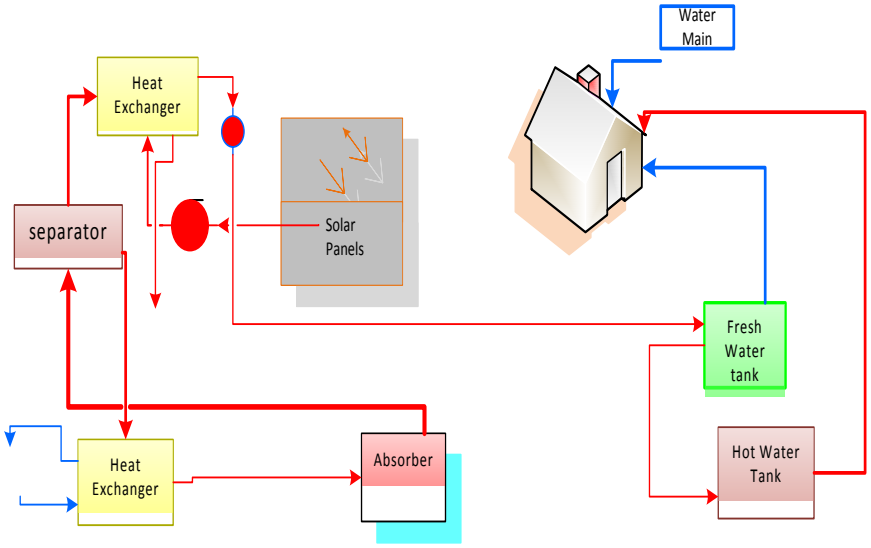

Figure 4.15: Distillation system.

4.3.7 Hot water storage tank

Hot water from the heat exchanger is stored in a hot water tank during the operation throughout long sunny months, and hot water from the hot thermal bank during the winter season is stored in the hot water tank and used accordingly.

Chapter 5: Model Development

In this chapter, general thermodynamic relations are presented and mathematical formulation of acoustic sound pressure level evaluation and seasonal load calculations, exergoeconomic analysis and optimization are presented.

"Exergy analysis is a method that uses the conservation of mass and conservation of energy principles, together with the Second Law of Thermodynamics, for the analysis, design, and improvement of energy and other systems" [1]:

5.1 Thermodynamic modeling

General Balance equations of unsteady system for a control volume, assuming kinetic, potential and chemical energies are negligible unless noted, are performed by using thermodynamic analysis as follows:

5.1.1 Mass analysis

The law of conservation of mass governs the mass balance equation:

$$\sum_i \dot{m}_i - \sum_e \dot{m}_e = \dot{m}_{stored} \tag{5.1}$$

where $\dot{m}$ is the mass flow rate and the subscripts *i* and *e* refer to the inlet and exit flow streams the control volume.

5.1.2 Energy analysis

The first law of thermodynamics for energy conservation is applied to all streams, heat and work inputs and outputs and for accumulated energy as follows:

$$\sum_i \dot{m}_\iota h_i - \sum_e \dot{m}_e h_e + \sum_i \dot{Q}_\iota - \sum_e \dot{Q}_e + \sum_i \dot{W}_\iota - \sum_e \dot{W}_e = \dot{E}_{stored} \tag{5.2}$$

where $\dot{Q}$, $\dot{W}$, $\dot{E}$, $\dot{m}_\iota h_i$, $\dot{m}_e h_e$, are heat, work, energy, and enthalpy in and out rates respectively.

5.1.3 Entropy analysis

The entropy generated within the control volume due to the process on hand is given by:

$$\sum_i \dot{m}_\iota s_i - \sum_e \dot{m}_e s_e + \sum_i \frac{\dot{Q}_\iota}{T_{source}} - \sum_e \frac{\dot{Q}_e}{T_{source}} + \dot{S}_{gene} = \dot{S}_{stored} \tag{5.3}$$

where $\dot{S}_{gen}\ is$ entropy generation rate and s is specific entropy.

5.1.4 Exergy analysis

The exergy content of a stream flowing in and out of the control volume is dependent on the substance flow and characteristics. Chemical exergy is associated with the departure of the chemical composition of a system from its chemical equilibrium and physical exergy is measured as a function of the thermodynamic state of the flow. Physical exergy is defined as the maximum useful work obtainable as a system interacts with an equilibrium state. Second law of thermodynamics is used to evaluate the exergy rate balance conducted on the control volume:

$$\sum_i \dot{m}_\iota[(h_i - h_0) - T_0(s_i - s_0)] - \sum_e \dot{m}_e[(h_e - h_0) - T_0(s_i - s_0)] + \sum_i \frac{\dot{Q}_\iota(T_{source} - T_0)}{T_{source}} -$$

$$\sum_e \frac{\dot{Q}_e(T_{source} - T_0)}{T_{source}} + \sum_i \dot{W}_i - \sum_e \dot{W}_e + \dot{E}_{X_{des}} = \dot{E}_{X_{accum}} \quad (5.4)$$

where $\dot{E}_{X_{des}}$ is exergy rate destructed for the process, $T_0\ and\ s_0$ are the reference temperature measured in *K* and specific entropy of the reference state respectively, T_{source} is the temperature measured in *K* for the system component where the thermal exergy is taking place.

5.2 Exergoeconomic analysis

Economic analysis based on exergy destruction or thermodynamic losses and capital costs will be examined in this study.

The basis for the analysis is well explained by [1] as: Amount input +Amount generated – Amount output – Amount consumed = Amount accumulated

Exergy costing associated with a steady state flow is dependent on the exergy balance of the system multiplied by its allocated cost defined as the average cost per unit of exergy in $/GJ [52]:

A flow cost rate $\dot{C}$ ($/h) is defined for each stream flow in and out of a system and the cost balance equation is written so that all terms are positive:

$$\dot{C}_i = \sum_i c_i \dot{m}_i[(h_i - h_0) - T_0(s_i - s_0)] \quad (5.5)$$

$$\dot{C}_e = \sum_e c_e \dot{m}_e[(h_e - h_0) - T_0(s_e - s_0)] \quad (5.6)$$

where c_i, c_e are the allocated exergetic cost for every in and out streams of the system components defined as the average cost per unit of exergy in US $/GJ.

$$\dot{C}_w = \left(\sum_i c_{w,i}\dot{W}_i - \sum_e c_{w,e}\dot{W}_e\right) \quad (5.7)$$

where the $\dot{C}_w$ is the total exergy cost associated with work,

$$\dot{C}_q = \sum_i c_{q,i}\frac{\dot{Q}_i(T_{source}-T_0)}{T_{source}} - \sum_e c_{q,e}\frac{\dot{Q}_e(T_{source}-T_0)}{T_{source}} \quad (5.8)$$

where $\dot{C}_q$ is the total cost associated with thermal exergy flow.

$$\dot{C}_{cinv} = IC\frac{(1+ir)^n}{(1+ir)^n-1}\left(\frac{1}{N}\right) \quad (5.9)$$

where $\dot{C}_{cinv}$ is the total capital investment, *IC* is initial capital.

$$\dot{C}_{o\,\&\,m} = FYM\frac{(1+ir)^n}{(1+ir)^n-1}\left(\frac{1}{N}\right) \quad (5.10)$$

where $\dot{C}_{o\,\&m}$ is the total maintenance and operation cost, ir is interest rate, n is life cycle in years, *N* is number of hours of operation in one year and *FYM* is first year maintenance cost.

$$\dot{C}_i + \dot{C}_q + \dot{C}_{capital\ investment} + \dot{C}_{operation\ and\ maintenance} = \dot{C}_e + \dot{C}_w \quad (5.11)$$

Equation (5.11) results in a set of equations that can be presented in a matrix form of the type (c = a / b) which solves for the allocated exergetic cost (c) for every stream component.

$$\dot{C}_{ex,des} = \left(\sum_j \dot{m}_j cost_{SFP_j} e_{xj}\right) \quad (5.12)$$

where $cost_{SFP_j}$ is the cost of the source that is generating the product, called the fuel, and can be obtained after evaluating equation: (5.11).

The total system cost is obtained as below:

$$\dot{C}_{tot} = \dot{C}_{ex,des} + \dot{C}_{cinv} + \dot{C}_{Oand\ M} \quad (5.13)$$

5.3 Exergoenvironmental analysis

In this research we attempt to achieve a net zero energy house where emissions of greenhouse gases are zero. The use of renewable energy systems to power the house and all other system components make it impossible to introduce any pollutants. In some systems, we have grid tied power configuration which if used the corresponding green gas emissions should be accounted for, even though the emissions were not produced directly by the house. One system is not tied to the grid and has a diesel generator that provides electricity when needed. Even though the production of pollutants is small, it will be accounted for and the cost will be charged to the total system for proper analysis and optimization.

5.4 Optimization analysis

In this research, a multiobjective optimization is used to minimize the total cost and maximize the exergetic efficiency. Multiobjective optimization is a genetic algorithm that deals with the minimization of a vector of objectives F(x) that can be the subject of a number of constraints or bounds and when maximization is needed, the F(x) is multiplied by a minus sign [53- 56].

- "The genetic algorithm begins by creating a random initial population and creates a sequence of new populations. At each step, the algorithm uses the individuals in the current generation to create the next population. To create the new population, the algorithm performs the following steps:
- Scores each member of the current population by computing its fitness value.
- Scales the raw fitness scores to convert them into a more usable range of values.
- Selects members, called parents, based on their fitness.
- Some of the individuals in the current population that have lower fitness are chosen as elite.
- These elite individuals are passed to the next population.
- Produces children from the parents. Children are produced either by making random changes to a single parent—mutation—or by combining the vector entries of a pair of parents—crossover.

- Replaces the current population with the children to form the next generation" [57] :

$$G_i(x) = 0, i = 1, \dots\dots\dots\dots\dots, k_e; G_i(x) \leq 0, i = k_e + 1, \dots k; l \leq xu \quad (5.14)$$

such that $\min_{x \in R^n} F(x)$

Since F(x) is a vector and if any of its components are competing then, there is no one solution to the problem. The concept of non-inferiority which is also called Pareto optimality must be used. This concept is based on the improvement of one objective while degrading the other. A programming code is presented in appendix C that solves the multiobjective optimization used in this study for system I.

In this research, Matlab function (gamultiobj) is used to find a local Pareto set x for the overall cost and exergy efficiency functions that are written in a Matlab file. The function (gamultiobj) uses an elitist genetic algorithm which favors individuals with better rank and individuals which can help increase the diversity of a population even if they have a lower fitness value. Diversity is maintained by limiting the number of individuals on the Pareto front and by favoring individuals that are relatively far away on the front [55].

The population size is set and a random initial population that satisfies the bounds is created. The tournament selection function with size 2 chooses parents for the next generation based on their scaled values from the fitness functions.

A crossover fraction for the next generation is set and an adaptive feasible mutation function which produces the remaining individuals in the next generation while satisfying the bounds is selected. An intermediate crossover function which combines two parents to form a new child by random weighted average of the parents is controlled by a ratio of 1. Movement of individuals between subpopulations is set to take place toward the last subpopulation with a 0.2 fraction and only 20 generations pass between migrations.

The following two parameters were used as multiobjective algorithm settings in order to perform the optimization:

- Distance measure function which measures the concentration of the population.

- Pareto front population factor keeps the fit population down to 0.85.

The variables in the fitness functions are weighted in importance by the criteria outlined above and most important are set by actual bounds that correspond to meteorological data and actual values. Most of the values in the exergetic fitness function are taken from the corresponding parametric study from 8.00 am to 5:00 pm while the cost fitness function values are taken from actual 2013 market values and the interest rate was selected between 4 and 9 % for duration of 20 years. The exergy destruction bound values are set by the parametric study values.

5.5 Acoustic sound pressure level analysis

A detailed programming code is presented in appendix B that solves for the optimal combination of acoustic and thermal insulation used for the house. Following the work done by [58, 59], the following equations determine the reflection coefficient of the tested material using the impedance tube experiment which is used to validate the results of the enclosure experiment:

$$\frac{Z}{\rho c} = J[\frac{H_{12}\, sin(kl) - sin\,(k(l-s)}{cos(k(l-s) - H_{12}\, cos(kl))} \tag{5.15}$$

$$\frac{Z}{\rho c} = x + ir \tag{5.16}$$

$$x = \rho c \frac{[R_e\,(H_{12})\, sin\,(k\,(2l-s) - \frac{1}{2}\{sin\,(k\,(2l-s)) + |H_{12}|^2 sin\,(2kl)\}]}{H_d} \tag{5.17}$$

$$r = \rho c \frac{[-I_m(H_{12}) sin\,(ks)]}{H_d} \tag{5.18}$$

where ρc is the characteristic impudence of air.

$$H_d = cos^2[k(l-s)] + |H_{12}|^2 cos^2(kl) \tag{5.19}$$

where I_m and R_e represent the real and imaginary parts, and l is the distance from the speaker to the first microphone. H_{12} is the transfer signal between the two microphone signals.

$$R_1(f) = \frac{H_{12}(f) - H_i(f)}{H_r(f) - H_{12}(f)} \tag{5.20}$$

$$R = R_1 e^{j2kl} \tag{5.21}$$

R is the reflection coefficient and α is the absorption coefficient.

$$\alpha = 1\text{-}|R_1|^2 \quad (5.22)$$

where $I_m \; and \; R_e$ represent the real and imaginary parts, and l is the distance from the speaker to the first microphone. H_{12} is the transfer signal between the two microphone signals?

A Matlab soft code is used to evaluate the transfer functions and is presented in Appendix B.

The following equation is used to evaluate the sound pressure level of the enclosure experiment after transforming voltage signals by Fast Fourier Transforms algorithm into pressure values:

$$SPL = 20log_{10}\left(\frac{P_{rms}}{P_0}\right) \quad (5.23)$$

where P_o = 20 x 10^{-6} and P_{rms} is a value obtained from the Fast Fourier Transforms (*FFT*).

5.6 Seasonal load calculations

Hourly analysis program (HAP) [60] developed by Carrier Corporation is used to calculate the loads for the proposed house.

"The software simulates hour-by-hour operation of all heating and air conditioning systems in the house and operation of all plant equipment and non-HVACs systems including lighting and appliances. It uses results of simulations to calculate total annual energy use and energy costs and generates tabular and graphical reports of hourly, daily, monthly and annual data"[60].

Detailed calculations are shown in appendix A.

Chapter 6: Case Study

6.1 Problem statement, assumptions and system inputs

A net zero energy house with one story flat roof structure and a total living area of 225 m^2 located in South Lebanon near the Litani River, is to be maximum powered by renewable energy systems with least greenhouse gases emissions and low noise pollution. Six individuals are living in the house and their potable water need is 30 l/day and hot water consumption is 120 l/day while the rest of the water needs are 300 l/day. Tables (A.11 to A.19) in Appendix A show the house architectural layers and components description.

Lebanon has a moderate climate where peak summer temperatures are at 32.8 ℃ most of the time and winter temperatures are around 5.6°c in average for a couple months and above 12 ℃ the rest of the time [61]. The following strategy is to be followed for reducing the energy requirements and noise pollution and producing hot and potable water:

- Constructing a good building envelope by optimizing the sizes of thermal and acoustic insulation used. The overall heat transfer coefficient for walls must not exceed 0.1W/m^2 K and for ceiling 0.075 W/m^2 K, while for acoustic insulation, the ability to attenuate a sound pressure level from 76 dB outside the house to 30 dB inside the house.
- Choosing the right orientation of the house.
- Using energy-efficient appliances and light fixtures.
- Using efficient water fixtures.
- Using high-efficiency mechanical systems.
- Maximizing the use of passive-solar cooling and heating techniques.
- Using solar thermal systems to heat space and water by thermal storage techniques and heat pumps.
- Maximizing renewable energy powered systems for space cooling.
- Producing potable water by systems powered by solar energy.

- Balancing electrical use, by grid-connected, photovoltaic, wind turbine, *ORC* turbines and hydro turbines.

The following assumptions are made for the energy and exergy analyses:

- All processes are steady-state and steady flow with negligible potential and kinetic energy effects and no chemical reactions.
- Heat transfer to the system and work transfer from the system are positive.
- Air behaves as an ideal gas.
- Heat transfer and refrigerant pressure drops in the tubing connecting the components are negligible since their lengths are short.
- Water leaving the evaporator is saturated vapor.
- Water leaving condenser is saturated liquid.
- Water leaving regenerator is saturated vapor.
- No LiBr solution crystallization occurs at the concentrations used.
- Natural heat losses from the various systems components are negligible.
- Water absorbed at the absorber is completely given off at the regenerator.
- Heat transferred by the blower to the room air stream is negligible.
- Reference states are set.
- Pressure drop inside system components is negligible.
- There are no heat losses from the system components unless noted.
- The vapor at the auxiliary condenser condenses completely.
- The outlet temperatures from the absorber, regenerator, and ORC evaporator correspond to equilibrium conditions of the mixing and separation respectively.
- The thermal physical properties of the working fluid are calculated using EES software.
- Thermodynamic equilibrium is achieved in all states.

The systems inputs are given in Table 6.1:

Table 6.1: Systems inputs.

System I		System II		System III	
T_o	298 K	T_o	298 K	T_o	298 K
P_o	101 kPa	P_o	101 kPa	P_o	101 kPa
T_{ev}	290 K	T_{ev}	290 K	T_{11}	296 K
T_{gen}	353 K	T_{gen}	353 K	T_{28}	299 K
T_{14}	290 K	T_{14}	290 K	T_{29}	T_{28}+15
P_{ev}	1.002 kPa	P_{ev}	1.002 kPa	$T_{htrs,con}$	302 K
P_{abs}	1.002 kPa	P_{abs}	1.002 kPa	T_{19}	Ts + 10
T_{con}	312 K	T_{con}	312 K	$T_{htrs,ev}$	T_{19} -3
P_{con}	7.381 kPa	P_{con}	7.381 kPa	$T_{hp,ev}$	278.72 K
P_{reg}	7.381 kPa	P_{reg}	7.381 kPa	T_s	353 K
T_{abs}	315 K	T_{abs}	315 K	$\dot{q}_s$	0.782kW/m²
P_{abs}	P_{ev}	P_{abs}	P_{ev}	$P_{htrs,con}$	4.08 kPa
P_{ev}	1.002 kPa	P_{ev}	1.002 kPa	$\dot{m}_{19}$	1.25 kg/s
T_{deh}	289 K	T_{deh}	289 K	$T_{hp,con}$	312.7 K
P_{deh}	101 kPa	P_{deh}	101 kPa	$T_{htrs,abs}$	378K
$P_{LDS,reg}$	4.82 kPa	$P_{LDS,reg}$	4.82 kPa	$T_{htrs,reg}$	T_{ev}
$T_{LDS,deh}$	86.63 K	$T_{LDS,deh}$	86.63 K	$P_{hp,ev}$	360 kPa
$P_{LDS,con}$	4.82 kPa	$P_{LDS,con}$	4.82 kPa	$\dot{m}_{17}$	0.4 kg/s
η_{trans}	0.75	$P_{ORC,ev}$	2.6 kPa	$P_{htrs,reg}$	4.08 kPa
η_{capac}	0.55	$T_{ORC,ev}$	354.6 K	$P_{htrs,abs}$	47.4 kPa
R	0.287 kJ/kg.K	$P_{ORC,con}$	0.49 kPa	$P_{htrs,ev}$	47.4 kPa
Cf	0.56	$T_{ORC,con}$	297 K	T_{sepv}	373K
ϖ_{turb}	3.79 v_e	$\dot{m}_{50}$	0.65 kg/s	P_{50}	1000kPa
P_a	101kPa	$\dot{m}_{61}$	1.4kg/s	T_{50}	343 K
CO_{pwr}	0.4	$T_{ORC,rect}$	338.6 K	$R_{pipe,emb}$	0.05 m
U_{ert}	0.0014kJ/sm^{2}K	ζ_{60}	0.96	γ	0.072 m^2/d

6.2 Thermodynamic modeling

The systems thermodynamic properties are evaluated by using EES software and all the corresponding thermodynamic equations are written in EES format. Several results are calculated by varying different parameters.

6.2.1 System I

Thermodynamic analysis of system I (Figure 4.1) composed of the following subsystems: absorption chiller, liquid desiccant system, solar system, hot water tank system, ground storage thermal bank and power system consisting of PV, wind turbine and diesel generator is carried out in the section below. Every subsystem will undergo a complete mass, energy, entropy, exergy and efficiency analysis for all its components.

6.2.1.1 Absorption chiller analysis

The thermodynamic analysis of the absorption chiller system is carried out where all balances and efficiencies equations are written below:

- Condenser analysis

The mass balance equations for the condenser are given as follows:

$$\dot{m}_7 = \dot{m}_8 = \dot{m}_w \tag{6.1}$$

$$\dot{m}_{11} = \dot{m}_{12} = \dot{m}_a \tag{6.2}$$

where *a* is subscript for air and *w* is for water.

The energy balance equations for the condenser are given as follows:

$$\dot{m}_7\, h_7 = \dot{m}_8 h_8 + \dot{Q}_{con} \tag{6.3}$$

$$\dot{m}_{11}\, h_{11} + \dot{Q}_{con} = \dot{m}_{12} h_{12} \tag{6.4}$$

The entropy balance equations for the condenser are given as follows:

$$\dot{m}_7\, s_7 + \dot{S}_{gene} = \dot{m}_8 s_8 + \frac{\dot{Q}_{con}}{T_{con}} \tag{6.5}$$

$$\dot{m}_{11} s_{11} + \dot{S}_{gene} + \frac{\dot{Q}_{con}}{T_{con}} = \dot{m}_{12} s_{12} \tag{6.6}$$

where $\dot{S}_{gene}$ is the entropy generated due to irreversible heat transfer.

The exergy balance equations for the condenser are given as follows:

$$\dot{m}_7 e_{x7} = \dot{m}_8 e_{x8} + \dot{Q}_{con}\left(1 - \frac{T_0}{T_{con}}\right) + \dot{E}_{x,w,con,des} \quad (6.7)$$

where $\dot{E}_{x.a.con,des}$ is given by:

$$\dot{E}_{x,w.con,des} = T_0 \dot{S}_{gene} \quad (6.8)$$

$$\dot{m}_{11} e_{x11} + \dot{Q}_{con}\left(1 - \frac{T_0}{T_{con}}\right) = \dot{m}_{12} e_{x12} + \dot{E}_{x.a.con,des} \quad (6.9)$$

where T_0 is the dead state temperature and $\dot{E}_{x.a.con,des}$ is given by:

$$\dot{E}_{x.a.con,des} = T_0 \dot{S}_{gene} \quad (6.10)$$

The exergetic efficiency equation is written as follows:

$$\psi_{con} = \frac{\dot{Q}_{con}\left(1 - {}^{T_0}/_{T_{con}}\right)}{\dot{m}_7(ex_7 - ex_8)} = \frac{\dot{m}_7(ex_7 - e_{x_8}) - \dot{E}_{x,w,con,des}}{\dot{m}_7(ex_7 - ex_8)} = 1 - \frac{\dot{E}_{x,w,con,des}}{\dot{m}_7(ex_7 - ex_8)} \quad (6.11)$$

- Expansion valve (solution) analysis

The mass balance equation for the expansion valve is given as follows:

$$\dot{m}_5 = \dot{m}_6 = \dot{m}_{sol} \quad (6.12)$$

The energy balance equation for the expansion valve is given as follows:

$$h_5 = h_6 \quad (6.13)$$

The entropy balance equation for the expansion valve is given as follows:

$$\dot{m}_6 s_6 + \dot{S}_{gene,sol} = \dot{m}_5 s_5 \quad (6.14)$$

The exergy balance equation for the expansion valve is given as follows:

$$\dot{m}_5 e_{x5} = \dot{m}_6 e_{x6} + \dot{E}_{x,sol,des} \quad (6.15)$$

where $\dot{E}_{x,sol,des}$ is given by:

$$\dot{E}_{x,sol,des} = T_0 \dot{S}_{sol,gene} \quad (6.16)$$

the exergy efficiency equation yields:

$$\psi_{exv_w} = 1 - \frac{\dot{E}_{x,sol,des}}{\dot{m}_5 e_{x5} - \dot{m}_6 e_{x6}} = 1 - \frac{\dot{m}_5 e_{x5} - \dot{m}_6 e_{x6}}{\dot{m}_5 e_{x5} - \dot{m}_6 e_{x6}} = 0 \quad (6.17)$$

- Expansion valve (water) analysis

The mass balance equation for the expansion valve is given as follows:

$$\dot{m}_8 = \dot{m}_9 = \dot{m}_w \tag{6.18}$$

The energy balance equation for the expansion valve is given as follows:

$$h_9 = h_8 \tag{6.19}$$

The entropy balance equation for the expansion valve is given as follows:

$$\dot{m}_8 s_8 + \dot{S}_{exv,w,gene} = \dot{m}_9 s_9 \tag{6.20}$$

The exergy balance equation for the expansion valve is given as follows:

$$\dot{m}_8 e_{x8} = \dot{m}_9 e_{x9} + \dot{E}_{x,exv,w,des} \tag{6.21}$$

where $\dot{E}_{x,exv,w,des}$ is given by:

$$\dot{E}_{x,exv,w,des} = T_0 \dot{S}_{exv,w,gene} \tag{6.22}$$

- Evaporator analysis

The mass balance equations for the evaporator are given as follows:

$$\dot{m}_9 = \dot{m}_{10} = \dot{m}_W \tag{6.23}$$

$$\dot{m}_{13} = \dot{m}_{14} = \dot{m}_a \tag{6.24}$$

The energy balance equations for the condenser are given as follows:

$$\dot{m}_9 h_9 + \dot{Q}_{eva} = \dot{m}_{10} h_{10} \tag{6.25}$$

$$\dot{m}_{13} h_{13} = \dot{m}_{14} h_{14} + \dot{Q}_{eva} \tag{6.26}$$

where h_9 is given by:

$$h_9 = h_8 \tag{6.27}$$

The entropy balance equations for the evaporator are given as follows:

$$\dot{m}_9 s_9 + \dot{S}_{eva,w,gene} + \frac{\dot{Q}_{eva}}{T_{eva}} = \dot{m}_{10} s_{10} \tag{6.27}$$

$$\dot{m}_{13} s_{13} + \dot{S}_{eva,a,gene} = \dot{m}_{14} s_{14} + \frac{\dot{Q}_{eva}}{T_{eva}} \tag{6.28}$$

The exergy balance equations for the evaporator are given as follows:

$$\dot{m}_9 e_{x9} + \dot{Q}_{eva}\left(1 - \frac{T_0}{T_{eva}}\right) = \dot{m}_{10} e_{x10} + \dot{E}_{x,eva,w,des} \quad (6.29)$$

$$\dot{m}_{13} e_{x13} = \dot{m}_{14} e_{x14} + \dot{Q}_{eva}\left(1 - \frac{T_0}{T_{eva}}\right) + \dot{E}_{x,eva,a,des} \quad (6.30)$$

where $\dot{E}_{x,eva,w,des}$ and $\dot{E}_{x,eva,w,des}$ are given by:

$$\dot{E}_{x,eva,w,des} = T_0 \dot{S}_{eva,w,gene} \quad (6.31)$$

$$\dot{E}_{x,eva,a,des} = T_0 \dot{S}_{eva,a,gene} \quad (6.32)$$

The exergetic efficiency is expressed as:

$$\psi_{eva} = \frac{\dot{Q}_{eva}\left({}^{T_0}/_{T_{eva}} - 1\right)}{\dot{m}_9(e_{x10} - e_{x9})} = \frac{\dot{m}_9(e_{x10} - e_{x_9}) - \dot{E}_{x\_eva\_des\_w}}{\dot{m}_9(e_{x10} - e_{x9})} = 1 - \frac{T_0 \dot{S}_{eva,w,gene}}{\dot{m}_9(e_{x10} - e_{x9})} \quad (6.33)$$

OR

Here our useful output is cooling the air which is re-circulated and the driving exergy gradient that causes the useful output which is also re-circulated is given by:

$$\psi_{eva} = \frac{-\dot{Q}_{eva}\left(1 - \frac{T_0}{T_{eva}}\right)}{\dot{m}_{13} e_{x13} - \dot{m}_{14} e_{x_{14}}} \quad (6.34)$$

- Heat exchanger analysis

The mass balance equations for the heat exchanger are given as follows:

$$\dot{m}_2 = \dot{m}_3 = \dot{m}_{wea,sol} \quad (6.35)$$

$$\dot{m}_4 = \dot{m}_5 = \dot{m}_{str,sol} \quad (6.36)$$

The energy balance equation for the heat exchanger is given as follows:

$$\dot{m}_2 h_2 + \dot{m}_4 h_4 = \dot{m}_3 h_3 + \dot{m}_5 h_5 \quad (6.37)$$

The effectiveness of the heat exchanger is given by:

$$\xi_{Hx} = \frac{\dot{m}_2 C_{p,2}(T_3 - T_2)}{(\dot{m}C_p)_{min}(T_4 - T_{2)})} = \frac{\dot{m}_4 C_{p,4}(T_4 - T_5)}{(\dot{m}C_p)_{min}(T_4 - T_{2)})} \quad (6.38)$$

but if $(\dot{m}C_p)_{min} = \dot{m}_4 C_{p,4}$ then:

$$\xi_{Hx} = \frac{(T_4 - T_5)}{(T_4 - T_{2)})} \quad (6.39)$$

Otherwise:

$$\xi_{Hx} = \frac{(T_3 - T_2)}{(T_4 - T_{2)})} \tag{6.40}$$

The entropy balance equation for the heat exchanger is given as follows:

$$\dot{m}_2 s_2 + \dot{S}_{hex,gene} + \dot{m}_4 s_4 = \dot{m}_3 s_3 + \dot{m}_5 s_5 \tag{6.41}$$

The exergy balance equation for the condenser is given as follows:

$$\dot{m}_2 e_{x2} + \dot{m}_4 e_{x4} = \dot{m}_3 e_{x3} + \dot{m}_5 e_{x5} + \dot{E}_{hex,des} \tag{6.42}$$

where $\dot{E}_{hex,des}$ is given by:

$$\dot{E}_{hex,des} = T_0 S_{\mathrm{hex},gene} \tag{6.43}$$

The exergetic efficiency of the heat exchanger is represented by:

$$\psi_{Hex} = \frac{\dot{m}_2 (e_{x_3} - e_{x_2})}{\dot{m}_4 (e_{x4} - e_{x5})} \tag{6.44}$$

- Pump analysis

The mass balance equation for the pump is given as follows:

$$\dot{m}_1 = \dot{m}_2 = \dot{m}_{wea,sol} \tag{6.45}$$

where (wea, sol) represents weak solution.

The energy balance equation for the pump is given as follows:

$$\dot{m}_1 h_1 + W_{pmp\_act} = \dot{m}_2 h_2 \tag{6.46}$$

The entropy balance equation for the pump is given as follows:

$$\dot{m}_1 s_1 + \dot{S}_{pmp,gene} = \dot{m}_2 s_2 \tag{6.47}$$

The exergy balance equation for the pump is given as follows:

$$\dot{m}_1 e_{x1} + \dot{W}_{pmp,act} = \dot{m}_2 e_{x2} + \dot{E}_{x,pmp,des} \tag{6.48}$$

where $\dot{E}_{x,pmp,des}$ is given by:

$$\dot{E}_{x,Pmp,des} = T_0 \dot{S}_{pmp,gene} \tag{6.49}$$

The pump efficiencies are evaluated as follows:

$$\psi_{pmp} = 1 - \frac{\dot{E}_{X,pmp,des}}{\dot{W}_{pmp,act}} \tag{6.50}$$

$$\eta_{pmp} = \frac{\dot{W}_{isen}}{\dot{W}_{act}} = \frac{\dot{m}_1 v}{\dot{m}_1 (h_2 - h_1)} (p_2 - p_1) \tag{6.51}$$

- Absorber analysis

The mass balance equations for the condenser are given as follows:

$$\dot{m}_{10} + \dot{m}_6 = \dot{m}_1 \tag{6.52}$$

$$x_1 \dot{m}_1 = x_6 \dot{m}_6 \tag{6.53}$$

The energy balance equation for the absorber is given as follows:

$$\dot{m}_{10} h_{10} + \dot{m}_6 h_6 = \dot{m}_1 h_1 + \dot{Q}_{abs} \tag{6.54}$$

The entropy balance equation for the absorber is given as follows:

$$\dot{S}_{abs,gene} + \dot{m}_{10} s_{10} + \dot{m}_6 s_6 = \dot{m}_1 s_1 + \frac{\dot{Q}_{abs}}{T_{abs}} \tag{6.55}$$

The exergy balance equation for the condenser is given as follows:

$$\dot{m}_{10} e_{x10} + \dot{m}_6 e_{x6} = \dot{m}_1 e_{x1} + \dot{E}_{x,abs,des} + \dot{Q}_{abs} \left(1 - \frac{T_o}{T_{abs}}\right) \tag{6.56}$$

where $\dot{E}_{x,abs,des}$ is given by:

$$\dot{E}_{x,abs,des} = T_o \dot{S}_{abs,gene} \tag{6.57}$$

The chemical exergy at the absorber $\dot{E}_{x,CH,abs}$ is given by [62] as:

$$\dot{E}_{x,CH,abs} = \frac{1}{\frac{x_{LiBr}}{(1-x_{LiBr}) m_{sol,gen}}} \left[\sum_{i=1}^{n} x_i \overline{E\_x\_o} + \overline{R} T_o \sum_{i=1}^{n} x_i \ln a_i\right] = \dot{Q}_{abs,ch} \left(1 - \frac{T_o}{T_{abs}}\right) \tag{6.58}$$

Here, the strong solution is the useful output and the driving exergy gradient is as shown in the equations of the efficiencies:

$$\psi_{abs} = 1 - \frac{\dot{E}_{x,abs,des}}{\dot{m}_{10} e_{x10} + \dot{m}_6 e_{x6} - \dot{m}_1 e_{x1}} \tag{6.59}$$

$$\eta_{abs} = \frac{\dot{Q}_{abs}}{\dot{m}_{10}\, h_{10} + \dot{m}_6\, h_6 - \dot{m}_1\, h_1} \tag{6.60}$$

- Regenerator analysis

The mass balance equations for the regenerator are given as follows:

$$\dot{m}_3 = \dot{m}_7 + \dot{m}_4 \tag{6.61}$$

$$x_3 \dot{m}_3 = x_4 \dot{m}_4 \tag{6.62}$$

The energy balance equation for the regenerator is given as follows:

$$\dot{m}_3 \mathrm{h}_3 + \dot{Q}_{gen} = \dot{m}_4 \mathrm{h}_4 + \dot{m}_7 \mathrm{h}_7 \tag{6.63}$$

The entropy balance equation for the regenerator is given as follows:

$$\dot{S}_{gen,gene} + \dot{m}_3 \mathrm{s}_3 + \frac{\dot{Q}_{gen}}{\mathrm{T_{gen}}} = \dot{m}_7 \mathrm{s}_7 + \dot{m}_4 \mathrm{s}_4 \tag{6.64}$$

The exergy balance equation for the regenerator is given as follows:

$$\dot{m}_3 e_{x3} + \dot{Q}_{gen}\left(1 - \frac{T_o}{T_{gen}}\right) = \dot{m}_7 e_{x7} + \dot{m}_4 e_{x4} + \dot{E}_{x,gen,des} \tag{6.65}$$

where $\dot{E}_{x,gen,des}$ is given by:

$$\dot{E}_{x,gen,des} = T_o \dot{S}_{gen,gene} \tag{6.66}$$

The chemical exergy at the regenerator is given by:

$$\dot{E}_{x,CH,gen} = \frac{1}{\frac{x_{LiBr}}{(1-x_{LiBr})m_{sol,gen}}} \left[\sum_{i=1}^{n} x_i \overline{E\_x\_o} + \overline{R} T_o \sum_{i=1}^{n} x_i \ln a_i\right] = \dot{Q}_{gen,ch}\left(1 - \frac{T_o}{T_{gen}}\right) \tag{6.67}$$

The regenerator efficiencies are given by:

$$\psi_{gen} = \frac{\dot{Q}_{gen}\left(1 - \frac{T_o}{T_{gen}}\right)}{\dot{m}_3 e_{x3} - (\dot{m}_7 e_{x7} + \dot{m}_4 e_{x4})} \tag{6.68}$$

$$\eta_{gen} = \frac{\dot{Q}_{gen}}{\dot{m}_4\, h_4 - (\dot{m}_7\, h_7 + \dot{m}_3\, h_3)} \tag{6.69}$$

- Absorption system overall COP

The overall absorption system energetic and exergetic coefficient of performance is described by:

$$COP_{\eta} = \frac{\dot{Q}_{eva}}{\dot{W}_{pmp} + \dot{Q}_{gen}} \quad (6.70)$$

$$COP_{\psi} = \frac{\dot{Q}_{eva}\left(1-\frac{T_o}{T_{eva}}\right)}{\dot{W}_{pmp}+Q_{gen}\left(1-\frac{T_o}{T_{gen}}\right)} \quad (6.71)$$

6.2.1.2 Solar system analysis

Thermodynamic analysis of the solar system is carried out where all balances and efficiencies equations are written below:

- Solar panels analysis

The thermodynamic analysis of the solar panel system is carried out through mass, energy, entropy and exergy balances:

The mass balance equation for the solar panels is given as follows:

$$\dot{m}_{19} = \dot{m}_{20} = \dot{m}_s \quad (6.72)$$

The energy balance equation for the solar panels is given as follows:

$$\dot{m}_{19}h_{19} + \dot{Q}_{s,net} = \dot{m}_{20}h_{20} \quad (6.73)$$

where $\dot{Q}_{S,net}\ is\ given\ by$:

$$\dot{Q}_{s,net} = A_s\dot{q}_s \quad (6.74)$$

The entropy balance equation for the solar panels is given as follows:

$$\dot{m}_{19}s_{19} + \dot{S}_{s,gene} + \frac{\dot{Q}_s}{T_{sun}} = \dot{m}_{20}s_{20} \quad (6.75)$$

The exergy balance equation for the solar panels is given as follows:

$$\dot{m}_{19}e_{x19} + \dot{Q}_s\left(1-\frac{T_0}{T_{sun}}\right) = \dot{m}_{20}e_{x20} + \dot{E}_{x,s,des} \quad (6.76)$$

where $\dot{E}_{x,S,des}$ is given by:

$$\dot{E}_{x,S,des} = T_o\dot{S}_{s,gene} \quad (6.77)$$

The efficiencies are given by the following equations:

$$\psi_s = \frac{\dot{m}_{20}(e_{x20} - e_{x19})}{\dot{Q}_s\left(1 - \frac{T_o}{T_{sun}}\right)} \quad (6.78)$$

$$\eta_s = \frac{\dot{m}_{19}((h_{20} - h_{19})}{\dot{Q}_s} \quad (6.79)$$

- Solar pump analysis

The mass balance equation for the solar pump is given as follows:

$$\dot{m}_{19} = \dot{m}_{16} = \dot{m}_s \quad (6.80)$$

The energy balance equation for the solar pump is given as follows:

$$\dot{m}_{16}h_{16} + \dot{W}_{Pmp,act} = \dot{m}_{19}h_{19} \quad (6.81)$$

The entropy balance equation for the solar pump is given as follows:

$$\dot{m}_{16}s_{16} + \dot{S}_{pmp,s,gene} = \dot{m}_{19}s_{19} \quad (6.82)$$

where $s_{19} = s_{16}$

The exergy balance equation for the solar pump is given as follows:

$$\dot{m}_{16}e_{x16} + \dot{W}_{Pmp,act} = \dot{m}_{19}e_{x19} + \dot{E}_{x,pmp,s,des} \quad (6.83)$$

where $\dot{E}_{x,pmp,s,des}$ is given by:

$$\dot{E}_{x,pmp,s,des} = T_o\dot{E}_{x,pmp,s,des} \quad (6.84)$$

The pump efficiencies are presented in the section below:

$$\psi_{pmp,s} = 1 - \frac{E_{x,pmp,des}}{W_{pmp,act}} \quad (6.85)$$

$$\eta_{pmp,s} = \frac{\dot{W}_{isen}}{\dot{W}_{act}} = \frac{\dot{m}_{14}v}{\dot{m}_{15}(h_{16} - h_{15})}(p_{16} - p_{15}) \quad (6.86)$$

6.2.1.3 Liquid desiccant system analysis

The thermodynamic analysis of the liquid desiccant system is carried out below through mass, energy, entropy and exergy balances for all system components.

- Dehumidifier analysis

The mass balance equations for the dehumidifier are given as follows:

$$\dot{m}_{32} + \dot{m}_{cond} = \dot{m}_{33} \tag{6.87}$$

$$x_{32}\,\dot{m}_{32} = x_{33}\,\dot{m}_{33} \tag{6.88}$$

$$\dot{m}_{40} = \dot{m}_{41} - \dot{m}_{cond} \tag{6.89}$$

where $\dot{m}_{cond}$ is water condensed from ambient air and *x* stands for mass concentration of LiBr solution.

The energy balance equation for the dehumidifier is given as follows:

$$\dot{m}_{32}h_{32} + \dot{m}_{40}h_{40} = \dot{m}_{33}h_{33} + \dot{m}_{41}h_{41} \tag{6.90}$$

The entropy balance equation for the dehumidifier is given as follows:

$$\dot{S}_{deh,gene} + \dot{m}_{32}s_{32} + \dot{m}_{cond}s_{cond} = \dot{m}_{32}s_{32} + \frac{\dot{Q}_{deh}}{T_{deh}} \tag{6.91}$$

The exergy balance equation for the dehumidifier is given as follows:

$$\dot{m}_{32}e_{x10} + \dot{m}_{cond}e_{x,cond} = \dot{m}_{33}e_{33} + \dot{E}_{x,deh,des} - \dot{Q}_{deh}\left(1 - \frac{T_o}{T_{deh}}\right) \tag{6.92}$$

where $\dot{E}_{x,deh,des}$ is given by:

$$\dot{E}_{x,deh,des} = T_o\dot{S}_{deh,gene} \tag{6.93}$$

The chemical exergy at the dehumidifier is given by:

$$\dot{E}_{x,CH,deh} = \frac{1}{\frac{x_{LiBr}}{(1-x_{LiBr})m_{sol,gen}}}\left[\sum_{i=1}^{n} x_i\overline{E\_x\_o} + \overline{R}T_o\sum_{i=1}^{n} x_i \ln a_i\right] = \dot{Q}_{deh,ch}\left(1 - \frac{T_o}{T_{deh}}\right) \tag{6.94}$$

The efficiencies of the dehumidifier are given by:

$$\psi_{deh} = \frac{-\dot{Q}_{deh}\left(1-\frac{T_o}{T_{deh}}\right)}{\dot{m}_{32}\,(\,e_{x33} - e_{x32}\,) + \dot{m}_{cond}\,e_{x,cond}} \tag{6.95}$$

$$\eta_{deh} = \frac{-\dot{Q}_{deh}}{\dot{m}_{32}(h_{33} - h_{32}) + \dot{m}_{cond}h_{cond}} \tag{6.96}$$

- Dehumidifier blower analysis

The mass balance equation for the dehumidifier blower is given as follows:

$$\dot{m}_{40} = \dot{m}_{41} = \dot{m}_a \tag{6.97}$$

The energy balance equation for the dehumidifier blower is given as follows:

$$\dot{m}_{40}h_{40} + \dot{W}_{blow} = \dot{m}_{41}h_{41} \quad (6.98)$$

where $\dot{W}_{blow}$ is the work done by the blower motor.

The entropy balance equation for the dehumidifier blower is given as follows:

$$\dot{m}_{40}s_{40} + \dot{S}_{blow,gene} = \dot{m}_{41}s_{41} \quad (6.99)$$

The exergy balance equation for the dehumidifier blower is given as follows:

$$\dot{m}_{40}e_{x40} + \dot{W}_{blow} + \dot{m}_{41}e_{x41} + \dot{E}_{x,blow,des} \quad (6.100)$$

where $\dot{E}_{x,blow,des}$ is given by:

$$\dot{E}_{x,blow,des} = T_o\dot{S}_{blow,gene} \quad (6.101)$$

The blower efficiency is given by:

$$\psi_{blow} = 1 - \frac{\dot{E}_{x,blow,des}}{\dot{W}_{blow}} \quad (6.102)$$

- Regenerator analysis

The mass balance equations for the regenerator are given as follows:

$$\dot{m}_{51} + \dot{m}_{29} = \dot{m}_{35} \quad (6.103)$$

$$x_{51}\dot{m}_{51} = x_{29}\dot{m}_{29} \quad (6.104)$$

$$\dot{m}_{24} = \dot{m}_{27} \quad (6.105)$$

The energy balance equation for the regenerator is given as follows:

$$\dot{m}_{68}h_{68} + \dot{m}_{24}h_{24} = \dot{m}_{29}h_{29} + \dot{m}_{27}h_{27} + \dot{m}_{35}h_{35} \quad (6.107)$$

The entropy balance equation for the regenerator is given as follows:

$$\dot{S}_{reg,gene} + \dot{m}_{68}s_{68} = \dot{m}_{29}s_{29} + \dot{m}_{35}s_{35} - \frac{\dot{Q}_{reg}}{T_{reg}} \quad (6.108)$$

The exergy balance equation for the regenerator is given as follows:

$$\dot{m}_{68}e_{x68} = \dot{m}_{29}e_{x29} + \dot{m}_{35}e_{x35} + \dot{E}_{x,reg,des} - \dot{Q}_{reg}\left(1 - \frac{T_o}{T_{reg}}\right) \quad (6.109)$$

where $\dot{E}_{x,reg,des}$ is given by:

$$\dot{E}_{x,reg,des} = T_o\, \dot{S}_{reg,gene} \tag{6.110}$$

The chemical exergy released at the regenerator is given by:

$$\dot{E}_{x,CH,reg} = \frac{1}{\frac{x_{LiBr}}{(1-x_{LiBr})m_{sol,gen}}} \left[\sum_{i=1}^{n} x_i \overline{E\_x\_o} + \overline{R} T_o \sum_{i=1}^{n} x_i \ln a_i\right] = \dot{Q}_{reg,ch}\left(1 - \frac{T_o}{T_{reg}}\right) \tag{6.111}$$

The efficiencies are given by:

$$\psi_{reg} = \frac{\dot{Q}_{reg}\left(1-\frac{T_o}{T_{deh}}\right)}{\dot{m}_{68}\, e_{x68} - (\dot{m}_{29}\, e_{x29} + \dot{m}_{35} e_{x35})} \tag{6.112}$$

$$\eta_{reg} = \frac{\dot{Q}_{reg}}{\dot{m}_{68} h_{68} - (\dot{m}_{35}\, h_{35} + \dot{m}_{29}\, h_{29})} \tag{6.113}$$

- Heat exchanger analysis

The mass balance equations for the heat exchanger are given as follows:

$$\dot{m}_{33} = \dot{m}_{34} \tag{6.114}$$

$$\dot{m}_{30} = \dot{m}_{31} \tag{6.115}$$

The energy balance equation for the heat exchanger is given as follows:

$$\dot{m}_{33} h_{33} + \dot{m}_{30} h_{30} = \dot{m}_{34} h_{34} + \dot{m}_{31} h_{31} \tag{6.116}$$

The entropy balance equation for the heat exchanger is given as follows:

$$\dot{S}_{LDS,hex,gene} + \dot{m}_{33} s_{33} + \dot{m}_{30} s_{30} = \dot{m}_{34} s_{34} + \dot{m}_{31} s_{31} \tag{6.117}$$

The exergy balance equations for the heat exchanger is given as follows:

$$\dot{m}_{34} e_{x34} + \dot{m}_{31} e_{x31} = \dot{m}_{33} e_{x33} + \dot{m}_{30} e_{x30} + \dot{E}_{x,LDS,hex,des} \tag{6.118}$$

where $\dot{E}_{x,LDS,hex,des}$ is given by:

$$\dot{E}_{x,LDS,hex,des} = T_o \dot{S}_{LDS,hex,gene} \tag{6.119}$$

The heat exchanger efficiency is derived as follows:

$$\psi_{hex} = \frac{\dot{m}_{34}\,(e_{x34} - e_{x33})}{\dot{m}_{30}\,(e_{x30} - e_{x31})} \tag{6.120}$$

- Cooling heat exchanger analysis

The mass balance equations for the cooling heat exchanger are given as follows:

$$\dot{m}_{13} = \dot{m}_{14} \tag{6.121}$$

$$\dot{m}_{32} = \dot{m}_{31} \tag{6.122}$$

The energy balance equation for the cooling heat exchanger is given as follows:

$$\dot{m}_{13}h_{13} + \dot{m}_{31}h_{31} = \dot{m}_{14}h_{14} + \dot{m}_{32}h_{32} \tag{6.123}$$

The entropy balance equation for the cooling heat exchanger is given as follows:

$$\dot{S}_{LDS,cooling,hex,gene} + \dot{m}_{13}s_{13} + \dot{m}_{13}s_{31} = \dot{m}_{14}s_{14} + \dot{m}_{32}s_{32} \tag{6.124}$$

The exergy balance equation for the cooling heat exchanger is given as follows:

$$\dot{m}_{13}e_{x13} + \dot{m}_{31}e_{x31} = \dot{m}_{32}e_{x32} + \dot{m}_{14}e_{x14} + \dot{E}_{x,LDS,cooling,hex,des} \tag{6.125}$$

where $\dot{E}_{x,LDS,cooling,hex,des}$ is given by:

$$\dot{E}_{x,LDS,cooling,hex,des} = T_o\dot{S}_{LDS,cooling,hex,gene} \tag{6.126}$$

The cooling heat exchanger exergetic efficiency is defined as follows:

$$\psi_{hex} = \frac{\dot{m}_{13}\,(e_{x14} - e_{x13})}{\dot{m}_{31}\,(e_{x31} - e_{x32})} \tag{6.127}$$

- Condenser analysis

The mass balance equations for the condenser are given as follows:

$$\dot{m}_{35} = \dot{m}_{36} \tag{6.128}$$

$$\dot{m}_{48} = \dot{m}_{49} \tag{6.129}$$

The energy balance equation for the condenser is given as follows:

$$\dot{m}_{35}h_{35} + \dot{m}_{48}h_{48} = \dot{m}_{36}h_{36} + \dot{m}_{49}h_{49} \tag{6.130}$$

The entropy balance equation for the condenser is given as follows:

$$\dot{S}_{LDS,con,gene} + \dot{m}_{35}s_{35} + \dot{m}_{48}s_{48} = \dot{m}_{36}s_{36} + \dot{m}_{49}s_{49} \tag{6.131}$$

The exergy balance equations for the condenser are given as follows:

$$\dot{m}_{35}\mathrm{e}_{x35} + \dot{m}_{48}\mathrm{e}_{x48} = \dot{m}_{36}\mathrm{e}_{x36} + \dot{m}_{49}e_{x49} + \dot{E}_{x,LDS,con,des} \quad (6.132)$$

where $\dot{E}_{x,LDS,con,des}$ is given by:

$$\dot{E}_{x,LDS,con,des} = T_o\dot{\mathrm{S}}_{LDS,con,gene} \quad (6.133)$$

The liquid desiccant condenser exergetic efficiency is defined as:

$$\psi_{LDS,con} = \frac{\dot{Q}_{con}(1-\frac{T_O}{T_{con}})}{\dot{m}_{48}\,(e_{x48} - e_{x49})} \quad (6.134)$$

- Desiccant pump analysis

The mass balance equation for the desiccant pump is given as follows:

$$\dot{m}_{29} = \dot{m}_{30} \quad (6.135)$$

The energy balance equation for the desiccant pump is given as follows:

$$\dot{m}_{29}h_{29} + \dot{W}_{pmp,act} = \dot{m}_{30}h_{30} \quad (6.136)$$

The entropy balance equation for the desiccant pump is given as follows:

$$\dot{m}_{29}s_{29} + \dot{S}_{Pmp,gene} = \dot{m}_{30}s_{30} \quad (6.137)$$

The exergy balance equation for the desiccant pump is given as follows:

$$\dot{m}_{29}e_{x29} + W_{Pmp,act} = \dot{m}_{30}e_{x30} + \dot{E}_{x,Pmp,des} \quad (6.138)$$

where $\dot{E}_{x,Pmp,des}$ is given by:

$$\dot{E}_{x,Pmp,des} = T_0\dot{S}_{Pmp,gene} \quad (6.139)$$

The desiccant pump efficiencies are defined as:

$$\psi_{Pump} = 1 - \frac{\dot{E}_{x,pmp,des}}{\dot{W}_{pmp,act}} \quad (6.140)$$

$$\eta_{pmp} = \frac{\dot{W}_{isen}}{\dot{W}_{act}} = \frac{\dot{m}_{29}v}{\dot{m}_{30}(h_{29}-h_{30})}(p_{30} - p_{29}) \quad (6.141)$$

- Expansion valve (solution) analysis

The mass balance equation for the expansion valve is given as follows:

$$\dot{m}_{34} = \dot{m}_{51} \tag{6.142}$$

The energy balance equation for the expansion valve is given as follows:

$$\dot{m}_{34} h_{34} = \dot{m}_{51} h_{51} \tag{6.143}$$

The entropy balance equation for the expansion valve is given as follows:

$$\dot{S}_{LDS,gene} = \dot{m}_{51} s_{51} - \dot{m}_{34} s_{34} \tag{6.144}$$

The exergy balance equation for the expansion valve is given as follows:

$$\dot{m}_{51} e_{x51} = \dot{m}_{34} e_{x34} + \dot{E}_{X,des} \tag{6.145}$$

where $\dot{E}_{x,LDS,des}$ is given by:

$$\dot{E}_{x,LDS,des} = T_0 \dot{S}_{LDS,gene} \tag{6.146}$$

The exergetic efficiency of the expansion valve is defines as follows:

$$\psi_{LDS,exv} = 1 - \frac{\dot{m}_{51} e_{x51} - \dot{m}_{34} e_{x34}}{\dot{m}_{51} e_{x51} - \dot{m}_{34} e_{x34}} = 0 \tag{6.147}$$

- Liquid desiccant system overall efficiencies

The overall energetic efficiency for the liquid desiccant system is defined as the desired product output divided by the useful fuel input as follows:

$$COP_{LDS,ov} = \frac{\dot{Q}_{LDS,deh} + \dot{m}_{36}(h_{35} - h_{36})}{\dot{Q}_{LDS,reg} + \dot{W}_{LDS,pmp} + \dot{Q}_{LDS,con}} \tag{6.148}$$

$$COP\psi_{LDS,ov} = \frac{\dot{Q}_{LDS,deh}(1 - \frac{T_0}{T_{deh}}) + \dot{m}_{36}(h_{35} - h_{36} - T_0(s_{35} - s_{36})}{\dot{Q}_{LDS,reg}(1 - \frac{T_0}{T_{reg}}) + \dot{W}_{LDS,pmp} + \dot{Q}_{LDS,con}(1 - \frac{T_0}{T_{con}})} \tag{6.149}$$

6.2.1.4 Hot water tank analysis

The thermodynamic analysis of the hot water tank system is carried out below through mass, energy, entropy and exergy balances for all system components.

The mass balance equations for the hot water tank are given as follows:

$$\dot{m}_{21} = \dot{m}_{18} \tag{6.150}$$

$$\dot{m}_{44} = \dot{m}_{26} \quad (6.151)$$

The energy balance equation for the hot water tank is given as follows:

$$\dot{m}_{21}\, h_{21} + \dot{m}_{44}\, h_{44} = \dot{m}_{26}\, h_{26} + \dot{m}_{18}\, h_{18} \quad (6.152)$$

The entropy balance equation for the hot water tank is given as follows:

$$\dot{S}_{hwt,gene} + \dot{m}_{21} s_{21} + \dot{m}_{44} s_{44} = \dot{m}_{26} s_{26} + \dot{m}_{18} s_{18} \quad (6.153)$$

The exergy balance equation for the hot water tank is given as follows:

$$\dot{m}_{21} \mathrm{e}_{x21} + \dot{m}_{44} \mathrm{e}_{x44} = \dot{m}_{26} \mathrm{e}_{x26} + \dot{m}_{1} e_{x18} + \dot{E}_{x,hwt,des} \quad (6.154)$$

where $\dot{E}_{x,hwt,des}$ is given by:

$$\dot{E}_{x,hwt,des} = T_o\, \dot{S}_{hwt,gene} \quad (6.155)$$

The efficiencies of the hot water tank are defined by:

$$\psi_{hwt} = \frac{\dot{m}_{26}(\mathrm{e}_{x26} - \mathrm{e}_{x44})}{\dot{m}_{21}(\mathrm{e}_{x21} - \mathrm{e}_{x18})} \quad (6.156)$$

$$\eta_{hwt} = \frac{\dot{m}_{26}(\mathrm{h}_{26} - \mathrm{h}_{44})}{\dot{m}_{21}(\mathrm{h}_{21} - \mathrm{h}_{18})} \quad (6.157)$$

6.2.1.5 Ground storage thermal bank analysis

The thermodynamic analysis of the ground thermal storage system is carried out below through mass, energy, entropy and exergy balances for all system components. Earth is used to store heat during the long summer months by circulating hot water powered by solar energy. Earth has a good property of slowly dissipating heat at the rate of 1 ℃ for every linear meter.

The mass balance equations for the ground storage thermal bank are given as follows:

$$\dot{m}_{43} = \dot{m}_{45} \quad (6.158)$$

$$\dot{m}_{25} = \dot{m}_{50} \quad (6.159)$$

The energy balance equations for the ground storage thermal bank during the winter and summer are given as follows respectively:

$$\dot{m}_{43} h_{43} + \dot{Q}_{soil} = \dot{m}_{45} h_{45} \quad (6.160)$$

$$\dot{m}_{25}h_{25} = \dot{m}_{50}h_{50} + \dot{Q}_{soil} \quad (6.161)$$

where $\dot{Q}_{soil}$, for large heat reservoir, is given by:

$$\dot{Q}_{soil} = U_{soil}A_{PIPE}T_{soil} \quad (6.162)$$

The energy balance equation for the ground storage thermal bank is given as follows:

$$\dot{S}_{gr,tb,gene} + \dot{m}_{43}s_{43} + \frac{\dot{Q}_{soil}}{T_{soil}} = \dot{m}_{45}s_{45} \quad (6.163)$$

The exergy balance equation for the ground storage thermal bank is given as follows:

$$\dot{m}_{43}e_{x43} + \dot{Q}_{soil}\left(1 - \frac{T_o}{T_{soil}}\right) = \dot{m}_{45}e_{x45} + \dot{E}_{x,gr,tb,des} \quad (6.164)$$

where $\dot{E}_{x,gr,tb,des}$ is given by:

$$\dot{E}_{x,gr,tb,des} = T_o\,\dot{S}_{gr,tb,gene} \quad (6.165)$$

The ground storage thermal bank exergetic efficiency is given by:

$$\psi_{gr,tb} = \frac{\dot{m}_{43}(e_{x45} - e_{x43})}{\dot{Q}_{soil}(1 - \frac{T_o}{T_{soil}})} \quad (6.166)$$

6.2.1.6 Photovoltaic/Thermal analysis

The analysis on the hybrid photovoltaic thermal system is carried using the approach of [1] as follows:

The mass balance equation on the photovoltaic thermal system is given as follows:

$$\dot{m}_{43} = \dot{m}_{53} = \dot{m}_w \quad (6.167)$$

The energy balance equation on the photovoltaic thermal system is as follows:

$$\dot{m}_{43}h_{43} + \dot{Q}_s = \dot{m}_{53}h_{53} + \dot{Q}_{loss} + \dot{P}_{elec} \quad (6.168)$$

where $\dot{Q}_{loss}$ and $\dot{P}_{elec}$ are given by:

$$\dot{Q}_{loss} = h_c A(T_{cell} - T_{amb}) \quad (6.169)$$

$$\dot{P}_{elec} = I_m V_m \quad (6.170)$$

w*here* I_m and V_m are the maximum current and voltage respectively while *A* is the total *PV* area, h_c is the heat convective heat transfer coefficient and T_{cell} are given by [1]:

$$h_c = 5.7 + 3.8V_{wind,vel} \quad (6.171)$$

$$T_{cell} = T_{amb} + \frac{(T_{cell,ref} - T_{amb})}{\dot{Q}_{s,ref}} \dot{Q}_s \quad (6.172)$$

The entropy balance equation on the photovoltaic thermal system is as follows [3]:

$$\Delta_{s,PVT} + \frac{\dot{Q}_{loss}}{T_{cell}} = C_{p,air} \mathrm{LN}(\frac{T_{cell}}{T_{amb}}) \quad (6.173)$$

where $\Delta_{s,PVT}$ is the change of entropy.

The exergy balance equation on the photovoltaic thermal system is as follows:

$$\dot{Q}_s \left(1 - \frac{T_o}{T_{sun}}\right) = \dot{p}_{elec} + h_c A (T_{cell} - T_{amb}) \left(1 - \frac{T_0}{T_{Cell}}\right) + \dot{E}_{x,PVT,des} \quad (6.174)$$

The efficiencies of the PV/T system are given as follows:

$$\psi_{PV/T} = \frac{\dot{P}_{elec} + h_c A (T_{cell} - T_{amb}) \left(1 - \frac{T_0}{T_{cell}}\right)}{A\dot{Q}_s (1 - \frac{T_o}{T_{sun}})} \quad (6.175)$$

$$\eta_{PV/T} = \frac{\dot{E}_{GH} + h_c A (T_{cell} - T_{amb})}{A\dot{Q}_s} \quad (6.176)$$

6.2.1.7 Wind turbine analysis

The wind turbine analysis is carried out using [1] approach:

- Wind turbine electric power

The electric power produced by the wind turbine is given as follows:

$$\dot{P}_{turb,elec} = \dot{P}_{turb} \eta_{trans} \, \eta_{capac} \quad (6.177)$$

where $\eta_{trans} and \, \eta_{capc}$ are the transmission and capacitance efficiencies of the wind turbine given by manufacturer while $\dot{P}_{turb}$ is the power produced by the wind turbine and is given by:

$$\dot{P}_{turb} = 0.5 \rho_{air} A_{sw} V_{avg}^3 C_{POW} \quad (6.178)$$

where A_{sw} is the swept area, C_{POW} is the power coefficient and V_{avg} is the average speed across the blades of the turbine and are given respectively as follows:

$$A_{sw} = \frac{\pi D^2}{4} \tag{6.179}$$

$$V_{avg} = 0.5\left(V_{turb,bl,tp,sp} + V_{a,i}\right) \tag{6.180}$$

where $V_{a,i}$ is the air inlet speed to the turbine and $V_{turb,bl,tp,sp}$ is the turbine tip blade speed and is given by:

$$V_{turb,bl,tp,sp} = \omega_{turb}\pi\frac{D}{60} \tag{6.181}$$

where D is the turbine diameter and ω_{turb} is the rotational speed

- Wind turbine efficiencies

$$\eta_{turb} = \frac{\dot{P}_{\text{turb,elec}}}{\dot{P}_{turb}} \tag{6.182}$$

$$\psi_{turb} = \frac{\dot{P}_{turb,elec}}{\dot{m}_{a,i}e_{x,a,i} - \dot{m}_{a,o}e_{x,a,o}} \tag{6.183}$$

To evaluate $e_{x,a,in}$ and $e_{x,a,o}$, we need the mass of air and the temperature and pressure before and after the turbine and are given by the following equations [1]:

$$T_{af,turb} = 35.74 + 0.6215T_{atm} - 35.75{V_{turb,bl,tp,sp}}^{0.16} + 0.4274T_{atm}{V_{turb,bl,tp,sp}}^{0.16} \tag{6.184}$$

$$T_{bf,turb} = 35.74 + 0.6215T_{atm} - 35.75{V_{a,in}}^{0.16} + 0.4274T_{atm}{V_{a\ ,in}}^{0.16} \tag{6.185}$$

$$\dot{m}_{a,i} = \rho_a A_{sw} V_{a\ ,i} \tag{6.186}$$

$$P_{bf,turb} = P_{atm} + 0.5\rho_{air}{V^2}_{a,i} \tag{6.187}$$

$$P_{af,turb} = P_{atm} + 0.5\rho_{air}V^2_{turb,bl,tp,sp} \tag{6.188}$$

the exergy balance on the wind turbine yields:

$$\dot{m}_{a,i}e_{x,a,in} + \frac{\dot{Q}_{\text{turb,loss}}}{T_{atm}} = 0.5\dot{m}_{a,i}\left(V^2_{a,i} - V^2_{a,o}\right) + \dot{m}_{a,i}C_P\left(T_{af,turb} - T_{bf,turb}\right) +$$

$$\dot{m}_{a,o}e_{x,ao} + \dot{m}_{a,i}T_o\left(c_p\text{LN}\left(\frac{T_{af,turb}}{T_{bf,turb}}\right) - R\text{LN}\left(\frac{P_{af,turb}}{P_{bf,turb}}\right)\right) \tag{6.189}$$

where $\dot{Q}_{\text{turb,loss}}$ is given by:

$$\dot{Q}_{\text{turb,loss}} = \dot{m}_{a,i}c_p\left(T_{atm} - \frac{T_{af,turb} + T_{bf,turb}}{2}\right) \tag{6.190}$$

6.2.1.8 System I overall efficiencies

The following equations calculate the energetic and exergetic efficiencies for the overall system.

$$\eta_{ov,sys} = \frac{\dot{Q}_{LDS,deh}+\dot{P}_{elec,PVT}+\dot{P}_{turb,elec}+h_c A_{PVT}(T_{cell}-T_{amb})+\dot{m}_{26}(h_{26}-h_{44})+\dot{m}_{36}(h_{35}-h_{36})}{\dot{q}_s(A_s+A_{PVT})+\dot{W}_{Pmp,tot}+0.5\rho_{air}A_{Swept}V_{avg}{}^3} \quad (6.191)$$

$$\psi_{ov,sys} = \frac{\dot{Q}_{eva}\left(\frac{T_0}{T_{air,in}}-1\right)+\dot{P}_{elec}+\dot{P}_{turb,elec}+h_c A_{PVT}(T_{cell}-T_{amb})\left(1-\frac{T_0}{T_{cell}}\right)}{\dot{q}_s(A_s+A_{PVT})\left(1-\frac{T_0}{T_{sun}}\right)+\dot{W}_{pmp,tot}+0.5\rho_{air}A_{Swept}V_{avg}{}^3}$$

$$+ \quad \frac{\dot{m}_{26}(h_{26}-h_{44}-T_0(s_{26}-s_{44})+\dot{m}_{36}(h_{35}-h_{36}-T_0(s_{35}-s_{36})}{\dot{q}_s(A_s+A_{PVT})\left(1-\frac{T_0}{T_{sun}}\right)+\dot{W}_{pmp,tot}+0.5\rho_{air}A_{Swept}V_{avg}{}^3} \quad (6.192)$$

6.2.2 System II

Thermodynamic analysis of system II, which is composed of absorption chiller, liquid desiccant system, solar system, hot water tank system and power system that consists of ORC and battery system, is carried out in the section below. Every subsystem will undergo a complete mass, energy, entropy, and exergy and energy efficiency analysis for all its components.

6.2.2.1 Organic Rankine cycle system analysis

- Condenser analysis

The mass balance equations for the condenser are given as follows:

$$\dot{m}_{61} = \dot{m}_{66} \quad (6.193)$$

$$\dot{m}_{59} + \dot{m}_{64} = \dot{m}_{50} \quad (6.194)$$

The energy balance equation for the condenser is given as follows:

$$\dot{m}_{61}h_{61} + \dot{m}_{59}h_{59} + \dot{m}_{64}h_{64} = \dot{m}_{66}h_{66} + \dot{m}_{50}h_{50} \quad (6.195)$$

$$\dot{Q}_{ORC,con} + \dot{m}_{61}h_{61} = \dot{m}_{66}h_{66} \quad (6.196)$$

The entropy balance equation for the condenser is given as follows:

$$\dot{m}_{61}s_{61} + \dot{m}_{59}s_{59} + \dot{m}_{64}s_{64} + \dot{S}_{ORC,con,gene} = \dot{m}_{66}s_{66+}\dot{m}_{50}s_{50} \quad (6.197)$$

The exergy balance equation for the condenser is given as follows:

$$\dot{m}_{61}e_{x61} + \dot{m}_{59}e_{x,59} + \dot{m}_{64}e_{x,64} = \dot{m}_{66}s_{66+}\dot{m}_{50}s_{50} + \dot{E}_{x,ORC,con,des} \quad (6.198)$$

where $\dot{E}_{x,ORC,con,des}$ is given by:

$$\dot{E}_{x,ORC,con,des} = T_0\dot{S}_{ORC,con,gene} \quad (6.199)$$

$$\eta_{,ORC,con} = \frac{\dot{Q}_{ORC,con}}{\dot{m}_{59}h_{59}+\dot{m}_{64}h_{64}-\dot{m}_{50}h_{50}} \quad (6.200)$$

$$\psi_{ORC,con} = \frac{\dot{Q}_{ORC,con}\left(1-{}^{T_0}/_{T_{con}}\right)}{\dot{m}_{59}(h_{59}-h_o-T_0(s_{59}-s_0)+\dot{m}_{64}(h_{64}-h_o-T_0(s_{64}-s_0)-\dot{m}_{50}(h_{50}-h_o-T_0(s_{50}-s_0)} \quad (6.201)$$

- Expansion valve analysis

The mass balance for the expansion valve is given as follows:

$$\dot{m}_{63} = \dot{m}_{64} \quad (6.202)$$

The energy balance equation for the expansion valve is given as follows:

$$h_{63} = h_{64} \quad (6.203)$$

The entropy balance equation for the expansion valve is given as follows:

$$\dot{S}_{ORC,exv,gene} = \dot{m}_{64}s_{64} - \dot{m}_{63}s_{63} \quad (6.204)$$

The exergy balance equation for the expansion valve is given as follows:

$$\dot{m}_{63}e_{x63} = \dot{m}_{64}e_{x64} + \dot{E}_{x,ORC,exv,des} \quad (6.205)$$

where $\dot{E}_{x,ORC,exv,des}$ is given by:

$$\dot{E}_{x,ORC,exv,des} = T_0\dot{S}_{ORC,exv,gene} \quad (6.206)$$

- Evaporator analysis

The mass balance equations for the evaporator are given as follows:

$$\dot{m}_{67} = \dot{m}_{43} \quad (6.207)$$

$$\dot{m}_{55} + \dot{m}_{65} = \dot{m}_{62} + \dot{m}_{57} \quad (6.208)$$

The energy balance equation for the evaporator is given as follows:

$$\dot{Q}_{ORC,eva} + \dot{m}_{43}h_{43} = \dot{m}_{67}h_{67} \quad (6.209)$$

$$\dot{m}_{55}h_{55} + \dot{m}_{65}h_{65} + \dot{Q}_{ORC,eva} = \dot{m}_{62}h_{62} + \dot{m}_{57}h_{57} \quad (6.210)$$

The entropy balance equation for the evaporator is given as follows:

$$\dot{m}_{55}s_{55} + \dot{m}_{65}s_{65} + \dot{S}_{ORC,eva,gene} + \frac{\dot{Q}_{ORC,eva}}{T_{eva}} = \dot{m}_{62}s_{62} + \dot{m}_{57}s_{57} \quad (6.211)$$

The exergy balance equation for the evaporator is given as follows:

$$\dot{m}_{55}e_{x55} + \dot{m}_{65}e_{x65} + \dot{Q}_{ORC,eva}\left(1 - \frac{T_0}{T_{eva}}\right) = \dot{m}_{62}e_{x62} + \dot{m}_{57}e_{x,57} + \dot{E}_{x,ORC,eva,des} \quad (6.212)$$

where $\dot{E}_{x,ORC,eva,des}$ is given by:

$$\dot{E}_{x,ORC,eva,des} = T_o\dot{S}_{ORC,eva,gene} \quad (6.213)$$

The evaporator efficiencies are given by:

$$\eta_{ORC,eva} = \frac{\dot{Q}_{ORC,eva}}{\dot{m}_{55}h_{55} + \dot{m}_{65}h_{65} - \dot{m}_{62}h_{62} - \dot{m}_{57}h_{57}} \quad (6.214)$$

$$\psi_{ORC,eva} = \frac{\dot{Q}_{ORC,eva}\left(1 - {}^{T_0}/_{T_{eva}}\right)}{\dot{m}_{55}(h_{55} - h_o - T_0(s_{55} - s_0) + \dot{m}_{65}(h_{65} - h_o - T_0(s_{65} - s_0) - \dot{m}_{57}(h_{57} - h_o - T_0(s_{57} - s_0) - \dot{m}_{62}(h_{62} - h_o - T_0(s_{62} - s_0)} \quad (6.215)$$

- Heat exchanger balance

The mass balance equations for the heat exchanger are given as follows:

$$\dot{m}_{53} = \dot{m}_{54} \quad (6.216)$$

$$\dot{m}_{62} = \dot{m}_{63} \quad (6.217)$$

The energy balance equation for the heat exchanger is given as follows:

$$\dot{m}_{53}h_{53} + \dot{m}_{62}h_{62} = \dot{m}_{63}h_{63} + \dot{m}_{54}h_{54} \quad (6.218)$$

The heat exchanger effectiveness is given by the following:

$$\xi_{hex} = \frac{\dot{m}_{53}C_{p,53}(T_{53} - T_{54})}{(\dot{m}C_p)_{min}(T_{62} - T_{53})} = \frac{\dot{m}_{62}C_{p,62}(T_{62} - T_{63})}{(\dot{m}C_p)_{min}(T_{62} - T_{53})} \quad (6.219)$$

If $(\dot{m}C_p)_{min} = \dot{m}_{62}C_{p,62}$

$$\xi_{hex} = \frac{(T_{62} - T_{63})}{(T_{62} - T_{53})} \quad (6.220)$$

Otherwise:

$$\xi_{hex} = \frac{(T_{54} - T_{53})}{(T_{62} - T_{53})} \quad (6.221)$$

The entropy balance equation for the heat exchanger is given as follows:

$$\dot{m}_{53} s_{53} + \dot{m}_{62} s_{62} + \dot{S}_{\mathrm{ORC,h}ex,gene} = \dot{m}_{63} s_{63} + \dot{m}_{54} s_{54} \quad (6.222)$$

The exergy balance equation for the heat exchanger is given as follows:

$$\dot{m}_{53} e_{x,53} + \dot{m}_{62} e_{x,62} = \dot{m}_{63} e_{x,63} + \dot{m}_{54} e_{x,54} + \dot{E}_{\mathrm{ORC,h}ex,des} \quad (6.223)$$

where $\dot{E}_{ORC,hex,des}$ is given by:

$$\dot{E}_{ORC,hex,des} = T_0 \dot{S}_{ORC,hex,gen} \quad (6.224)$$

The heat exchanger exergetic efficiency is described by:

$$\psi_{Hex} = \frac{\dot{m}_{53}(e_{x,54} - e_{x,53})}{\dot{m}_4(e_{x,62} - e_{x,63})} \quad (6.225)$$

- Pump analysis

The mass balance equation for the pump is given as follows:

$$\dot{m}_{50} = \dot{m}_{51} \quad (6.226)$$

The energy balance equation for the pump is given as follows:

$$\dot{m}_{50} h_{50} + \dot{W}_{ORC,pmp,act} = \dot{m}_{51} h_{51} \quad (6.227)$$

The entropy balance equation for the pump is given as follows:

$$\dot{m}_{50}\, s_{50} + \dot{S}_{ORC,pmp,gene} = \dot{m}_{51} s_{51} \quad (6.228)$$

The exergy balance equation for the pump is given as follows:

$$\dot{m}_{50} e_{x50} + \dot{W}_{ORC,pmp,act} = \dot{m}_{51} e_{x51} + \dot{E}_{x,ORC,pmp,des} \quad (6.229)$$

where $\dot{E}_{x,ORC,pmp,des}$ is given by:

$$\dot{E}_{x,ORC,pmp,des} = T_o \dot{S}_{ORC,pmp,gene} \quad (6.230)$$

The pump efficiencies are given by:

$$\psi_{ORC,Pmp} = 1 - \frac{\dot{E}_{x,ORC,pmp,des}}{\dot{W}_{ORC,pmp,act}} \quad (6.231)$$

$$\eta_{Pmp} = \frac{\dot{W}_{ORC,pmp,isen}}{\dot{W}_{ORC,pmp,act}} = \frac{\dot{m}_{50} v_{50}}{\dot{m}_{50}(h_{51} - h_{50})}(p_{51} - p_{50}) \quad (6.232)$$

- Rectifier analysis

The mass balance equations for the rectifier are given as follows:

$$\dot{m}_{52} = \dot{m}_{56} \quad (6.233)$$

$$\dot{m}_{57} = \dot{m}_{58} + \dot{m}_{65} \quad (6.234)$$

The energy balance equations for the rectifier are given as follows:

$$\dot{Q}_{ORC,rect} + \dot{m}_{52} h_{52} = \dot{m}_{56} h_{56} \quad (6.235)$$

$$\dot{m}_{57} h_{57} = \dot{m}_{58} h_{58} + \dot{m}_{65} h_{65} + \dot{Q}_{ORC,rect} \quad (6.236)$$

The entropy balance equation for the rectifier is given as follows:

$$\dot{m}_{57} s_{57} + \dot{S}_{ORC,rect,gene} = \dot{m}_{58} s_{58} + \dot{m}_{65} s_{65} + \frac{\dot{Q}_{ORC,rect}}{T_{rect}} \quad (6.237)$$

The energy balance equation for the rectifier is given as follows:

$$\dot{m}_{57} e_{x57} = \dot{m}_{58} e_{x58} + \dot{m}_{65} e_{x65} + \dot{Q}_{ORC,rec}\left(1 - \frac{T_o}{T_{rect}}\right) + \dot{E}_{x,ORC,rect,des} \quad (6.238)$$

where $\dot{E}_{x,ORC,rect,des}$ is given by:

$$\dot{E}_{x,ORC,rect,des} = T_o \dot{S}_{ORC,rect,gene} \quad (6.239)$$

The rectifier efficiencies are described by:

$$\psi_{ORC,rec} = \frac{\dot{Q}_{ORC,rec}\left(1 - {}^{T_0}/_{T_{rec}}\right)}{\dot{m}_{57}(h_{57} - h_o - T_0(s_{57} - s_0) - \dot{m}_{58}(h_{58} - h_o - T_0(s_{58} - s_0) - \dot{m}_{65}(h_{65} - h_o - T_0(s_{65} - s_0)} \quad (6.240)$$

$$\eta_{ORC,rec} = \frac{\dot{Q}_{ORC,rec}}{\dot{m}_{57} h_{57} - \dot{m}_{58} h_{58} - \dot{m}_{65} h_{65}} \quad (6.241)$$

6.2.2.2 Absorption chiller analysis

The thermodynamic analysis of the absorption chiller system is carried out where all balances and efficiencies equations are written below:

- Condenser analysis

The mass balance equations for the condenser are given as follows:

$$\dot{m}_7 = \dot{m}_8 = \dot{m}_w \tag{6.242}$$

$$\dot{m}_{11} = \dot{m}_{12} = \dot{m}_a \tag{6.243}$$

where *a* is subscript for air and *w* is for water.

The energy balance equations for the condenser are given as follows:

$$\dot{m}_7\, h_7 = \dot{m}_8 h_8 + \dot{Q}_{con} \tag{6.244}$$

$$\dot{m}_{11}\, h_{11} + \dot{Q}_{con} = \dot{m}_{12} h_{12} \tag{6.245}$$

The entropy balance equations for the condenser are given as follows:

$$\dot{m}_7\, s_7 + \dot{S}_{gene} = \dot{m}_8 s_8 + \frac{\dot{Q}_{con}}{T_{con}} \tag{6.246}$$

$$\dot{m}_{11} s_{11} + \dot{S}_{gene} + \frac{\dot{Q}_{con}}{T_{con}} = \dot{m}_{12} s_{12} \tag{6.247}$$

where $\dot{S}_{gene}$ is the entropy generated due to irreversible heat transfer.

The exergy balance equations for the condenser are given as follows:

$$\dot{m}_7 e_{x7} = \dot{m}_8 e_{x8} + \dot{Q}_{con}\left(1 - \frac{T_0}{T_{con}}\right) + \dot{E}_{x,w,con,des} \tag{6.248}$$

where $\dot{E}_{x.a.con,des}$ is given by:

$$\dot{E}_{x,w.con,des} = T_0 \dot{S}_{gene} \tag{6.249}$$

$$\dot{m}_{11} e_{x11} + \dot{Q}_{con}\left(1 - \frac{T_0}{T_{con}}\right) = \dot{m}_{12} e_{x12} + \dot{E}_{x.a.con,des} \tag{6.250}$$

where T_0 is the dead state temperature and $\dot{E}_{x.a.con,des}$ is given by:

$$\dot{E}_{x.a.con,des} = T_0 \dot{S}_{gene} \tag{6.251}$$

The exergetic efficiency equation for the condenser is written as follows:

$$\psi_{con} = \frac{\dot{Q}_{con}\left(1 - {}^{T_0}/_{T_{con}}\right)}{\dot{m}_7 (ex_7 - ex_8)} = \frac{\dot{m}_7 (ex_7 - e_{x_8}) - \dot{E}_{x,w,con,des}}{\dot{m}_7 (ex_7 - ex_8)} = 1 - \frac{\dot{E}_{x,w,con,des}}{\dot{m}_7 (ex_7 - ex_8)} \tag{6.252}$$

- Expansion valve (solution) analysis

The mass balance equation for the expansion valve is given as follows:

$$\dot{m}_5 = \dot{m}_6 = \dot{m}_{sol} \tag{6.253}$$

The energy balance equation for the expansion valve is given as follows:

$$h_5 = h_6 \tag{6.254}$$

The entropy balance equation for the expansion valve is given as follows:

$$\dot{m}_6 s_6 + \dot{S}_{gene,sol} = \dot{m}_5 s_5 \tag{6.255}$$

The exergy balance equation for the expansion valve is given as follows:

$$\dot{m}_5 e_{x5} = \dot{m}_6 e_{x6} + \dot{E}_{x,sol,des} \tag{6.256}$$

where $\dot{E}_{x,sol,des}$ is given by:

$$\dot{E}_{x,sol,des} = T_0 \dot{S}_{sol,gene} \tag{6.257}$$

The exergy efficiency equation yields:

$$\psi_{exv_w} = 1 - \frac{\dot{E}_{x,sol,des}}{\dot{m}_5 e_{x5} - \dot{m}_6 e_{x6}} = 1 - \frac{\dot{m}_5 e_{x5} - \dot{m}_6 e_{x6}}{\dot{m}_5 e_{x5} - \dot{m}_6 e_{x6}} = 0 \tag{6.258}$$

- Expansion valve (water) analysis

The mass balance equation for the expansion valve is given as follows:

$$\dot{m}_8 = \dot{m}_9 = \dot{m}_w \tag{6.259}$$

The energy balance equation for the expansion valve is given as follows:

$$h_9 = h_8 \tag{6.260}$$

The entropy balance equation for the expansion valve is given as follows:

$$\dot{m}_8 s_8 + \dot{S}_{exv,w,gene} = \dot{m}_9 s_9 \tag{6.261}$$

The exergy balance equation for the expansion valve is given as follows:

$$\dot{m}_8 e_{x8} = \dot{m}_9 e_{x9} + \dot{E}_{x,exv,w,des} \tag{6.262}$$

where $E_{x,exv,w,des}$ is given by:

$$E_{x,exv,w,des} = T_0 \dot{S}_{exv,w,gene} \quad (6.263)$$

- Evaporator analysis

The mass balance equations for the evaporator are given as follows:

$$\dot{m}_9 = \dot{m}_{10} = \dot{m}_W \quad (6.264)$$

$$\dot{m}_{13} = \dot{m}_{14} = \dot{m}_a \quad (6.265)$$

The energy balance equations for the condenser are given as follows:

$$\dot{m}_9 h_9 + \dot{Q}_{eva} = \dot{m}_{10} h_{10} \quad (6.266)$$

$$\dot{m}_{13} h_{13} = \dot{m}_{14} h_{14} + \dot{Q}_{eva} \quad (6.267)$$

where h_9 is given by:

$$h_9 = h_8 \quad (6.268)$$

The entropy balance equations for the evaporator are given as follows:

$$\dot{m}_9 s_9 + \dot{S}_{eva,w,gene} + \frac{\dot{Q}_{eva}}{T_{eva}} = \dot{m}_{10} s_{10} \quad (6.269)$$

$$\dot{m}_{13} s_{13} + \dot{S}_{eva,a,gene} = \dot{m}_{14} s_{14} + \frac{\dot{Q}_{eva}}{T_{eva}} \quad (6.270)$$

The exergy balance equations for the evaporator are given as follows:

$$\dot{m}_9 e_{x9} + \dot{Q}_{eva}\left(1 - \frac{T_0}{T_{eva}}\right) = \dot{m}_{10} e_{x10} + \dot{E}_{x,eva,w,des} \quad (6.271)$$

$$\dot{m}_{13} e_{x13} = \dot{m}_{14} e_{x14} + \dot{Q}_{eva}\left(1 - \frac{T_0}{T_{eva}}\right) + \dot{E}_{x,eva,a,des} \quad (6.272)$$

where $\dot{E}_{x,eva,w,des}$ and $\dot{E}_{x,eva,w,des}$ are given by:

$$\dot{E}_{x,eva,w,des} = T_0 \dot{S}_{eva,w,gene} \quad (6.273)$$

$$\dot{E}_{x,eva,a,des} = T_0 \dot{S}_{eva,a,gene} \quad (6.274)$$

The exergetic efficiency is expressed as:

$$\psi_{eva} = \frac{\dot{Q}_{eva}\left({}^{T_0}/_{T_{eva}} - 1\right)}{\dot{m}_9(e_{x10} - e_{x9})} = \frac{\dot{m}_9(e_{x10} - e_{x9}) - \dot{E}_{x\_eva\_des\_w}}{\dot{m}_9(e_{x10} - e_{x9})} = 1 - \frac{T_0 \dot{S}_{eva,w,gene}}{\dot{m}_9(e_{x10} - e_{x9})} \quad (6.275)$$

Here, our useful output is cooling the air which is re-circulated and the driving exergy gradient that causes the useful output which is also re-circulated is given by:

$$\psi_{eva} = \frac{-\dot{Q}_{eva}\left(1-\frac{T_0}{T_{eva}}\right)}{\dot{m}_{13}e_{x13}-\dot{m}_{14}e_{x_{14}}} \quad (6.276)$$

- Heat exchanger analysis

The mass balance equations for the heat exchanger are given as follows:

$$\dot{m}_2 = \dot{m}_3 = \dot{m}_{wea,sol} \quad (6.277)$$

$$\dot{m}_4 = \dot{m}_5 = \dot{m}_{str,sol} \quad (6.278)$$

The energy balance equation for the heat exchanger is given as follows:

$$\dot{m}_2 h_2 + \dot{m}_4 h_4 = \dot{m}_3 h_3 + \dot{m}_5 h_5 \quad (6.279)$$

The effectiveness of the heat exchanger is given by:

$$\xi_{Hx} = \frac{\dot{m}_2 C_{p,2}(T_3-T_2)}{(\dot{m}C_p)_{min}(T_4-T_{2)})} = \frac{\dot{m}_4 C_{p,4}(T_4-T_5)}{(\dot{m}C_p)_{min}(T_4-T_{2)})} \quad (6.280)$$

but if $(\dot{m}C_p)_{min} = \dot{m}_4 C_{p,4}$ then:

$$\xi_{Hx} = \frac{(T_4-T_5)}{(T_4-T_{2)})} \quad (6.290)$$

Otherwise:

$$\xi_{Hx} = \frac{(T_3-T_2)}{(T_4-T_{2)})} \quad (6.291)$$

The entropy balance equation for the heat exchanger is given as follows:

$$\dot{m}_2 s_2 + \dot{S}_{hex,gene} + \dot{m}_4 s_4 = \dot{m}_3 s_3 + \dot{m}_5 s_5 \quad (6.292)$$

The exergy balance equation for the condenser is given as follows:

$$\dot{m}_2 e_{x2} + \dot{m}_4 e_{x4} = \dot{m}_3 e_{x3} + \dot{m}_5 e_{x5} + \dot{E}_{hex,des} \quad (6.293)$$

where $\dot{E}_{hex,des}$ is given by:

$$\dot{E}_{hex,des} = T_0 S_{\mathrm{hex,gene}} \quad (6.294)$$

The exergetic efficiency of the heat exchanger is represented by:

$$\psi_{Hex} = \frac{\dot{m}_2(e_{x_3} - e_{x_2})}{\dot{m}_4(e_{x4} - e_{x5})} \quad (6.295)$$

- Pump analysis

The mass balance equation for the pump is given as follows:

$$\dot{m}_1 = \dot{m}_2 = \dot{m}_{wea,sol} \quad (6.296)$$

where wea, sol represents weak solution

The energy balance equation for the pump is given as follows:

$$\dot{m}_1 h_1 + W_{pmp,act} = \dot{m}_2 h_2 \quad (6.297)$$

The entropy balance equation for the pump is given as follows:

$$\dot{m}_1 s_1 + \dot{S}_{pmp,gene} = \dot{m}_2 s_2 \quad (6.298)$$

The exergy balance equation for the pump is given as follows:

$$\dot{m}_1 e_{x1} + \dot{W}_{pmp,act} = \dot{m}_2 e_{x2} + \dot{E}_{x,pmp,des} \quad (6.299)$$

where $\dot{E}_{x,pmp,des}$ is given by:

$$\dot{E}_{x,Pmp,des} = T_0 \dot{S}_{pmp,gene} \quad (6.300)$$

The pump exergetic efficiency is evaluated as follows:

$$\psi_{pmp} = 1 - \frac{\dot{E}_{X,pmp,des}}{\dot{W}_{pmp,act}} \quad (6.301)$$

- Absorber analysis

The mass balance equations for the absorber are given as follows:

$$\dot{m}_{10} + \dot{m}_6 = \dot{m}_1 \quad (6.302)$$

$$x_1 \dot{m}_1 = x_6 \dot{m}_6 \quad (6.303)$$

The energy balance equation for the absorber is given as follows:

$$\dot{m}_{10} h_{10} + \dot{m}_6 h_6 = \dot{m}_1 h_1 + \dot{Q}_{abs} \quad (6.304)$$

The entropy balance equation for the absorber is given as follows:

$$\dot{S}_{abs,gene} + \dot{m}_{10}\, s_{10} + \dot{m}_6\, s_6 = \dot{m}_1\, s_1 + \frac{\dot{Q}_{abs}}{T_{abs}} \quad (6.305)$$

The exergy balance equations for the absorber are given as follows:

$$\dot{m}_{10} e_{x10} + \dot{m}_6 e_{x6} = \dot{m}_1\, e_{x1} + \dot{E}_{x,abs,des} + \dot{Q}_{abs}\left(1 - \frac{T_o}{T_{abs}}\right) \quad (6.306)$$

where $\dot{E}_{x,abs,des}$ is given by:

$$\dot{E}_{x,abs,des} = T_o\, \dot{S}_{abs,gene} \quad (6.307)$$

The chemical exergy at the absorber is evaluated as follows:

$$\dot{E}_{x,CH,abs} = \frac{1}{\frac{x_{LiBr}}{(1-x_{LiBr})m_{sol,gen}}}\left[\sum_{i=1}^{n} x_i \overline{E\_x\_o} + \overline{R} T_o \sum_{i=1}^{n} x_i \ln a_i\right] = \dot{Q}_{abs,ch}\left(1 - \frac{T_o}{T_{abs}}\right) \quad (6.308)$$

Here, the strong solution is the useful output and the driving exergy gradient is as shown in the equations of the efficiencies:

$$\psi_{abs} = 1 - \frac{\dot{E}_{x,abs,des}}{\dot{m}_{10}\, e_{x10} + \dot{m}_6 e_{x6} - \dot{m}_1 e_{x1}} \quad (6.309)$$

$$\eta_{abs} = \frac{\dot{Q}_{abs}}{\dot{m}_{10}\, h_{10} + \dot{m}_6\, h_6 - \dot{m}_1\, h_1} \quad (6.310)$$

- Regenerator analysis

The mass balance equations for the regenerator are given as follows:

$$\dot{m}_3 = \dot{m}_7 + \dot{m}_4 \quad (6.311)$$

$$x_3 \dot{m}_3 = x_4 \dot{m}_4 \quad (6.312)$$

The energy balance equation for the regenerator is given as follows:

$$\dot{m}_3 h_3 + \dot{Q}_{gen} = \dot{m}_4 h_4 + \dot{m}_7 h_7 \quad (6.313)$$

The entropy balance equation for the regenerator is given as follows:

$$\dot{S}_{gen,gene} + \dot{m}_3 s_3 + \frac{\dot{Q}_{gen}}{T_{gen}} = \dot{m}_7 s_7 + \dot{m}_4 s_4 \quad (6.314)$$

The exergy balance equations for the regenerator are given as follows:

$$\dot{m}_3 e_{x3} + \dot{Q}_{gen}\left(1 - \frac{T_o}{T_{gen}}\right) = \dot{m}_7 e_{x7} + \dot{m}_4 e_{x4} + \dot{E}_{x,reg,des} \quad (6.315)$$

where $\dot{E}_{x,gen,des}$ are given by:

$$\dot{E}_{x,gen,des} = T_o \dot{S}_{gen,gene} \tag{6.316}$$

The chemical exergy at the regenerator is given as follows:

$$\dot{E}_{x,CH,gen} = \frac{1}{\frac{x_{LiBr}}{(1-x_{LiBr})m_{sol,gen}}} \left[\sum_{i=1}^{n} x_i \overline{E\_x\_o} + \overline{R} T_o \sum_{i=1}^{n} x_i \ln a_i\right] = \dot{Q}_{gen,ch} \left(1 - \frac{T_o}{T_{gen}}\right) \tag{6.317}$$

The regenerator efficiencies are given by:

$$\psi_{gen} = \frac{\dot{Q}_{gen}\left(1-\frac{T_o}{T_{gen}}\right)}{\dot{m}_3 e_{x3} - (\dot{m}_7 e_{x7} + \dot{m}_4 e_{x4})} \tag{6.318}$$

$$\eta_{gen} = \frac{\dot{Q}_{gen}}{\dot{m}_4 h_4 - (\dot{m}_7 h_7 + \dot{m}_3 h_3)} \tag{6.319}$$

- Absorption system overall COPs

The overall absorption system energetic and exergetic coefficients of performance are described by:

$$COP_{\eta} = \frac{\dot{Q}_{eva}}{\dot{W}_{pmp} + \dot{Q}_{gen}} \tag{6.320}$$

$$COP_{\psi} = \frac{\dot{Q}_{eva}\left(1-\frac{T_o}{T_{eva}}\right)}{\dot{W}_{pmp} + \dot{Q}_{gen}\left(1-\frac{T_o}{T_{gen}}\right)} \tag{6.321}$$

6.2.2.3 Solar panels system analysis

The mass balance equations for the solar panels are given as follows:

$$\dot{m}_{19} = \dot{m}_{20} \tag{6.322}$$

$$\dot{m}_{43} = \dot{m}_{67} \tag{6.323}$$

The energy balance equation for the solar panels is given as follows:

$$\dot{m}_{43} h_{43} + \dot{m}_{19} h_{19} + \dot{Q}_S = \dot{m}_{20} h_{20} + \dot{m}_{67} h_{67} \tag{6.324}$$

The entropy balance equation for the solar panels is given as follows:

$$\dot{m}_{43} s_{43} + \dot{m}_{19} s_{19} + \dot{S}_{s,gene} + \frac{\dot{Q}_s}{T_{sun}} = \dot{m}_{20} s_{20} + \dot{m}_{67} s_{67} \tag{6.325}$$

The exergy balance equation for the solar panels is given as follows:

$$\dot{m}_{43}e_{x43} + \dot{m}_{19}e_{x19} + \dot{Q}_s\left(1 - \frac{T_0}{T_{sun}}\right) = \dot{m}_{20}e_{x20} + \dot{m}_{67}e_{x67} + \dot{E}_{x,S,des} \quad (6.326)$$

where $\dot{E}_{x,s,des}$ is given by:

$$\dot{E}_{x,s,des} = T_0\dot{S}_{s,gene} \quad (6.327)$$

The efficiencies are given as:

$$\psi_s = \frac{\dot{m}_{20}(e_{x20} - e_{x19}) + \dot{m}_{67}(e_{x67} - e_{x43})}{\dot{Q}_s\left(1 - \frac{T_0}{T_{sun}}\right)} \quad (6.328)$$

$$\eta_s = \frac{\dot{m}_{19}((h_{20} - h_{19}) + \dot{m}_{67}((h_{67} - h_{43})}{\dot{Q}_s} \quad (6.329)$$

- Solar pump analysis

The mass balance equation for the solar pump is given as follows:

$$\dot{m}_{16} = \dot{m}_{19} \quad (6.330)$$

The energy balance equation for the solar pump is given as follows:

$$\dot{m}_{16}h_{16} + \dot{W}_{pmp,act} = \dot{m}_{19}h_{19} \quad (6.331)$$

The entropy balance equation for the solar pump is given as follows:

$$\dot{m}_{16}s_{16} + \dot{S}_{pmp,s,gene} = \dot{m}_{19}s_{19} \quad (6.332)$$

The exergy balance equation for the solar pump is given as follows:

$$\dot{m}_{16}e_{x16} + \dot{W}_{pmp,act} = \dot{m}_{19}e_{x19} + \dot{E}_{x,pmp,s,des} \quad (6.333)$$

where $\dot{E}_{x,pmp,s,des}$ is given by:

$$\dot{E}_{x,pmp,s,des} = T_0\dot{S}_{pmp,s,gene} \quad (6.334)$$

The pump efficiencies are described by:

$$\psi_{pmp,s} = 1 - \frac{\dot{E}_{x,pmp,des}}{\dot{W}_{pmp,act}} \quad (6.335)$$

$$\eta_{pmp,s} = \frac{\dot{W}_{isen}}{\dot{W}_{act}} = \frac{\dot{m}_{16}v_{16}}{\dot{m}_{19}(h_{19} - h_{16})}(p_{19} - p_{16}) \quad (6.336)$$

6.2.2.4 Liquid desiccant system analysis

The thermodynamic analysis of the liquid desiccant system is carried out below through mass, energy, entropy and exergy balances for all system components.

- Dehumidifier analysis

The mass balance equations for the dehumidifier are given as follows:

$$\dot{m}_{32} + \dot{m}_{cond} = \dot{m}_{33} \tag{6.337}$$

$$x_{32}\,\dot{m}_{32} = x_{33}\,\dot{m}_{33} \tag{6.338}$$

$$\dot{m}_{40} = \dot{m}_{41} - \dot{m}_{cond} \tag{6.339}$$

where $\dot{m}_{cond}$ is water condensed from ambient air and *x* stands for mass concentration of LiBr solution.

The energy balance equation for the dehumidifier is given as follows:

$$\dot{m}_{32}h_{32} + \dot{m}_{40}h_{40} = \dot{m}_{33}h_{33} + \dot{m}_{41}h_{41} \tag{6.340}$$

The entropy balance equation for the dehumidifier is given as follows:

$$\dot{S}_{deh,gene} + \dot{m}_{32}s_{32} + \dot{m}_{cond}s_{cond} = \dot{m}_{32}s_{32} + \frac{\dot{Q}_{deh}}{T_{deh}} \tag{6.341}$$

The exergy balance equation for the dehumidifier is given as follows:

$$\dot{m}_{32}e_{x10} + \dot{m}_{cond}e_{x,cond} = \dot{m}_{33}e_{33} + \dot{E}_{x,deh,des} - \dot{Q}_{deh}\left(1 - \frac{T_o}{T_{deh}}\right) \tag{6.342}$$

where $\dot{E}_{x,deh,des}$ is given by:

$$\dot{E}_{x,deh,des} = T_o\dot{S}_{deh,gene} \tag{6.343}$$

The chemical exergy at the dehumidifier is given by:

$$\dot{E}_{x,CH,deh} = \frac{1}{\frac{x_{LiBr}}{(1-x_{LiBr})m_{sol,gen}}}\left[\sum_{i=1}^{n} x_i\overline{E\_x\_o} + \overline{R}T_o\sum_{i=1}^{n} x_i \ln a_i\right] = \dot{Q}_{deh,ch}\left(1 - \frac{T_o}{T_{deh}}\right) \tag{6.344}$$

$$\psi_{deh} = \frac{-\dot{Q}_{deh}\left(1-\frac{T_o}{T_{deh}}\right)}{\dot{m}_{32}\,(\,e_{x33} - e_{x32}\,) + \dot{m}_{cond}\,e_{x,cond}} \tag{6.345}$$

$$\eta_{deh} = \frac{-\dot{Q}_{deh}}{\dot{m}_{32}(h_{33} - h_{32}) + \dot{m}_{cond}h_{cond}} \tag{6.346}$$

- Dehumidifier blower analysis

The mass balance equation for the dehumidifier blower is given as follows:

$$\dot{m}_{40} = \dot{m}_{41} = \dot{m}_a \tag{6.347}$$

The energy balance equation for the dehumidifier blower is given as follows:

$$\dot{m}_{40} h_{40} + \dot{W}_{blow} = \dot{m}_{41} h_{41} \tag{6.348}$$

where $\dot{W}_{blow}$ is the work done by the blower motor.

The entropy balance equation for the dehumidifier blower is given as follows:

$$\dot{m}_{40} s_{40} + \dot{S}_{blow,gene} = \dot{m}_{41} s_{41} \tag{6.349}$$

The exergy balance equation for the dehumidifier blower is given as follows:

$$\dot{m}_{40} e_{x40} + \dot{W}_{blow} + \dot{m}_{41} e_{x41} + \dot{E}_{x,blow,des} \tag{6.350}$$

where $\dot{E}_{x,blow,des}$ is given by:

$$\dot{E}_{x,blow,des} = T_o \dot{S}_{blow,gene} \tag{6.351}$$

The blower efficiency is given by:

$$\psi_{blow} = 1 - \frac{\dot{E}_{x,blow,des}}{\dot{W}_{blow}} \tag{6.352}$$

- Regenerator analysis

The mass balance equations for the regenerator are given as follows:

$$\dot{m}_{51} + \dot{m}_{29} = \dot{m}_{35} \tag{6.353}$$

$$x_{51} \dot{m}_{51} = x_{29} \dot{m}_{29} \tag{6.354}$$

$$\dot{m}_{24} = \dot{m}_{27} \tag{6.355}$$

The energy balance equation for the regenerator is given as follows:

$$\dot{m}_{68} h_{68} + \dot{m}_{24} h_{24} = \dot{m}_{29} h_{29} + \dot{m}_{27} h_{27} + \dot{m}_{35} h_{35} \tag{6.356}$$

The entropy balance equation for the regenerator is given as follows:

$$\dot{S}_{reg,gene} + \dot{m}_{68} s_{68} = \dot{m}_{29} s_{29} + \dot{m}_{35} s_{35} - \frac{\dot{Q}_{reg}}{T_{reg}} \tag{6.357}$$

The exergy balance equation for the regenerator is given as follows:

$$\dot{m}_{68}e_{x68} = \dot{m}_{29}e_{x29} + \dot{m}_{35}e_{x35} + \dot{E}_{x,reg,des} - \dot{Q}_{reg}\left(1 - \frac{T_o}{T_{reg}}\right) \quad (6.358)$$

where $\dot{E}_{x,reg,des}$ is given by:

$$\dot{E}_{x,reg,des} = T_o\,\dot{S}_{reg,gene} \quad (6.359)$$

The chemical exergy at the regenerator is given by:

$$\dot{E}_{x,CH,reg} = \frac{1}{\frac{x_{LiBr}}{(1-x_{LiBr})m_{sol,gen}}}\left[\sum_{i=1}^{n} x_i\overline{E\_x\_o} + \overline{R}T_o\sum_{i=1}^{n} x_i \ln a_i\right] = \dot{Q}_{reg,ch}\left(1 - \frac{T_o}{T_{reg}}\right) \quad (6.360)$$

The efficiencies are given by:

$$\psi_{reg} = \frac{\dot{Q}_{reg}\left(1-\frac{T_o}{T_{deh}}\right)}{\dot{m}_{68}\,e_{x68} - (\dot{m}_{29}\,e_{x29} + \dot{m}_{35}e_{x35})} \quad (6.361)$$

$$\eta_{reg} = \frac{\dot{Q}_{reg}}{\dot{m}_{68}h_{68} - (\dot{m}_{35}\,h_{35} + \dot{m}_{29}\,h_{29})} \quad (6.362)$$

- Heat exchanger analysis

The mass balance equations for the heat exchanger are given as follows:

$$\dot{m}_{33} = \dot{m}_{34} \quad (6.363)$$

$$\dot{m}_{30} = \dot{m}_{31} \quad (6.364)$$

The energy balance equation for the heat exchanger is given as follows:

$$\dot{m}_{33}h_{33} + \dot{m}_{30}h_{30} = \dot{m}_{34}h_{34} + \dot{m}_{31}h_{31} \quad (6.365)$$

The entropy balance equation for the heat exchanger is given as follows:

$$\dot{S}_{LDS,hex,gene} + \dot{m}_{33}s_{33} + \dot{m}_{30}s_{30} = \dot{m}_{34}s_{34} + \dot{m}_{31}s_{31} \quad (6.366)$$

The exergy balance equation for the heat exchanger is given as follows:

$$\dot{m}_{34}e_{x34} + \dot{m}_{31}e_{x31} = \dot{m}_{33}e_{x33} + \dot{m}_{30}e_{x30} + \dot{E}_{x,LDS,hex,des} \quad (6.367)$$

where $\dot{E}_{x,LDS,hex,des}$ is given by:

$$\dot{E}_{x,LDS,hex,des} = T_o\dot{S}_{LDS,hex,gene} \quad (6.368)$$

The heat exchanger efficiency is derived as follows:

$$\psi_{hex} = \frac{\dot{m}_{34}\,(e_{x34} - e_{x33})}{\dot{m}_{30}\,(e_{x30} - e_{x31})} \tag{6.369}$$

- Cooling heat exchanger analysis

The mass balance equations for the cooling heat exchanger are given as follows:

$$\dot{m}_{13} = \dot{m}_{14} \tag{6.370}$$

$$\dot{m}_{32} = \dot{m}_{31} \tag{6.371}$$

The energy balance equation for the cooling heat exchanger is given as follows:

$$\dot{m}_{13}h_{13} + \dot{m}_{31}h_{31} = \dot{m}_{14}h_{14} + \dot{m}_{32}h_{32} \tag{6.372}$$

The entropy balance equation for the cooling heat exchanger is given as follows:

$$\dot{S}_{LDS,cooling,hex,gene} + \dot{m}_{13}s_{13} + \dot{m}_{13}s_{31} = \dot{m}_{14}s_{14} + \dot{m}_{32}s_{32} \tag{6.373}$$

The exergy balance equation for the cooling heat exchanger is given as follows:

$$\dot{m}_{13}e_{x13} + \dot{m}_{31}e_{x31} = \dot{m}_{32}e_{x32} + \dot{m}_{14}e_{x14} + \dot{E}_{x,LDS,cooling,hex,des} \tag{6.374}$$

where $\dot{E}_{x,LDS,cooling,hex,des}$ is given by:

$$\dot{E}_{x,LDS,cooling,hex,des} = T_o\dot{S}_{LDS,cooling,hex,gene} \tag{6.375}$$

The cooling heat exchanger exergetic efficiency is defined as follows:

$$\psi_{hex} = \frac{\dot{m}_{13}\,(e_{x14} - e_{x13})}{\dot{m}_{31}\,(e_{x31} - e_{x32})} \tag{6.376}$$

- Condenser analysis

The mass balance equations for the condenser are given as follows:

$$\dot{m}_{35} = \dot{m}_{36} \tag{6.377}$$

$$\dot{m}_{48} = \dot{m}_{49} \tag{6.378}$$

The energy balance equation for the condenser is given as follows:

$$\dot{m}_{35}h_{35} + \dot{m}_{48}h_{48} = \dot{m}_{36}h_{36} + \dot{m}_{49}h_{49} \tag{6.379}$$

The entropy balance equation for the condenser is given as follows:

$$\dot{S}_{LDS,con,gene} + \dot{m}_{35}s_{35} + \dot{m}_{48}s_{48} = \dot{m}_{36}s_{36} + \dot{m}_{49}s_{49} \quad (6.380)$$

The exergy balance equation for the condenser is given as follows:

$$\dot{m}_{35}e_{x35} + \dot{m}_{48}e_{x48} = \dot{m}_{36}e_{x36} + \dot{m}_{49}e_{x49} + \dot{E}_{x,LDS,con,des} \quad (6.381)$$

where $\dot{E}_{x,LDS,con,des}$ is given by:

$$\dot{E}_{x,LDS,con,des} = T_o\dot{S}_{LDS,con,gene} \quad (6.382)$$

The condenser exergetic efficiency is defined as:

$$\psi_{LDS,con} = \frac{\dot{Q}_{con}(1-\frac{T_O}{T_{con}})}{\dot{m}_{48}\,(e_{x48} - e_{x49})} \quad (6.383)$$

- Desiccant pump analysis

The mass balance for the desiccant pump is given as follows:

$$\dot{m}_{29} = \dot{m}_{30} \quad (6.384)$$

The energy balance equation for the desiccant pump is given as follows:

$$\dot{m}_{29}h_{29} + \dot{W}_{pmp,act} = \dot{m}_{30}h_{30} \quad (6.385)$$

The entropy balance equation for the desiccant pump is given as follows:

$$\dot{m}_{29}s_{29} + \dot{S}_{Pmp,gene} = \dot{m}_{30}s_{30} \quad (6.386)$$

The exergy balance equation for the desiccant pump is given as follows:

$$\dot{m}_{29}e_{x29} + \dot{W}_{Pmp,act} = \dot{m}_{30}e_{x30} + \dot{E}_{x,Pmp,des} \quad (6.387)$$

where $\dot{E}_{x,Pmp,des}$ is given by:

$$\dot{E}_{x,Pmp,des} = T_0\dot{S}_{Pmp,gene} \quad (6.388)$$

The desiccant pump efficiencies are defined as:

$$\psi_{Pump} = 1 - \frac{\dot{E}_{x,pmp,des}}{\dot{W}_{pmp,act}} \quad (6.389)$$

$$\eta_{pmp} = \frac{\dot{W}_{isen}}{\dot{W}_{act}} = \frac{\dot{m}_{29}v}{\dot{m}_{30}(h_{29}-h_{30})}(p_{30} - p_{29}) \quad (6.390)$$

- Expansion valve (solution) analysis

The mass balance equation for the expansion valve is given as follows:

$$\dot{m}_{34} = \dot{m}_{51} \tag{6.391}$$

The energy balance equation for the expansion valve is given as follows:

$$\dot{m}_{34} h_{34} = \dot{m}_{51} h_{51} \tag{6.392}$$

The entropy balance equation for the expansion valve is given as follows:

$$\dot{S}_{LDS,gene} = \dot{m}_{51} s_{51} - \dot{m}_{34} s_{34} \tag{6.393}$$

The exergy balance equation for the expansion valve is given as follows:

$$\dot{m}_{51} e_{x51} = \dot{m}_{34} e_{x34} + \dot{E}_{X,des} \tag{6.394}$$

where $\dot{E}_{x,LDS,des}$ is given by:

$$\dot{E}_{x,LDS,des} = T_0 \dot{S}_{LDS,gene} \tag{6.395}$$

The exergetic efficiency of the expansion valve is defines as follows:

$$\psi_{LDS,exv} = 1 - \frac{\dot{m}_{51} e_{x51} - \dot{m}_{34} e_{x34}}{\dot{m}_{51} e_{x51} - \dot{m}_{34} e_{x34}} = 0 \tag{6.396}$$

- Liquid desiccant system overall efficiencies

The overall energetic efficiency for the LDS is defined as the desired product output divided by the useful fuel input as follows:

$$COP_{LDS,ov} = \frac{\dot{Q}_{LDS,deh} + \dot{m}_{36}(h_{35} - h_{36})}{\dot{Q}_{LDS,reg} + \dot{W}_{LDS,pmp} + \dot{Q}_{LDS,con}} \tag{6.397}$$

$$COP\psi_{LDS,ov} = \frac{\dot{Q}_{LDS,deh}(1 - \frac{T_0}{T_{deh}}) + \dot{m}_{36}(h_{35} - h_{36} - T_0(s_{35} - s_{36})}{\dot{Q}_{LDS,reg}(1 - \frac{T_0}{T_{reg}}) + \dot{W}_{LDS,pmp} + \dot{Q}_{LDS,con}(1 - \frac{T_0}{T_{con}})} \tag{6.398}$$

6.2.2.5 Hot water tank analysis

The thermodynamic analysis of the hot water tank system is carried out below through mass, energy, entropy and exergy balances for all system components.

The mass balance equations for the hot water tank are given as follows:

$$\dot{m}_{21} = \dot{m}_{18} \tag{6.399}$$

$$\dot{m}_{44} = \dot{m}_{26} \tag{6.400}$$

The energy balance equation for the hot water tank is given as follows:

$$\dot{m}_{21}\, h_{21} + \dot{m}_{44}\, h_{44} = \dot{m}_{26}\, h_{26} + \dot{m}_{18}\, h_{18} \tag{6.401}$$

The entropy balance equation for the hot water tank is given as follows:

$$\dot{S}_{hwt,gene} + \dot{m}_{21} s_{21} + \dot{m}_{44} s_{44} = \dot{m}_{26} s_{26} + \dot{m}_{18} s_{18} \tag{6.402}$$

The exergy balance equation for the hot water tank is given as follows:

$$\dot{m}_{21} \mathrm{e}_{x21} + \dot{m}_{44} \mathrm{e}_{x44} = \dot{m}_{26} \mathrm{e}_{x26} + \dot{m}_{1} e_{x18} + \dot{E}_{x,hwt,des} \tag{6.403}$$

where $\dot{E}_{x,hwt,des}$ is given by:

$$\dot{E}_{x,hwt,des} = T_o\, \dot{S}_{hwt,gene} \tag{6.404}$$

The efficiencies of the hot water tank are defined by:

$$\psi_{hwt} = \frac{\dot{m}_{26}(\mathrm{e}_{x26} - \mathrm{e}_{x44})}{\dot{m}_{21}(\mathrm{e}_{x21} - \mathrm{e}_{x18})} \tag{6.405}$$

$$\eta_{hwt} = \frac{\dot{m}_{26}(\mathrm{h}_{26} - \mathrm{h}_{44})}{\dot{m}_{21}(\mathrm{h}_{21} - \mathrm{h}_{18})} \tag{6.406}$$

6.2.2.6 System II overall efficiencies analysis

The overall system efficiencies is evaluated by dividing the desired energy outputs of the cooled air, produced power, fresh and hot water by the total energy inputs of solar and pumps as follows:

$$\eta_{ov,sys} = \frac{\dot{Q}_{LDS,deh} + \dot{m}_{36}(h_{35} - h_{36}) + \dot{P}_{ORC,turb,elec} + \dot{m}_{26}(h_{26} - h_{44}) + \dot{m}_{36}(h_{35} - h_{36})}{\dot{q}_s(A_s) + \dot{W}_{Pmp,tot}} \tag{6.407}$$

$$\psi_{ov,sys} = \frac{\dot{Q}_{LDS,deh}\left(\frac{T_0}{T_{deh}} - 1\right) + \dot{P}_{ORC,turb,elec} + \dot{m}_{26}(h_{26} - h_{44} - T_0(s_{26} - s_{44})}{\dot{q}_s(A_s)\left(1 - \frac{T_0}{T_{sun}}\right) + \dot{W}_{Pmp,tot}} +$$

$$\frac{\dot{m}_{36}(h_{35} - h_{36} - T_0(s_{35} - s_{36})}{\dot{q}_s(A_s)\left(1 - \frac{T_0}{T_{sun}}\right) + \dot{W}_{Pmp,tot}} \tag{6.408}$$

6.2.3 System III

Thermodynamic analysis of system III, which is composed of heat transformer, solar panels, heat pump, distillation system, ground storage heating and cooling thermal banks and power system consisting of PV, hydro and battery system, is carried out in the section below. Every subsystem will undergo a complete mass, energy, entropy, exergy and efficiency analysis for all its components.

6.2.3.1 Heat transformer analysis

The thermodynamic analysis of the heat transformer system is carried out below through mass, energy, entropy and exergy balances for all system components.

- Condenser analysis

The mass balance equations for the condenser are given as follows:

$$\dot{m}_1 = \dot{m}_2 \tag{6.409}$$

$$\dot{m}_{28} = \dot{m}_{29} \tag{6.410}$$

The energy balance equations for the condenser are given as follows:

$$\dot{m}_1 h_1 = \dot{m}_2 h_2 + \dot{Q}_{con} \tag{6.411}$$

$$\dot{m}_{28} h_{28} + \dot{Q}_{con} = \dot{m}_{29} h_{29} \tag{6.412}$$

The entropy balance equations for the condenser are given as follows:

$$\dot{m}_1 s_1 + \dot{S}_{con,gene} = \dot{m}_2 s_2 + \frac{\dot{Q}_{con}}{T_{con}} \tag{6.413}$$

$$\dot{m}_{28} s_{28} + \dot{S}_{con,gene} + \frac{\dot{Q}_{con}}{T_{con}} = \dot{m}_{29} s_{29} \tag{6.415}$$

The exergy balance equations for the condenser are given as follows:

$$\dot{m}_1 e_{x1} = \dot{m}_2 e_{x2} + \dot{Q}_{con}\left(1 - \frac{T_o}{T_{con}}\right) + \dot{E}_{x,con,des} \tag{6.416}$$

$$\dot{m}_{28} e_{x28} + \dot{Q}_{con}\left(1 - \frac{T_o}{T_{con}}\right) = \dot{m}_{29} e_{x29} + \dot{E}_{x.con,des} \tag{6.417}$$

where $\dot{E}_{x,con,des}$ is given by:

$$\dot{E}_{x,con,des} = T_o \dot{S}_{con,gene} \tag{6.418}$$

The efficiencies of the condenser are given as:

$$\eta_{con} = \frac{\dot{Q}_{con}}{\dot{m}_1(h_1 - h_2)} \tag{6.419}$$

$$\psi_{con} = \frac{\dot{Q}_{con}\left(1 - {}^{T_0}/_{T_{con}}\right)}{\dot{m}_1(e_{x1} - e_{x2})} \tag{6.420}$$

- expansion valve (solution) analysis

The mass balance equation for the expansion valve is given as follows:

$$\dot{m}_7 = \dot{m}_6 \tag{6.421}$$

The energy balance equation for the expansion valve is given as follows:

$$h_7 = h_6 \tag{6.422}$$

The entropy balance equation for the expansion valve is given as follows:

$$\dot{m}_6 s_6 + \dot{S}_{gene,sol} = \dot{m}_7 s_7 \tag{6.423}$$

The exergy balance equation for the expansion valve is given as follows:

$$\dot{m}_6 e_{x6} = \dot{m}_7 e_{x7} + \dot{E}_{x,sol,des} \tag{6.424}$$

where $\dot{E}_{x,sol,des}$ is given by:

$$\dot{E}_{x,sol,des} = T_0 \dot{S}_{gene,sol} \tag{6.425}$$

The exergetic efficiency of the expansion valve is given as follows:

$$\psi_{sol} = 1 - \frac{\dot{E}_{x,sol,des}}{\dot{m}_6 e_{x6} - \dot{m}_7 e_{x7}} \tag{6.426}$$

- Evaporator analysis

The mass balance equations for the evaporator are given as follows:

$$\dot{m}_3 = \dot{m}_4 \tag{6.427}$$

$$\dot{m}_{20} = \dot{m}_{21} \tag{6.428}$$

The energy balance equations for the evaporator are given as follows:

$$\dot{m}_3 h_3 + \dot{Q}_{eva} = \dot{m}_4 h_4 \quad (6.429)$$

$$\dot{m}_{20} h_{20} = \dot{m}_{21} h_{21} + \dot{Q}_{eva} \quad (6.430)$$

The entropy balance equations for the evaporator are given as follows:

$$\dot{m}_3 s_3 + \dot{S}_{eva,gene} + \frac{\dot{Q}_{eva}}{T_{eva}} = \dot{m}_4 s_4 \quad (6.431)$$

$$\dot{m}_{20} s_{20} + \dot{S}_{eva,gene} = \dot{m}_{21} s_{21} + \frac{\dot{Q}_{eva}}{T_{eva}} \quad (6.432)$$

The exergy balance equations for the evaporator are given as follows:

$$\dot{m}_3 e_{x3} + \dot{Q}_{eva}\left(1 - \frac{T_0}{T_{eva}}\right) = \dot{m}_4 e_{x4} + \dot{E}_{x,eva,des} \quad (6.433)$$

$$\dot{m}_{20} e_{x20} = \dot{m}_{21} e_{x21} + \dot{Q}_{eva}\left(1 - \frac{T_0}{T_{eva}}\right) + \dot{E}_{x,eva,des} \quad (6.434)$$

where $\dot{E}_{x,eva,des}$ is given by:

$$\dot{E}_{x,eva,des} = T_0 \dot{S}_{eva,gene} \quad (6.435)$$

The efficiencies of the heat transformer evaporator are given by:

$$\eta_{eva} = \frac{\dot{Q}_{eva}}{\dot{m}_4 (h_4 - h_3)} \quad (6.436)$$

$$\psi_{eva} = \frac{\dot{Q}_{eva}\left({}^{T_0}/_{T_{eva}} - 1\right)}{\dot{m}_4 (e_{x4} - e_{x3})} \quad (6.437)$$

- Absorber analysis

The mass balance equations for the absorber are given as follows:

$$\dot{m}_{10} + \dot{m}_4 = \dot{m}_5 \quad (6.438)$$

$$\dot{m}_{12} = \dot{m}_{13} \quad (6.439)$$

$$x_{10}\, \dot{m}_{10} = x_5\, \dot{m}_5 \quad (6.440)$$

The energy balance equation for the absorber is given as follows

$$\dot{m}_{10} h_{10} + \dot{m}_4 h_4 = \dot{m}_5 h_5 + \dot{m}_{13} h_{13} - \dot{m}_{12} h_{12} \quad (6.441)$$

The entropy balance equation for the absorber is given as follows

$$\dot{m}_{10}s_{10} + \dot{m}_4 s_4 + \dot{S}_{abs,gene} = \dot{m}_1 s_1 + \dot{m}_{13} s_{13} - \dot{m}_{12} s_{12} + \frac{\dot{Q}_{abs,ch}}{T_{abs}} \quad (6.442)$$

The exergy balance equation for the absorber is given as follows:

$$\dot{m}_{10} e_{x10} + \dot{m}_4 e_{x4} + \dot{m}_{12} e_{x12} = \dot{m}_5 e_{x5} + \dot{E}_{x,abs,des} + \dot{m}_{13} e_{x13} \quad (6.443)$$

where $\dot{E}_{x,abs,des}$ is given by:

$$\dot{E}_{x,abs,des} = T_o \, \dot{S}_{abs,gene} \quad (6.444)$$

The chemical exergy at the absorber is given by:

$$\dot{E}_{x,CH,abs} = \frac{1}{\frac{x_{LiBr}}{(1-x_{LiBr})m_{sol,abs}}} \left[\sum_{i=1}^{n} x_i \overline{E,x,o} + \overline{R} T_o \sum_{i=1}^{n} x_i \, ln \, a_i\right] = \dot{Q}_{abs,ch}\left(1 - \frac{T_o}{T_{abs}}\right) \quad (6.445)$$

The efficiency equations of the absorber are written as follows:

$$\psi_{abs} = \frac{\dot{Q}_{abs}\left(1-\frac{T_o}{T_{abs}}\right)}{\dot{m}_5 e_{x5} - (\dot{m}_4 e_{x4} + \dot{m}_{10} e_{x10})} \quad (6.446)$$

$$\eta_{abs} = \frac{\dot{Q}_{abs}}{\dot{m}_5 \, h_5 - (\dot{m}_4 \, h_4 + \dot{m}_{10} \, h_{10})} \quad (6.447)$$

- Regenerator analysis

The mass balance equations for the regenerator are given as follows:

$$\dot{m}_7 = \dot{m}_8 + \dot{m}_1 \quad (6.448)$$

$$\dot{m}_{23} = \dot{m}_{24} \quad (6.449)$$

$$x_7 \dot{m}_7 = x_8 \dot{m}_8 \quad (6.450)$$

The energy balance equation for the regenerator is given as follows:

$$\dot{m}_7 h_7 + \dot{m}_{23} h_{23} = \dot{m}_8 h_8 + \dot{m}_1 h_1 + \dot{m}_{24} h_{24} \quad (6.451)$$

The entropy balance equation for the regenerator is given as follows:

$$\dot{S}_{gen,gene} + \dot{m}_7 s_7 + \dot{m}_{23} s_{23} = \dot{m}_8 s_8 + \dot{m}_1 s_1 + \dot{m}_{24} s_{24} + \frac{\dot{Q}_{gen,ch}}{T_{gen}} \quad (6.452)$$

The exergy balance equation for the regenerator is given as follows:

$$\dot{m}_7 e_{x7} + \dot{m}_{23} e_{x23} = \dot{m}_8 e_{x8} + \dot{m}_1 e_{x1} + \dot{m}_{24} e_{x24} + \dot{E}_{x,gen,des} \quad (6.453)$$

where $\dot{E}_{x,gen,des}$ is given by:

$$\dot{E}_{x,gen,des} = T_o \, \dot{s}_{gen,gene} \quad (6.454)$$

The chemical exergy at the regenerator is given by:

$$\dot{E}_{x,CH,gen} = \frac{1}{\frac{x_{LiBr}}{(1-x_{LiBr})m_{sol,gen}}} \left[\sum_{i=1}^{n} x_i \overline{E,x,o} + \overline{R} T_o \sum_{i=1}^{n} x_i \ln a_i\right] = \dot{Q}_{reg,ch}\left(1 - \frac{T_o}{T_{gen}}\right) \quad (6.455)$$

The efficiencies of the regenerator are described as follows:

$$\psi_{abs} = \frac{\dot{Q}_{gen}\left(1-\frac{T_o}{T_{gen}}\right)}{(\dot{m}_7 e_{x7} - (\dot{m}_8 e_{x8} + \dot{m}_1 e_{x1})} \quad (6.456)$$

$$\eta_{abs} = \frac{\dot{Q}_{gen}}{\dot{m}_7 \, h_7 - (\dot{m}_8 \, h_8 + \dot{m}_1 \, h_1)} \quad (6.457)$$

- Heat exchanger analysis

The mass balance equations for the heat exchanger are given as follows:

$$\dot{m}_5 = \dot{m}_6 \quad (6.458)$$

$$\dot{m}_9 = \dot{m}_{10} \quad (6.459)$$

The energy balance equation for the heat exchanger is given as follows:

$$\dot{m}_5 h_5 + \dot{m}_9 h_9 = \dot{m}_6 h_6 + \dot{m}_{10} h_{10} \quad (6.460)$$

The energy balance equation for the heat exchanger is given as follows:

$$\dot{m}_5 s_5 + \dot{m}_9 s_9 + \dot{S}_{hex,gene} = \dot{m}_6 s_6 + \dot{m}_{10} s_{10} \quad (6.461)$$

The entropy balance equation for the heat exchanger is given as follows:

$$\dot{m}_5 e_{x5} + \dot{m}_9 e_{x9} = \dot{m}_6 e_{x6} + \dot{m}_{10} e_{x10} + \dot{E}_{x,hex,des} \quad (6.462)$$

where $\dot{E}_{x,hex,des}$ is given as follows:

$$\dot{E}_{x,hex,des} = T_o \, \dot{S}_{hex,gene} \quad (6.463)$$

The heat exchanger exergetic efficiency is given by:

$$\psi_{hex} = \frac{\dot{m}_{10} \, e_{x10} - \dot{m}_9 \, e_{x9}}{\dot{m}_5 \, e_{x5} - \dot{m}_6 \, e_{x6}} \quad (6.464)$$

6.2.3.2 Solar system analysis

The thermodynamic analysis of the solar system is carried out below through mass, energy, entropy and exergy balances for all system components.

- Solar panels analysis

The mass balance equation for the solar panels, on water, is given as follows:

$$\dot{m}_{27} = \dot{m}_{18} \tag{6.465}$$

The energy balance equation for the solar system panels, on water, is given as follows:

$$\dot{m}_{27}h_{27} + \dot{Q}_s = \dot{m}_{18}h_{18} \tag{6.466}$$

The entropy balance equation for the solar system panels, on water, is given as follows:

$$\dot{m}_{27}s_{27} + \dot{S}_s + \frac{\dot{Q}_s}{T_{sun}} = \dot{m}_{18}s_{18} \tag{6.467}$$

The exergy balance equation for the solar system panels, on water, is given as follows:

$$\dot{m}_{27}e_{x27} + \dot{Q}_s\left(1 - \frac{T_o}{T_{sun}}\right) = \dot{m}_{18}e_{x18} + \dot{E}_{x,S,des} \tag{6.468}$$

where $\dot{E}_{x,S,des}$ is given as follows:

$$\dot{E}_{x,S,des} = T_o\dot{S}_{s,gene} \tag{6.469}$$

The solar panels system efficiencies are given as:

$$\psi_s = \frac{\dot{m}_{27}(e_{x18} - e_{x27})}{\dot{Q}_s\left(1 - \frac{T_0}{T_{sun}}\right)} \tag{6.470}$$

$$\eta_s = \eta_{coll}\left(\frac{\dot{m}_{27}(h_{18} - h_{27})}{\dot{Q}_s}\right) \tag{6.471}$$

- Solar pump analysis

The mass balance equation of the solar pump is given as follows:

$$\dot{m}_{26} = \dot{m}_{27} \tag{6.472}$$

The energy balance equation of the solar pump is given as follows:

$$\dot{m}_{26}h_{26} + \dot{W}_{pmp,act} = \dot{m}_{27}h_{27} \tag{6.473}$$

The entropy balance equation of the solar pump is given as follows

$$\dot{m}_{26}s_{26} + \dot{S}_{pmp,gene} = \dot{m}_{27}s_{27} \quad (6.474)$$

The exergy balance equation of the solar pump is given as follows:

$$\dot{m}_{26}e_{x26} + \dot{W}_{Pmp,s,act} = \dot{m}_{27}e_{x27} + +\dot{E}_{x,pmp,s,des} \quad (6.475)$$

where $\dot{E}_{x,pmp,s,des}$ is given by:

$$\dot{E}_{x,pmp,s,des} = T_0\dot{S}_{pmp,s,gene} \quad (6.476)$$

The efficiencies of the solar pump are described as follows:

$$\psi_{pmp,s} = 1 - \frac{\dot{E}_{x,pmp,s,des}}{\dot{W}_{Pmp,act}} \quad (6.477)$$

$$\eta_{pmp,s} = \frac{\dot{W}_{isen}}{\dot{W}_{act}} = \frac{\dot{m}_{26}v_{26}}{\dot{m}_{26}(h_{27}-h_{26})}(p_{27} - p_{26}) \quad (6.478)$$

6.2.3.3 Ground source heat pump analysis

The thermodynamic analysis of the heat pump is carried out below through mass, energy, entropy and exergy balances for all system components.

Heat pump cooling cycle analysis

- Heat exchanger IV

The mass balance equations for heat exchanger IV are given as follows:

$$\dot{m}_{51} = \dot{m}_{48} \quad (6.479)$$

$$\dot{m}_{50} = \dot{m}_{53} \quad (6.480)$$

The energy balance equation for heat exchanger IV is given as follows:

$$\dot{m}_{51}h_{51} + \dot{m}_{50}h_{50} = \dot{m}_{48}h_{48} + \dot{m}_{53}h_{53} \quad (6.481)$$

The entropy balance equation for heat exchanger IV is given as follows:

$$\dot{m}_{51}s_{51} + \dot{S}_{hexIV,gene} + \dot{m}_{50}s_{50} = \dot{m}_{48}s_{48} + \dot{m}_{53}s_{53} \quad (6.482)$$

The exergy balance equations for heat exchanger IV is given as follows:

$$\dot{m}_{51}e_{x51} + \dot{m}_{50}e_{x50} = \dot{m}_{48}e_{x48} + \dot{m}_{53}e_{x53} + \dot{E}_{hexIV,des} \quad (6.483)$$

where $\dot{E}_{hexIV,des}$ is given by:

$$\dot{E}_{hexIV,des} = T_0 \dot{S}_{hexIV,gene} \quad (6.484)$$

The exergetic efficiency of heat exchanger IV is given as follows:

$$\psi_{hexIV} = \frac{\dot{m}_{51}(e_{x48} - e_{x51})}{\dot{m}_{50}(e_{x50} - e_{x53})} \quad (6.485)$$

- Condenser analysis

The mass balance equations for the condenser are given as follows:

$$\dot{m}_{54} = \dot{m}_{31} \quad (6.486)$$

$$\dot{m}_{32} = \dot{m}_{30} \quad (6.487)$$

The energy balance equations for the condenser are given as follows:

$$\dot{m}_{54} h_{54} + \dot{m}_{32} h_{32} = \dot{m}_{33} h_{33} + \dot{m}_{30} h_{30} \quad (6.488)$$

$$\dot{Q}_{con} + \dot{m}_{32} h_{32} = \dot{m}_{30} h_{30} \quad (6.489)$$

The entropy balance equation for the condenser is given as follows:

$$\dot{m}_{54} s_{54} + \dot{S}_{con,gene} = \dot{m}_{31} s_{31} + \frac{\dot{Q}_{con}}{T_{con}} \quad (6.490)$$

The exergy balance equation for the condenser is given as follows:

$$\dot{m}_{54} e_{x54} + \dot{m}_{32} e_{x32} = \dot{m}_{31} e_{x31} + \dot{m}_{30} e_{x30} + \dot{E}_{con,des} \quad (6.491)$$

where $\dot{E}_{con,des}$ is given by:

$$\dot{E}_{con,des} = T_0 \dot{S}_{con,gene} \quad (6.492)$$

The condenser exergetic efficiency is given by:

$$\psi_{con} = \frac{\dot{Q}_{con}\left(1 - \frac{T_0}{T_{con}}\right)}{\dot{m}_{54}(e_{x54} - e_{x31})} \quad (6.493)$$

- Evaporator analysis

The mass balance equations for the evaporator are given as follows:

$$\dot{m}_{52} = \dot{m}_{33} \quad (6.494)$$

$$\dot{m}_{55} = \dot{m}_{56} \quad (6.495)$$

The energy balance equations for the evaporator are given as follows:

$$\dot{m}_{55}h_{55} + \dot{m}_{33}h_{33} = \dot{m}_{56}h_{56} + \dot{m}_{52}h_{52} \quad (6.496)$$

$$\dot{m}_{55}h_{55} = \dot{Q}_{ev} + \dot{m}_{56}h_{56} \quad (6.497)$$

The entropy balance equation for the evaporator is given as follows:

$$\dot{m}_{53}s_{53} + \dot{S}_{ev,gene} + \frac{\dot{Q}_{ev}}{T_{ev}} = \dot{m}_{52}s_{52} \quad (6.498)$$

The exergy balance equation for the evaporator is given as follows:

$$\dot{m}_{55}e_{x55} + \dot{m}_{33}e_{x33} = \dot{m}_{56}e_{x56} + \dot{m}_{52}e_{x52} + \dot{E}_{ev,des} \quad (6.499)$$

where $\dot{E}_{ev,des}$ is given as follows:

$$\dot{E}_{ev,des} = T_0\dot{S}_{ev,gene} \quad (6.500)$$

The exergetic efficiency of the evaporator is described by:

$$\psi_{ev} = \frac{\dot{Q}_{ev}\left(\frac{T_0}{T_{ev}}-1\right)}{\dot{m}_{52}(e_{x52}-e_{x33})} \quad (6.501)$$

The coefficient of performance of the GSHP is:

$$COP_{hp,cool} = \frac{\dot{Q}_{ev}+\dot{Q}_{hexIV}}{\dot{W}_{comp}} \quad (6.502)$$

Heat pump heating cycle analysis

- Heat exchanger IV analysis

The thermodynamic analysis of the heat pump system is carried out below through mass, energy, entropy and exergy balances for all system components.

The mass balance equations for heat exchanger IV are given as follows:

$$\dot{m}_{51} = \dot{m}_{48} \quad (6.503)$$

$$\dot{m}_{50} = \dot{m}_{53} \quad (6.504)$$

The energy balance equation for heat exchanger IV is given as follows:

$$\dot{m}_{51}h_{51} + \dot{m}_{50}h_{50} = \dot{m}_{48}h_{48} + \dot{m}_{53}h_{53} \quad (6.505)$$

The entropy balance equation for heat exchanger IV is given as follows:

$$\dot{m}_{51}s_{51} + \dot{S}_{hexIV,gene} + \dot{m}_{50}s_{50} = \dot{m}_{48}s_{48} + \dot{m}_{53}s_{53} \quad (6.506)$$

The exergy balance equations for heat exchanger IV is given as follows:

$$\dot{m}_{51}e_{x51} + \dot{m}_{50}e_{x50} = \dot{m}_{48}e_{x48} + \dot{m}_{53}e_{x53} + \dot{E}_{hexIV,des} \quad (6.507)$$

where $\dot{E}_{hexIV,des}$ is given by:

$$\dot{E}_{hexIV,des} = T_0\dot{S}_{hexIV,gene} \quad (6.508)$$

The exergetic efficiency of heat exchanger IV is given as follows:

$$\psi_{hexIV} = \frac{\dot{m}_{51}(e_{x48}-e_{x51})}{\dot{m}_{50}(e_{x50}-e_{x53})} \quad (6.509)$$

- Condenser analysis

The mass balance equations for the condenser are given as follows:

$$\dot{m}_{49} = \dot{m}_{31} \quad (6.510)$$

$$\dot{m}_{32} = \dot{m}_{30} \quad (6.511)$$

The energy balance equations for the condenser are given as follows:

$$\dot{m}_{34}h_{34} + \dot{m}_{32}h_{32} = \dot{m}_{49}h_{49} + \dot{m}_{30}h_{30} \quad (6.512)$$

$$\dot{Q}_{con} + \dot{m}_{30}h_{30} = \dot{m}_{32}h_{32} \quad (6.513)$$

The entropy balance equation for the condenser is given as follows:

$$\dot{m}_{31}s_{31} + \frac{\dot{Q}_{con}}{T_{con}} + \dot{S}_{con,gene} = \dot{m}_{49}s_{49} \quad (6.514)$$

The exergy balance equation for the condenser is given as follows:

$$\dot{m}_{31}e_{x31} + \dot{m}_{32}e_{x32} = \dot{m}_{49}e_{x49} + \dot{m}_{30}e_{x30} + \dot{E}_{con,des} \quad (6.515)$$

where $\dot{E}_{con,des}$ is given by:

$$\dot{E}_{con,des} = T_0\dot{S}_{con,gene} \quad (6.516)$$

The condenser exergetic efficiency is given by:

$$\psi_{con} = \frac{\dot{Q}_{con}\left(\frac{T_0}{T_{con}}-1\right)}{\dot{m}_{31}(e_{x49}-e_{x31})} \quad (6.517)$$

- Evaporator analysis

The mass balance equations for the evaporator are given as follows:

$$\dot{m}_{52} = \dot{m}_{34} \quad (6.528)$$

$$\dot{m}_{55} = \dot{m}_{56} \quad (6.519)$$

The energy balance equations for the evaporator are given as follows:

$$\dot{m}_{55}h_{55} + \dot{m}_{52}h_{52} = \dot{m}_{56}h_{56} + \dot{m}_{34}h_{34} \quad (6.520)$$

$$\dot{Q}_{ev} + \dot{m}_{55}h_{55} = \dot{m}_{56}h_{56} \quad (6.521)$$

The entropy balance equation for the evaporator is given as follows:

$$\dot{m}_{52}s_{52} + \dot{S}_{ev,gene} = \dot{m}_{34}s_{34} + \frac{\dot{Q}_{ev}}{T_{ev}} \quad (6.522)$$

The exergy balance equation for the evaporator is given as follows:

$$\dot{m}_{55}e_{x55} + \dot{m}_{52}e_{x52} = \dot{m}_{56}e_{x56} + \dot{m}_{34}e_{x34} + \dot{E}_{ev,des} \quad (6.523)$$

where $\dot{E}_{ev,des}$ is given as follows:

$$\dot{E}_{ev,des} = T_0\dot{S}_{ev,gene} \quad (6.524)$$

The exergetic efficiency of the evaporator is described by:

$$\psi_{ev} = \frac{\dot{Q}_{ev}\left(1-\frac{T_0}{T_{ev}}\right)}{\dot{m}_{52}(e_{x52}-e_{x34})} \quad (6.525)$$

The coefficient of performance of the GSHP is:

$$COP_{hp,heat} = \frac{\dot{Q}_{ev}+\dot{Q}_{hexIV}}{\dot{W}_{comp}} \quad (6.526)$$

The analysis for the heat pump compressor does not change for both cooling and heating cycle so it is introduced once.

- Compressor analysis

The mass balance equation for the compressor is given as follows:

$$\dot{m}_{49} = \dot{m}_{50} \quad (6.527)$$

The energy balance equation for the compressor is given as follows:

$$\dot{m}_{49}h_{49} + \dot{W}_{comp} = \dot{m}_{50}h_{50} \quad (6.538)$$

The entropy balance equation for the compressor is given as follows:

$$\dot{m}_{49}h_{49} + \dot{S}_{comp,gene} = \dot{m}_{50}h_{50} \quad (6.529)$$

The energy balance equation for the compressor is given as follows:

$$\dot{m}_{49}e_{x49} = \dot{m}_{50}e_{x50} + \dot{E}_{x,comp,des} \quad (6.530)$$

where $\dot{E}_{x,comp,des}$ is given by:

$$\dot{E}_{x,comp,des} = T_0\dot{S}_{comp,gene} \quad (6.531)$$

The exergetic efficiency of the compressor is given by:

$$\psi_{comp} = \frac{\dot{m}_{50}e_{x50} - \dot{m}_{49}e_{x49}}{\dot{W}_{comp}} \quad (6.533)$$

6.2.3.4 Distillation system analysis

The thermodynamic analysis of the distillation system is carried out below through mass, energy, entropy and exergy balances.

- Separation vessel analysis

The mass balance equation for the separation vessel is given as follows:

$$\dot{m}_{13} = \dot{m}_{16} + \dot{m}_{14} = \dot{m}_{12} \quad (6.534)$$

The energy balance equation for the separation vessel is given as follows:

$$\dot{m}_{13}h_{13} = \dot{m}_{16}h_{16} + \dot{m}_{14}h_{14} \quad (6.535)$$

The entropy balance equation for the separation vessel is given as follows:

$$\dot{m}_{13}s_{13} + \dot{S}_{sepv,gene} = \dot{m}_{16}s_{16} + \dot{m}_{14}s_{14} \quad (6.536)$$

The exergy balance equation for the separation vessel is given as follows:

$$\dot{m}_{13}e_{x13} = \dot{m}_{16}e_{x16} + \dot{m}_{14}e_{x14} + \dot{E}_{sepv,des} \quad (6.537)$$

The exergetic efficiency of the separation vessel is given by:

$$\psi_{sepv} = \frac{\dot{m}_{14}\, e_{x14}}{\dot{m}_{13} e_{x13}} \tag{6.538}$$

- Auxiliary condenser (heat exchanger III) analysis

The mass balance equations for heat exchanger III are given as follows:

$$\dot{m}_{13} = \dot{m}_{16} + \dot{m}_{14} = \dot{m}_{12} \tag{6.539}$$

$$\dot{m}_{14} = \dot{m}_{15} \tag{6.540}$$

$$\dot{m}_{18} = \dot{m}_{19} \tag{6.541}$$

The energy balance equation for heat exchanger III is given as follows:

$$\dot{m}_{14} h_{14} + \dot{m}_{18} h_{18} = \dot{m}_{15} h_{15} + \dot{m}_{19} h_{19} \tag{6.542}$$

The entropy balance equation for heat exchanger III is given as follows:

$$\dot{m}_{14} s_{14} + \dot{m}_{18} s_{18} + \dot{S}_{hexIII,gene} = \dot{m}_{15} s_{15} + \dot{m}_{19} s_{19} \tag{6.543}$$

The exergy balance equation for heat exchanger III is given as follows:

$$\dot{m}_{14} e_{x14} + \dot{m}_{18} e_{x18} = \dot{m}_{15} e_{x15} + \dot{m}_{19} e_{x19} + \dot{E}_{x,des} \tag{6.544}$$

The exergetic efficiency for heat exchanger III is given by:

$$\psi_{hexIII} = \frac{\dot{m}_{14}\, e_{x19} - \dot{m}_{18}\, e_{x18}}{\dot{m}_{14}\, e_{x14} - \dot{m}_{15}\, e_{x15}} \tag{6.545}$$

- Heat exchanger I analysis

The mass balance equations for heat exchanger I are given as follows:

$$\dot{m}_{16} = \dot{m}_{12} \tag{6.546}$$

$$\dot{m}_{11} = \dot{m}_{17} \tag{6.547}$$

The energy balance equation for heat exchanger I is given as follows:

$$\dot{m}_{16} h_{16} + \dot{m}_{11} h_{11} = \dot{m}_{12} h_{12} + \dot{m}_{17} h_{17} \tag{6.548}$$

The entropy balance equation for heat exchanger I is given as follows:

$$\dot{m}_{16} s_{16} + \dot{m}_{11} s_{11} + \dot{S}_{hexI,gene} = \dot{m}_{12} s_{12} + \dot{m}_{17} s_{17} \tag{6.549}$$

The exergy balance equations for heat exchanger I is given as follows:

$$\dot{m}_{16}e_{x16} + \dot{m}_{11}e_{x11} = \dot{m}_{12}e_{x12} + \dot{m}_{17}e_{x17} + \dot{E}_{x,hexI,des} \quad (6.550)$$

The exergetic efficiency for heat exchanger I is given as follows:

$$\psi_{hexI} = \frac{\dot{m}_{17}\, e_{x17} - \dot{m}_{14}\, e_{x14}}{\dot{m}_{16}\, e_{x16} - \dot{m}_{12}\, e_{x12}} \quad (6.551)$$

6.2.3.5 Thermal bank analysis

The following thermodynamic analysis evaluates the exergy efficiency of the ground storage thermal bank designated as thermal bank in the schematic diagram by applying mass, energy, entropy and exergy balances to all system components.

- Ground storage heating thermal bank analysis

The mass balance for ground storage heating thermal bank is given as follows:

$$\dot{m}_{46} = \dot{m}_{43} \quad (6.552)$$

The energy balance equation for ground storage heating thermal bank is given as follows:

$$\dot{m}_{46}h_{46} = \dot{m}_{43}h_{43} + \dot{Q}_{gr} \quad (6.553)$$

where $\dot{Q}_{gr}$ is given by:

$$\dot{Q}_{gr} = U_{gr}\left(T_{gr,fnl} - T_{gr,int}\right)2\pi r_{pipe}l_{pipe} \quad (6.554)$$

The entropy balance equation for ground storage heating thermal bank is given as follows:

$$\dot{m}_{46}s_{46} + \dot{S}_{tb,gene} = \dot{m}_{43}s_{43} + \frac{\dot{Q}_{gr}}{T_{gr}} \quad (6.555)$$

where exergy destruction for ground storage heating thermal bank is given as follows:

$$\dot{E}_{x,tb,des} = T_o\, \dot{S}_{tb,gene} \quad (6.556)$$

The exergetic efficiency for ground storage heating thermal bank is as follows:

$$\psi_{tb} = \frac{\dot{Q}_{gr}\,(1 - \frac{T_o}{T_{gr,fnl}}}{\dot{m}_{46}\,(h_{46} - h_{43} - T_o\,(s_{46} - s_{43}))} \quad (6.557)$$

- Ground storage cooling thermal bank analysis

The following thermodynamic analysis evaluates the exergy efficiency of the ground storage thermal bank designated as cooling bank in the schematic diagram.

The mass balance equation for ground storage cooling thermal bank is given as follows:

$$\dot{m}_{42} = \dot{m}_{40} \tag{6.558}$$

The energy balance equation for ground storage cooling thermal bank is given as follows:

$$\dot{m}_{42} h_{42} = \dot{m}_{40} h_{40} + \dot{Q}_{gr,cool} \tag{6.559}$$

where $\dot{Q}_{gr,cool}$ is given by:

$$\dot{Q}_{gr,cool} = U_{gr}\left(T_{gr,cool,fnl} - T_{gr,int}\right) 2\pi r_{pipe} l_{pipe} \tag{6.560}$$

The entropy balance equation for ground storage cooling thermal bank is given as follows:

$$\dot{m}_{42} s_{42} + \dot{S}_{gr.cool,gene} = \dot{m}_{40} s_{40} + \frac{\dot{Q}_{gr,cool}}{T_{gr,cool}} \tag{6.561}$$

where exergy destruction for ground storage cooling thermal bank is given as follows:

$$\dot{E}_{x,gr,cool,des} = T_o \dot{S}_{gr,cool,gene} \tag{6.562}$$

The exergetic efficiency for ground storage heating thermal bank is as follows:

$$\psi_{gr,cool} = \frac{\dot{Q}_{gr,cool}\left(1 - \frac{T_o}{(T_{gr,cool,fnl} + 273)}\right)}{\dot{m}_{42}\left(h_{42} - h_{40} - T_o\left(s_{42} - s_{40}\right)\right.} \tag{6.563}$$

6.2.3.6 Photovoltaic analysis

The following methodology is employed to analyse and evaluate the power output of the PV system. The effect of the PV cell temperature will be considered in the optimization and the time step will be taken as 100 minutes. The total amount of solar radiation striking the horizontal surface on the earth which is available from metrological data is not the amount of radiation striking the surface of the PV array. Therefore the global solar radiation incident on the surface of the PV array is calculated as follows [63]:

$$\bar{\dot{q}}_{Tot} = (\overline{\dot{q}_b} + \overline{\dot{q}_d}) R_b + \overline{\dot{q}_d}(1 - A_i)\left(\frac{1+\cos\beta}{2}\right)\left(1 + f_{cloud} sin^3\left(\frac{\beta}{2}\right)\right) + \bar{\dot{q}} r_g \left(\frac{1-\cos\beta}{2}\right) \tag{6.564}$$

such that the value of $\frac{\overline{\dot{q}_d}}{\bar{\dot{q}}}$ is determined from the following equation :

$$\frac{\overline{\dot{q}_d}}{\bar{\dot{q}}} = \begin{cases} 1 - 0.09C & for\ C \leq 0.22 \\ 0.9511 - 0.1604C + 4.388C^2 - 16.638C^3 + 12.336C^4 & for 0.22 < C \leq 0.8 \\ 0.165 & for\ C > 0.8 \end{cases} \quad (6.565)$$

$$\bar{\dot{q}} = \overline{\dot{q}_b} + \overline{\dot{q}_d} \quad (6.566)$$

where $\bar{\dot{q}}_{Tot}$ is the total solar radiation incident on the surface of the PV and is composed of the beam, diffused and ground reflected radiation averaged over the time step.

The energy balance equation on the PV array yields:

$$\tau\alpha\bar{\dot{q}}_{Tot} = \eta_c\bar{\dot{q}}_{tot} + U(T_{cell} - T_a) \quad (6.567)$$

where the solar energy absorbed by the PV array ($\tau\alpha\bar{\dot{q}}_{Tot}$) is equal to the electrical output ($\eta_c\bar{\dot{q}}_{Tot}$) plus the heat transfer ($U(T_{cell} - T_a)$) to the surroundings.

Rearranging Eq. (6.567) to calculate the PV cell temperature yields:

$$T_{cell} = T_a + \bar{\dot{q}}_{tot}\left(\frac{\tau\alpha}{U}\right)\left(1 - \frac{\eta_c}{\tau\alpha}\right) \quad (6.568)$$

But, at no load operation $\eta_c = 0$ and nominal cell operating temperature the ($\frac{\tau\alpha}{U}$) is replaced by:

$$\frac{\tau\alpha}{U} = \frac{T_{cell,nom} - T_{a,nom}}{\bar{\dot{q}}_{Tot,nom}} \quad (6.569)$$

where $T_{cell,nominal}$ is manufacturer's reported PV nominal cell temperature at $\bar{\dot{q}}_{Tot,nominal} = 0.8\ \frac{kW}{m^2}$ and $T_{a,nominal}$ =20 ℃ .

Substituting Eq. (6.569) into (6.568) yields:

$$T_{cell} = T_a + \bar{\dot{q}}_{tot}\left(\frac{T_{cell,nom} - T_{a,nom}}{\bar{\dot{q}}_{Tot,nom}}\right)\left(1 - \frac{\eta_c}{\tau\alpha}\right) \quad (6.570)$$

where $\tau\alpha = 0.9$, note that $\frac{\eta_c}{\tau\alpha}$ is relatively small compared to unity

$$\eta_{mp} = \eta_{mp,STC}\left(1 + \partial(T_{cell} - T_{cell,STC})\right) \quad (6.571)$$

where η_{mp} is the efficiency of the PV array at its maximum power point and $\eta_{mp,STC}$ is the maximum power point efficiency under standard test conditions. $T_{cell,STC} = 25$℃ is

the PV cell temperature under standard test conditions. ∂ is the temperature coefficient of power $\frac{\%}{℃}$ and is always negative because the efficiency of the PV array decreases with increasing cell temperature:

$$T_{cell} = \frac{T_{amb}+(T_{cell,nom}-T_{a,nom})\left(\frac{\bar{q}_{tot}}{\bar{q}_{tot,nom}}\right)\left(1-\frac{\eta_{mp,STC}\left(1+\alpha_p(T_{cell}-T_{cell,STC})\right)}{\tau\alpha}\right)}{1+(T_{cell,nom}-T_{a,nom})\left(\frac{\bar{q}_{tot}}{\bar{q}_{tot,nom}}\right)\left(\frac{\alpha_p\eta_{mp,STC}}{\tau\alpha}\right)} \quad (6.572)$$

Here, the temperatures are in Kelvin.

Once the PV cell temperature is calculated at every time step, the corresponding PV power output is calculated by:

$$\dot{P}_{output} = \dot{P}_{nominal} f_{PV}\left(\frac{\bar{q}_{tot}}{\bar{q}_{nominal}}\right)\left(1+\alpha_p(T_{cell}+T_{cell,STC}\right) \quad (6.573)$$

where $\dot{P}_{output}$ is the PV array output power and $\dot{P}_{nominal}$ is the rated capacity of PV array,f_{PV} is a derating factor for PV power output due to soil, age, wiring losses, etc.

6.2.3.7 Battery analysis

The following equations evaluate the battery charge and discharge power:

$$\dot{P}_{batt,disch} = \left(\frac{k\dot{z}_1 e^{-k\Delta t}+\dot{z}_{\text{batt}}kx(1-e^{-k\Delta t})}{1-e^{-k\Delta t}+x(k\Delta t-1+e^{-k\Delta t}}\right) \quad (6.574)$$

$$\dot{P}_{batt,chg} = \left(\frac{-\dot{z}_{theo}kx+k\dot{z}_1 e^{-k\Delta t}+\dot{z}_{\text{batt}}kx\left(1-e^{-k\Delta t}\right)}{1-e^{-k\Delta t}+x(k\Delta t-1+e^{-k\Delta t}}\right) \quad (6.575)$$

$$\dot{z}_{\text{batt}} = \dot{z}_1 + \dot{z}_2 \quad (6.576)$$

where $\dot{z}_1$ stands for the available energy kWh in the battery at the beginning of the time step Δt and $\dot{z}_2$ is the bound energy kWh in the battery at the beginning of the time step while x is the battery capacity ratio (unit-less) and k is the battery rate constant.

6.2.3.8 Hydro analysis

The following equations calculate the hydro turbine nominal and actual power after evaluating the effective head (h_{eff}).

$$\dot{P}_{hyd,nom} = \frac{\eta_{hyd}\rho_w \dot{V}_{design} g h_{dist}}{1000} \quad (6.577)$$

where η_{hyd} is hydro turbine efficiency and $\dot{V}_{design}$ is the design flow rate while g is the gravitational acceleration and h_{dist} is the available hydro head distance.

$$\dot{P}_{hyd} = \frac{\eta_{hyd}\rho_w \dot{V}_{design} g h_{eff}}{1000} \tag{6.578}$$

$$h_{eff} = h_{dist}\left(1 - f_{fric}\right) \tag{6.579}$$

where h_{eff} is the effective hydro head and f_{fric} is the frictional loss in the hydro pipeline, expressed as a fraction of the available head.

6.2.3.9 System III and its subsystems overall efficiencies

The following equations give the energetic and exergetic efficiencies for the overall system and the overall subsystems.

$$\eta_{ov} = \frac{\dot{P}_{hyd}+\dot{P}_{PV}+\dot{m}_{15}(h_{14}-h_{15})+\dot{m}_{45}(h_{45}-h_{51})+\dot{Q}_{hp,ev}}{\dot{P}_{pmp,tot}+\dot{W}_{comp}+\dot{q}_s A_s} \tag{6.580}$$

$$\psi_{ov} = \frac{\dot{P}_{hyd}+\dot{P}_{PV}+\dot{m}_{15}(h_{14}-h_{15}-T_o(s_{14}-s_{15}))+\dot{m}_{45}(h_{45}-h_{51}-T_o(s_{45}-s_{51}))+\dot{Q}_{hp,ev}\left(1-\frac{T_0}{T_{hp,ev}}\right)}{\dot{P}_{pmp,tot}+\dot{W}_{comp}+\dot{q}_s A_s\left(1-\frac{T_0}{T_{sun)}}\right)} \tag{6.581}$$

- Overall heat transformer system efficiencies

$$\eta_{htrs,ov} = \frac{\dot{Q}_{abs}}{\dot{P}_{pmps}+\dot{Q}_{gen}+\dot{Q}_{ev}} \tag{6.582}$$

$$\psi_{htrs,ov} = \frac{\dot{Q}_{abs}\left(1-\frac{T_0}{T_{abs}}\right)}{\dot{P}_{pmps}+\dot{Q}_{gen}\left(1-\frac{T_0}{T_{gen}}\right)+\dot{Q}_{ev}\left(1-\frac{T_0}{T_{ev}}\right)} \tag{6.583}$$

- Overall distillation system efficiencies

$$\eta_{desal,ov} = \frac{\dot{m}_{15}h_{15}}{\dot{P}_{pmps}+\dot{Q}_{s,net}} \tag{6.584}$$

$$\psi_{desal,ov} = \frac{\dot{m}_{15}(h_{15}-h_o-T_o(s_{15}-s_o))}{\dot{P}_{pmp,tot}+\dot{Q}_s\left(1-\frac{T_0}{T_{sun}}\right)} \tag{6.585}$$

- GSHP system overall efficiencies

The following equations evaluate the energetic, exergetic and reversible coefficient of performance of the ground source heat pump for cooling and heating cycles with a heat exchanger and without a heat exchanger.

Cooling cycle

$$COP_{hp,cyc} = \frac{\dot{Q}_{ev}}{\dot{W}_{comp}} \tag{6.586}$$

$$COP_{hp,cool,rev} = \frac{(T_{ev}+273)}{(T_{con}-T_{ev})} \tag{6.587}$$

$$COP_{\psi,hp,cool} = \frac{\dot{Q}_{ev}(1-\frac{T_o}{T_{ev}})}{\dot{W}_{comp}} \tag{6.588}$$

$$COP_{hp,cool,+hex} = \frac{\dot{Q}_{ev}+\dot{Q}_{hex}}{\dot{W}_{comp+\dot{W}_{pmp}}} \tag{6.589}$$

$$COP_{\psi,hp,cool,+hex} = \frac{\dot{Q}_{ev}(1-\frac{T_o}{T_{ev}})+\dot{Q}_{hex}(1-\frac{T_o}{T_{50}})}{\dot{W}_{comp}+\dot{W}_{pmp}} \tag{6.590}$$

Heating cycle

$$COP_{hp,heat} = \frac{\dot{Q}_{ev,heat}}{\dot{W}_{comp}} \tag{6.591}$$

$$COP_{hp,heat,rev} = \frac{(T_{ev,heat}+273)}{(T_{ev,heat}-T_{con})} \tag{6.592}$$

$$COP_{\psi,hp,heat} = \frac{\dot{Q}_{ev,heat}(1-\frac{T_0}{T_{ev}})}{\dot{W}_{comp}} \tag{6.593}$$

$$COP_{hp,heat,+hex} = \frac{\dot{Q}_{ev,heat}+\dot{Q}_{ev,hex}}{\dot{W}_{comp+\dot{W}_{pmp}}} \tag{6.594}$$

$$COP_{\psi,hp,heat,+hex} = \frac{\dot{Q}_{ev,heat}(1-\frac{T_0}{T_{ev}})+\dot{Q}_{ev,hex}(1-\frac{T_0}{T_{50}})}{\dot{W}_{comp+\dot{W}_{pmp}}} \tag{6.595}$$

Chapter 7: Results and Discussion

The design of a net-zero energy house is established by following the procedures outlined in section 6.1. The developed systems that provide the house with electricity, hot and fresh water and seasonal air-conditioning are shown in Figures 4.8, 4.9 and 4.10.

First, thermal and acoustic sizes, of insulation materials chosen for this study are determined and the heat load calculations are carried out. Secondly, the total electrical *kW* needed for the house is calculated, and then the optimum power system is selected based on minimum NPC, minimum CO_2 emissions and maximum renewable energy fraction. After which, energy and exergy analyses are conducted to assess the overall system performance along with exergo-economic analysis. Finally, the selected system is optimized for minimizing overall system cost and maximizing exergetic efficiency. Assessment for zero energy house classification is investigated.

7.1 Calculating the thermal and acoustic insulation material sizes

After conducting the impedance tube and enclosure experiments (Appendix D) a Matlab code (Appendix B) is generated to produce the results as shown in Figures 7.1 and 7.2.

An examination of Figure 7.1 indicates that the sound pressure level *SPL* of the ambient noise plus the 1000*Hz* sinusoidal noise is 75 dB, while the *SPL* of the tested specimen of one inch rigid expanded polystyrene foam and 3 inch Roxul fiber glass insulation combined as one layer is 35 dB, which means that a reduction of 40 dB is achieved by using an enclosure of (1″+3″) combination.

The second experiment, using the same noise conditions, but this time a (2″ + 3″) combination of the above same material is tested and the measured *SPL* as seen in Figure 7.1 is 15 dB. Therefore, the 1″ rigid expanded polystyrene foam has the power to attenuate 20 dB and is equal to that of the 3″ fiber glass insulation. These results are verified by the impedance tube experiment as shown in Figure 7.2 where the two specimens used in experiments 1 and 2 above have the same reflection coefficient. The thermal and acoustic insulation sizes that satisfy the problem statement are determined by

a software code which optimizes the thicknesses to be at, 4.1″ and 2.3″ for the wall and 4.72″and 2.3″ for the roof structures.

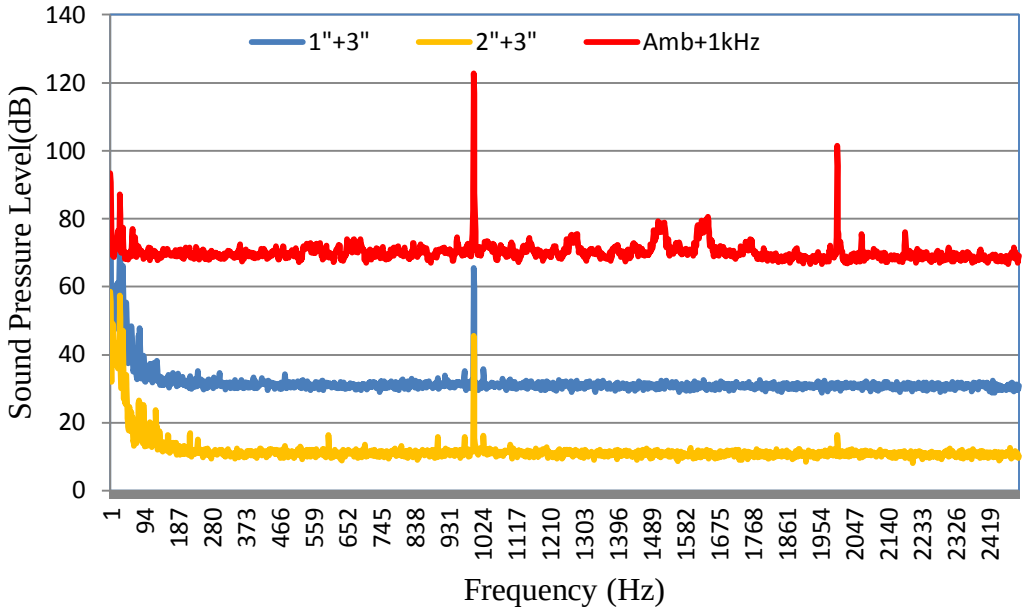

Figure 7.1: Sound pressure Level for ambient noise +1000 *Hz* sinusoidal wave vs. a combination of (1" + 3", 2″+3″) materials measured at different frequencies.

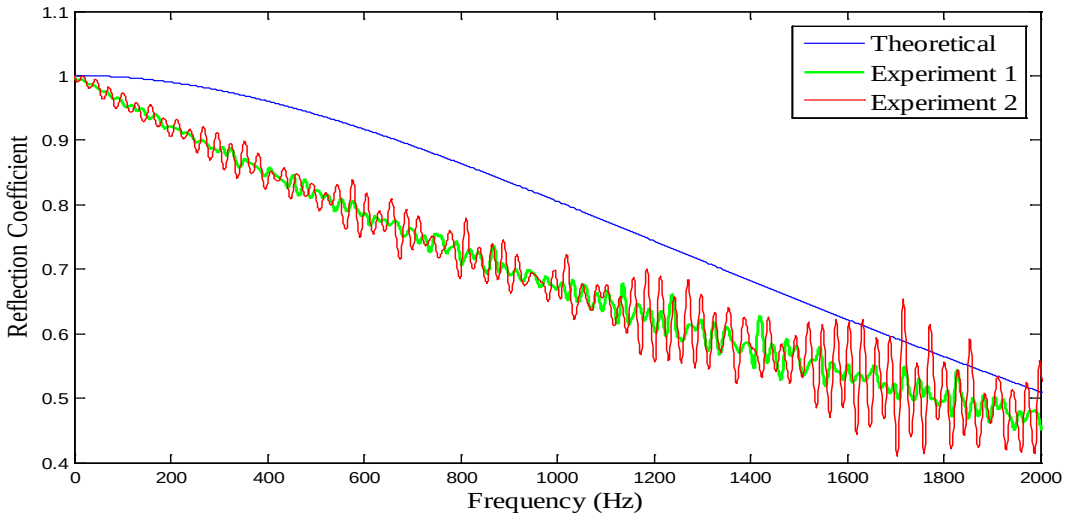

Figure 7.2: Reflection coefficients of materials used in experiments 1 and 2 vs. the theoretical coefficient of open impedance tube measured at various frequencies.

7.2 Calculating the seasonal heat loads

The building wall and roof compositions are finalized by the previous step and the rest of the design criteria are carried out to enable savings in energy requirements. Special care is given to the glass to wall ratio as not to exceed 20%. Summer and winter loads are calculated using Carrier's *HAP* for design temperatures as shown in Table 7.1. The building heat transfer coefficients are set low to minimize the seasonal loads and the results obtained by the simulation software are 4601*W* for summer cooling and 1703 *W* for winter heating.

Table 7.1: Design temperature values for summer cooling and winter heating.

Air temperature	Cooling	Heating
Outside dry bulb (℃)	32.8	5.6
Outside wet bulb (℃)	25.6	1.8
Inside dry bulb (℃)	23	21.1
Inside relative humidity (%)	50	50

7.3 Calculating the total connected load

After determining the heat loads of the house, the total peek electrical usage is calculated at 4.3 kW and the average electrical daily demand is 90kWh/day, which is the basis for our modeling and optimization.

7.4 System I results

7.4.1 Optimized power system

The basis for our power system optimization is to minimize the total NPC of the power system and the CO_2 emissions. Huge numbers of simulations are conducted and the following power configuration as shown in Table 7.2 is composed of 12 kW PV array, 10 kW wind turbine, 20 batteries of 2 volts capacity each, 5kw inverter and rectifier each. The total net present cost of the system is $56,558.00 as seen in table 7.3. Figure 7.3 and table 7.4 shows the cash flow for the various components of the selected optimized renewable energy system with values of the initial, replacement, maintenance and operation, fuel consumption and salvage costs.

Table 7.2: System I optimized renewable energy power system architecture.

PV Array	12 kW
Wind turbine	1 Generic 10kW
Diesel Generator 1	2 kW
Battery	20 Hoppecke 24 OPzS 3000
Inverter	5 kW
Rectifier	5 kW

Table 7.3: Optimized renewable energy power system cost summary.

Total net present cost	$ 56,558
Levelized cost of energy	$ 0.127/kWh
Operating cost	$ 411/yr

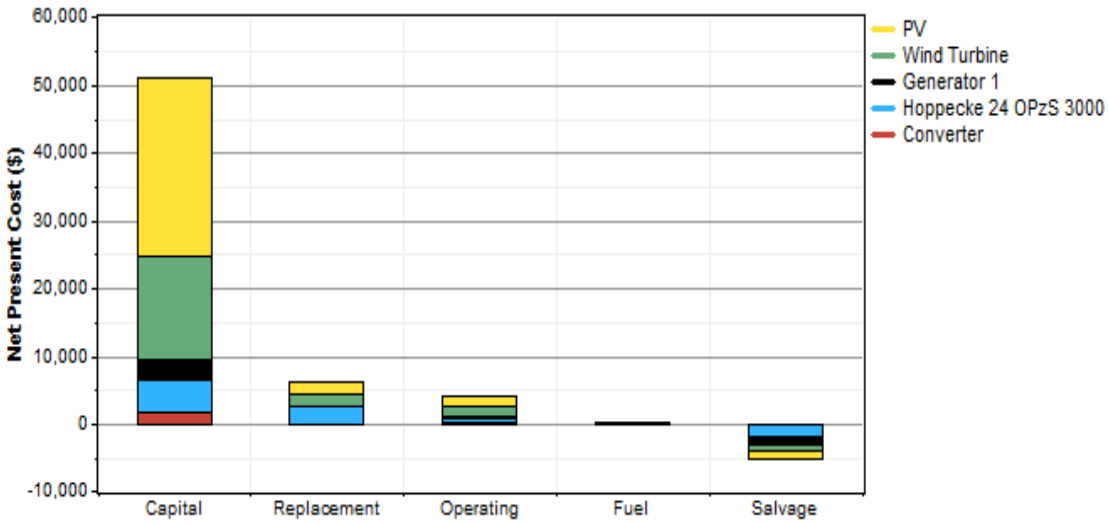

Figure 7.3: System I optimized renewable energy power system cash flow summary.

The salvage values are shown as negative in Figure 7.3, when in fact, they are revenue and hence positive. The values shown in the figure are plotted with a reverse sign for clarity reasons and so are the values in table 7.4.

Table 7.5 gives the optimized renewable energy power system annualized cost with the photovoltaic system being the highest at $/yr 2,129.00 followed by the wind turbine at $/yr 1,259.00 with a total annualized system cost of $/yr 4,162.00. The annualized cost is

determined in order to evaluate the levelized cost of energy which is given as the annualized cost divided by the total annual electrical load served.

Table 7.4: Optimized renewable energy power system net present costs.

Component	Capital Cost ($)	Replacement Cost ($)	Operation and Maintenance Cost ($)	Fuel Cost ($)	Salvage Revenue ($)	Total ($)
PV	26,400	1,999	1,631	0	-1,095	28,934
10kW	15,000	1,666	1,359	0	-913	17,112
Generator 1	3,000	0	408	303	-1,260	2,451
Hoppecke 24 OPzS 3000	5,000	2,610	544	0	-1,810	6,343
Converter	1,571	0	146	0	0	1,717
System	50,971	6,275	4,087	303	-5,078	56,558

Table 7.5: Optimized renewable energy power system annualized costs.

Component	Capital Cost ($)	Replacement Cost ($)	Operation and Maintenance Cost ($)	Fuel Cost ($)	Salvage Cost ($)	Total Cost ($)
PV	1,943	147	120	0	-81	2,129
Wind Turbine	1,104	123	100	0	-67	1,259
Generator 1	221	0	30	22	-93	180
Batteries	368	192	40	0	-133	467
Converter	116	0	11	0	0	126
System	3,751	462	301	22	-374	4,162

Table 7.6: Optimized renewable energy power system electrical configuration.

Component	Production (kWh/yr)	Fraction (%)
PV array	28,566	54
Wind turbine	24,654	46
Generator 1	73	0
Excess electricity	14,982	28.1
Renewable fraction	-	0.998

As seen in table 7.6, the PV array has the highest electrical production 28,566.00 kWh/year, while, the wind turbine produces kWh/year 28,566.00 and the generator 73 kWh/year. There is an excess electricity of kWh/year 14,982.00 and the systems total renewable fraction is 0.998.

Table 7.7 and Figure 7.4 outline the electrical configuration and PV electrical output respectively. The efficiency of the PV arrays is 27.2% and the levelized cost of electricity is 0.0745 $/kWh.

Table 7.8 and Figure 7.5 show the electrical configuration and wind turbine electrical output respectively. The efficiency of the wind turbine is 28.1% and the levelized cost of electricity is 0.0511 $/kWh. The wind penetration is 75.1% which is the average power output of the wind turbine divided by the average primary load.

Table 7.7: PV electrical configuration.

Quantity	Value
Rated capacity	12 kW
Mean output	3.26 kW
Mean output	78.3 kWh/d
Capacity factor	27.20%
Total production	28566 kWh/yr
Maximum output	13.4 kW
PV penetration	87%
Hours of operation	4378 h/yr
Levelized cost	0.0745 $/kWh

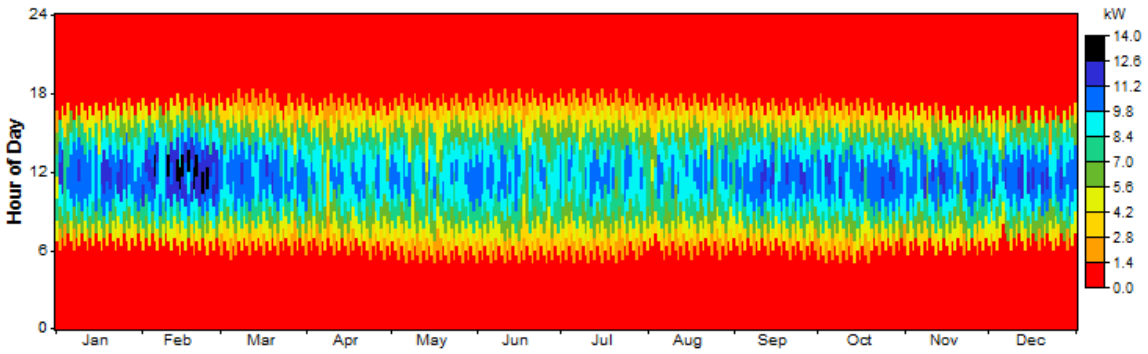

Figure 7.4: PV system electrical production.

Table 7.8: DC wind turbine electrical configuration.

Variable	Value
Total rated capacity	10.0 kW
Mean output	2.81 kW
Capacity factor	28.1%
Total production	24,654 kWh/yr
Minimum output	0.00 kW
Maximum output	9.97 kW
Wind penetration	75.1%
Hours of operation	7,628 h/yr
Levelized cost	0.0511 $/kWh

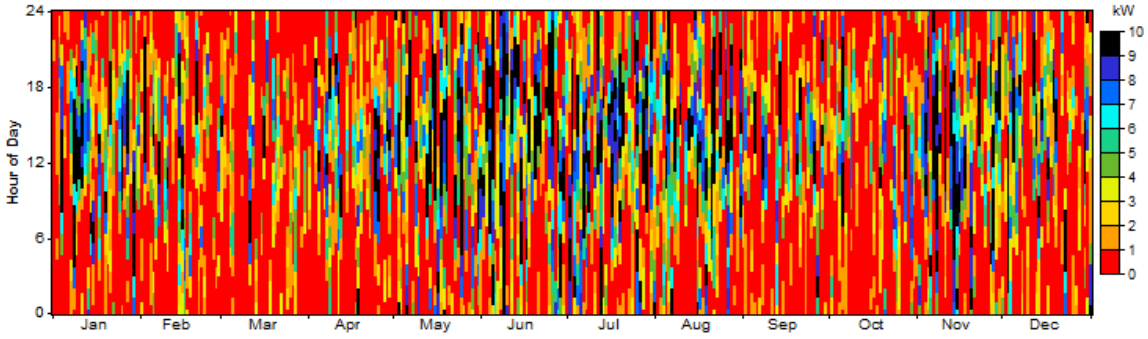

Figure 7.5: DC wind turbine system electrical production.

The diesel generator electrical configuration and power outputs are shown in Table 7.9 and Figure 7.7 respectively. The generator produces 72.9 kWh/year and starts 10 times at 60 h/year of operation. It consumes 27.8 l/year at a fuel energy input 274kWh/yr. The mean electrical efficiency is 26.6%.

Table 7.9: Diesel generator electrical configuration.

Quantity	Value
Hours of operation	60 h/yr
Number of starts	10 starts/yr
Capacity factor	0.416%
Fixed generation cost	0.828 $/h
Marginal generation cost	0.200 $/kWh
Electrical production	72.9 kWh/yr
Mean electrical output	1.22 kW
Min. electrical output	0.600 kW
Max. electrical output	2.00 kW
Fuel consumption	27.8 L/yr
Specific fuel consumption	0.382 L/kWh
Fuel energy input	274 kWh/yr

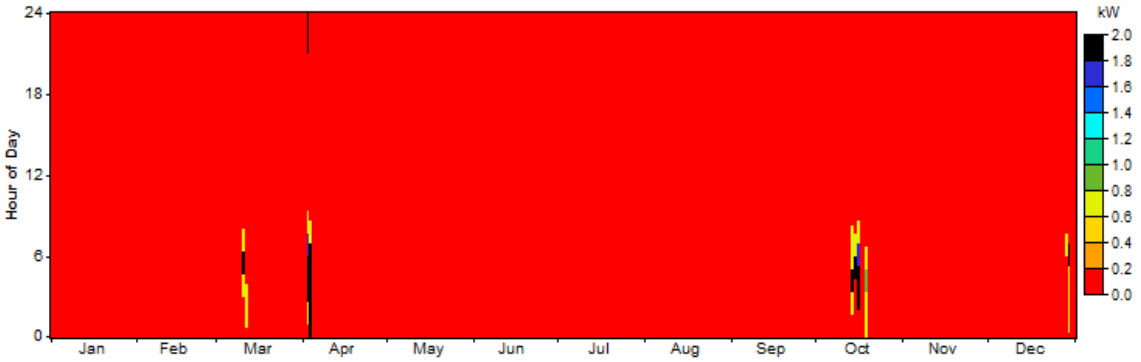

Figure 7.6: Diesel generator electrical production.

Table 7.10 gives the battery system architecture where 20 batteries are connected in parallel with a Bus voltage of 2 volts each.

Table 7.11 indicates the battery system electrical configuration where the usable nominal capacity is 84.00 kWh, while the battery bank autonomy, the ratio of the battery bank size to the electric load is 22.4 *h* and the annual throughput, the amount of energy that cycle through the battery bank in one year is 12,303.00 kWh /yr.

Table 7.10: Battery system architecture.

Quantity	Value
String size	1
Strings in parallel	20
Batteries	20
Bus voltage (V)	2

Figure 7.7 shows the yearly battery system charging state for 24 hours a day in percentage form. It is noticed that the minimum state of charge of 30% is not broken during the optimization as recommended by the manufacturer.

Table 7.11: Battery system electrical configuration.

Quantity	Value
Nominal capacity	120 kWh
Usable nominal capacity	84.0 kWh
Autonomy	22.4 h
Lifetime throughput	203,920 kWh
Energy in	13,245 kWh/yr
Energy out	11,410 kWh/yr
Storage depletion	-2.37 kWh/yr
Losses	1,838 kWh/yr
Annual throughput	12,303 kWh/yr

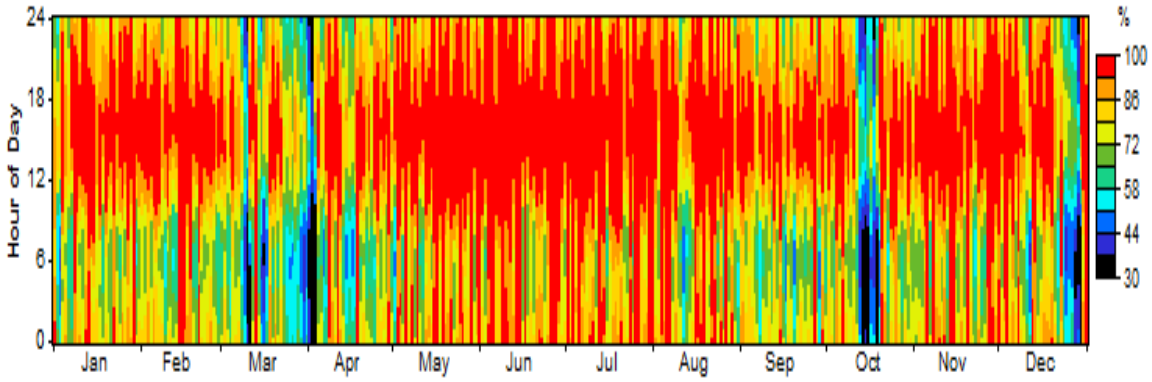

Figure 7.7: Battery system charging state (%).

The electrical configuration of the converter system is presented in Table 7.12. The rated capacity is 5.00 kW with efficiency of 74.8%. The energy losses are 3639 kWh/year for 8755 hours of operation and the maximum output is 4.33 kW.

Table 7.12: Converter system electrical configuration.

Quantity	Inverter	Rectifier	Units
Capacity	5.00	5.00	kW
Mean output	3.74	0.00	kW
Minimum output	0.00	0.00	kW
Maximum output	4.33	0.00	kW
Capacity factor	74.8	0.0	%
Hours of operation	8,755	0	hrs/yr
Energy in	36,404	0	kWh/yr
Energy out	32,764	0	kWh/yr
Losses	3,639	0	kWh/yr

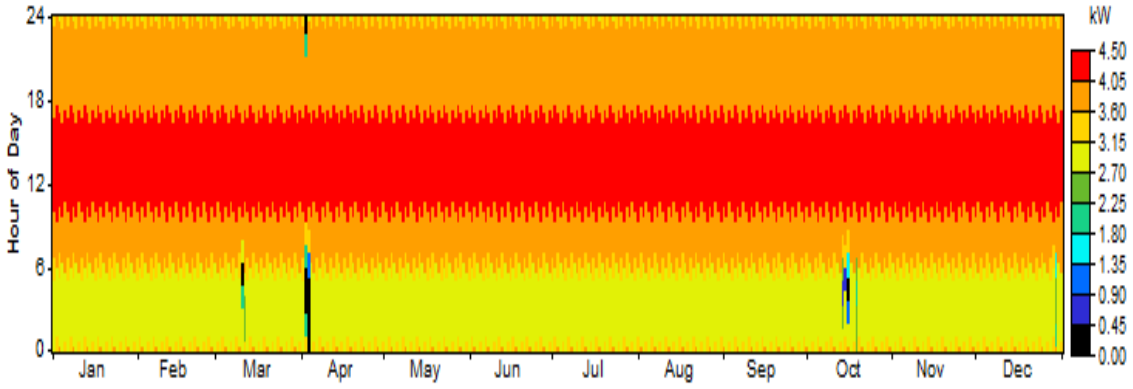

Figure 7.8: Inverter electrical output.

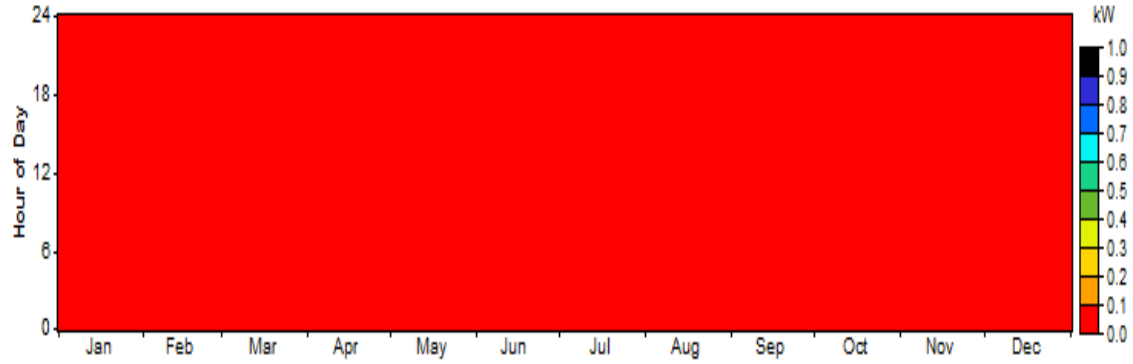

Figure 7.9: Rectifier electrical output.

Table 7.13: Optimized renewable energy power system emissions.

Pollutant	Annual Emissions (kg)
Carbon dioxide	73.3
Carbon monoxide	0.181
Unburned hydrocarbons	0.02
Particulate matter	0.0136
Sulfur dioxide	0.147
Nitrogen oxides	1.61

Table 7.13 gives the yearly green gases emissions in *kg* for the selected optimal power system where CO_2 is highest at 73.3 kg/yr followed by nitrogen oxides at 1.61 kg/yr

The inverter and rectifier monthly electrical outputs are shown in Figures 7.8, 7.9 for 24 hours a day. The inverter output power is a maximum between 11:00 am and 17:00 pm while the rectifier output is zero.

Table 7.14 indicates different power system configurations with corresponding total net present cost. The best optimum power structure corresponds to power scheme 1 with NPC of $56,558.00. Removing the diesel generator and wind turbine from the power structure as in schemes 6, 7, and 8 increases the NPC between $15,000.00 and $25,000.00 as compared to scheme 1 ,while eliminating the PV system as in schemes 9,10 and 11 raises the NPC between $27,000.00 and $30,000.00.

Table 7.14: Total NPC for different renewable system configurations [64].

Power Structure	PV Capacity (kW)	Wind Turbine (Capacity) (kW)	Diesel Generator Capacity (kW)	Battery Quantity and Type (Hoppecke 24 OPzS 3000)	Converter Capacity (kW)	Total NPC ($)
1	12	1x10	2	20	5	56,558
2	12	1x10	0	36	6	58,085
3	14	1x10	0.5	18	5	59,149
4	10	1x10	4	32	5.5	59,193
5	20	0	0	60	6	71,915
6	24	0	0	40	6	76,017
7	30	0	0	14	5	81,952
8	0	3x8.1	3.5	40	10	83,100
9	0	2x8.1	4	60	5	85,005

7.4.2 Exergy analysis results

A sensitivity analysis on the system components is carried out by varying several parameters. EES software is used to calculate all the system properties and develop the parametric studies.

The effect of keeping these parameters, $T_o = 25^{\circ}C$, $T_{eva} = 7^{\circ}C$, $T_{gen,} = 80^{\circ}C$ $and\ T_{w,eva} = 17^{\circ}C$ constant, designated here as the reference system, are shown for the overall COP for the absorption chiller, liquid desiccant system and the overall system efficiencies in Figures 7.10 and 7.11 respectively.

The energetic COP, varies from 0.24 to 0.14 and from 0.3 to 0.1 for the LDS and absorption chiller respectively, at 8.00 am and 2:00 pm, due to increase in generator heat as seen in Figure 7.10 while the exergetic COP, varies from 0.14 to 0.07 and from 0.09 to 0.04 for the LDS and absorption chiller respectively, at 8.00 am and 2:00 pm.

The overall efficiency varies between 80% and 46% at 8.00am and 2.00 pm due to solar and velocity changes while the overall system exergy varies between 41 % and 26 % at 8.00 am and 2.00 pm. These results clearly indicate that the exergetic analysis represents a better sensitivity analysis of the system performance than energy.

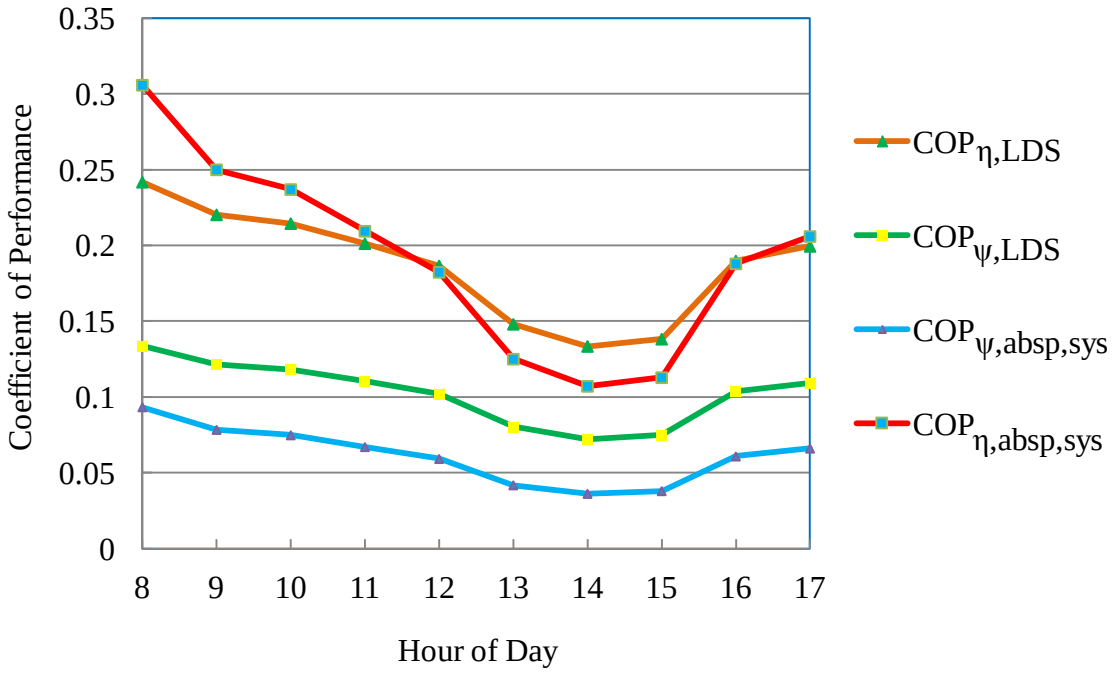

Figure 7.10: Energy and exergy coefficients of performance for the absorption chiller and liquid desiccant system.

Figure 7.12 shows the system thermal heats for several components. The percentage and values of exergy destruction for system components are presented in figures 7.13 and 7.14. The system component efficiencies are presented in figure 7.15. The absorber followed by the regenerator and LDS condenser has the highest exergy destruction rate, because, chemical exergy losses caused by heat of solution, due to absorption and desorption and the high energy needed to condense the steam at the condenser.

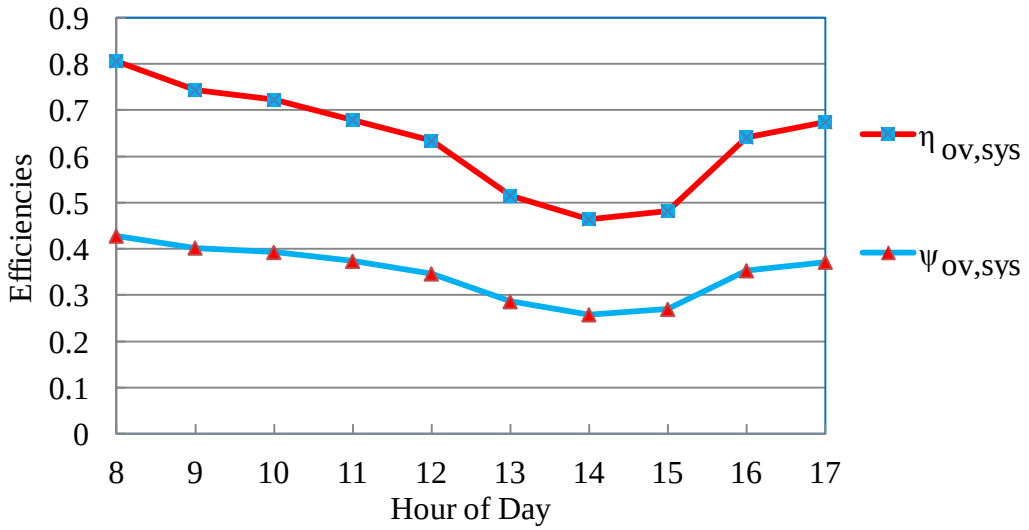

Figure 7.11: Energy and exergy efficiencies of the overall system.

The efficiency of the photovoltaic thermal system was improved by an average of 35%, while the exergetic efficiency by 5%, as shown in Figure 7.16. The behavior of the PV/T system energy efficiency curve differs from that of the PV, because, changes in air velocity affects the heat losses.

Changing the reference temperature as shown in Figures 7.17 and 7.18, causes the exergetic COP, of the absorption system to increase from 0.06 to about 0.1 at maximum T_0 because the factor $\dot{Q}_{gen}\left(1-\frac{T_0}{T_{gen}}\right)$ decreases more than $\dot{Q}_{eva}\left(\frac{T_0}{T_{ev}}-1\right)$. The exergetic COP, of the LDS system decreases from 0.13 to about 0.04 at 2:00 pm, because the numerator in the exergy equation decreases more than the denominator when T_0 increases. While the overall exergy efficiency has the factor $\left(1-\frac{T_0}{T_{Sun}}\right)$ in the

denominator which is not affected by the range of changes in T_0 since T_{sun} is large and the numerator was affected slightly by T_0 causing an unnoticeable decrease. The energetic COP doesn't change because T_0 has no influence on it.

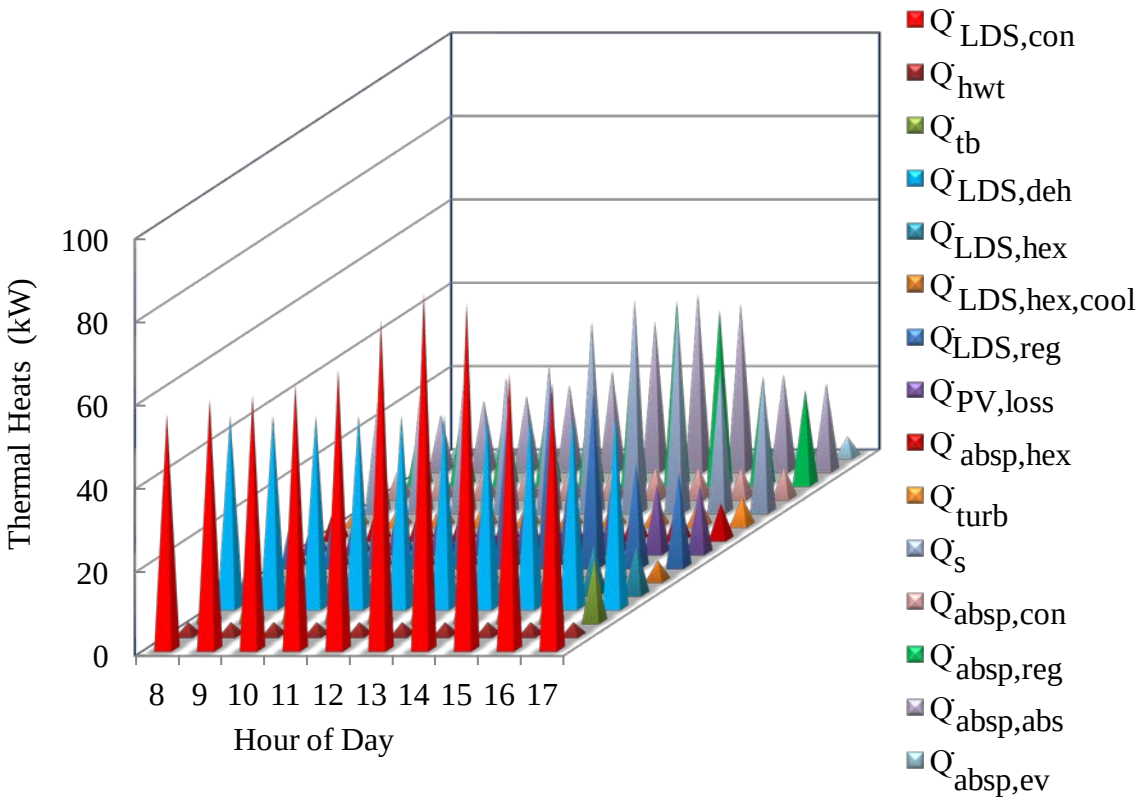

Figure 7.12: System thermal heats at different hours.

Figures 7.19 and 7.20 show comparison of COP's and overall efficiencies to the reference case of Figures 7.10 and 7.11. All parameters are fixed except for temperature of regenerators that change from 77℃ at 8:00 am to 87 ℃ at 5:00 pm at increments of 1℃ . COP of absorption chiller increases with increase in regenerator temperature and decreases with decrease in regenerator temperature, while the COP of the LDS system follow the same path as the absorption chiller but with modest variation in the COP due to other influences in the COP equation. Also, the overall and exergetic efficiencies doesn't show any changes with regenerator temperature changes, because, the changes

are about 10℃ and the influence of the regenerator on the overall efficiencies is modest as compared to other factors as shown in the corresponding equations.

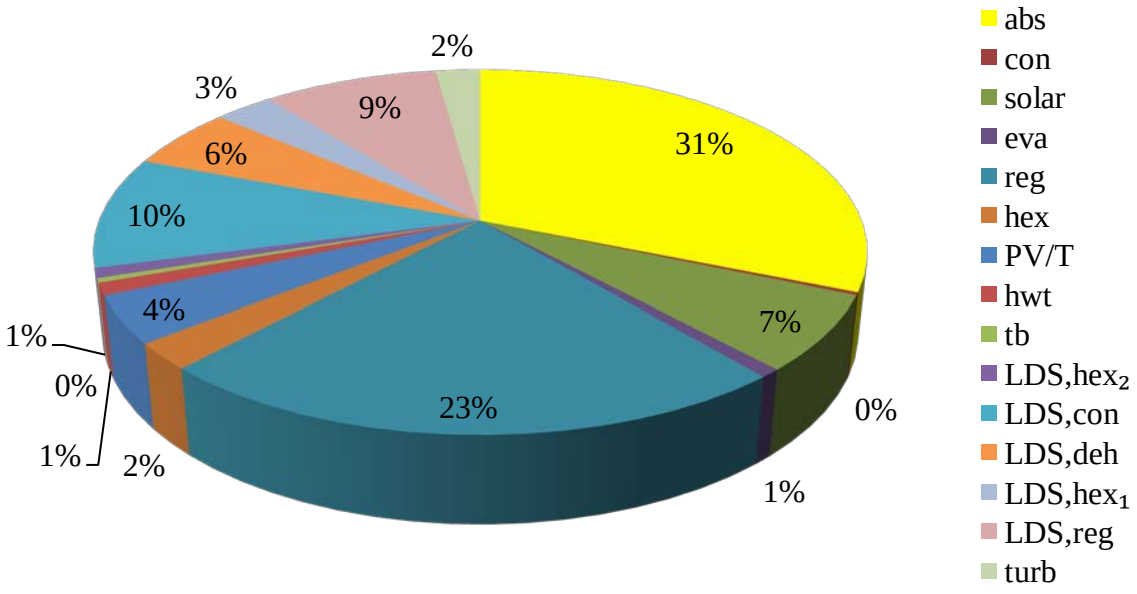

Figure 7.13: Percentage of total exergy destruction at reference system parameters.

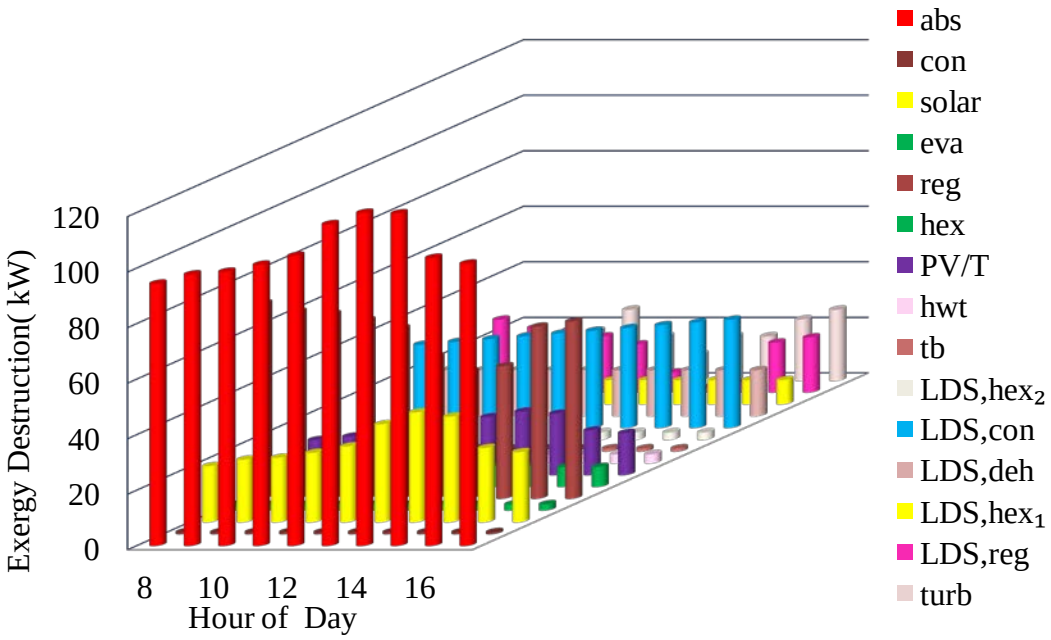

Figure 7.14: Exergy destruction for system components at reference system parameters.

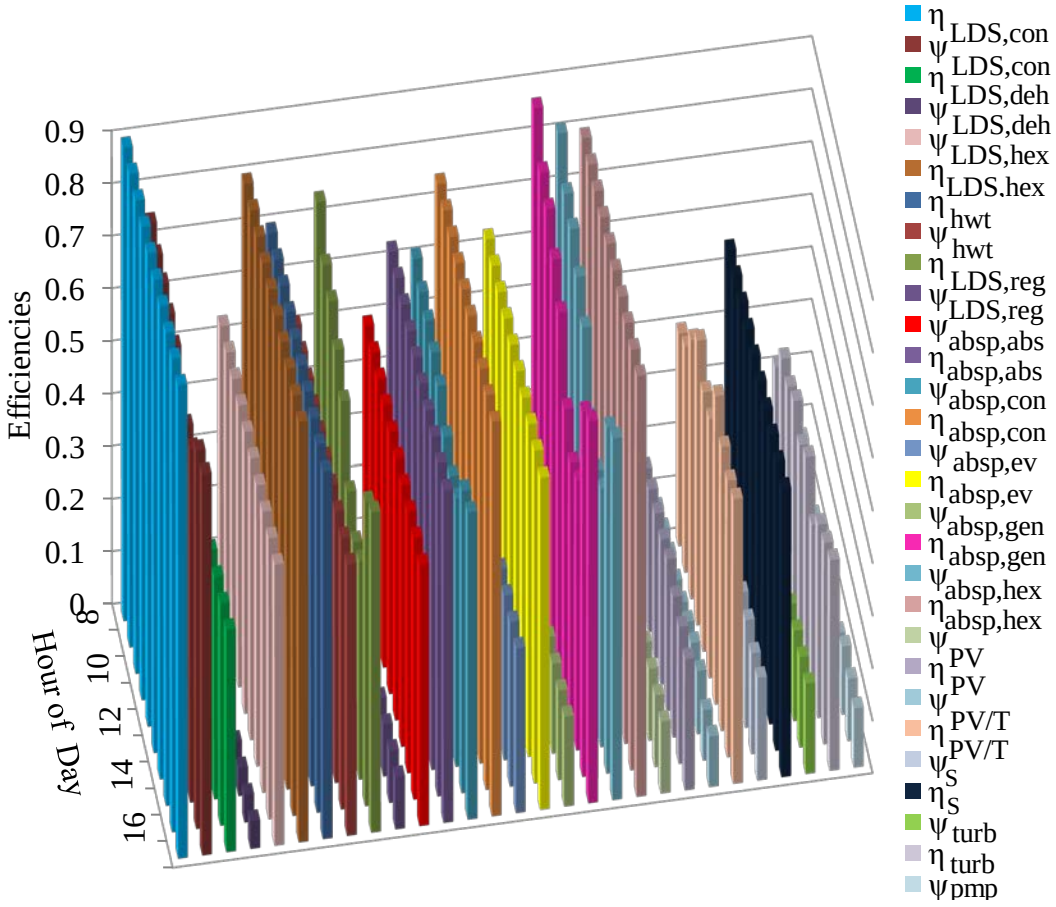

Figure 7.15: Exergy and energy efficiencies of various system components.

In Figures 7.21 and 7.20, the temperature of the evaporator is varying from 13˚C at 8:00 am to 4˚C at 5:00 pm at decrements of 1˚C, *while* $T_{gen} = 80$˚C $, T_o = 25$˚C$, T_a =$ 20˚C remains constant. We notice that the COP and exergetic COP of absorption chiller and LDS increase with decrease in evaporator temperature and decrease with increase in evaporator temperature as expected, because of changes in $\dot{Q}_{eva}$ and $\dot{Q}_{LDS,deh}$. The overall efficiency is not affected by variation in the evaporator temperature because the influence is minimal. Overall system exergy efficiency varies unnoticeably due to

limitations of $\dot{Q}_{LDS,deh}$ on the process at the specified temperatures in comparison to other parameters in the overall system exergy equation.

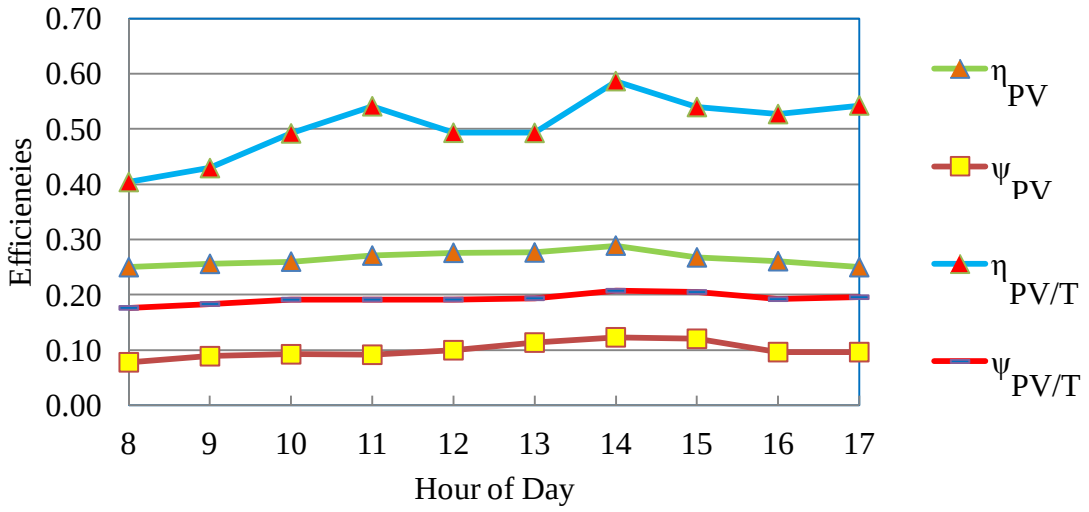

Figure 7.16: Effect of modifying the PV system to PV/T on efficiencies.

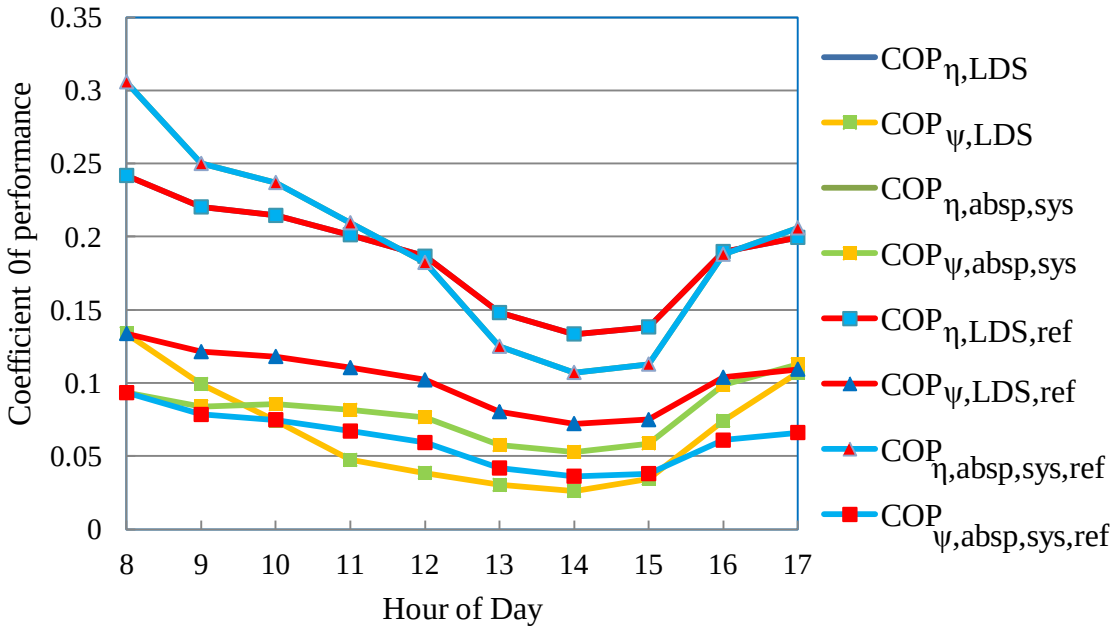

Figure 7.17: Energy and exergy coefficients of performance of the absorption and LDS systems at variable dead state temperature vs. the reference system.

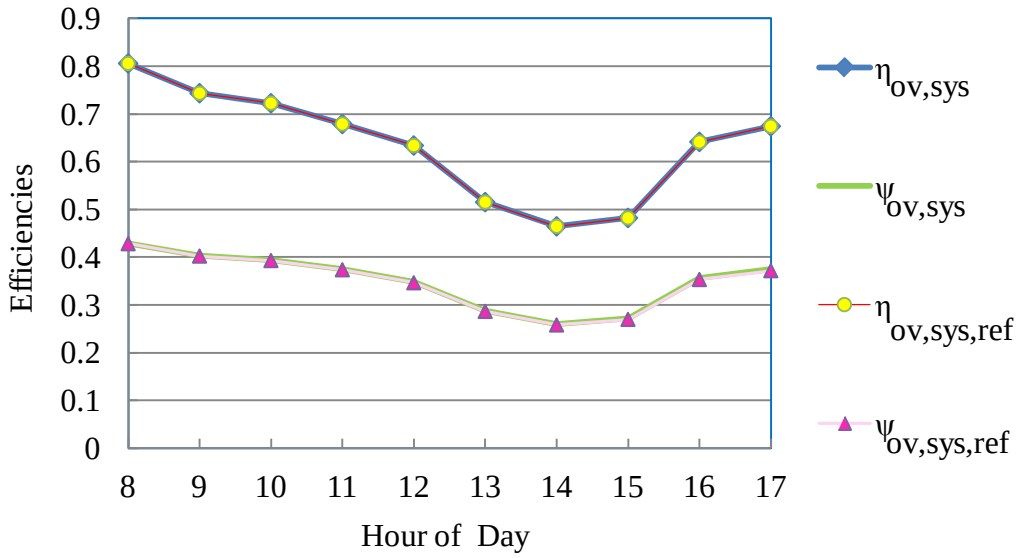

Figure 7.18: Energy and exergy efficiency of the overall system at variable dead state temperature vs. the reference system.

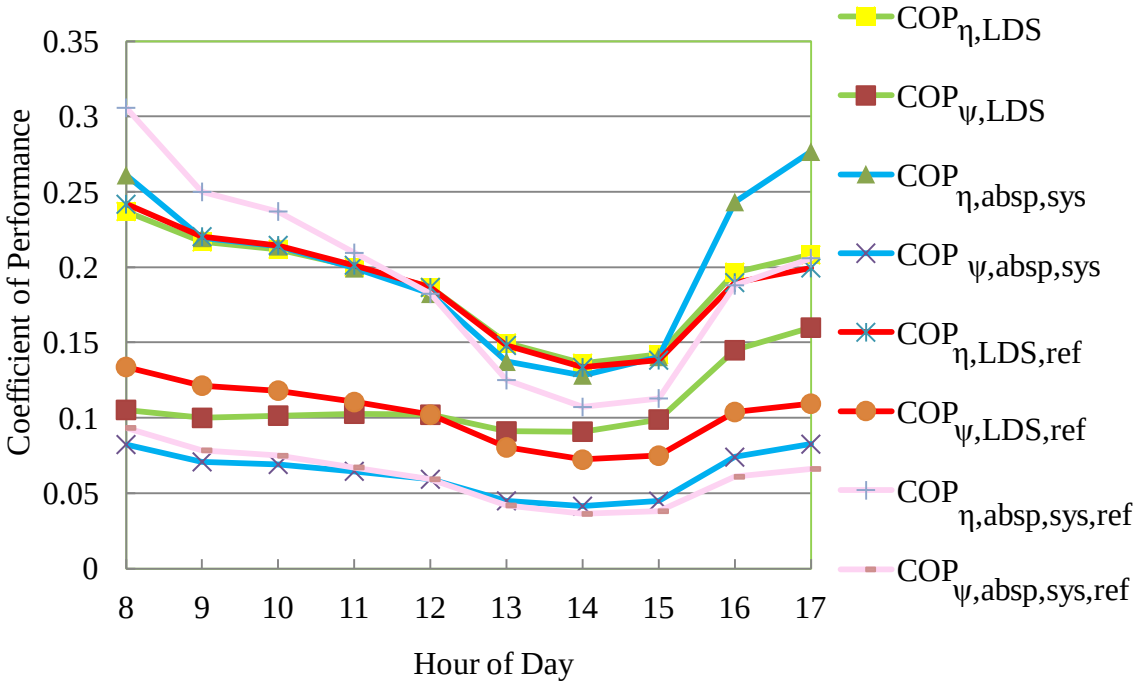

Figure 7.19: Energy and exergy coefficients of performance of the absorption and LDS systems at variable regenerator temperature vs. the reference system.

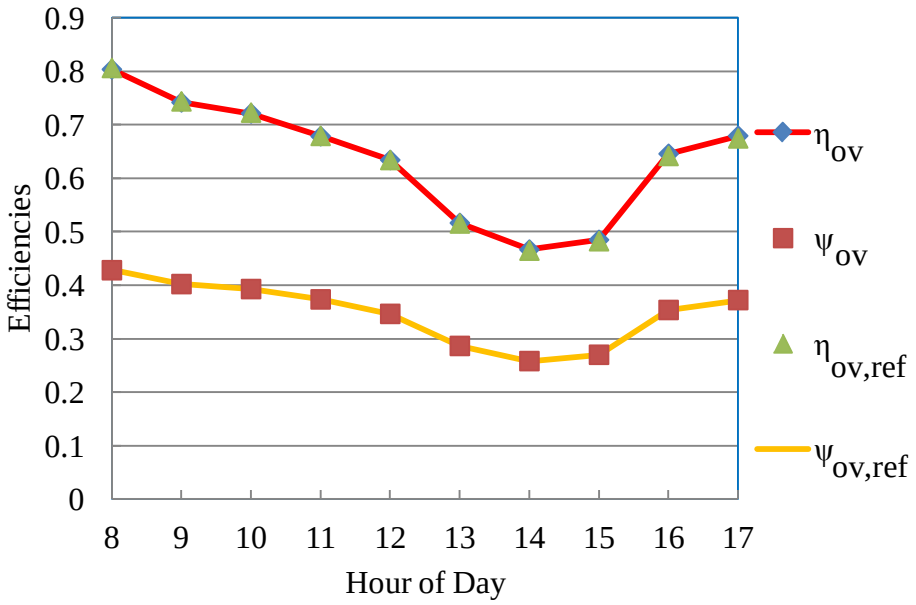

Figure 7.20: Energy and exergy efficiency of the overall system at variable regenerator temperature vs. the reference system.

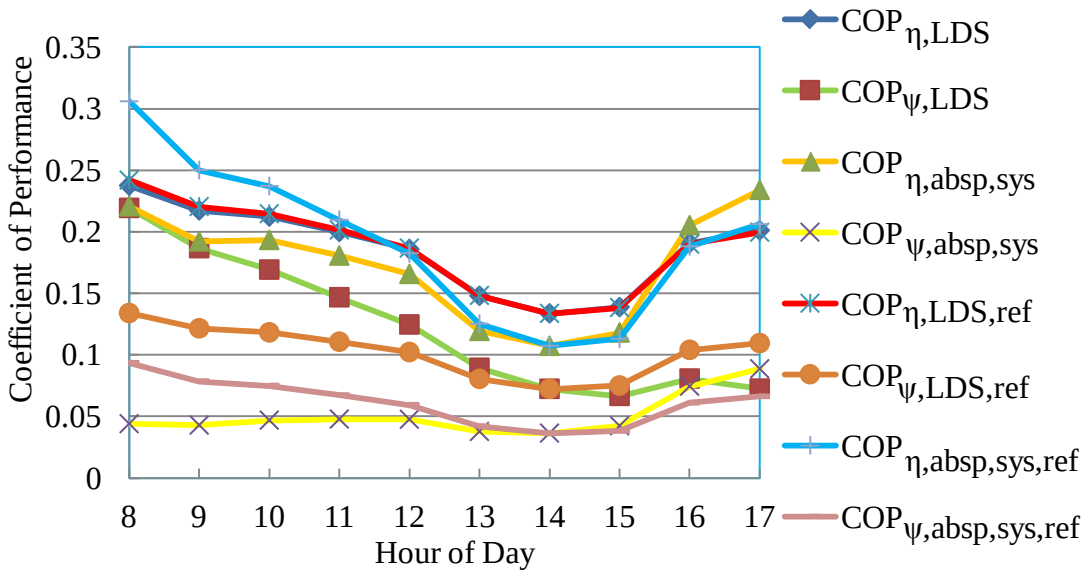

Figure 7.21: Energy and exergy coefficients of performance of the absorption and LDS systems at variable evaporator temperature vs. the reference system.

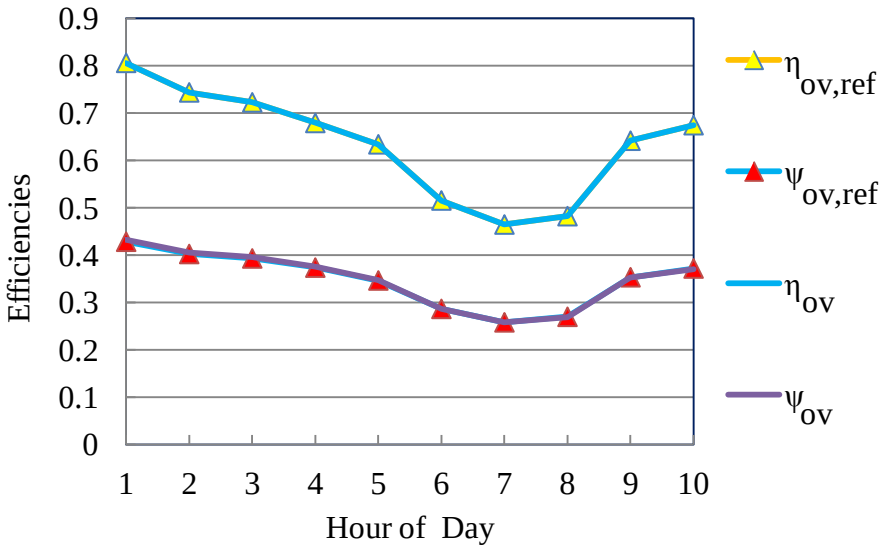

Figure 7.22: Energy and exergy efficiencies of the overall system at variable evaporator temperature vs. the reference system.

.

In Figures 7.23 and 7.24, the effect of changing the ambient temperature from 27˚C at 8:00 am to 32.8˚C at 1:00 pm and back to 29 ˚C at 5:00 pm at increments of 1˚C on the COP of the absorption chiller and LDS systems and the overall energetic and exergetic efficiency is shown. The COP and exergetic COP of the absorption chiller are not changed from those of the reference system, because, the ambient air has no influence on it. While the COP and exergetic COP of the LDS decrease with increasing ambient air because $\dot{Q}_{LDS,con}$ and $\dot{Q}_{LDS,reg}$ increase and they outweigh the increase of$\dot{Q}_{LDS,deh}$.

The energetic and exergetic efficiencies of the overall system decrease with decreasing ambient temperature due to the same reasoning of decreasing values of $\dot{Q}_{LDS,con}$, $\dot{Q}_{LDS,reg}$ and $\dot{Q}_{LDS,deh}$.

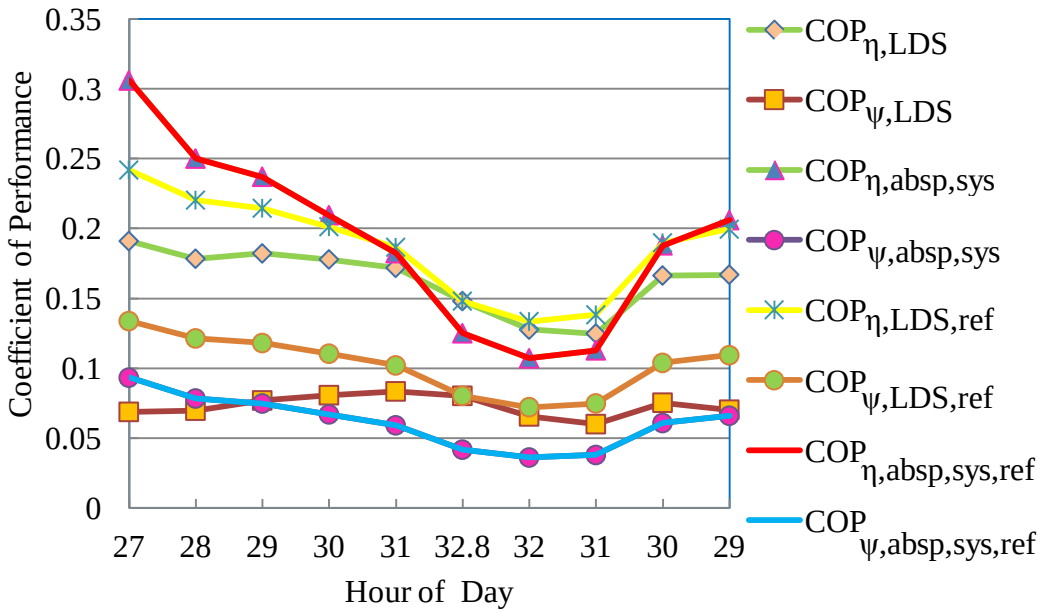

Figure 7.23: Energy and exergy coefficient's of the absorption and LDS systems at variable T_{amb} vs. the reference system.

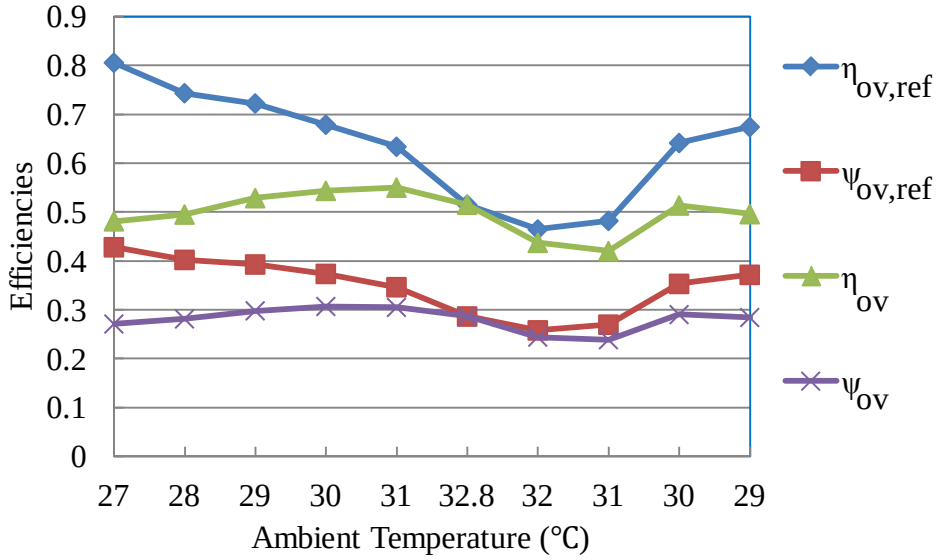

Figure 7.24: Energy and exergy efficiencies of the overall system at variable T_{amb} vs. the reference system.

7.4.3 Exergo-economic analysis and optimization results

The exergoeconomic analysis is conducted to calculate the total initial cost of the system equipments, operation and maintenance and exergy destruction. Optimization using multi-objective technique is carried out for minimum total system cost and maximum overall system exergy efficiency. The Pareto Front is plotted in Figure 7.25, where the overall exergy efficiency ranges from 48.52 % to 49.32 % at a total cost of $/h 0.99173 to $/h 0.99192.

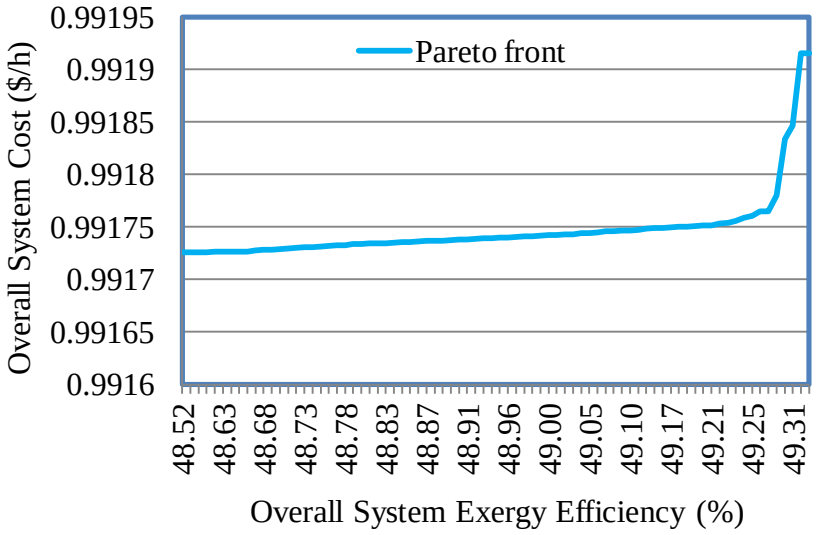

.

Figure 7.25: Optimal solution curve for the overall system exergy efficiency vs. the total overall cost of the system.

7.5 System II results

7.5.1 Optimization of the power system

The optimization is carried out to find the best optimum system of ORC and batteries that would meet the electrical demand load of the house shown in Figure 7.26 and the optimized system architecture is given in Table 7.15. The total net present cost of the system is $52,505.00 and the levelized cost of energy is $0.118/kWh as seen in Table 7.16.

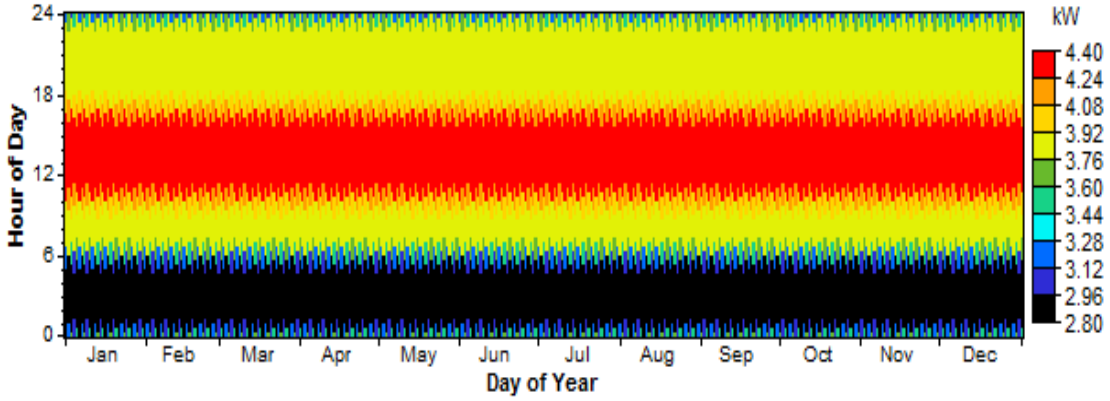

Figure 7.26: Data map of the connected primary load to the house.

Table 7.15: System II Optimized renewable energy power system architecture.

ORC	12 kW
Battery	18 Hoppecke 24 OPzS 3000
Inverter	10 kW
Rectifier	10 kW

Table 7.16: Optimized renewable energy power system cost summary.

Total net present cost	$ 52,505
Levelized cost of energy	$ 0.118/kWh
Operating cost	$ 1,104/yr

Table 7.17 gives the net present cost of the optimized renewable energy power system components for capital, replacement; operation and maintenance, salvage and total costs. ORC system has the highest total cost of $36,440.00. Figures 7.27 and 7.28 show cash flow summary and annualized cost for the various optimized renewable energy power system components.

The salvage revenue indicates that money is made but the (-) sign is considered in the cash flow figures for clarity of values of the system components net present cost. In other words the salvage values in Table 7.17 are (+) and the rest are (-).

Table 7.17: Optimized renewable energy power system components net present costs.

Component	Capital Cost ($)	Replacement Cost ($)	Maintenance and Operation Cost ($)	Salvage Revenue ($)	Total NPC ($)
ORC	30,000	2,221	5,436	-1,217	36,440
Batteries	4,500	5,237	2,446	-1,836	10,347
Converter	3,000	0	2,718	0	5,718
System	37,500	7,458	10,600	-3,053	52,505

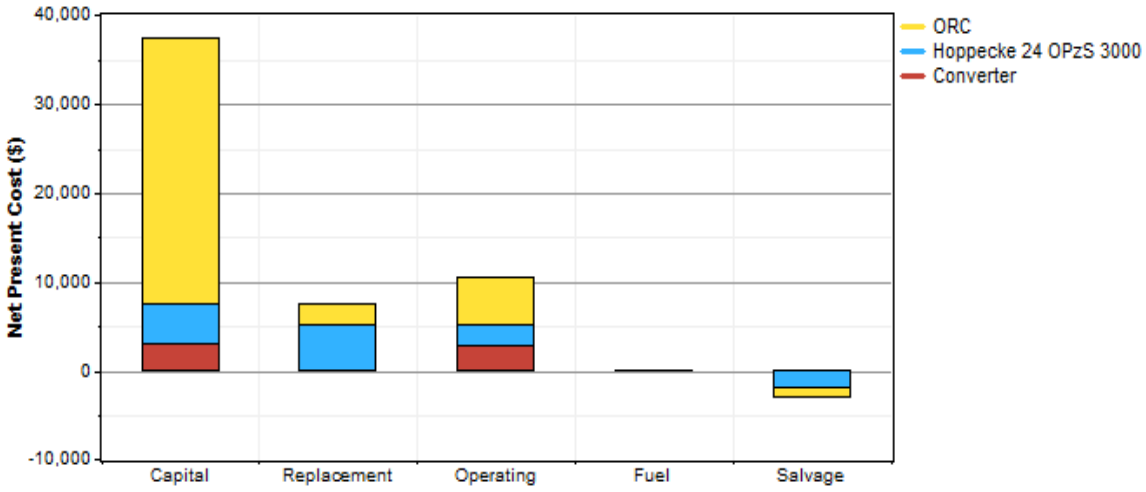

Figure 7.27: System II optimized renewable energy power system cash flow summary.

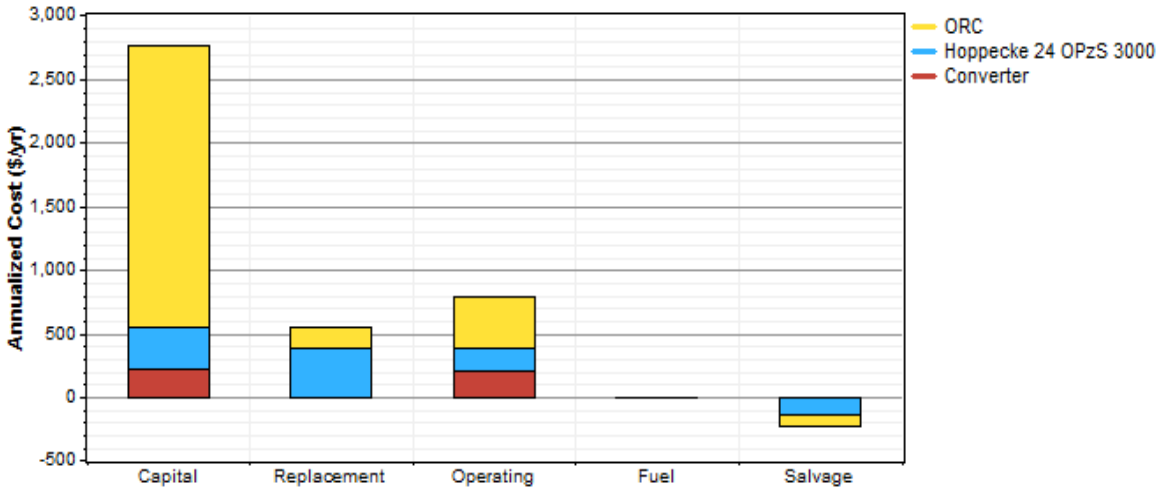

Figure 7.28: Optimized renewable energy power system annualized cash flow summary.

Figure 7.29 shows the nominal cash flow, which is the actual income minus the cost that is anticipated in a particular year. Figure 7.30 predicts the discounted cash flow which is the nominal cash flow discounted to year zero by a discount factor.

The discount factor is a ratio used to calculate the present value of a cash flow (time value of money) that occurs in any year of the project lifetime. Table 7.18 indicates that the total electrical production of the ORC system is 47,610.00kWh/yr and the total connected load is 32,836.00kWh/yr. Table 7.19 indicates that the ORC turbine nominal capacity is 15kW while the mean output is 12 kW at efficiency of 80%.

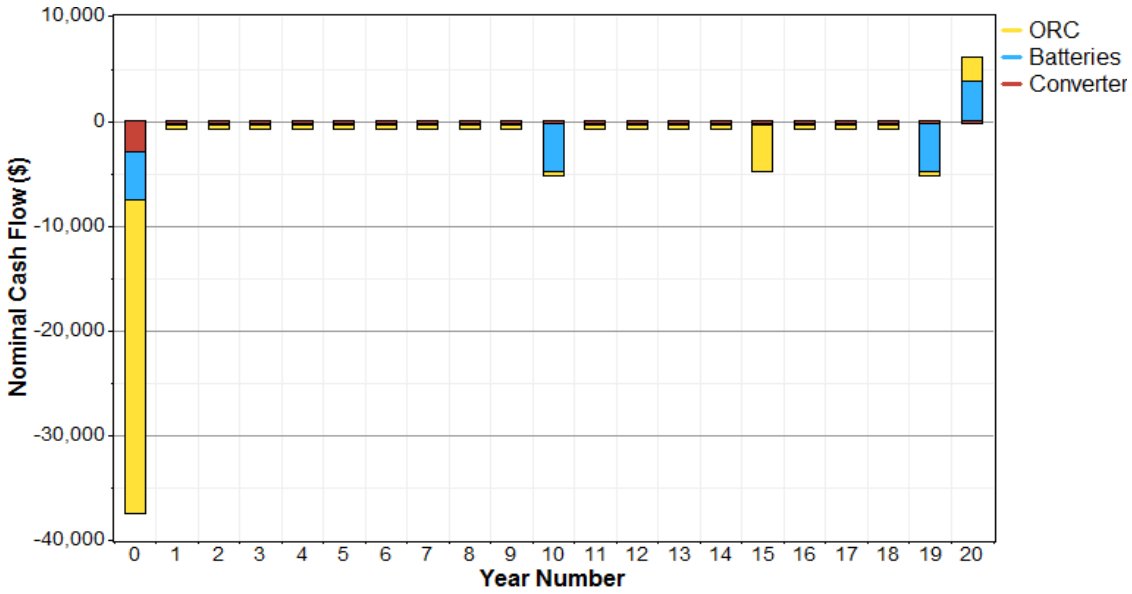

Figure 7.29: Optimized renewable energy power system nominal cash flow summary.

Table 7.20 indicates that 18 batteries are configured by optimization and connected in parallel to meet the demand load when the ORC power system is not working.

Table 7.21 gives the nominal power capacity of the batteries of 108kWh/day with an annual throughput of 19,324.00kWh/yr. Storage depletion of 18.1kWh/yr and losses of 2,857.00kWh/yr. The expected life is 9.50 years and the battery bank autonomy (the ratio of the battery bank size to the electric load) is 20.2 h. Figure 7.31 shows the optimized battery system monthly state of charge in percentage value.

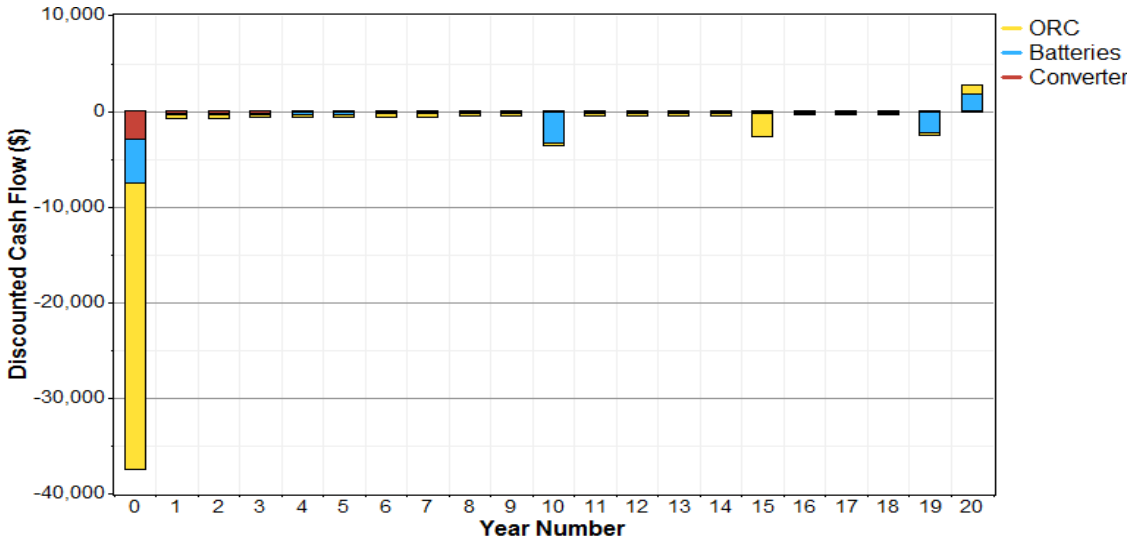

Figure 7.30: Optimized renewable energy power system discounted cash flow summary.

Table 7.18: Optimized renewable energy power system electrical configuration.

Component	Annual Power (kWh)	Fraction
ORC	47,610	100%
Connected load	32,836	100%

Table 7.19: Organic Rankine turbine power system configuration.

Quantity	Value
Rated capacity	15.0 kW
Mean output	12 kW
Capacity factor	80 %
Total production	47,610 kWh/yr

Table 7.20: Battery system architecture.

Quantity	Value
String size	1
Strings in parallel	18
Batteries	18
Bus voltage (V)	2

Table 7.21: Battery system electrical configuration.

Quantity	Value
Nominal capacity	108 kWh
Usable nominal capacity	75.6 kWh
Autonomy	20.2 h
Lifetime throughput	183,528 kWh
Battery wear cost	0.026 $/kWh
Energy in	20,796 kWh/yr
Energy out	17,920 kWh/yr
Storage depletion	18.1 kWh/yr
Losses	2,857 kWh/yr
Annual throughput	19,324 kWh/yr
Expected life	9.50 yr

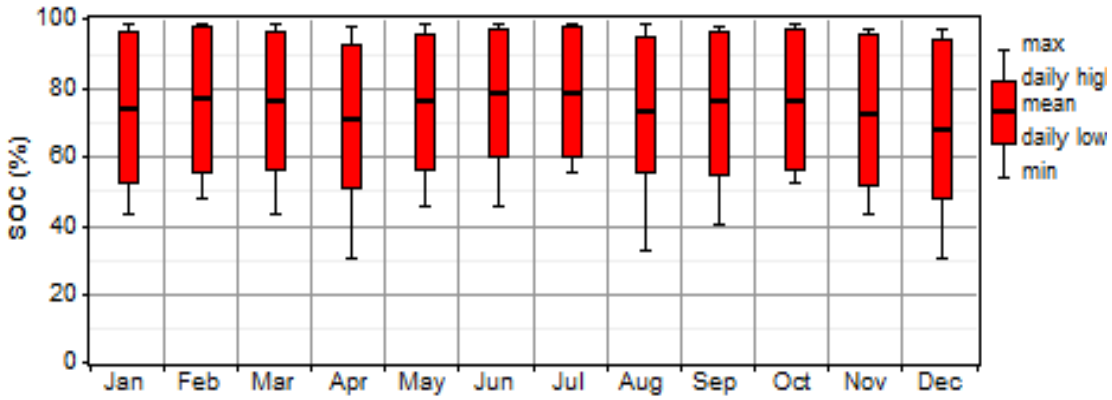

Figure 7.31: Battery system monthly statistics state of charge.

Figures (7.33, 7.35, 7.37, 7.39) and Figures (7.34, 7.36, 7.38, 7.40) show optimized power system components hourly production versus the connected load and optimized battery system charging, discharging and battery power content at different times of the year respectively. It's worth mentioning that the graphs show that the selected battery bank system is sized properly to accommodate the electrical demand of the house whenever the ORC system electricity is not available or sufficient. It is clear that the

battery power supply offset the demand. The figures are samples from the data calculated for the whole year. The discharge, charge and battery power content graphs show the behavior of the battery bank system during charging and discharging stages and their effect on the battery energy content.

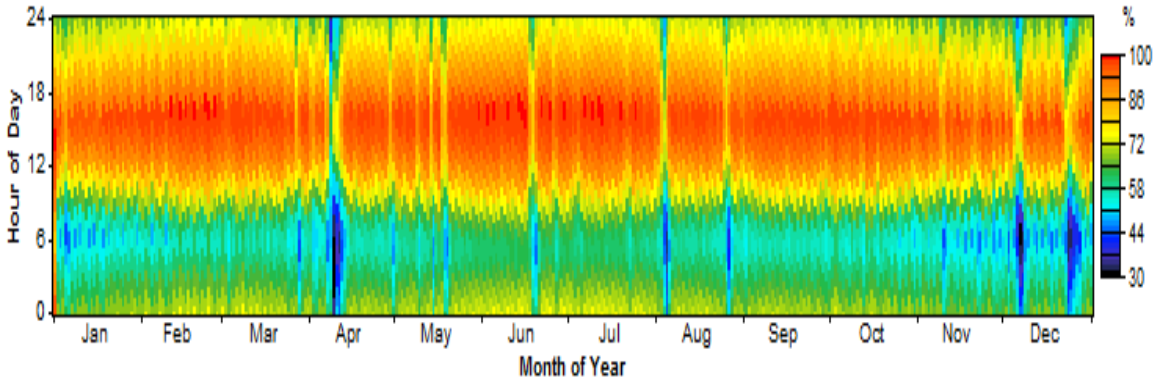

Figure 7.32: Battery bank state of charge (%).

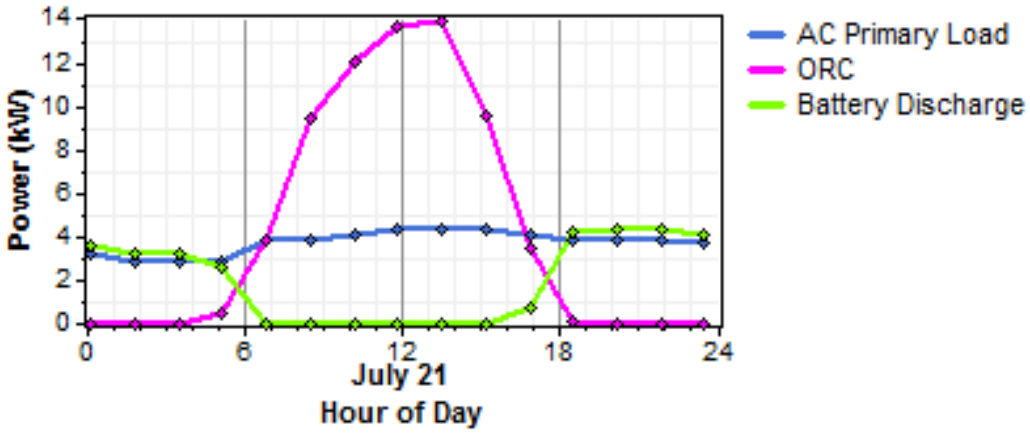

Figure 7.33: Optimized power system components hourly production versus the connected load on July 21.

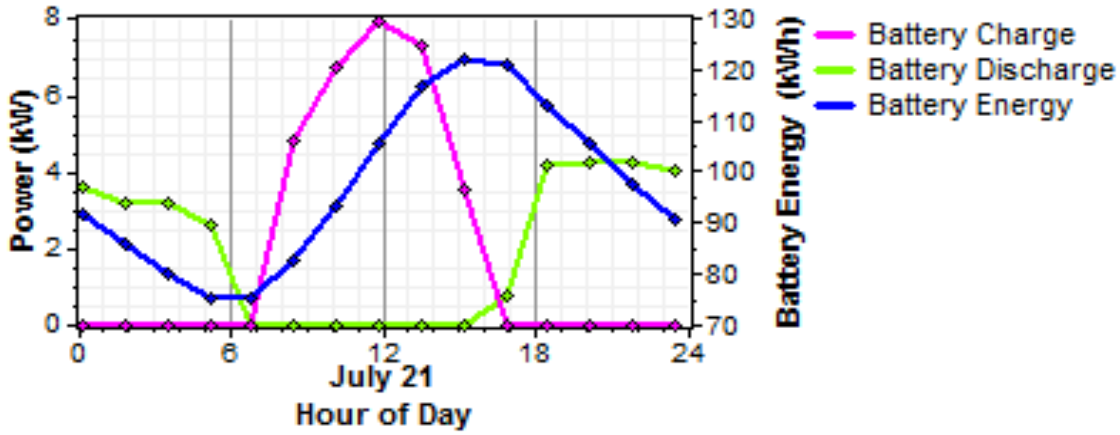

Figure 7.34: Optimized battery system charging, discharging and power content on July 21.

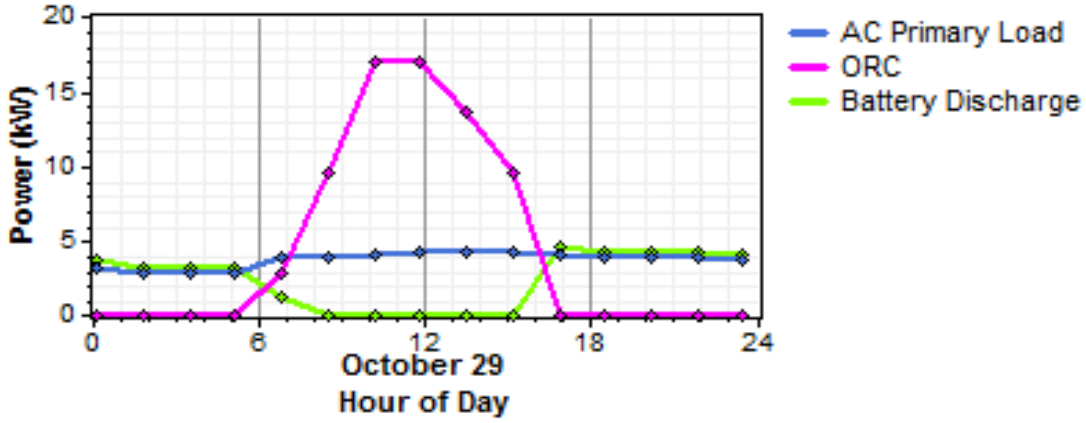

Figure 7.35: Optimized power system components hourly production versus the connected load on October 29.

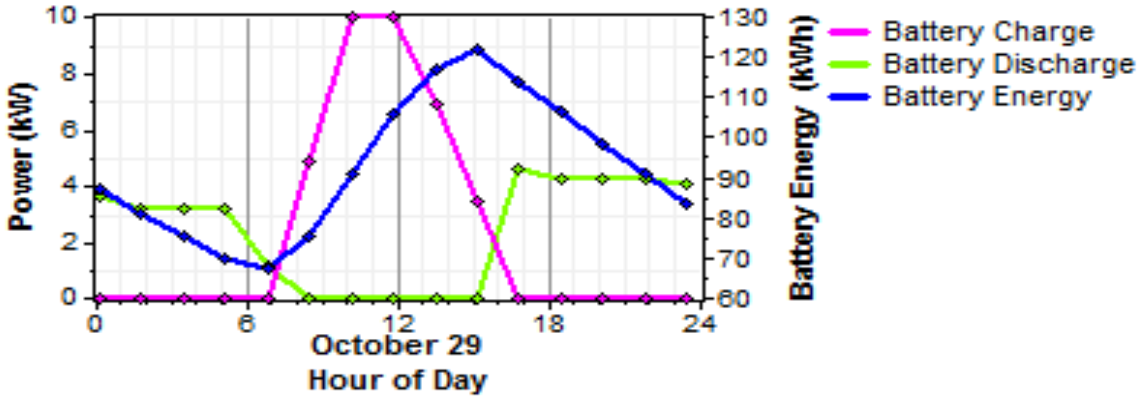

Figure 7.36: Optimized battery system charging, discharging and battery power content on October 29.

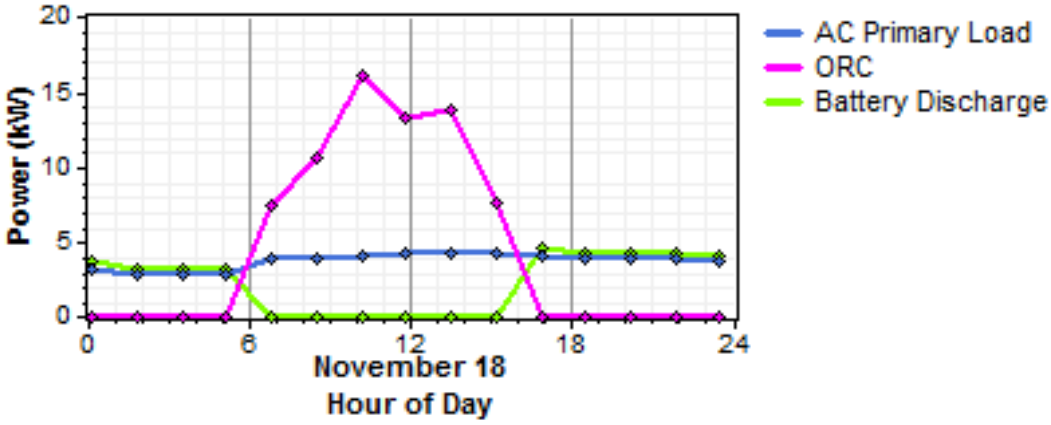

Figure 7.37: Optimized power system components hourly production versus the connected load on November 18.

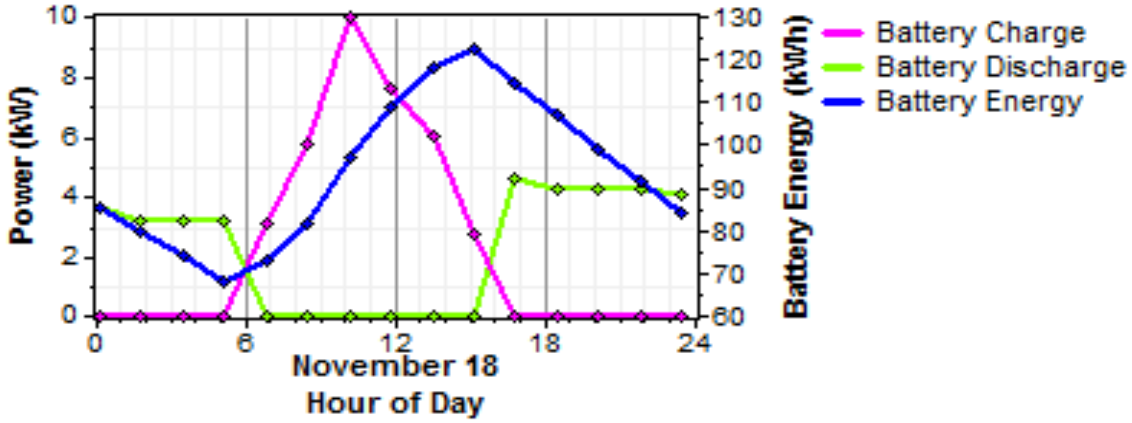

Figure 7.38: Optimized battery system charging, discharging and battery power content on November 18.

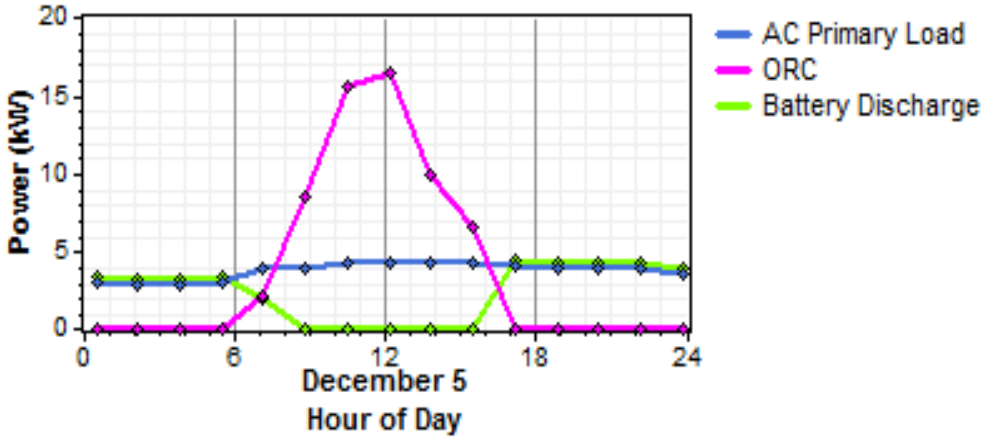

Figure 7.39: Optimized power system components hourly production versus the connected load on December 5.

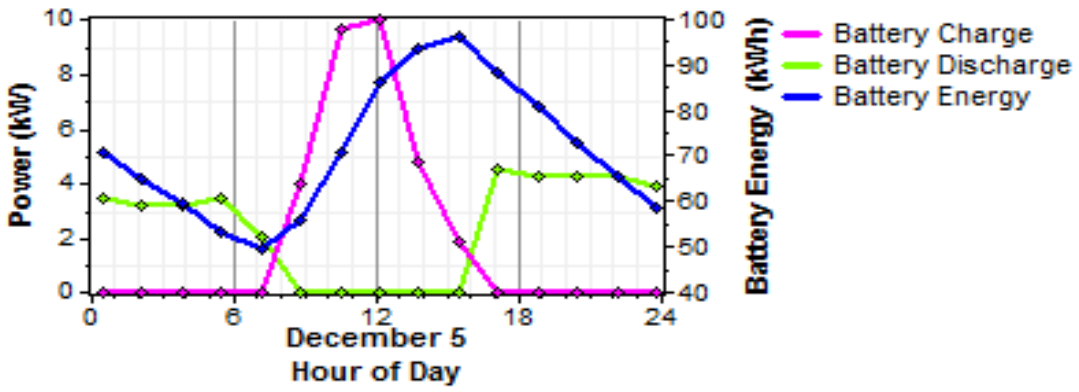

Figure 7.40: Optimized battery system charging, discharging and battery power content on December 5.

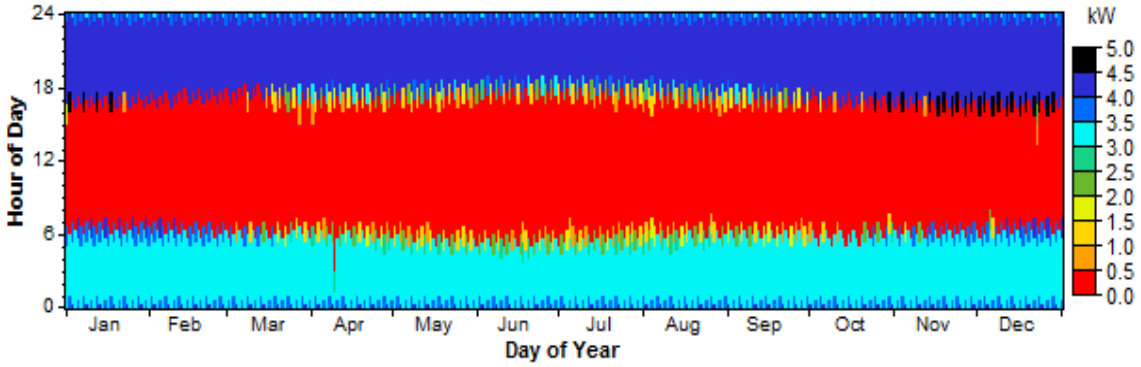

Figure 7.41: Battery system power discharge scheme.

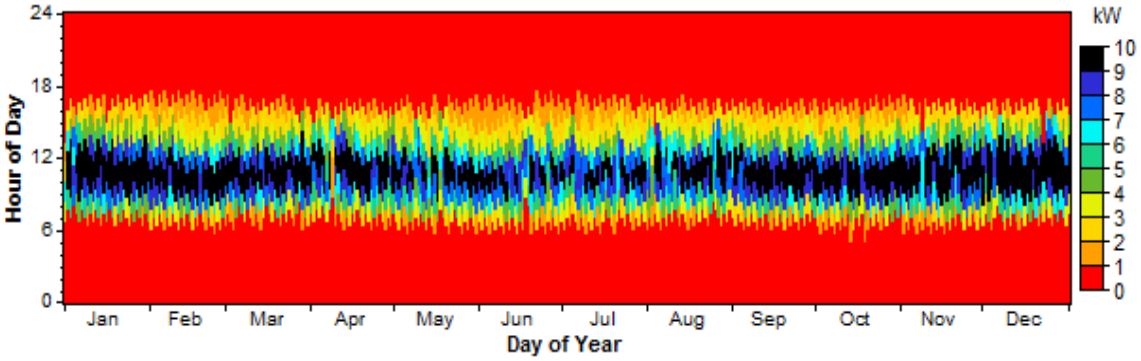

Figure 7.42: Battery system power charge scheme.

Figures 7.41 and 7.42 show the the yearly hour by hour power discharge and charge rate of the batteries, where between 6:00 am and 18:00 pm charging occurs for most of the time and discharge occurs outside this time range.

Table 7.22 gives the converter system electrical configuration with an inverter and rectifier of 10 kW capacities each. The rectifier is used to transform *AC* to *DC* to charge the batteries while the inverter is used to transform battery *DC* to *AC* to supply the house with electricity when *AC* from the ORC system is not available or sufficient. The inverter is supplied with 17,920.00kWh/yr while 1,792.00kWh/yr of energy is lost, while the rectifier is supplied by 24,465.00kWh/yr with 3,670.00kWh/yr of energy losses. The efficiencies are 18.4% and 23.7% for the inverter and rectifier respectively.

Table 7.22: Converter system electrical configuration.

Quantity	Inverter	Rectifier	Units
Capacity	10.0	10.0	kW
Mean output	1.8	2.4	kW
Maximum output	4.2	10.0	kW
Capacity factor	18.4	23.7	%
Hours of operation	4,998	3,758	hrs/yr
Energy in	17,920	24,465	kWh/yr
Energy out	16,128	20,796	kWh/yr
Losses	1,792	3,670	kWh/yr

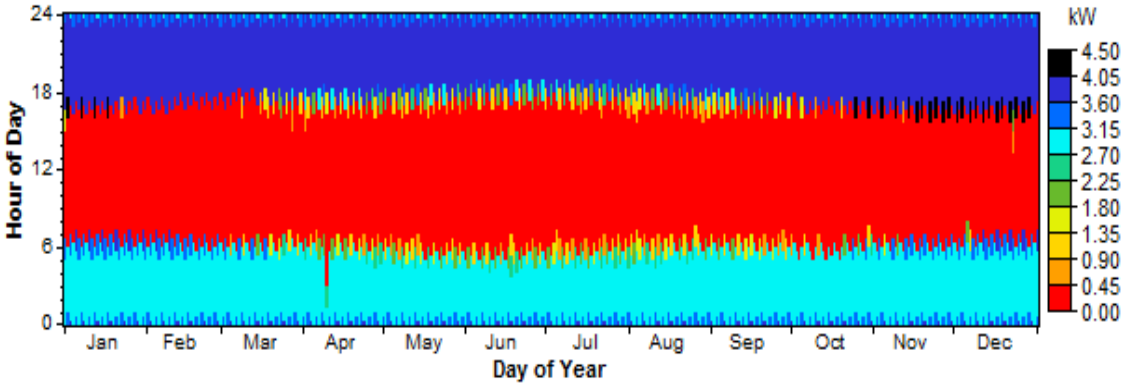

Figure 7.43: Inverter hourly output power.

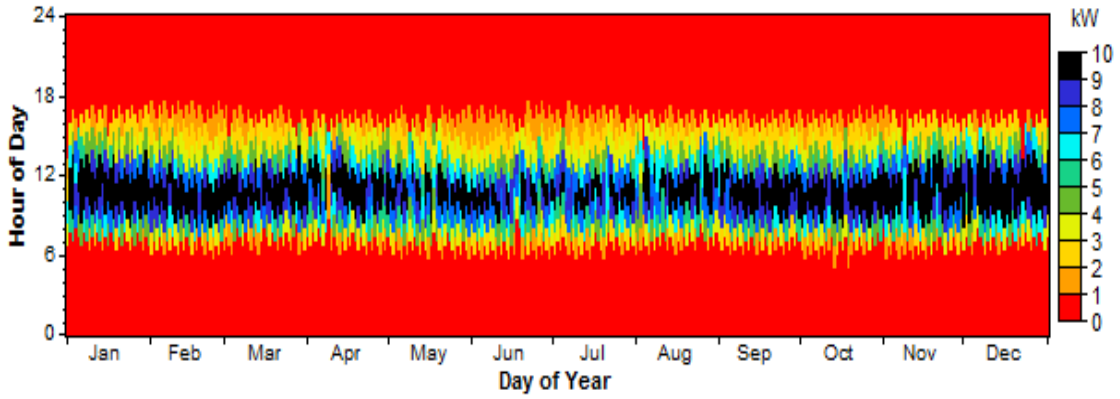

Figure 7.44: Rectifier hourly output power.

Figure 7.43 and 7.44 show monthly output power, at different hours of the day, for the inverter and rectifier. The simulations produce zero pollutants emissions.

7.5.2 Exergy analysis results

A sensitivity analysis on the system components is carried out by varying several parameters. EES software is used to calculate all the system properties and develop the parametric studies.

The effect of keeping parameters, $T_o = 25^{\circ}\text{C}$, $T_{eva} = 7^{\circ}\text{C}$, $T_{gen} = 80^{\circ}\text{C}$, $T_{w,eva} = 7^{\circ}\text{C}$ $and\ T_{w,eva,return} = 17^{\circ}\text{C}$ constant, designated here as the reference system, is shown for the overall COP for the absorption chiller, liquid desiccant system, organic Rankine cycle and the overall system efficiencies in Figure 7.45. The energetic COP varies around 0.65 for the LDS and from 1.058 at 8.00 am to 0.813 at 2.00 pm and 0.9805 at 5.00 pm for the absorption chiller, due to effect of solar energy. The exergetic COP varies around 0.275 for the LDS and from 0.3861 to 0.2697 to 0.3489 for the absorption chiller, at 8.00 am, 2:00 pm and 5:00 pm.

The overall system exergetic efficiency varies between 44.76%, 23.57% and 36.22% at 8.00 am, 2.00 pm and 5.00 pm, due to solar energy changes, while the overall system efficiency varies between 60%, 36.62% and 53.95% at 8.00 am, 2.00 pm and 5.00 pm respectively.

These results clearly indicate that the exergetic analysis represents a better sensitivity analysis of the system performance than energy.

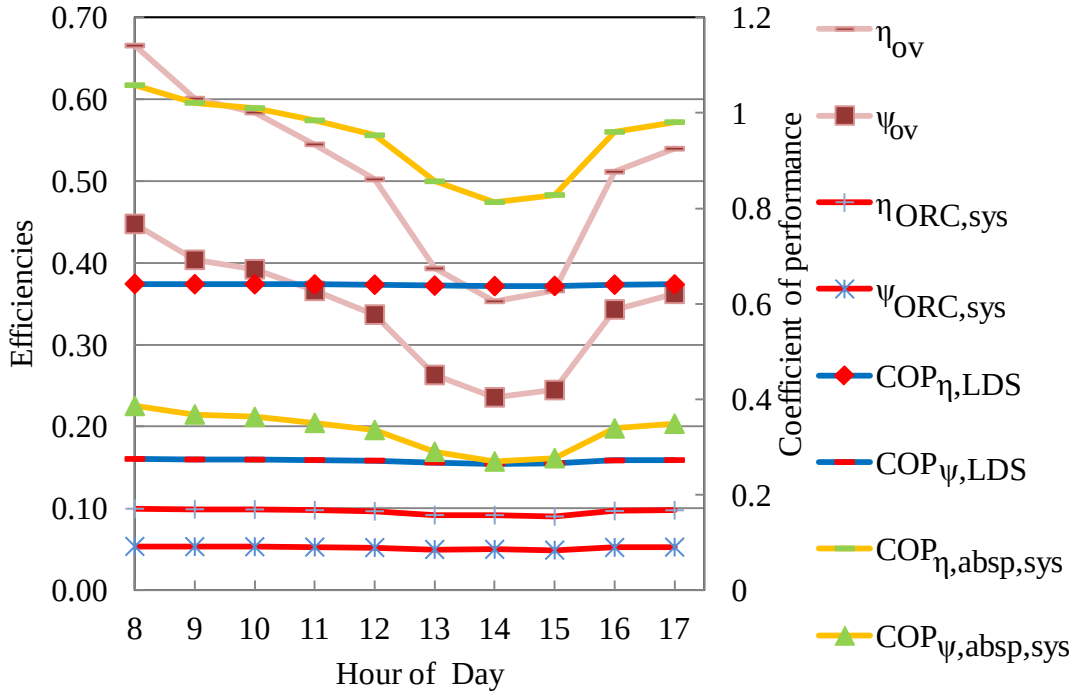

Figure 7.45: Energetic and exergetic COP of the absorption chiller and efficiencies of the ORC, LDS and overall system at reference parameters.

Figure 7.46 shows the energetic and exergetic efficiencies of the various individual components of the system. This figure is very important in identifying which component of the system needs to be worked on to improve its performance, and thus it's efficiency.

Figure 7.47 shows exergy destruction for the different system components where the absorber, LDS regenerator, ORC evaporator and absorption chiller regenerator have the highest values due to chemical exergy destruction caused by absorption and desorption processes. These values will be used later in evaluating the cost of exergy destruction in the exergoeconomic analysis and the multi-objective optimization. Also, they are important in indicating which processes have high irreversibility.

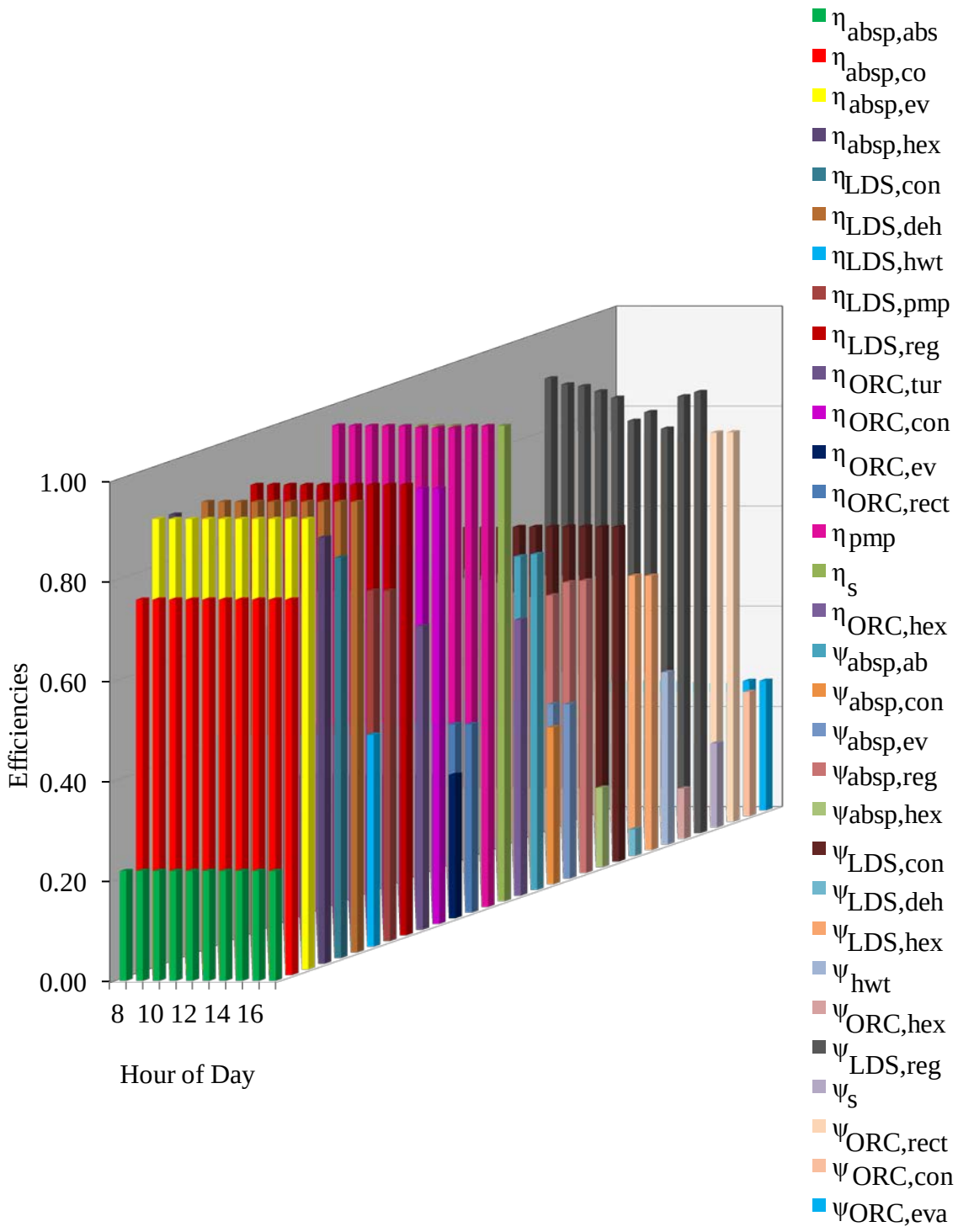

Figure 7.46: Exergy and energy efficiencies of various system components.

Figure 7.48 shows thermal heat values for different system components with the evaporator of the organic Rankine cycle, having the highest value followed by the liquid desiccant system condenser. This graph indicates the thermal heat needed to complete the processes on hand.

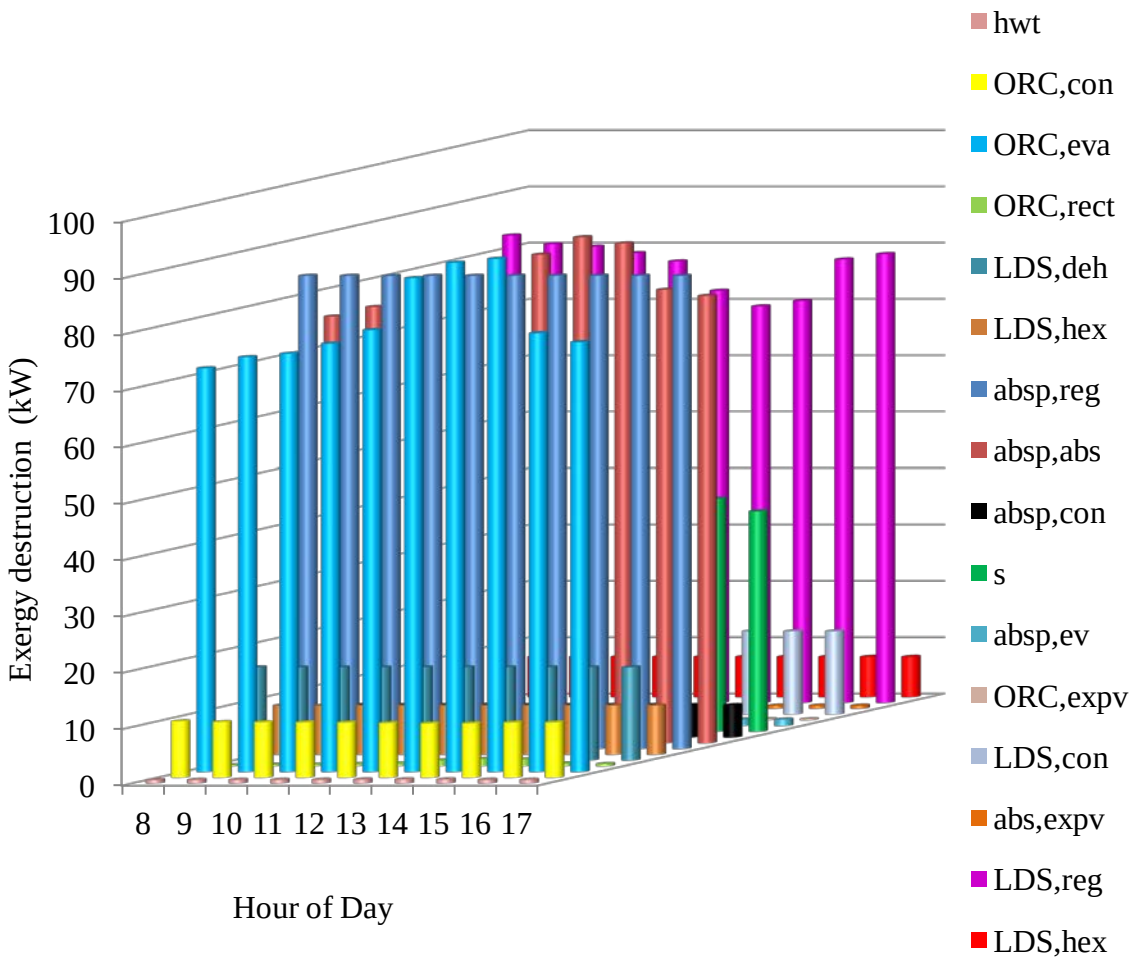

Figure 7.47: Exergy destruction for systems components at constant reference parameters.

Changing the reference temperature as shown in Figure 7.49, causes the exergetic COP, of the absorption system to increase from 0.3861 at 8:00 am to about 0.6061 at maximum T_0 because the factor $\dot{Q}_{gen}\left(1-\frac{T_0}{T_{gen}}\right)$ decreases more than $\dot{Q}_{eva}\left(\frac{T_0}{T_{ev}}-1\right)$. The

exergetic and energetic COP, of the LDS system doesn't change much from the reference system because the changes in the reference temperature are small and occur in both numerator and denominator, while the overall exergy efficiency has the factor $\left(1-\frac{T_0}{T_{Sun}}\right)$ in the denominator which is not affected by the range of changes in T_o, since T_{Sun} is large and the numerator is affected slightly by T_0 causing an unnoticeable decrease. The energetic COP doesn't change because T_0 has no influence on it. Similarly the energetic and exergetic efficiencies of the ORC system follow the same reasoning as the overall efficiencies.

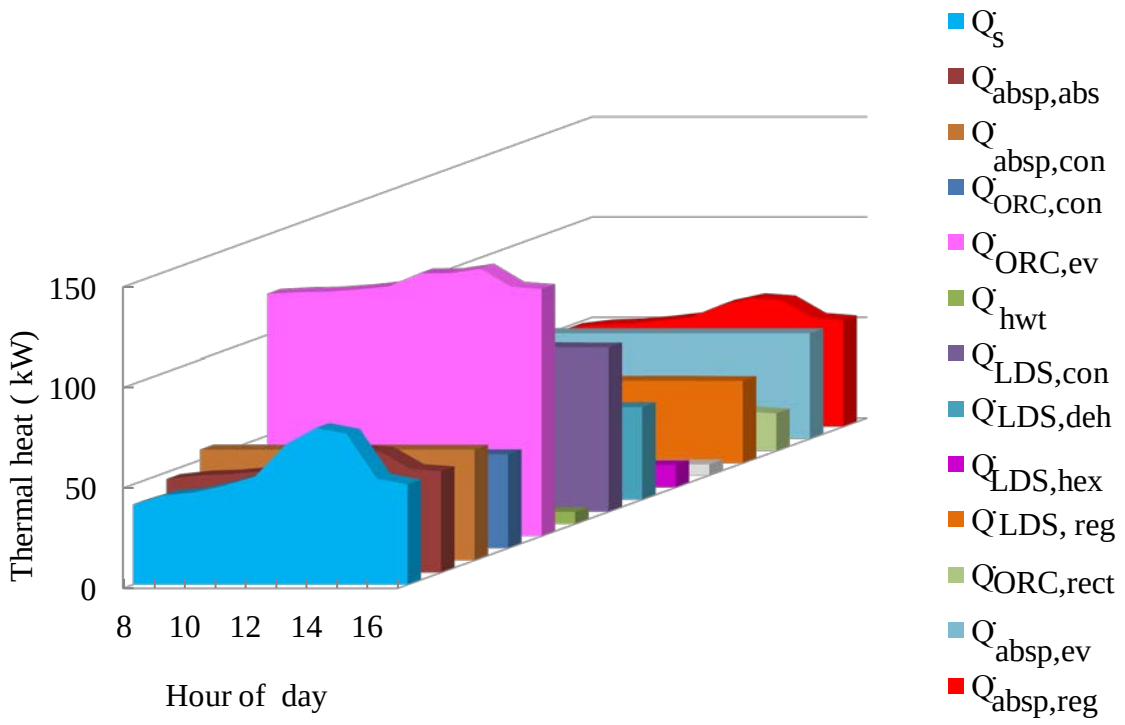

Figure 7.48: System thermal heats at different hours for reference system.

In Figure 7.50, the temperature of the evaporator is varying from 7˚C at 8:00 am to 14˚C at 3:00 pm at increments of 1˚C and decreases to 6˚C and 5˚C at 4:00 pm and 5:00 pm, $while\ T_{gen} = 80˚C\ , T_o = 25˚C, T_{eva,return} = 17˚C$ remains constant. After comparing Figure 7.50 to Figure 7.45 we notice that the COP and exergetic COP of the

absorption chiller decrease with increase in evaporator's temperature and increase with decrease in evaporator's temperature as expected, due to changes in$\dot{Q}_{\text{eva}}$.

The COP of the LDS system increases unnoticeably with increasing evaporator temperature, because, the thermal heat at the LDS regenerator and condenser increases while $\dot{Q}_{LDS,deh}$ doesn't change. The exergetic COP increases from 0.275 at $T_{eva} = 7^{\circ}\text{C}$ to 0.4313 at $T_{eva} = 14^{\circ}\text{C}$ and drops to 0.2249 at $T_{eva} = 5^{\circ}\text{C}$, because, the thermal heat at the LDS regenerator and condenser increases while $\dot{Q}_{LDS,deh}$ don't change.

The overall energy efficiency is not affected by variation in the evaporator's temperature because it has no influence on it. Overall system exergy efficiency varies slightly at the lowest evaporator temperature due to the small weight of $\dot{Q}_{LDS,deh}$ in comparison to other parameters in the overall system exergy equation.

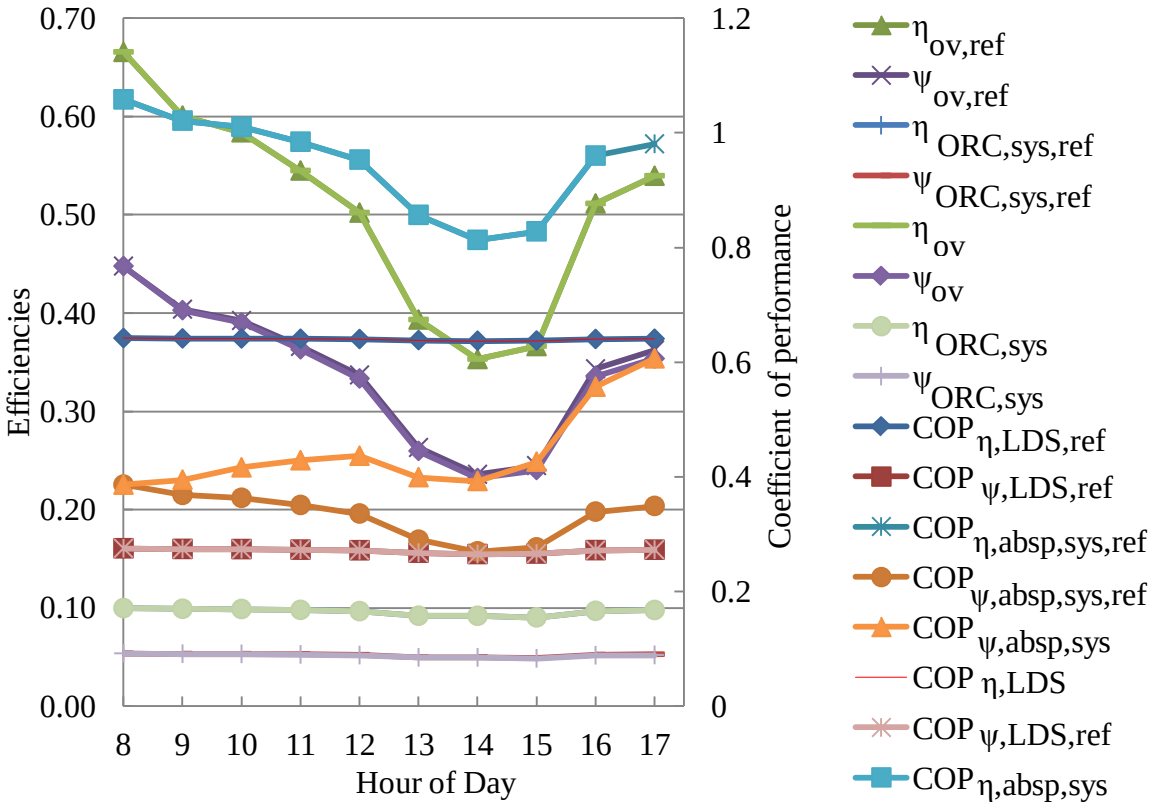

Figure 7.49: Energetic and exergetic COP of the absorption chiller and efficiencies of the ORC, LDS and overall system at variable dead state temperature vs. the reference system.

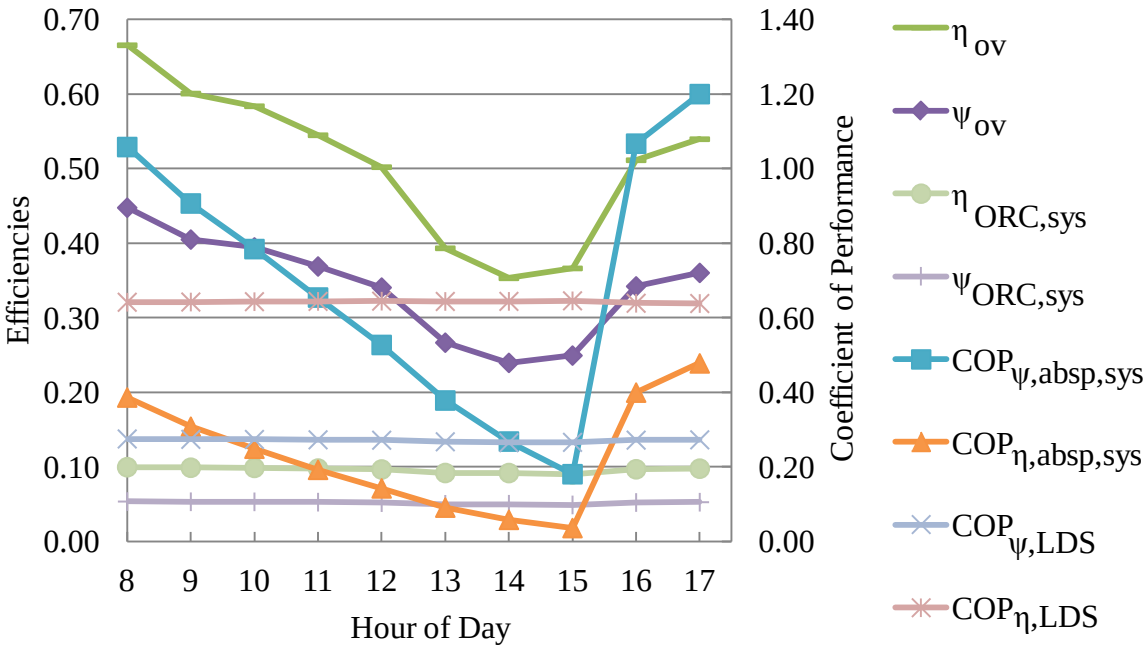

Figure 7.50: Energetic and exergetic COP of the absorption chiller and efficiencies of the ORC, LDS and overall system at variable evaporator temperature.

Figure 7.51 shows comparison of the coefficients of performance and overall efficiencies to the reference case of Figure 7.45. All parameters are fixed except for temperature of regenerators that changed from 80℃ at 8:00 am to 89 ℃ at 5:00 pm at increments of 1℃ . COP of absorption chiller is not affected while the exergetic COP decreases with increasing regenerator temperature because of the factor $\left(1-\frac{T_0}{T_{gen}}\right)$.

COP of the LDS system decreases slightly with the temperature range taken because of increasing regenerator's temperature which is in the denominator of the COP equation. The exergetic COP decreases from 0.275 at $T_{gen} = 80℃$ to 0.2278 at $T_{gen} = 89℃$. Also, the overall and exergetic efficiencies don't show any changes with regenerator temperature changes, because, the changes are about 10℃ and the influence of the regenerator on the overall efficiencies is modest as compared to other factors as shown in the relevant equations.

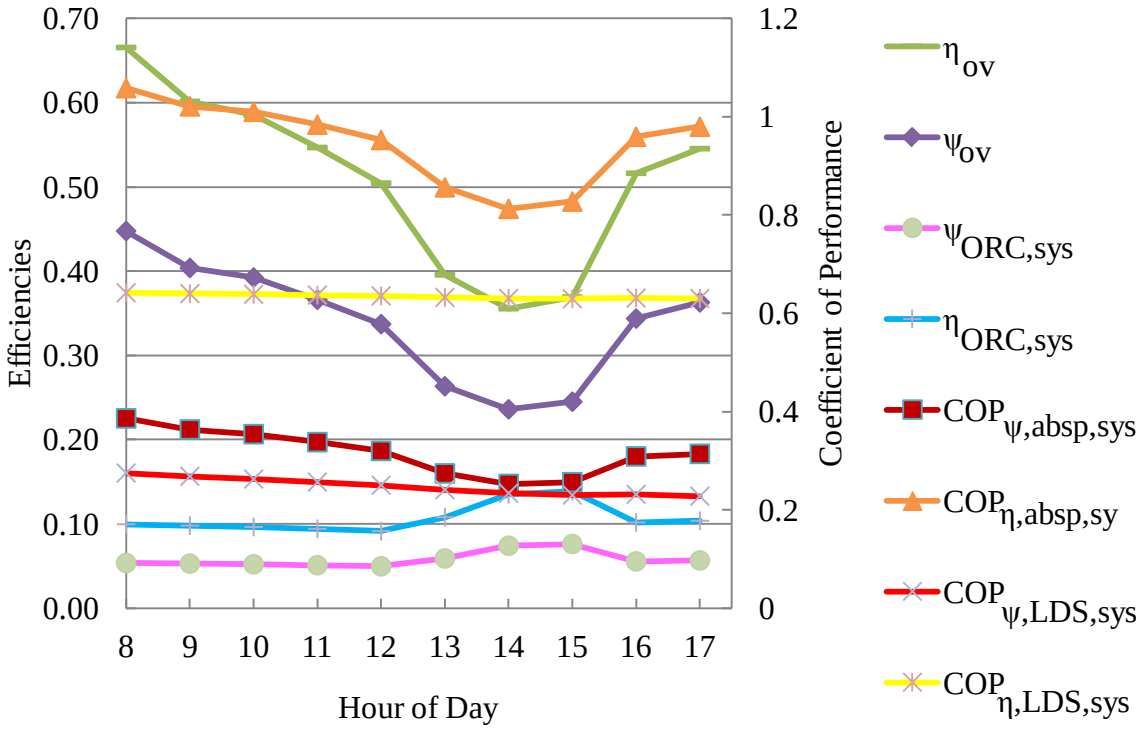

Figure 7.51: Energetic and exergetic COP of the absorption chiller and efficiencies of the ORC, LDS and overall system at variable regenerator temperature vs. the reference system.

7.5.3 Exergo-economic analysis and optimization results

The exergoeconomic analysis is conducted to calculate the total cost of the system equipments, operation and maintenance and exergy destruction. Optimization using multiobjective technique is carried out for minimum total system cost and maximum overall system exergy efficiency.

The Pareto Front is plotted in Figure 7.52, where the overall exergy efficiency ranges from 58.7921% to 58.7948% at a total cost of $/h 0.0.827609252 to $/h 0.0.82761333. The maximum overall system exergy efficiency is 44.67% and increases to 58.8% by optimization, using multivariable objective genetic algorithm with 21 variables. The initial system net present cost is $117,700.00 compared to $128,500.00 after running the optimization.

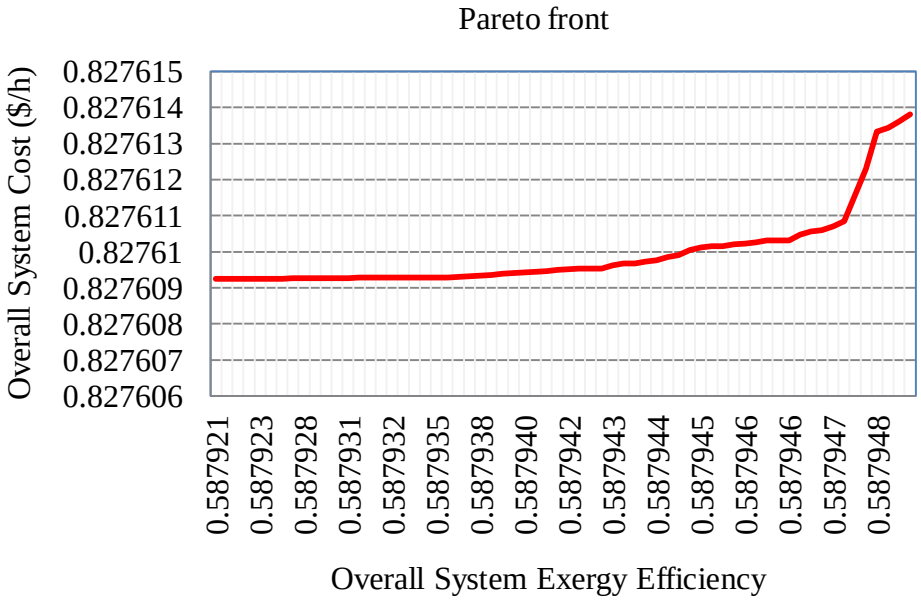

Figure 7.52: Optimal solution curve for the overall system exergy efficiency vs. the total overall cost of the system.

7.6 System III results

7.6.1 Optimized power system

Table 7.23 shows the optimization sensitivity case of the power system, which is carried out for minimum NPC and maximum renewable energy fraction at a hydro head of 30 m, design flow rate of 10 *l*/s, hydro turbine efficiency of 80% and hydro head loss of 21.7%.

Table 7.23: Optimization sensitivity case.

Hydro Head:	30 m
Hydro Design Flow Rate:	10 l/s
Hydro Turbine Efficiency:	80%
Hydro Head Loss:	21.70%

The optimization yields a power system configuration of 6 kW PV array, 2.35 kW hydro turbine, 4 batteries and 2 kW converter as given in Table 7.24. Table 7.25 gives the total net present cost for the optimized power system as $40,420.00 and the levelized cost of energy at 0.091 $/kWh.

Table 7.24: System III Power architecture.

PV Array	6 kW
Hydro	2.35 kW
Battery	4 Hoppecke 24 OPzS 3000
Inverter	2 kW
Rectifier	2 kW

Table 7.25: Optimized power system cost summary.

Total net present cost	$ 40,420
Levelized cost of energy	$ 0.091/kWh

Figure 7.53 shows the cash flow summary for the different optimized power system components with the NPC of $23077.00, $14,083.00, $2116.00, $1144.00 for hydro, PV, batteries and converter respectively, while Figure 7.54 shows the NPC of the optimized power system by cost type for the capital, replacement, operating and salvage.

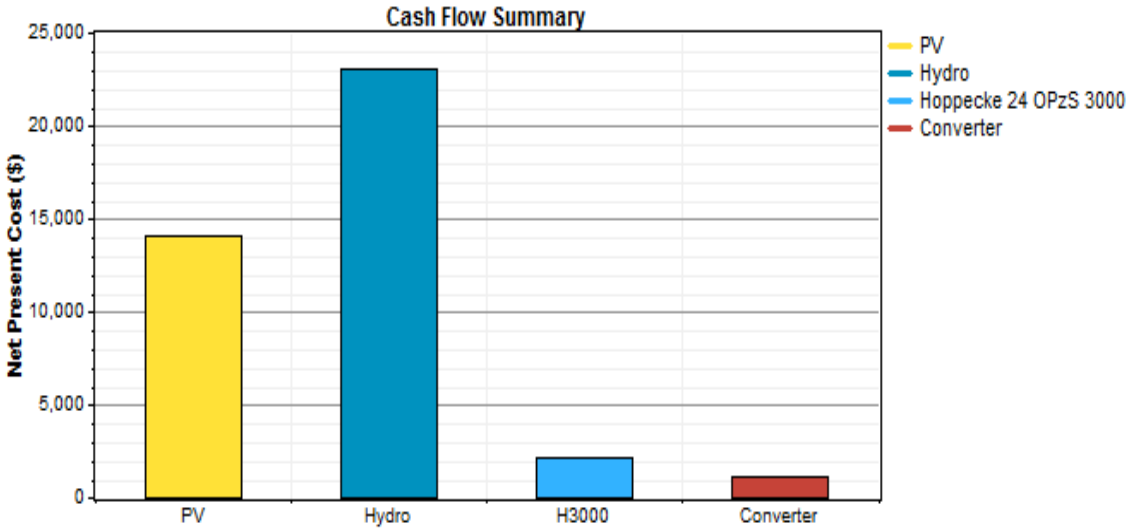

Figure 7.53: System III optimized power system cash flow summary by component.

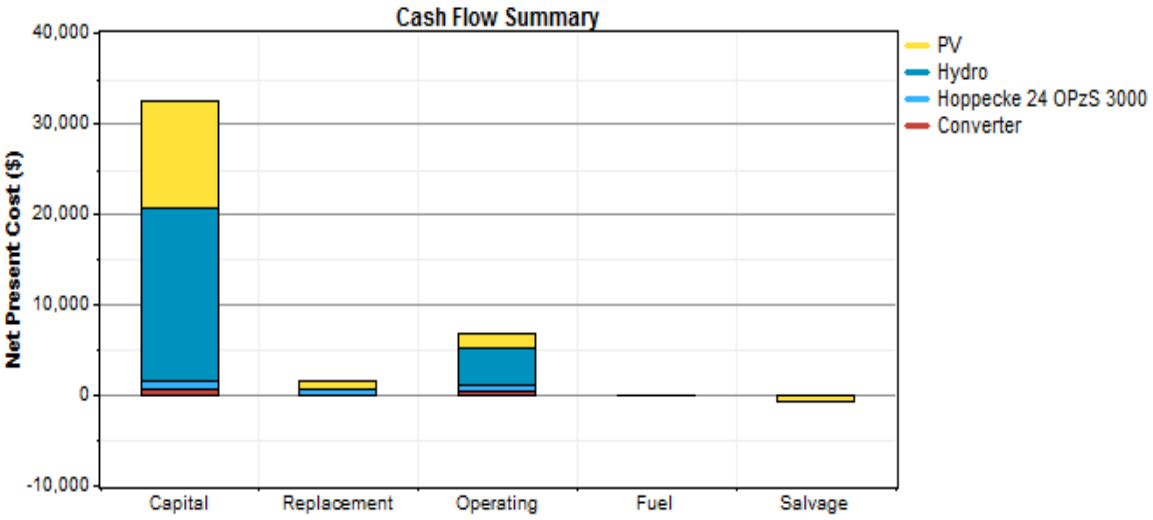

Figure 7.54: Optimized power system cash flow summary by cost type.

Figure 7.55 shows the discounted cash flow of the optimized power system to year zero as $-12,000.00, $-19,000.00, $-1000.00, $-600.00 for PV, hydro, batteries and converter respectively.

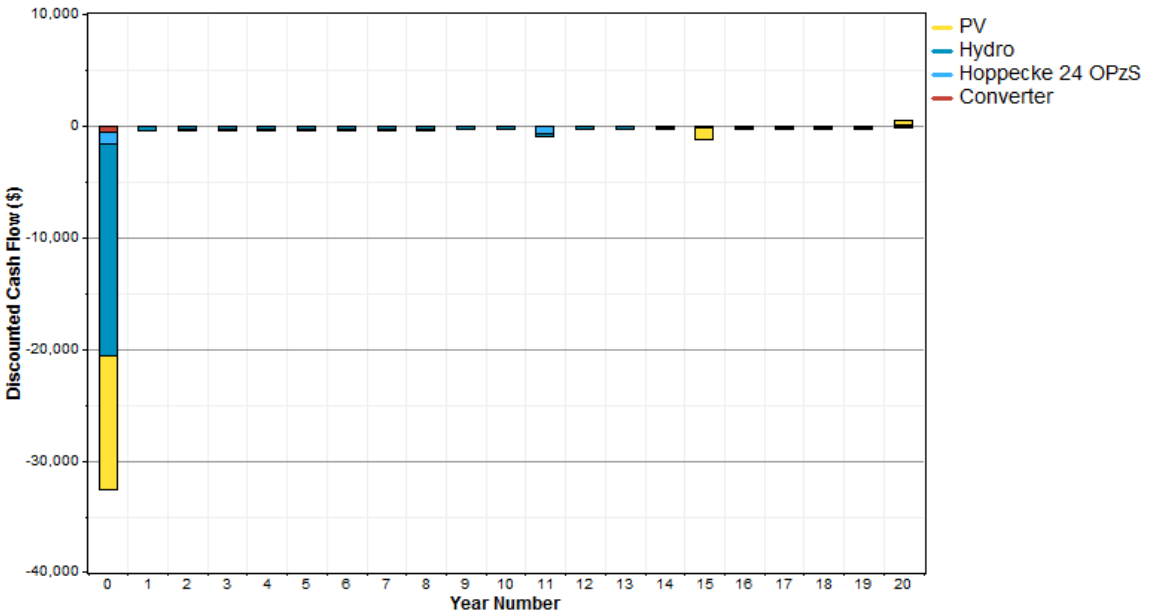

Figure 7.55: Optimized power system discounted cash flow by component.

Table 7.26 gives optimized power system components, electrical production and percentage of total power, where the hydro turbine system produces annually 24,224.00 kWh and the PV system 14,283.00 kWh. Excess annual power production of 4052 kWh is produced over the total needed load of 32,850.00 kWh as given in Table 7.27.

Table 7.26: Optimized power system electrical configuration.

Component	Annual Production (kWh)	Fraction (%)
PV array	14,283	37
Hydro turbine	24,224	63
Total	38,507	100
Excess electricity	4,052	-
Unmet load	0.00	-
Capacity shortage	0.00	-
Renewable fraction	-	1.00

Table 7.27: Total load connected to the NZEH.

Load	Annual Consumption (kWh)	Fraction (%)
AC primary load	32,850	100
Total	32,850	100

Figure 7.56 shows the monthly average electrical production of the optimized power system components with the hydro producing more than the PV system as shown. Table 7.28 gives the electrical configuration of the optimized PV array system with a rated capacity of 6 kW and total annual production of 14,283 kWh for 4378 hours of operation with an efficiency of 27.2%, while Figure 7.57 shows the monthly electrical production of the optimized PV system for different hours of the day.

Table 7.29 gives the hydro turbine electrical specifications with a total annual production of 24,224 kWh at a mean output 2.77 kW, with a hydro penetration of 73.7% which is the average power output of the hydro turbine divided by the average primary load. The levelized cost of energy is 0.0701 %/kWh, which is defined here as the average

cost per kWh of useful electrical energy produced by the system and results from dividing the annualized cost of producing electricity by the total electric load served. Figure 7.58 shows the optimized hydropower system monthly output 2.77 kW every hour of the day. The nominal power of the hydro system is 2.35 kW. This would be the power produced by the hydro turbine given the available head and a stream flow equal to the design flow rate of the hydro turbine.

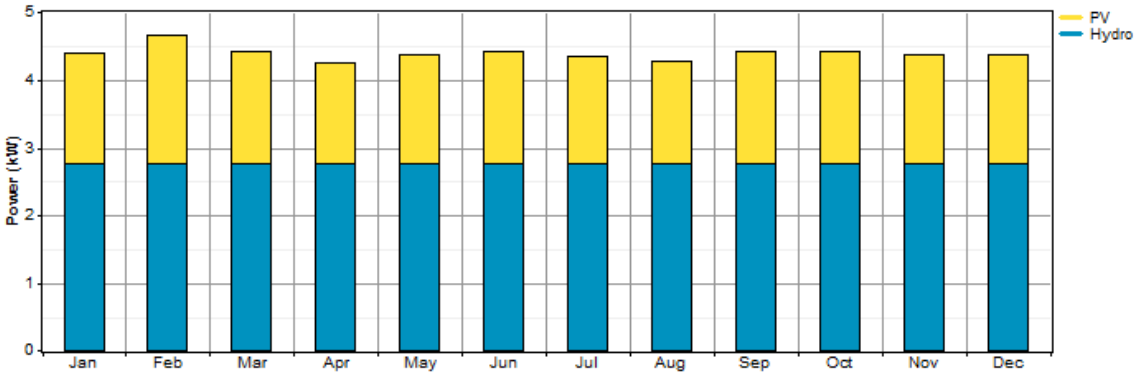

Figure 7.56: Optimized power system monthly average electrical production.

Table 7.28: PV electrical configuration.

Quantity	Value
Rated capacity	6.00 kW
Mean output	1.63 kW
Mean output	39.1 kWh/d
Capacity factor	27.2%
Total production	14,283 kWh/yr
Minimum output	0.00 kW
Maximum output	6.68 kW
PV penetration	43.5%
Hours of operation	4,378 h/yr
Levelized cost	0.0725 $/kWh

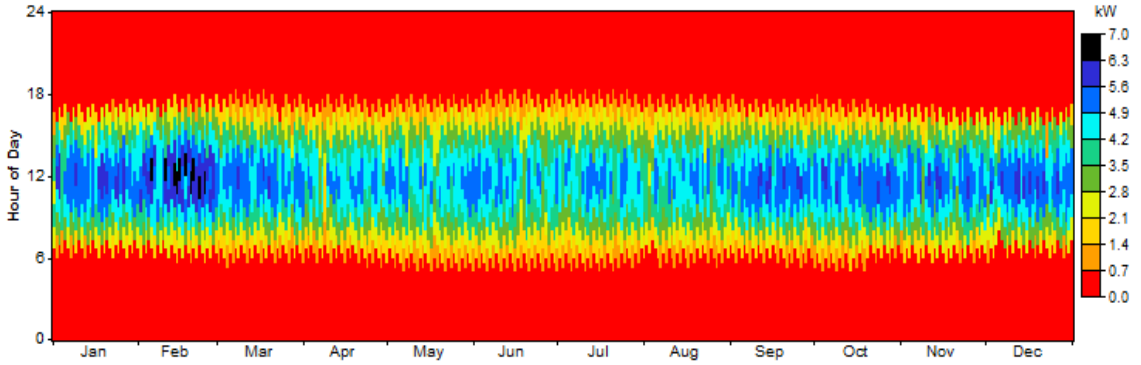

Figure 7.57: Optimized PV system electrical production.

Table 7.29: Hydro turbine electrical configuration.

Quantity	Value
Nominal capacity	2.35 kW
Mean output	2.77 kW
Capacity factor	117%
Total annual production	24,224 kWh
Minimum output	2.77 kW
Maximum output	2.77 kW
Hydro penetration	73.7%
Annual hours of operation	8,760 h
Levelized cost	0.0701 $/kWh

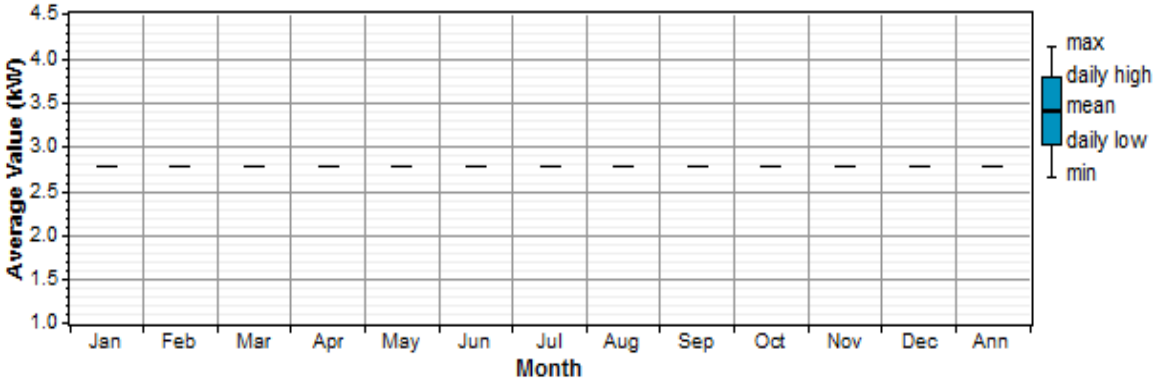

Figure 7.58: Optimized hydropower system output.

Table 7.30 indicates the batteries system architecture with 4 batteries in parallel rated at a Bus voltage of 2 volts each, while Table 7.31 gives the nominal power capacity of the batteries at 24.00 kWh with life time throughput (the total amount of energy that cycles through the battery bank during its life) of 40,784.00 kWh, storage depletion of 5.81kWh/yr and losses of 546.00 kWh/yr. The expected life is 10.90 years and the battery bank autonomy (the ratio of the battery bank size to the electric load) is 4.48 hrs.

Table 7.30: Battery system architecture.

Quantity	Value
String size	1
Strings in parallel	4
Batteries	4
Bus voltage (V)	2

Table 7.31: Battery system electrical configuration.

Quantity	Value
Nominal capacity	24.0 kWh
Usable nominal capacity	16.8 kWh
Autonomy	4.48 h
Lifetime throughput	40,784 kWh
Battery wear cost	0.026 $/kWh
Average energy cost	0.000 $/kWh
Energy in	4,009 kWh/yr
Energy out	3,457 kWh/yr
Storage depletion	5.81 kWh/yr
Losses	546 kWh/yr
Annual throughput	3,728 kWh/yr
Expected life	10.9 yr

Figures 7.59, 7.60, 7.61 and 7.62 show the yearly hour by hour battery bank state of charge percentage, power discharge, content and charge rates of the batteries respectively, where, between 6:00 am and 18:00 pm charging occurs for most of the time and discharge occurs outside this time range, while the battery energy content spreads throughout the hours of the day and % state of charge is maximum between 12:00 pm and 17:00 pm.

Figures (7.63, 7.64) show optimized power system components hourly production versus the connected load and Figure 7.65 shows optimized battery system charging, discharging and battery power content at different times of the year respectively. It's worth mentioning that the graphs show that the selected battery bank system is sized properly to accommodate the electrical demand of the house whenever the PV system electricity is not available or sufficient. It is clear that the battery power supply offset the demand.

The figures are samples from the data calculated for the whole year. The discharge, charge and battery power content graphs show the behavior of the battery bank system and how each increases and decreases.

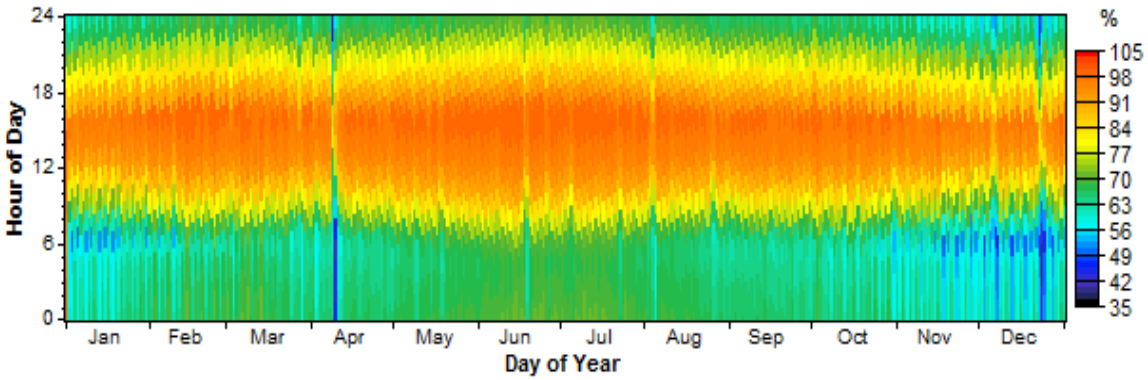

Figure 7.59: Battery system state of charge (%).

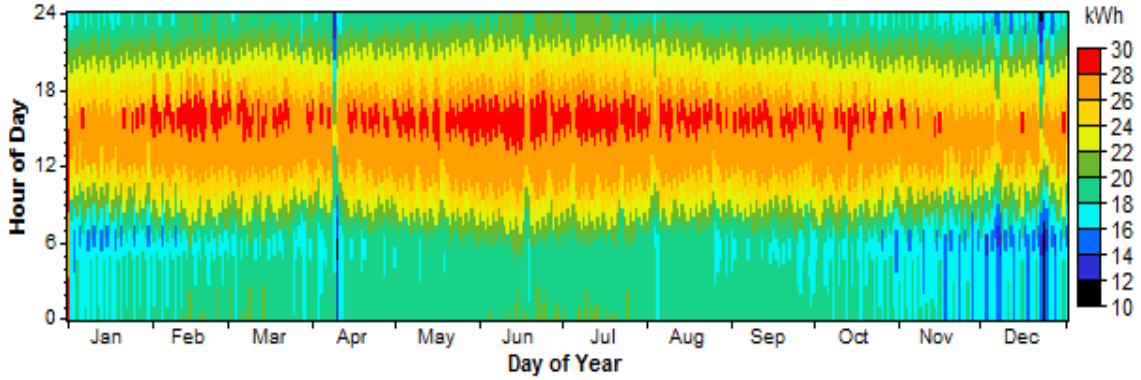

Figure 7.60: Battery system energy content.

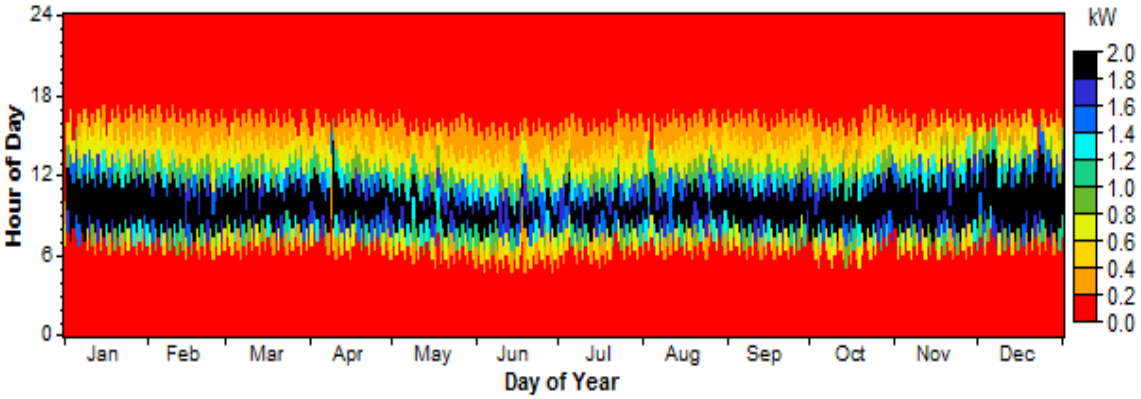

Figure 7.61: Battery system power charge scheme.

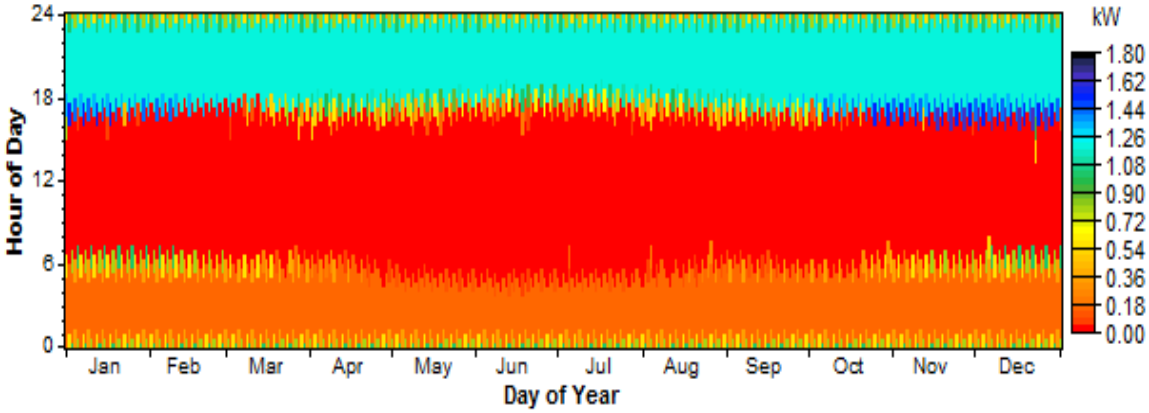

Figure 7.62: Battery system power discharge scheme.

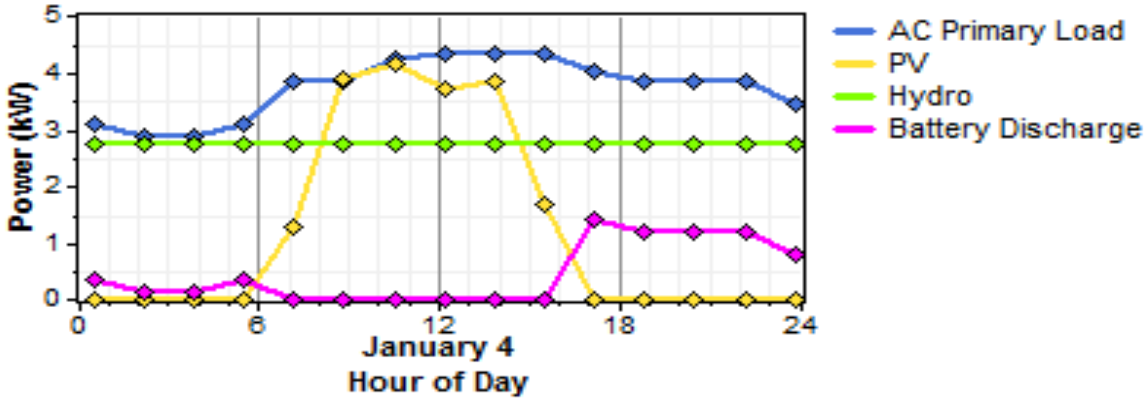

Figure 7.63: Optimized power system component's hourly production on January 4 for different hours of

the day.

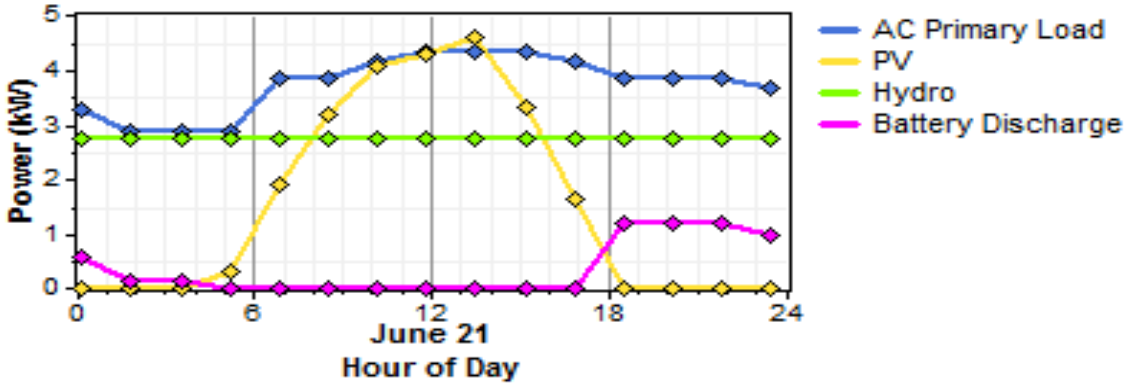

Figure 7.64: Optimized power system component's hourly production on June 21 for different hours of the day.

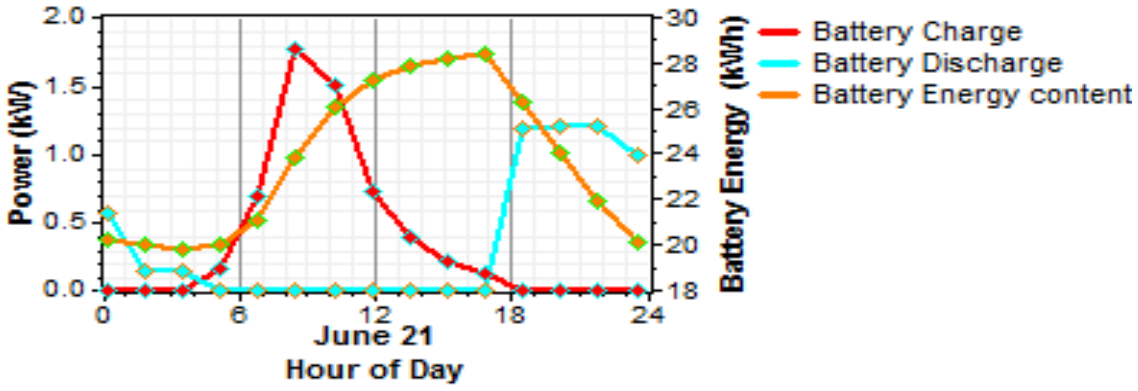

Figure 7.65: Optimized battery system state of charge, discharge and energy content on June 21 for different hours of day.

Table 7.32 gives the converter system electrical configuration with an inverter and rectifier of 2 kW capacities each. The rectifier is used to transform *AC* to *DC* to charge the batteries while the inverter is used to transform battery *DC* to *AC* to supply the house with electricity when *AC* from the PV system is not available or sufficient. The inverter is supplied by 3,457.00kWh/yr with energy losses of 346.00kWh/yr, while the rectifier is supplied by 4,716.00kWh/yr with energy losses of 707.00kWh/yr. The efficiencies are 17.8% and 22.9% for the inverter and rectifier respectively.

Figure 7.66 and 7.67 shows the inverter and rectifier monthly output power at different hours of the day. The simulations produce a zero pollutants emissions.

Table 7.32: Converter system electrical configuration.

Quantity	Inverter	Rectifier	Units
Capacity	2.00	2.00	kW
Mean output	0.36	0.46	kW
Maximum output	1.47	2.00	kW
Capacity factor	17.8	22.9	%
Hours of operation	4,888	3,872	hrs/yr
Annual energy in	3,457	4,716	kWh
Annual energy out	3,111	4,009	kWh
Annual losses	346	707	kWh

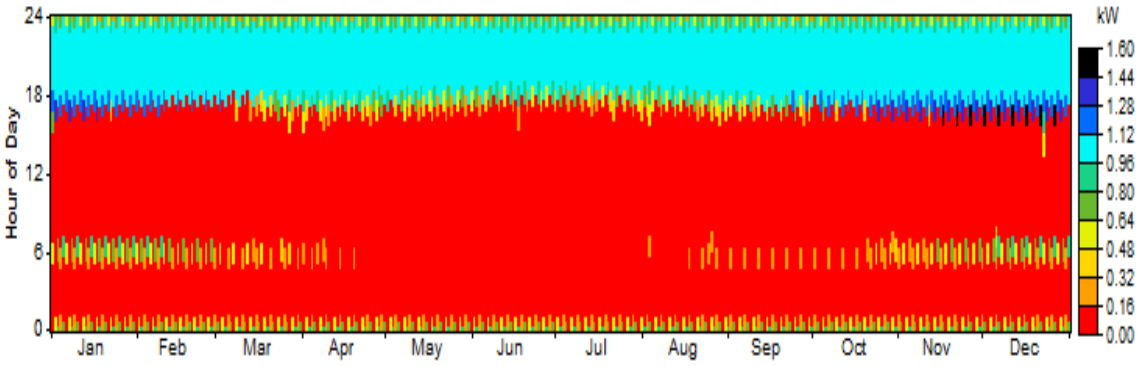

Figure 7.66: Inverter hourly output power.

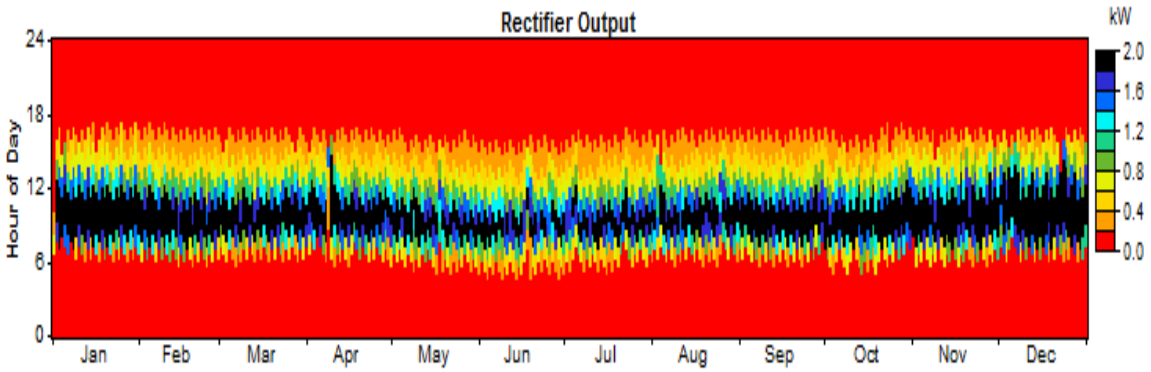

Figure 7.67: Rectifier hourly output power.

A sensitivity analysis is carried out using the optimal system type (OST) graph which gives the highest-level view of the sensitivity results. Figure 7.68 shows that the optimal total NPC of the optimized power system with hydro turbine efficiency (η_{hyd}=80%) and hydro head loss (f_h = 21.7%) decreases as the sensitivity variables of design flow rate ($\dot{V}$) and hydro head (l) increases, while Figure 7.69 shows that the optimal total NPC of the optimized power system with hydro turbine efficiency (η_{hyd}=80%) and hydro head loss (f_h = 30 %) increases due to increase in hydro head loss as compared to Figure 7.68.

Figures 7.70 and 7.71 show the optimal total NPC of the optimized power system with η_{hyd}=70%, f_h = 21.7% and η_{hyd}=60%, f_h = 21.7% respectively versus the sensitivity variables design flow rate ($\dot{V}$) and hydro head (l). As the turbine efficiency decreases while keeping all other parameters fixed the NPC increases from the values shown in Figure 7.68.

Figures 7.72, 7.73 and 7.74 show the total NPC of the power system with the total electrical load being superimposed for η_{hyd}= (60, 70, 80) % and f_h = (21.7, 21.7, 21.7) % respectively. The graphs show that as the hydro turbine efficiency decreases the total NPC increases and the total electrical production depends on optimized PV and hydro capacities for fixed hydro head loss.

Figure 7.75 shows the surface plot (primary variable values are identified by a surface region) of the PV capacity with the hydro capacity superimposed at η_{hyd}= 80%

and f_h = 21.7%, versus the sensitivity variables of design flow rate ($\dot{V}$) and hydro head (h_{eff}). The hydro capacity increases as the hydro head and flow rate increases, while the PV capacity decreases.

Figure 7.76, shows the surface plot of the hydro capacity with the battery number superimposed at η_{hyd}= 80% and f_h = 21.7%, versus the sensitivity's variables of design flow rate ($\dot{V}$) and hydro head (h_{eff}). As the hydro head and flow rate decreases the number of batteries increases while the hydro capacity decreases.

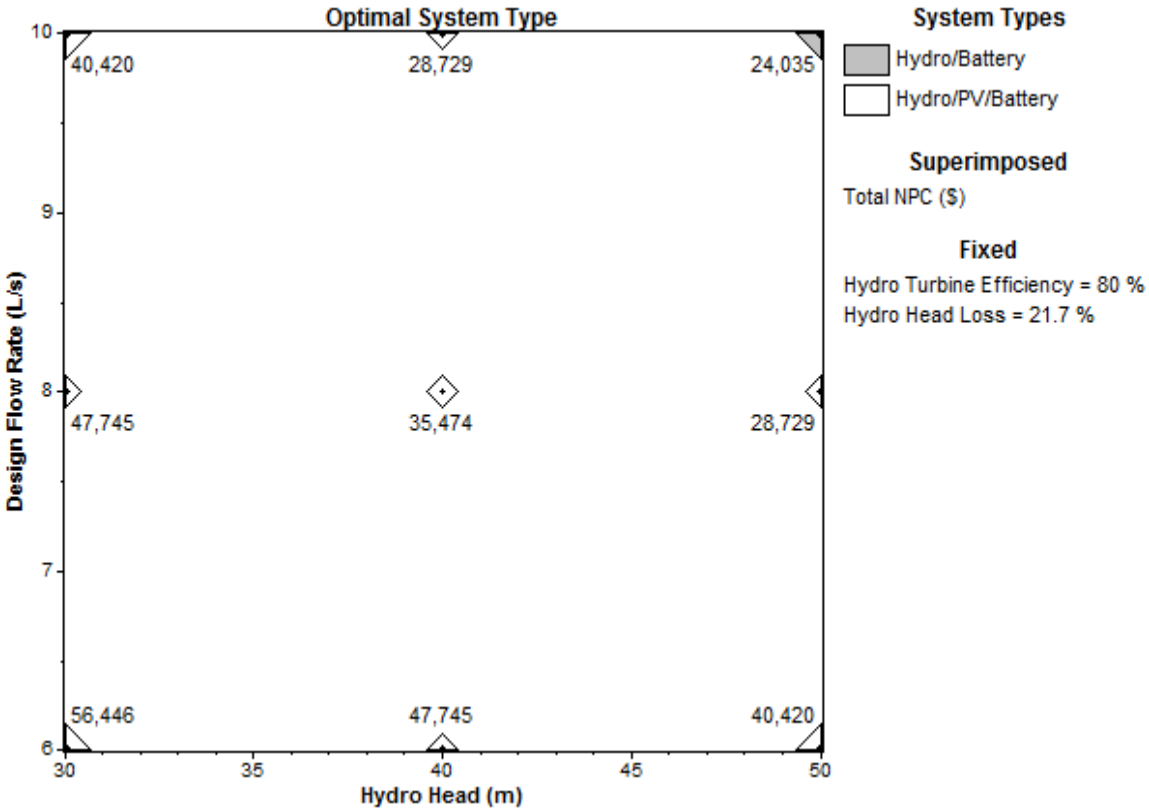

Figure 7.68: Total NPC for optimal system configuration at η_{hyd} = 80% and f_h= 21.7%.

Figure 7.77 shows a spider graph (which is used when multiple variables have different values and a best estimate is considered in the analysis to cover the range of uncertainty, then the most sensitive variable to the optimized goal can be identified) of the total NPC vs. the hydro head, design flow rate, hydro turbine efficiency and hydro

head loss. It is clear that the design flow rate has the steepest graph followed by the hydro head and thus the total NPC is most sensitive to it.

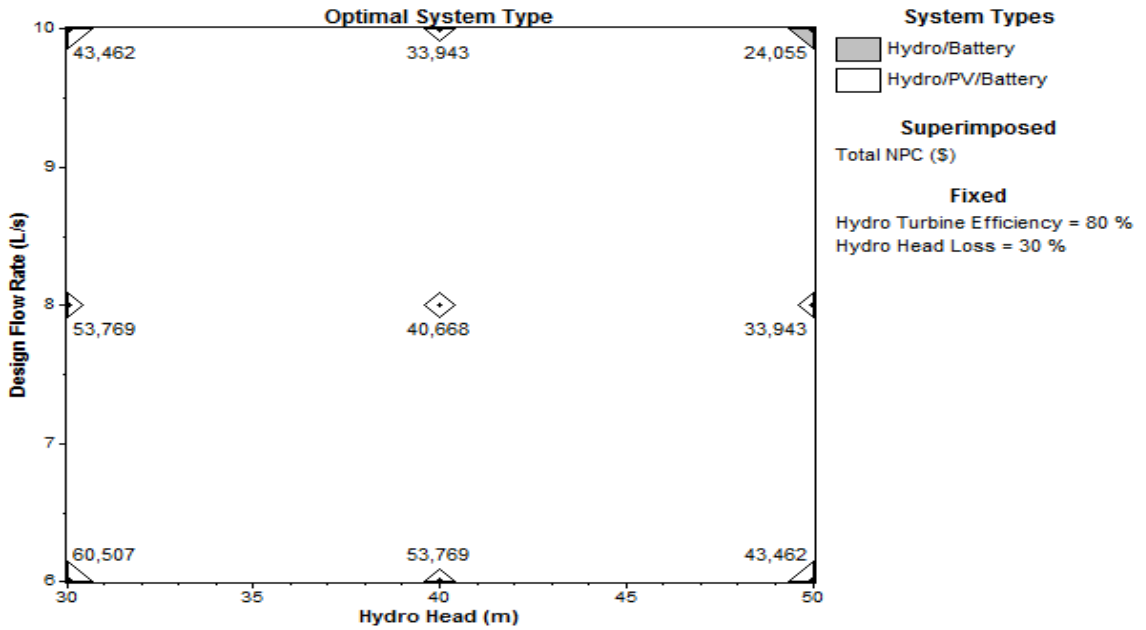

Figure 7.69: Total NPC for optimal system configuration at η_{hyd} = 80% and f_h = 30%.

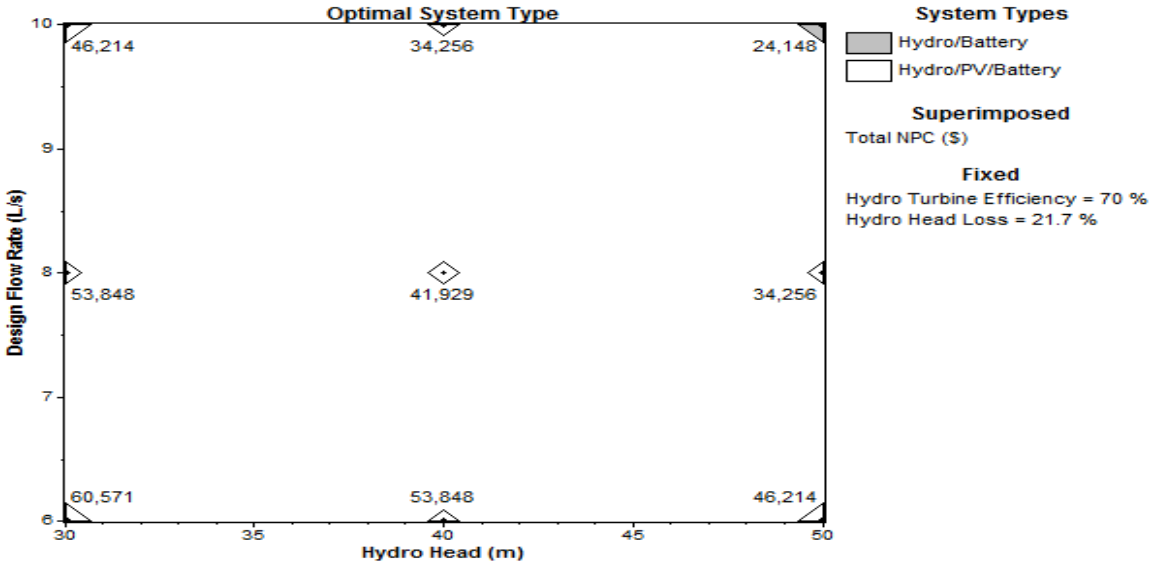

Figure 7.70: Total NPC for optimal system configuration at ηhyd = 70% and fh = 21.7%.

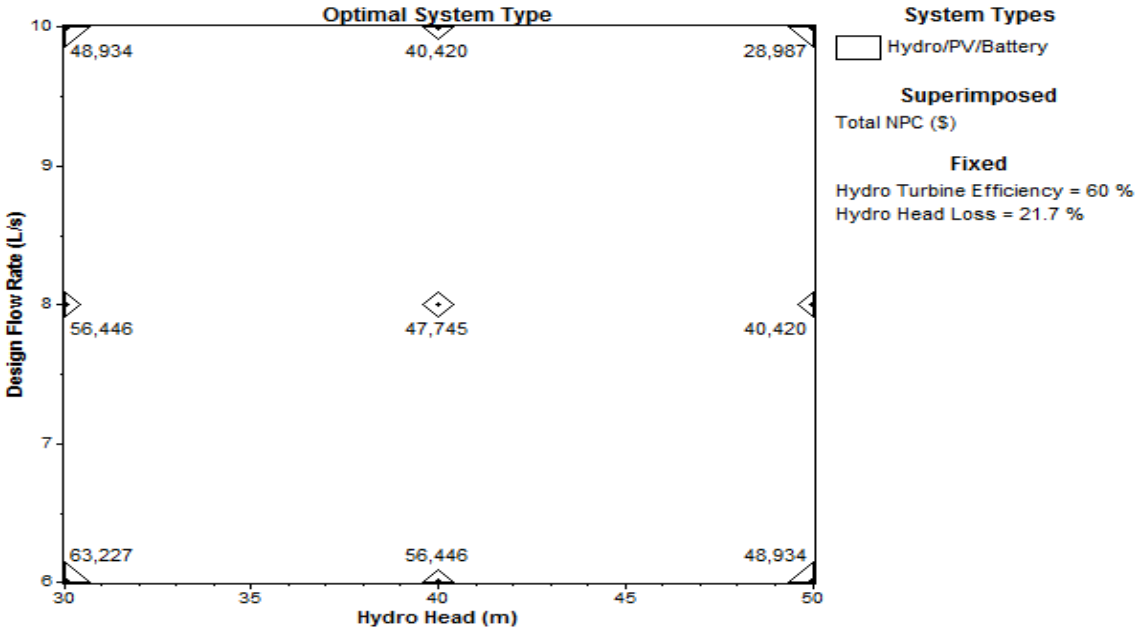

Figure 7.71: Total NPC for optimal system configuration at η_{hyd} = 60% and f_h = 21.7%.

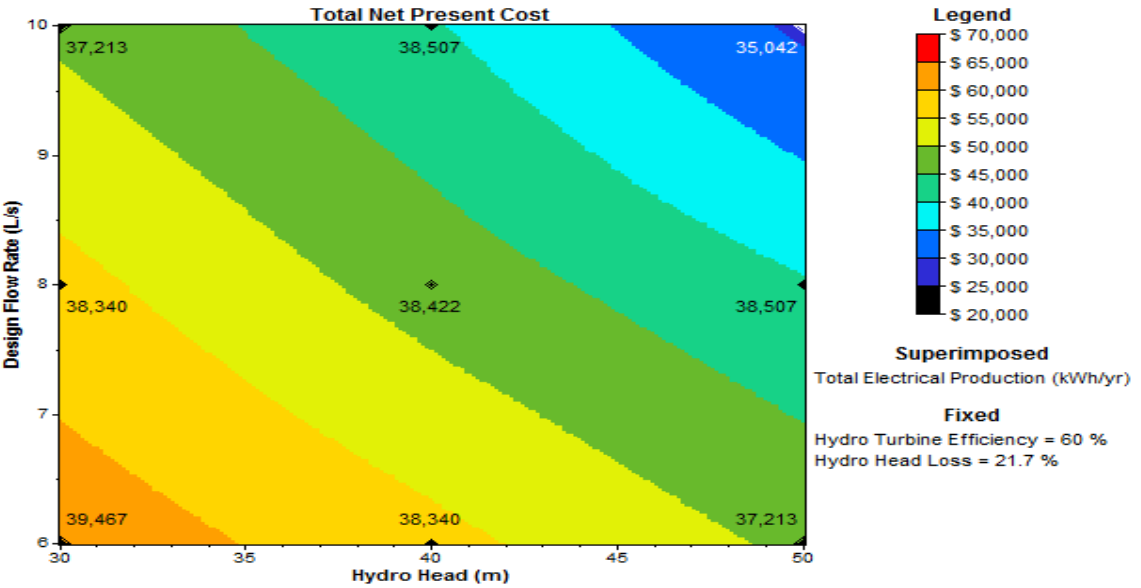

Figure 7.72: Surface plot of the total NPC and electrical production of the optimized power system at η_{hyd} = 60% and f_h = 21.7%.

Figure 7.78 shows that the total NPC decreases as the hydro head increases, but the total electrical production of the optimized power system decreases from 30 m to 40 m

hydro head, because of the PV-hydro power system combination, and then increases, because the hydro capacity increases faster and its electrical production contribution becomes larger above 40 m hydro head.

Figure 7.79 shows the effect of the flow rate on the total NPC and total electrical production of the optimized power system at constant η_{hyd}= 70%, $f_h = 21.7\%$ and $h_{eff} = 30\ m$. As the design flow rate increases the total NPC decreases sharply while the total electrical production decreases moderately up to 8 *l/s* and then decreases sharply to 10 l/s, because, the hydro head is fixed at 30 m.

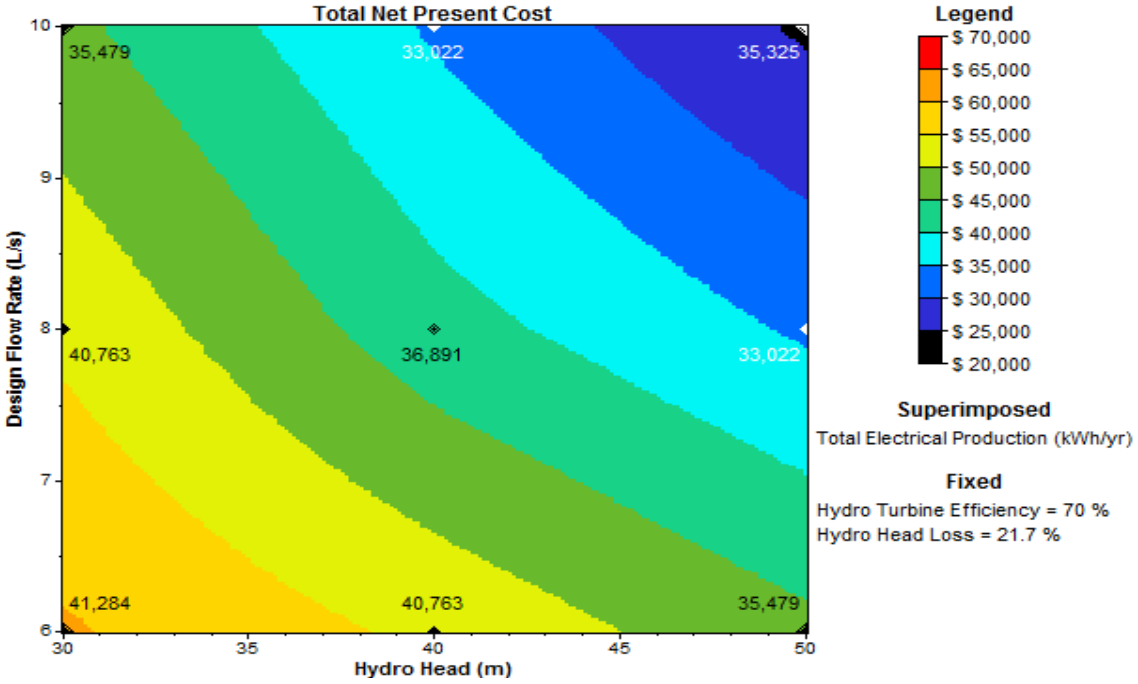

Figure 7.73: Surface plot of the total NPC and electrical production of the optimized power system at η_{hyd} = 70% and f_h = 21.7%.

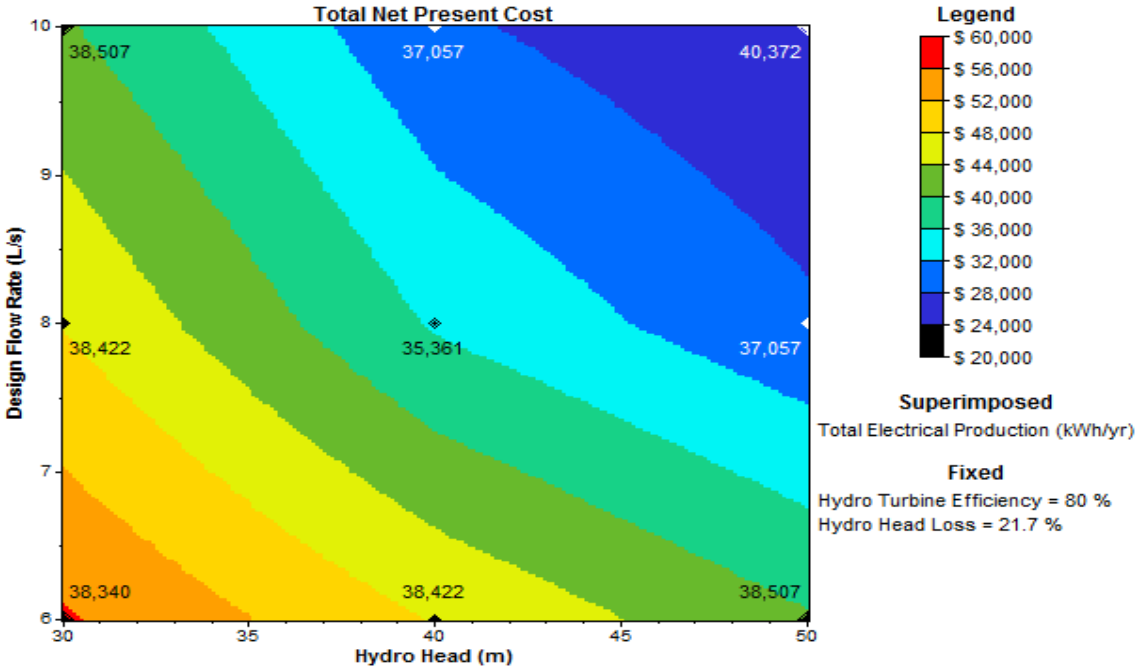

Figure 7.74: Surface plot of the total NPC and electrical production of the optimized power system at η_{hyd} = 80% and f_h = 21.7% .

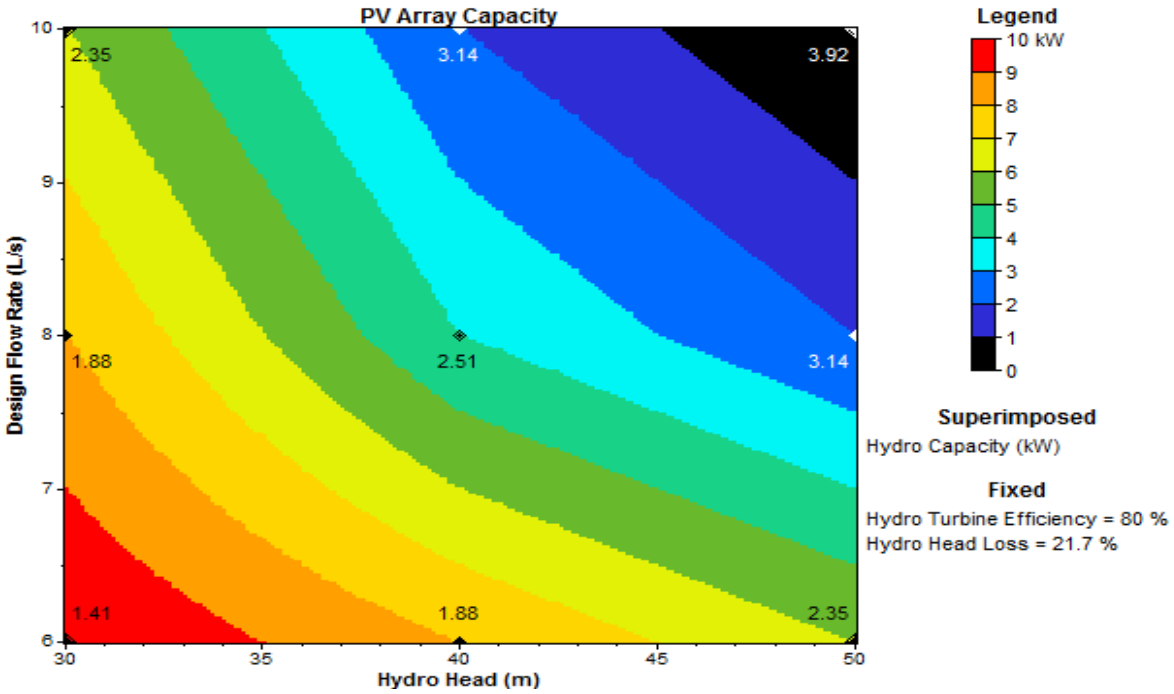

Figure 7.75: Surface plot of the PV and corresponding superimposed hydro capacity of the optimized power system at η_{hyd} = 80% and f_h = 21.7%.

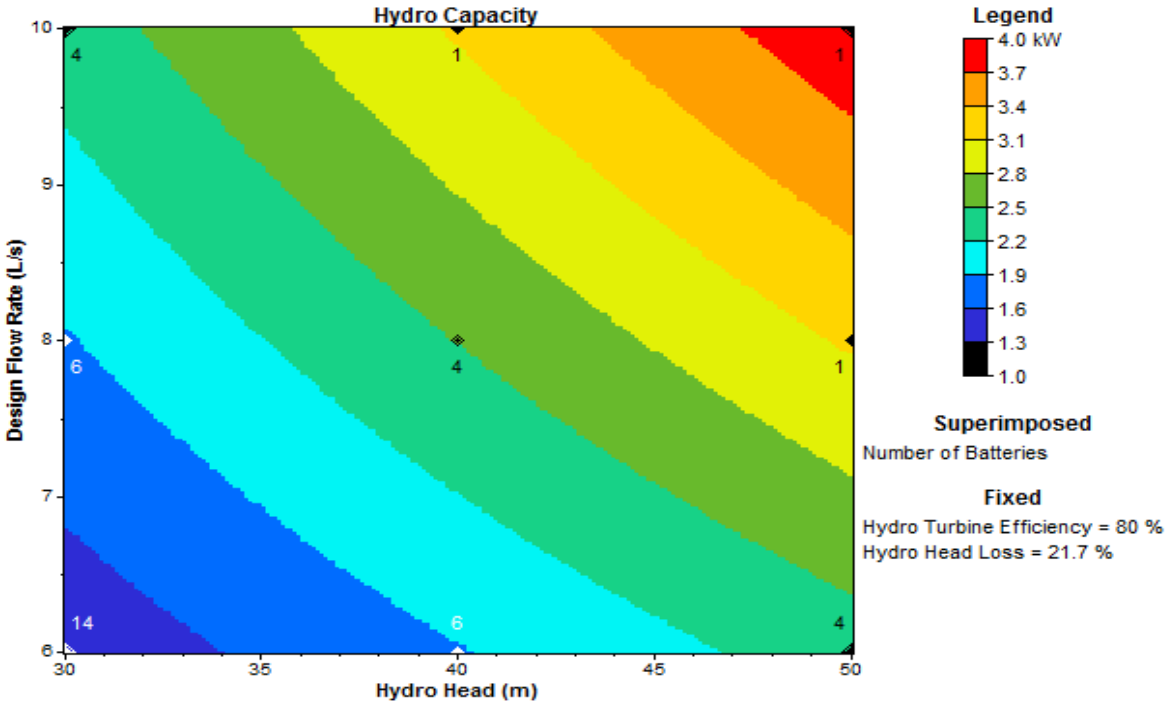

Figure 7.76: Surface plot of the hydro power capacity and corresponding number of batteries for the optimized power system at η_{hyd} = 80% and f_h = 21.7%.

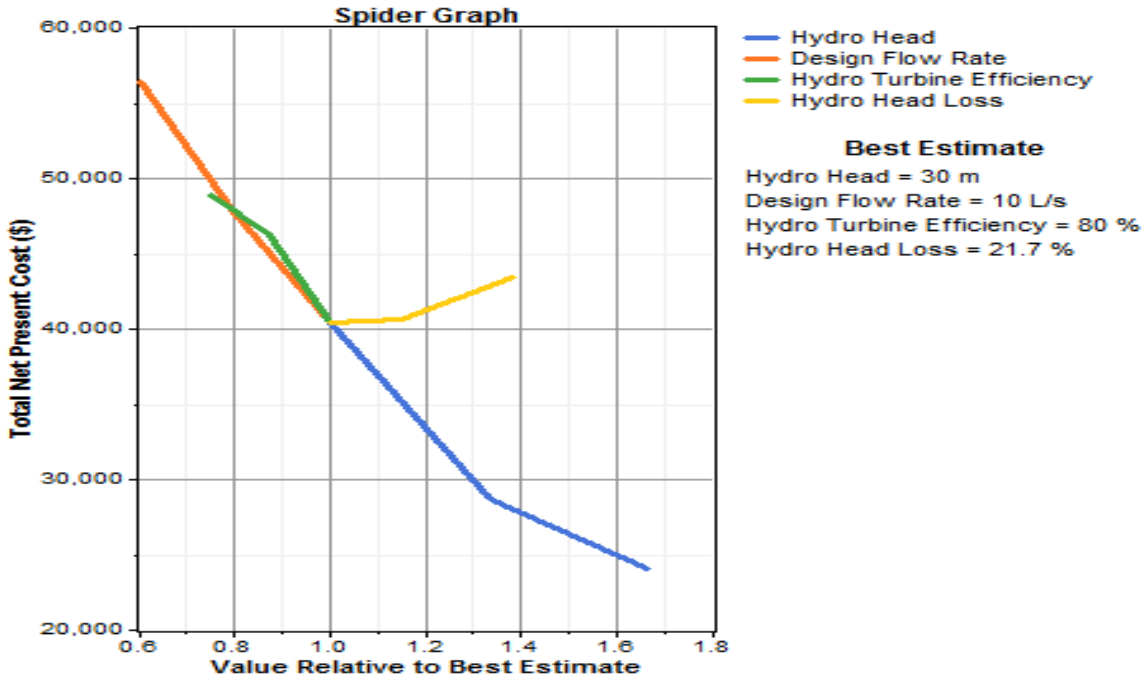

Figure 7.77: Spider graph of the optimized hydro system at the best estimate parameters selected vs. the variables η_{hyd}, f_h, h_{eff}, and $\dot{V}design$.

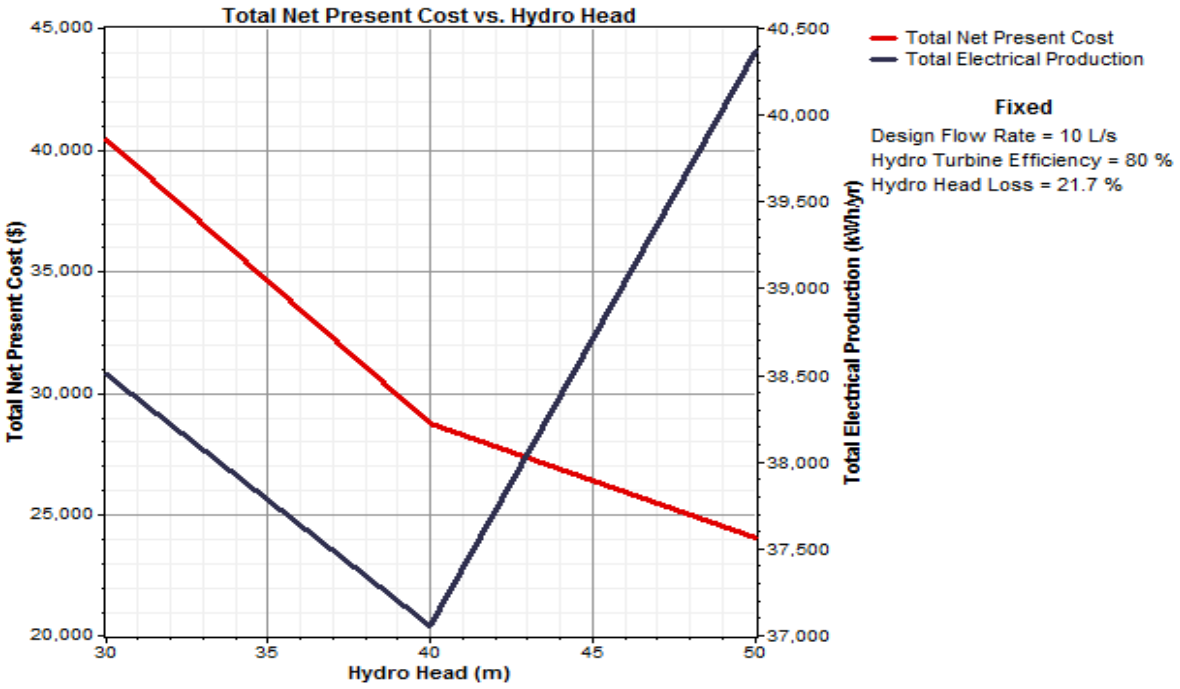

Figure 7.78: Total NPC and electrical production vs. hydro head.

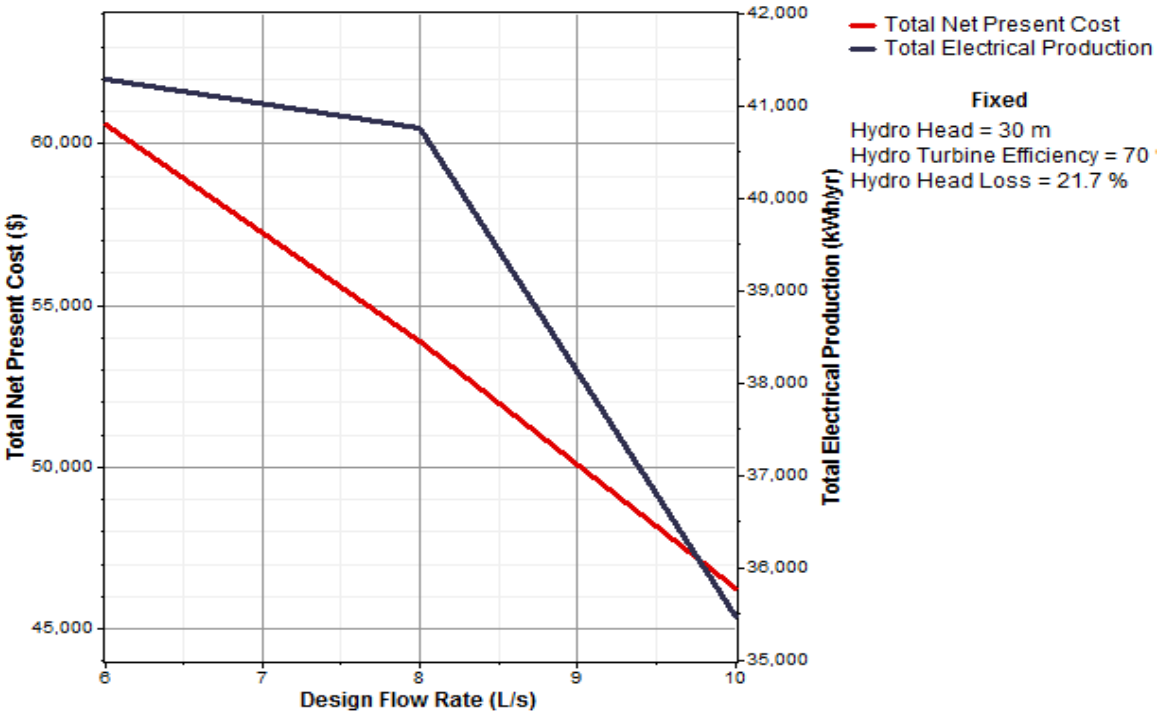

Figure 7.79: Total NPC and electrical production vs. flow rate.

7.6.2 Exergy analysis results

A sensitivity analysis on the system components is carried out by varying several parameters. Engineering equation solver (EES) software is used to calculate all the system properties and develop the parametric studies. The effects of keeping parameters, $T_o = 25^{\circ}C$, T_con = 29˚C, $T_{hp,con} = 39.37^{\circ}C$ *and* $T_{hp,ev} = 5.82^{\circ}C$ constant, designated here as the reference system, are shown for the COP of the heat transformer and the efficiencies for the distillation and overall systems in Figure 7.80. The energetic COP varies from 0.66 for the heat transformer at 8:00 am to 0.7 at 2:00 pm and 0.67 at 5:00 pm, while the exergetic COP varies around 0.55, 0.47 and 0.45 at 8:00 am, 2:00 pm and 5:00 pm respectively. The distillation system energetic efficiency varies between 71 %, 38 % and 64.1 % at 8.00 am; 2:00 pm and 5:00 pm, while the exergetic efficiency varies between 40 %, 18 % and 31 % at 8.00 am, 2:00 pm and 5.00 pm. The overall proposed system energetic efficiency varies from 0.92, 0.52, and 0.78 at 8:00 am, 2:00 pm and 5:00 pm respectively while the exergetic efficiency varies from 0.5, 0.37 and 0.51 correspondingly. The effect of solar energy dictates the behavior of the efficiencies graphs.

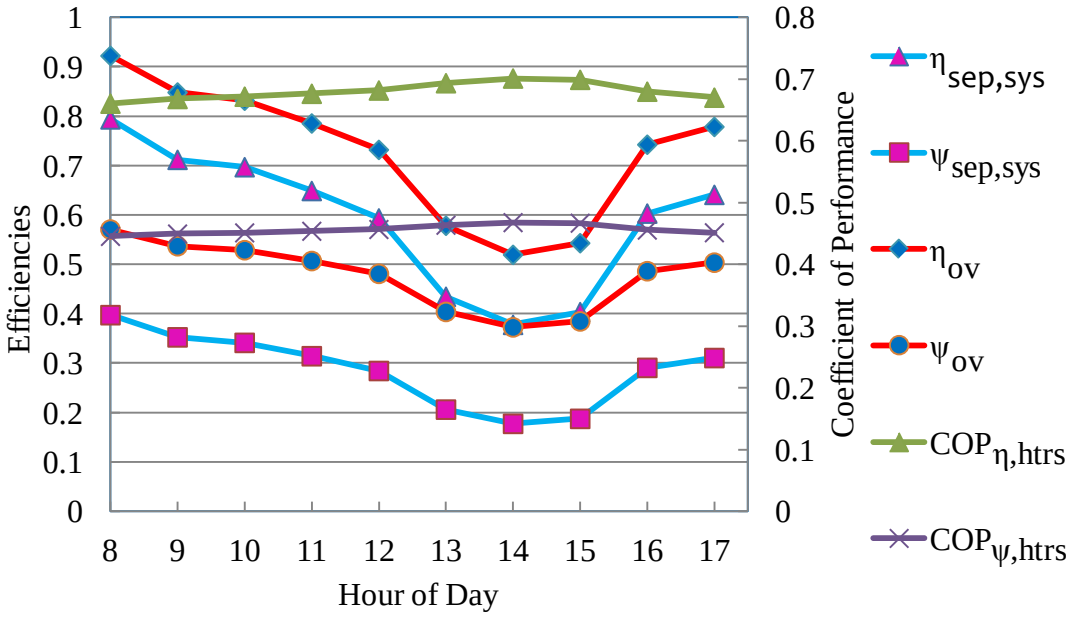

Figure 7.80: Energetic and exergetic COP of the heat transformer system and efficiencies of the distillation and overall systems at reference parameters.

Figure 7.81 shows the exergy destruction for the various developed systems components where the absorber followed by the regenerator, evaporator and condenser have the highest values due to absorption and desorption and latent heats.

Figure 7.82 shows the energetic and exergetic coefficient of performance of the GSHP cooling cycle with and without a heat exchanger for heating water at constant condensing pressure and variable evaporator pressures. The energetic COP decreases with decreasing evaporator pressure because the compressor has to work more due to lower suction pressure and constant condensing pressure.

The exegetic COP increases with increasing evaporator pressure because the exergetic thermal heat decreases more than the exergetic input work by the compressor as seen in the COP_{ψ} equation.

The effect of adding a heat exchanger to heat water at the discharge of the compressor is noted by the change in the energy and exergy COP of the GSHP. The addition of a heat exchanger improves the energy and exergy efficiencies.

The energetic and exergetic COP of the GSHP during the heating cycle with and without a heat exchanger are given in Table 7.33. The heat exchanger addition to the GSHP increases its COP.

Figure 7.83 shows the energy and exergy efficiencies for the individual components of the proposed system at the reference system parameters. This graph is important since it aids in improving any system component if possible.

Table 7.33: GSHP COP for heating cycle.

GSHP	COP_{η}	COP_{ψ}
Heat exchanger added	2.32	0.2287
Heat exchanger excluded	1.083	0.1139

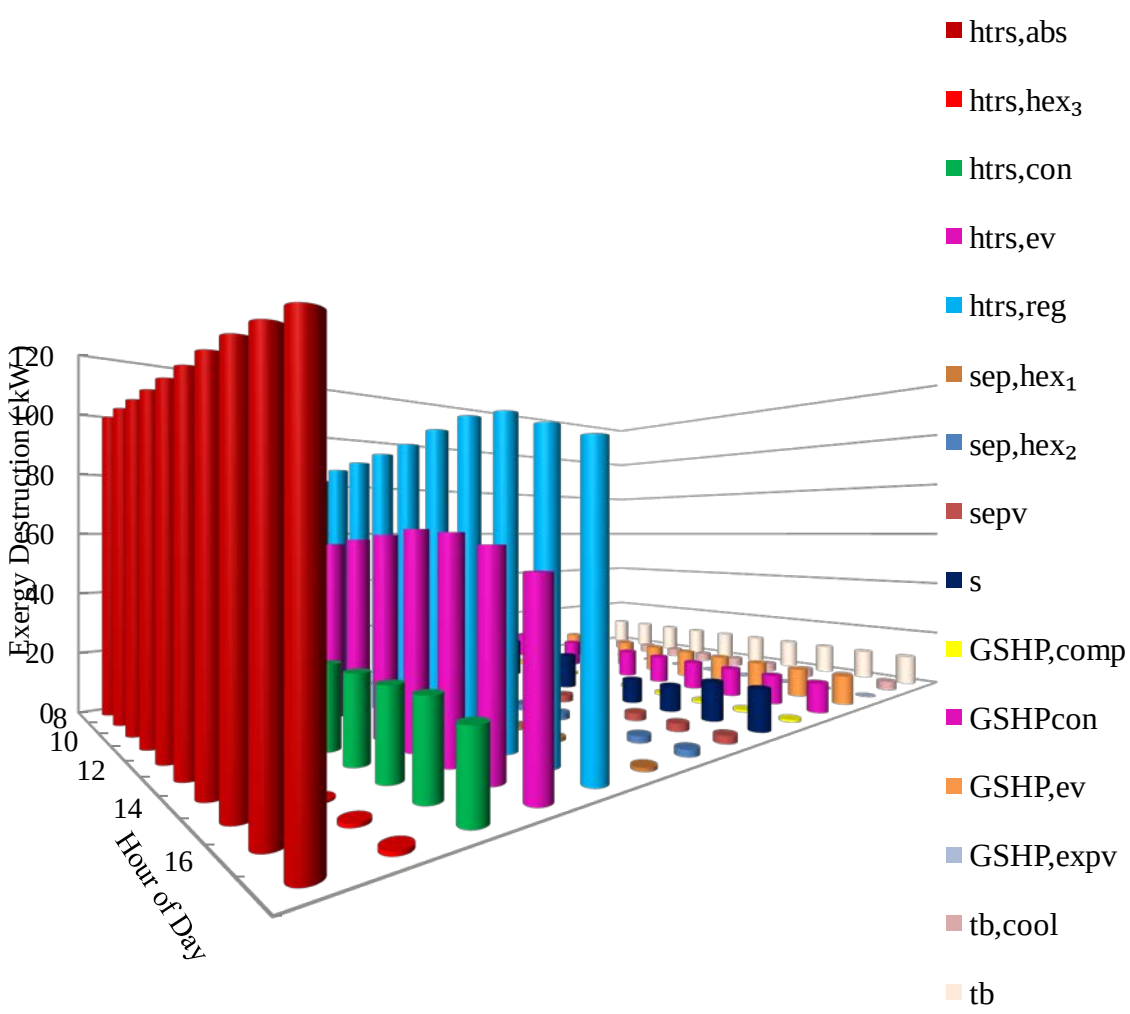

Figure 7.81: Exergy destruction for system components at constant reference parameters.

Figure 7.84 shows the energetic and exergetic efficiencies of the overall developed system and major systems at variable reference temperature. The energetic COP and efficiencies are not affected by varying the reference temperature. The exergetic COP of the heat transformer increases slightly because the numerator increases and the denominator decreases in the corresponding equation thus eliminating remarkable changes, while the exergetic efficiency of the distillation and overall proposed system vary slightly from the reference case because the effect of T_{sun} in the denominator of the corresponding equation.

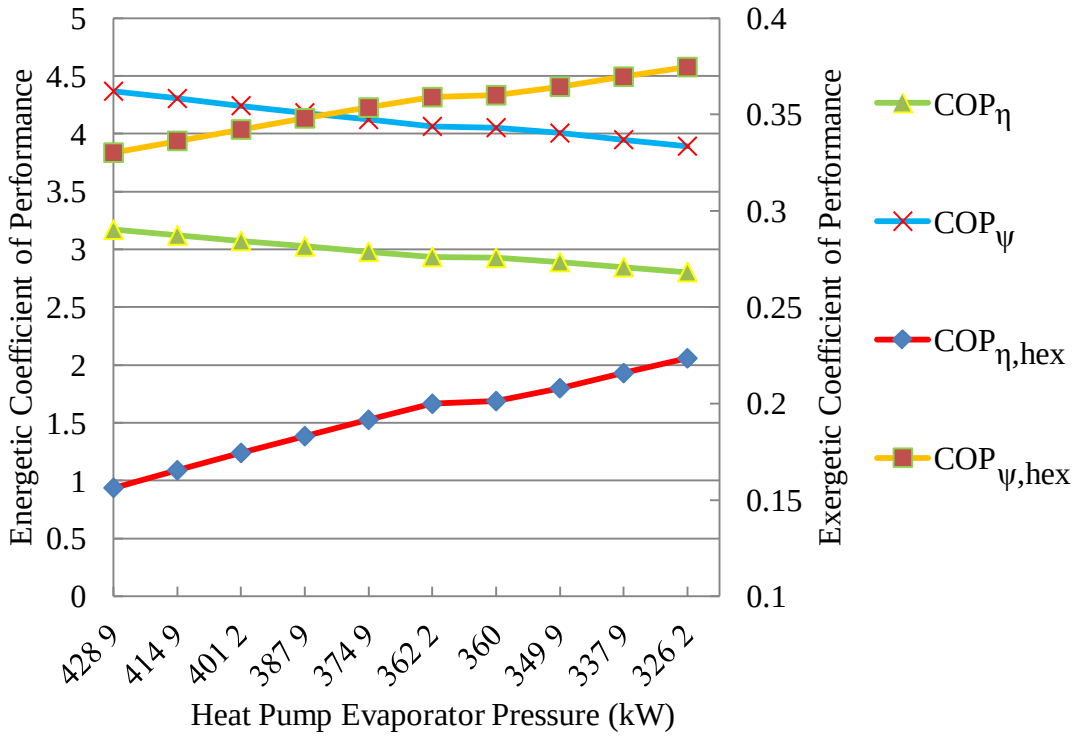

Figure 7.82: Energetic and exergetic COP of the GSHP with and without a heat exchanger at variable evaporator pressure for the cooling cycle.

Figure 7.85 shows that the increase in the reference temperature causes slight increase in the exergy efficiency of most of the individual components, except for the condenser where it decreases to approach zero as the reference temperature equals the condenser temperature and to negative as it exceeds it and that is expected.

Figure 7.86 shows exergy destruction for the various system components at variable reference temperature with modest effect on the system, because, the temperatures considered are varied slightly around the reference temperature (298K) from (294 to 303K) to resemble the actual setting of the research and the rest of the parametric variables.

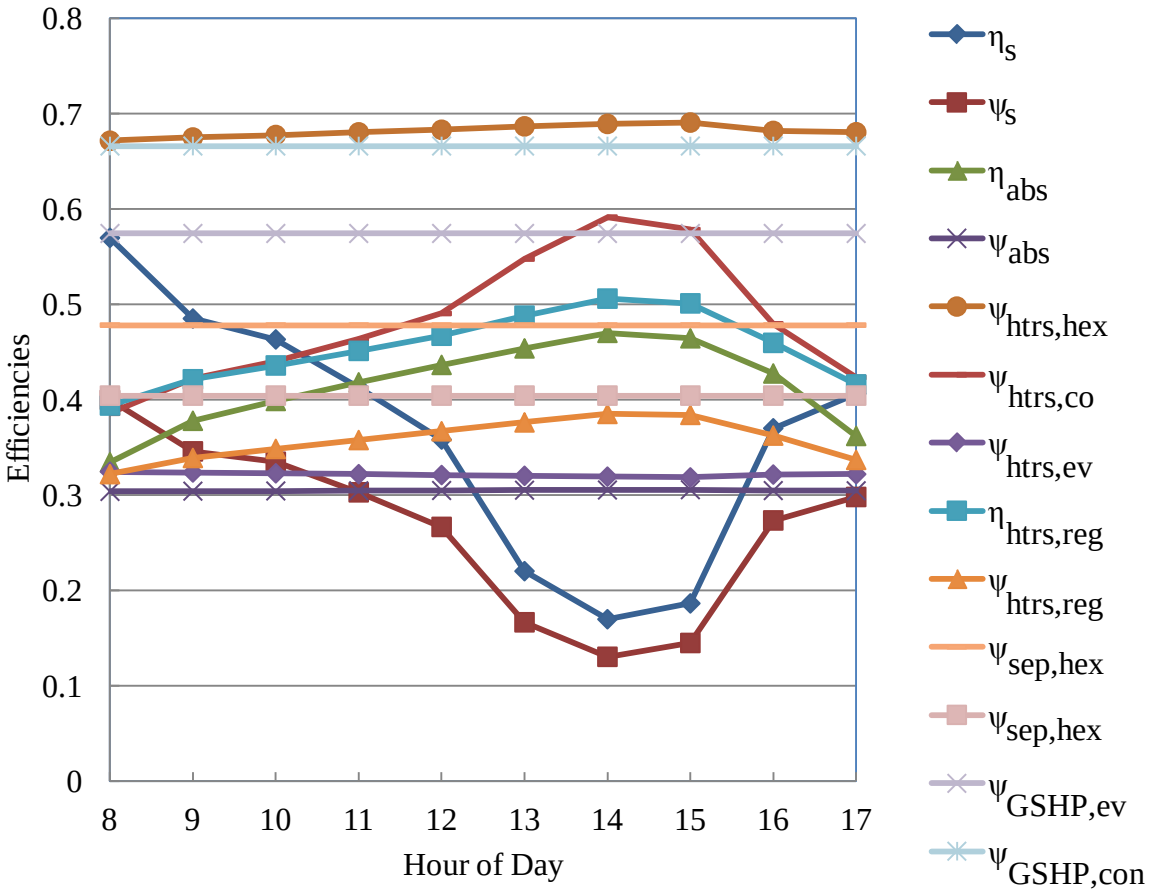

Figure 7.83: Exergy and energy efficiencies of various system components at reference parameters.

Figure 7.87 shows that the reversible COP of the GSHP decreases from 10 to 7.8 with decrease in evaporator pressure from 429.9 kPa to 326.2 kPa while keeping the condensing temperature constant and the total load constant.

The compressor work increases with decreasing evaporator pressure at constant condensing temperatures and fixed cooling load due to lower suction pressures at the inlet to the compressor.

The GSHP reversible COP and compressor work graphs exhibit the same trend but in reverse order.

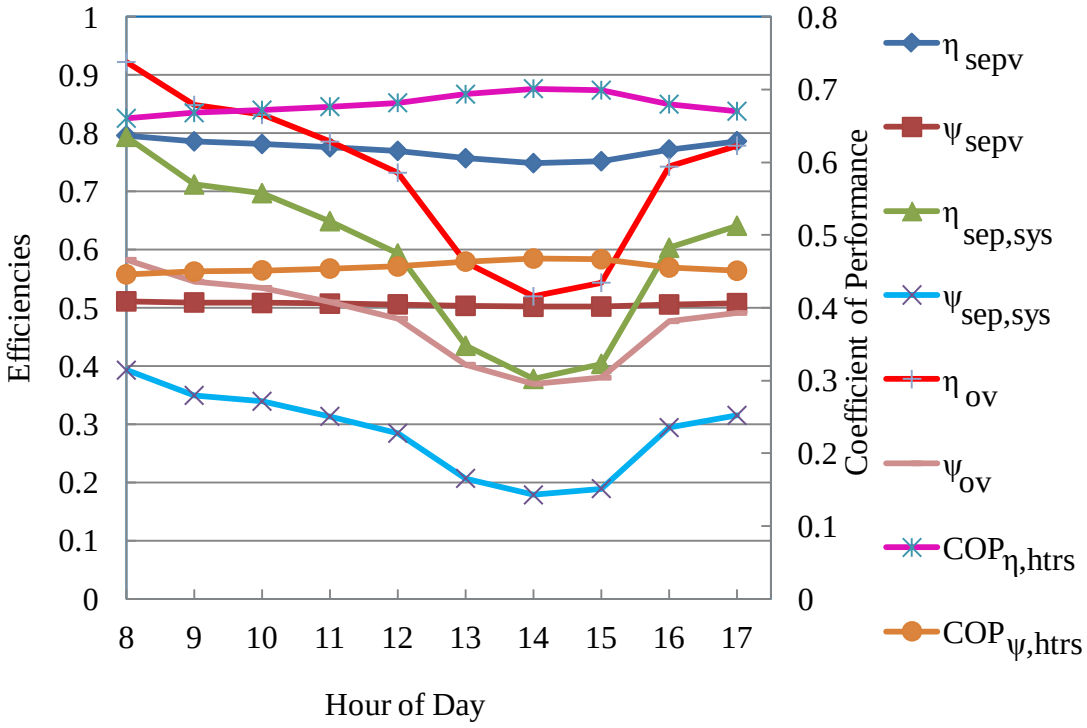

Figure 7.84: Energetic and exergetic COP of the heat transformer system and efficiencies of the separation and overall systems at variable reference temperature.

Figure 7.88 shows the effect of changing the GSHP condenser pressure on the exergy and energy COP with and without a heat exchanger while keeping all other parameters constant. The energetic COP for the GSHP without a heat exchanger varies from 2.9 to 2.8 as pressure increases from 839.2 kPa to 122 kPa while the values decreases from 4.1 to 4 with the inclusion of a heat exchanger to heat water at the discharge line of the compressor. As the condenser pressure increases while the evaporator pressure and cooling load remain constant the compressor works harder and the COP decreases.

The Exergetic COP doesn't change much for both cases of the GSHP with and without the heat exchanger because the decrease in the evaporator thermal heat is constant while the decrease in the compressor work is very small and meets that of the evaporator thermal heat. The addition of a heat exchanger to the GSHP improves the energetic COP from 2.9 to 3.7 and the exergetic COP from 0.21 to 0.33.

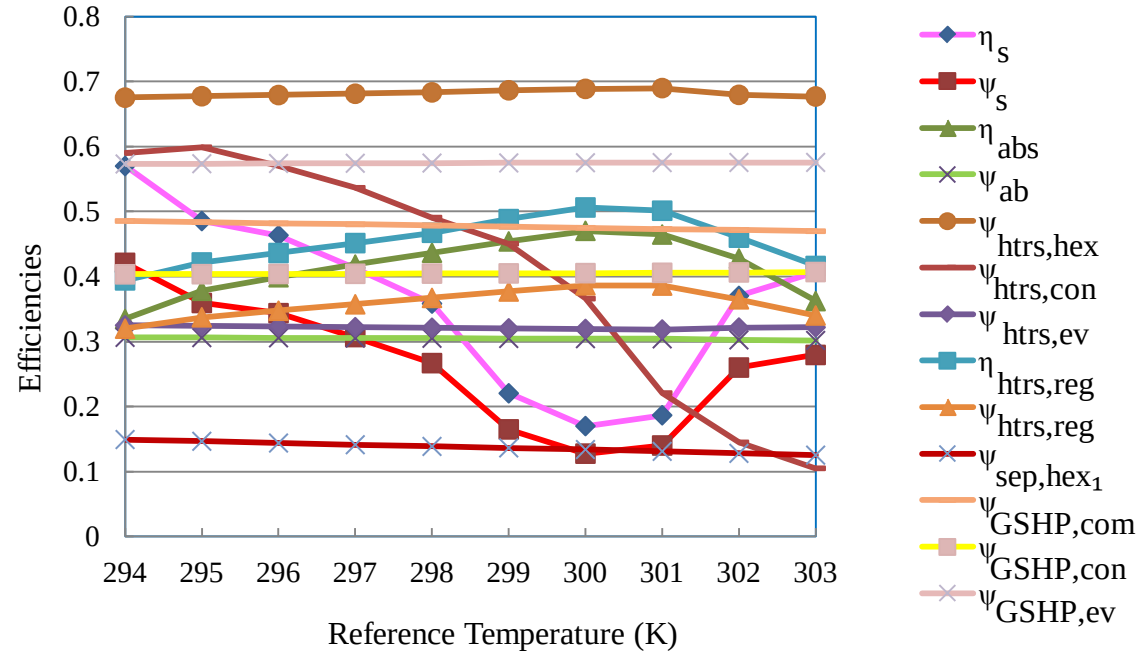

Figure 7.85: Exergy and energy efficiencies of various system components at variable dead state temperature.

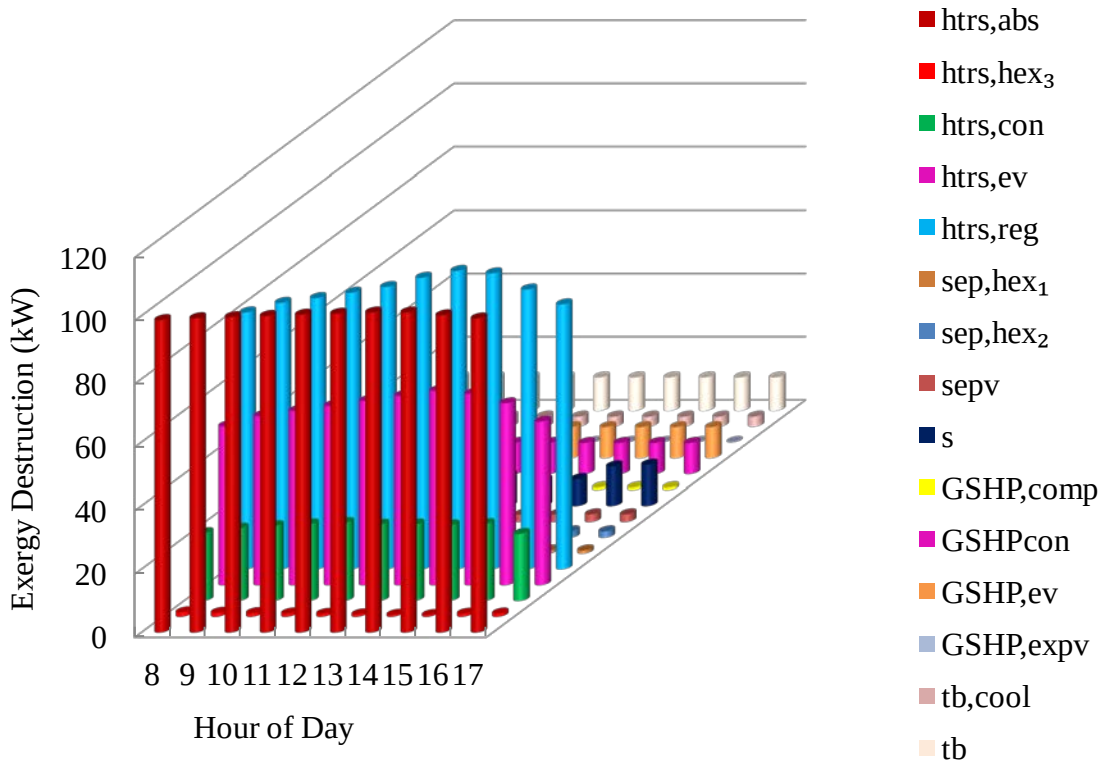

Figure 7.86: Exergy destruction for system components at variable reference temperature.

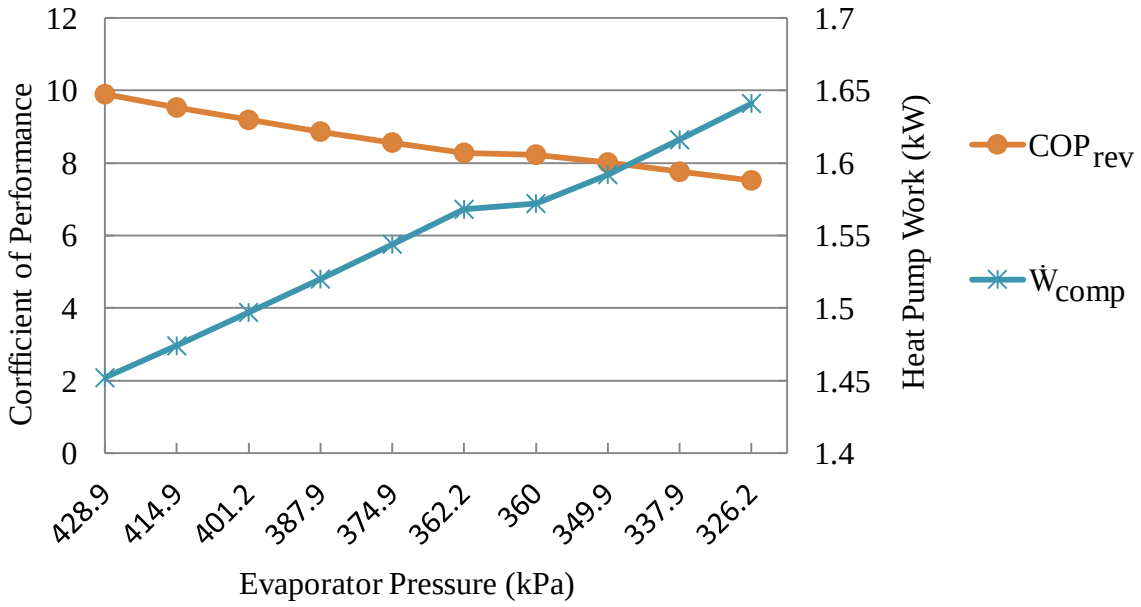

Figure 7.87: Effect of the evaporator pressure on the reversible COP and compressor work of the GSHP at constant reference temperature.

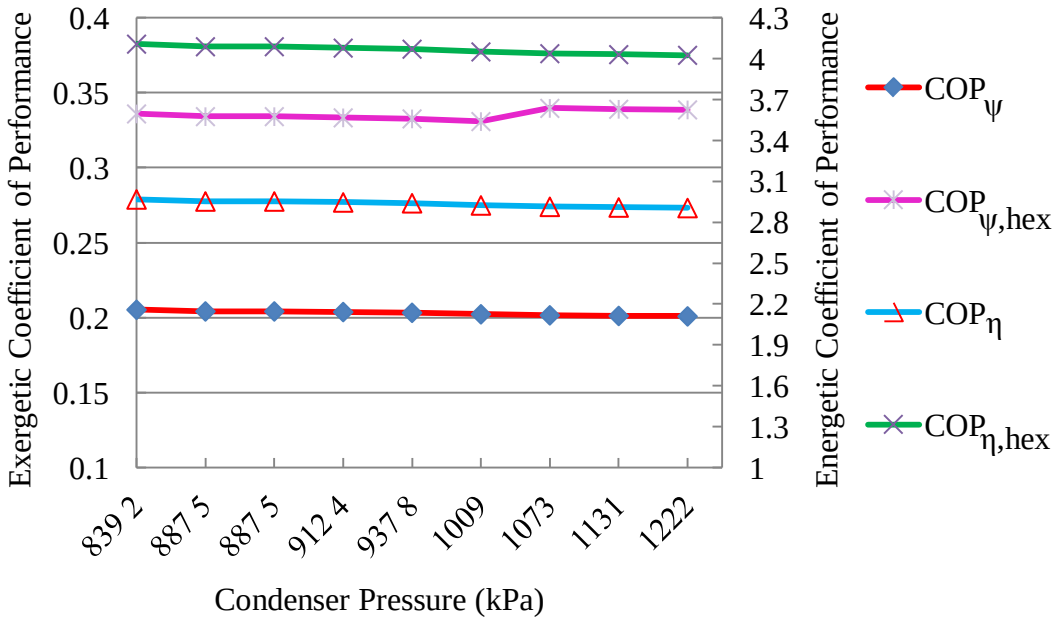

Figure 7.88: Energetic and exergetic COP of the GSHP cooling cycle at variable condenser pressure with and without a heat exchanger.

7.6.3 Exergoeconomic analysis and optimization results

Exergoeconomic analysis is conducted to calculate the total cost of the system equipments, operation and maintenance and exergy destruction. Optimization using multi-objective technique is carried out for minimum total system cost and maximum overall system exergy efficiency. The Pareto Front is plotted in Figure 7.89 where the overall exergy efficiency ranged from 65.41% to 65.46 % at a total cost of 0.646 $/h to 0.647 $/h. The maximum overall system exergy efficiency is 57.1% at reference case and is increased to 65.5% by optimization. The initial system net present cost is $68,192.25 compared to $74,384.00 after running the optimization.

In this case, 300 generations with a population size of 120 is used where it undergoes tournament selection criteria to choose parents for the next generation. The tournament selection Figure 7.90 chooses each parent by choosing 2 players at random and then choosing the best individual out of that set to be a parent. The reproduction crossover fraction of 80% which specifies the fraction of the next generation, other than elite children, that are produced by cross over. The genetic algorithm makes small random changes in the individuals in the population to create mutation children which provide genetic diversity by randomly generating directions that are adaptive with respect to the last successful or unsuccessful generation. The feasible region is bounded by the 21 constraints. A step length is chosen along each direction so that linear constraints and bounds are satisfied and the crossover of individuals occurs by combining two individuals or parents and taking their weighted average considered in this case to be 1 to form a crossover child for the next generation. A migration fraction of 20% of individuals moves between sub-populations from the smaller of the two sub-populations in intervals of 20 generations. When migration occurs, the best individuals from one sub-population replace the worst individuals in another subpopulation. Individuals that migrate from one sub-population to another are copied.

Finally, the Pareto front population fraction of 0.85 is selected so that individuals are kept on the first Pareto front while the solver selects individuals from higher fronts.

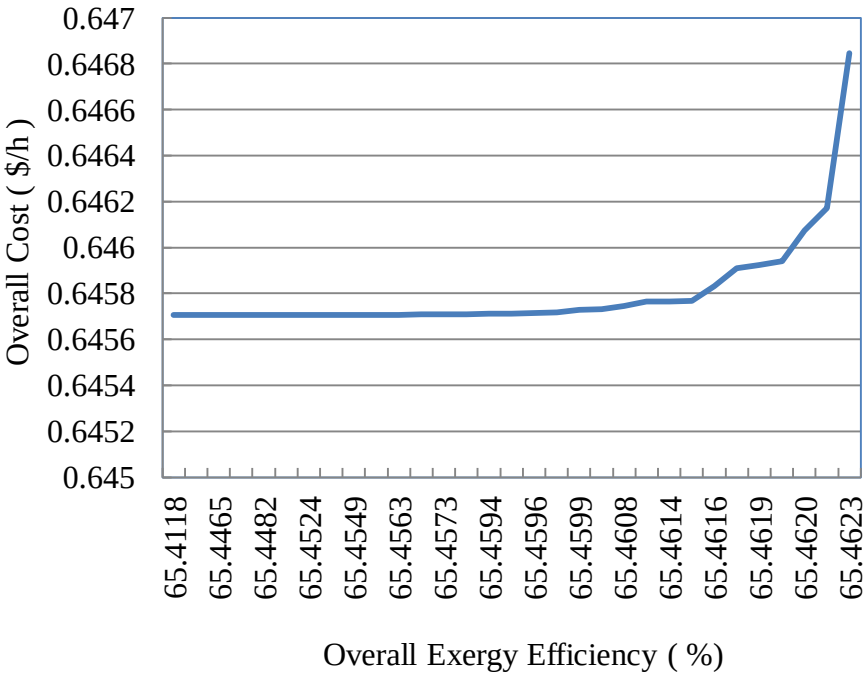

Figure 7.89: Pareto front for the overall system cost vs. the overall exergy efficiency.

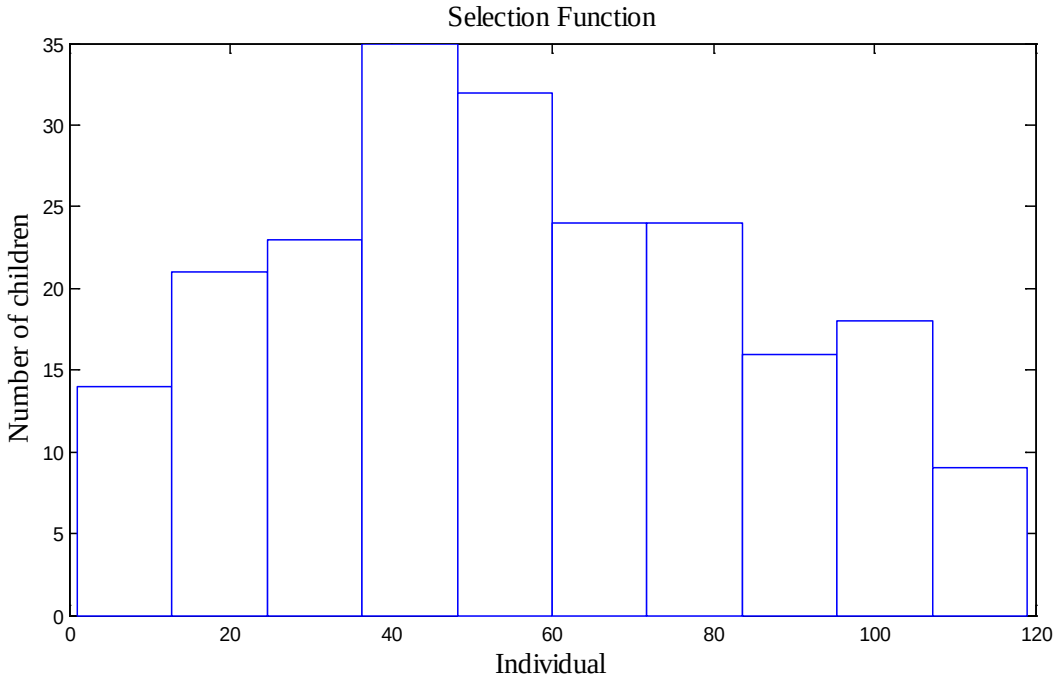

Figure 7.90: Histogram of the parents.

Figure 7.91 shows the rank structure where the Pareto plots the fraction of individuals in each Pareto hierarchy. Individuals ranked 1 are best, rank 2 individuals are dominated only by rank 1 individuals and so on.

Figure 7.92 shows the average distance measure between individuals in every population, while Figure 7.93 shows the average Pareto distance measure between individuals for the 300 populations. Figure 7.94 shows the average Pareto spread around 0.98 which is the change in distance measure of individuals with respect to the previous generation.

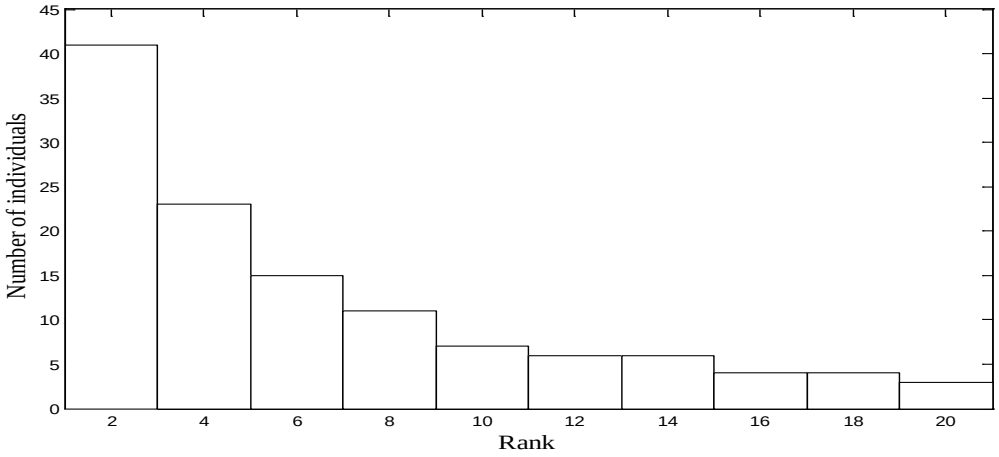

Figure 7.91: Rank histogram.

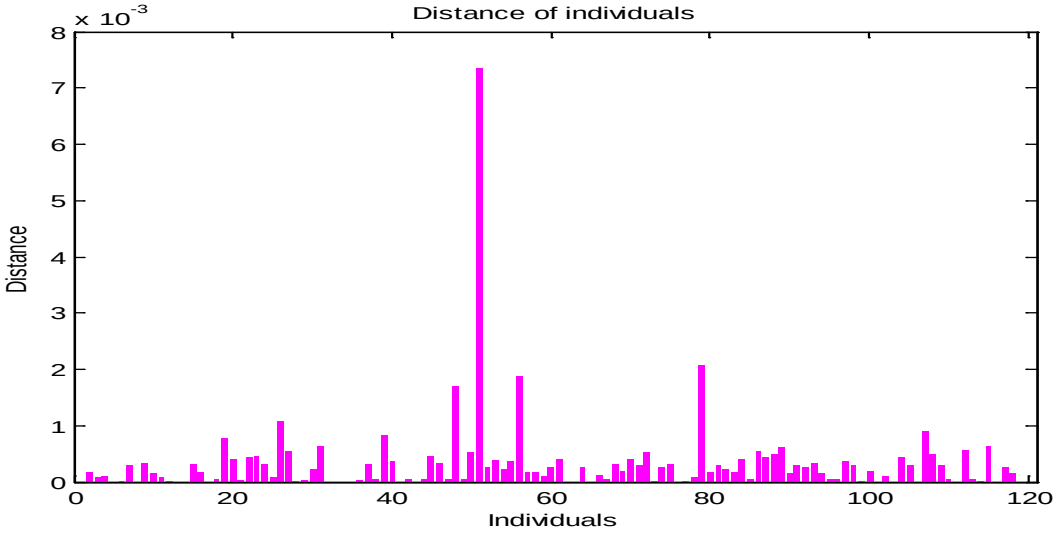

Figure 7.92: Distance between individuals in one population.

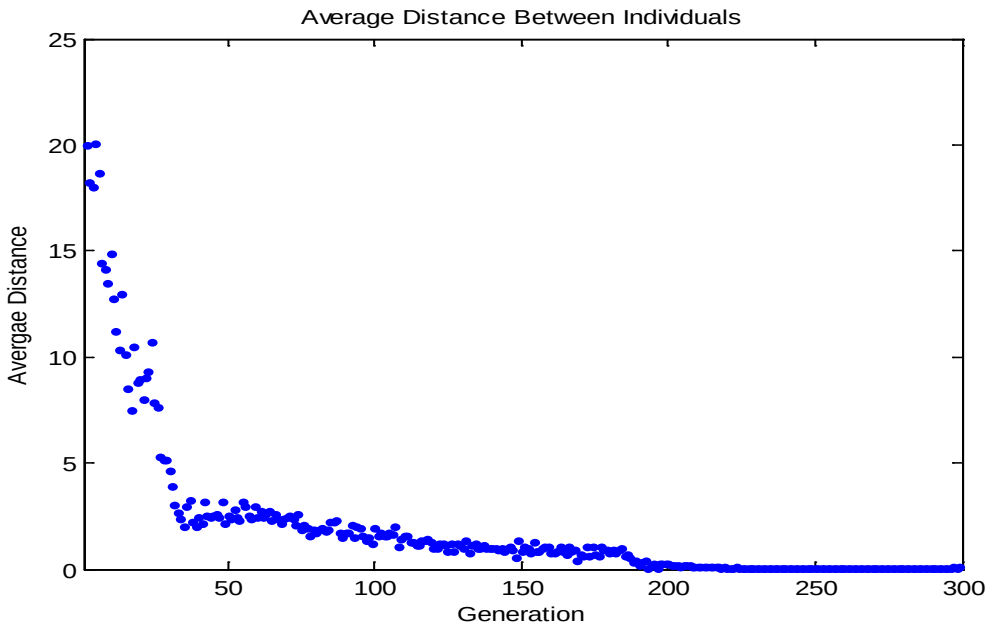

Figure 7.93: Average Pareto distance.

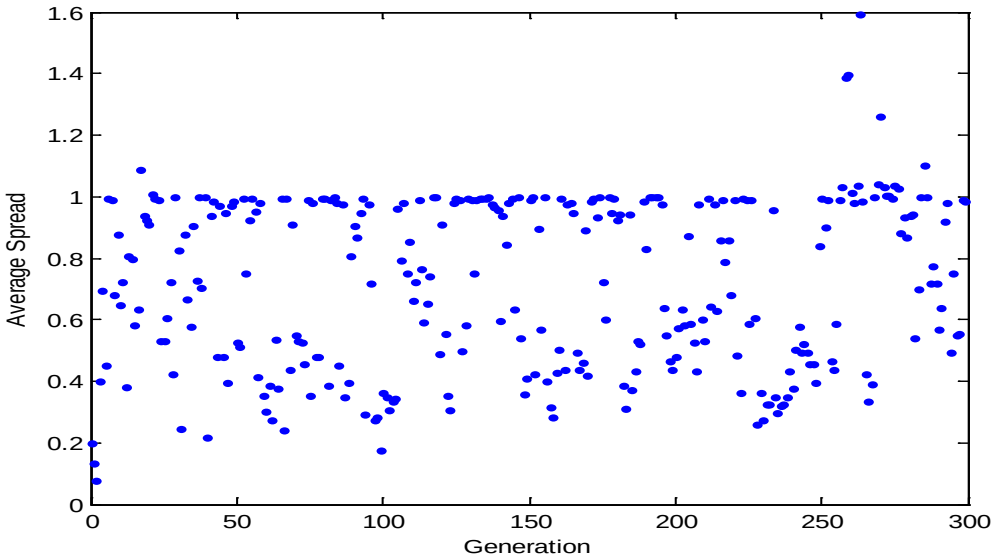

Figure 7.94: Average Pareto spread.

Chapter 8: Conclusions and Recommendations

This study develops three novel integrated energy systems, for multigeneration applications to meet the demands of power, seasonal air-conditioning, hot and fresh water for building energy applications which result in net zero energy houses or buildings.

8.1 Conclusions

The following findings can be extracted from this research:

8.1.1 System I

- The optimal power system with total NPC = $56,558.00 and renewable energy fraction of 0.998 with 73.3 kg/yr CO_2 emissions provides a net-zero energy house.
- The levelized cost of energy is $0.127/kWh.
- The exergy results show that the absorption chillers' regenerator and absorber and the LDS regenerator are the main sources of irreversibility due to chemical exergy associated with sorption and desorption processes.
- The exergy analysis of the system efficiencies shows a lower performance of the system components in comparison to energy.
- The exergoeconomic analysis yields a total system cost of $107,000.00.
- The multiobjective optimization improves the overall exergy efficiency from the original design by 10% with a total system net present cost increase of 8%.
- The hot water produced at the hot water tank during sunshine is 0.0078 l/s which satisfy the requirement of the house.
- The hot water produced from the ground thermal storage during winter season is 0.0068 l/s which satisfy the requirement of the house.
- The fresh water produced is 0.01364 l/s which satisfy the requirement of the house.
- The desired power, seasonal air-conditioning, hot and fresh water for the NZEH are achieved by the developed system.

8.1.2 System II

- The optimal power system with total NPC of $52,505.00 and renewable energy fraction of 1.00 with zero kg/yr CO_2 emissions provides a NZEH.
- The levelized cost of energy is $0.118/kWh.
- The exergy results show that the ORC evaporator, absorption chillers' regenerator and absorber and the LDS regenerator are the main sources of irreversibility due to chemical exergy associated with sorption and desorption processes.
- The exergy analysis of the system efficiencies shows a lower performance of the system components in comparison to energy.
- The exergoeconomic analysis yields a total system cost of $117,700.00.
- The exergy analysis yields maximum overall system exergy efficiency of 44.67%.
- The multiobjective optimization improves the overall system exergy efficiency by 14.1%.
- The overall system exergetic efficiency varies between 44.76 %, 23.57 % and 36.22 % at 8.00 am, 2.00 pm and 5.00 pm, due to solar energy changes, while the overall system energetic efficiency varies between 60 %, 36.62 % and 53.95 % at 8.00 am, 2.00 pm and 5.00 pm respectively.
- The fresh water produced is 0.01364 l/s which satisfy the requirement of the house.
- The hot water produced at the hot water tank during sunshine is 0.0078 l/s which satisfy the requirement of the house.
- The desired power, seasonal air-conditioning, hot and fresh water for the NZEH are achieved by the developed system.

8.1.3 System III

- The optimal power system with total NPC $40,420.00 and renewable energy fraction of 1.00 with zero kg/yr CO_2 emissions provides a NZEH.
- The levelized cost of energy is 0.091 $/kWh.

- The exergy results show that the heat transformers' absorber and regenerator are the main sources of irreversibility due to chemical exergy associated with sorption and desorption processes.
- The exergy analysis of the system efficiencies shows a lower performance of the system components in comparison to energy.
- The exergoeconomic analysis yields a total system NPC of $68,192.25.
- The exergy analysis yields maximum overall system exergy efficiency of 57.1%.
- The multiobjective optimization improves the overall system exergy efficiency by 8.4% at an overall system total NPC increase of $6,191.75.
- The overall system exergetic efficiency varies from 0.57 to 0.37 and 0.51 at 8:00 am, 2:00 pm and 5:00 pm respectively due to solar changes.
- The hot and fresh water produced by the distillation system is 0.0184 l/s which satisfy the requirement of the house.
- The hot water produced from the ground thermal storage during winter season is 0.0068 l/s which satisfy the requirement of the house.
- The desired power, seasonal air-conditioning, hot and fresh water for the NZEH are achieved by the developed system.
- System III will be used for the present house since its location allows for the use of hydro turbine and the total system NPC is the lowest.

8.2 Recommendations

The three developed novel systems can be used anywhere in the world with adjustment to meteorological data. It is recommended to select the system that best fits the resources available. It is worth noting that human awareness and performance is crucial to transforming any community to net zero energy homes concept. Hence, it is imperative to engage a home owner in the early design stages in order to consume power efficiently and learns to live sustainably. Future studies should complement and integrate these resourceful multigenerational systems with the following:

- The developed systems should be built and tested for net zero energy houses and performance assessment.

- The analysis should be performed for different regions of the world and the effect on total NPC values and efficiencies to be investigated.
- Hydrogen production should be integrated with these systems.
- The electricity production from fuel cells should be investigated and the feasibility of the integrated system should be considered.
- The solar collector system and PV system should be replaced by solar tracking systems and investigation of their effect on the total NPC and efficiencies noted.
- Using building integrated photovoltaic's with the developed systems in order to increase efficiencies of the overall system should be carried out
- Replacing the wind turbine used by the new 80% efficient Dutch wind turbine known as Archimedes and noting the changes on the system performance and efficiencies should be evaluated.
- Building design should accommodate for day lighting, passive ventilation and the use of green house solarium which might have reasonable effect on the system's NPC and efficiencies should be investigated.

References

[1] Dincer I, Rosen M, "Exergy: Energy, Environment and Sustainable Development," *Elsevier, Second Edition*; 2007

[2] Dincer I, "Renewable energy and sustainable development: a crucial review," *Renewable and Sustainable Energy Reviews*; 2000; 4(2): 157-175.

[3] http://www.epa.gov/cleanenergy.

[4] http://naturalresources.house.gov.

[5] NASA Langley Research Center, "Radiation Budget," 2006

[6] Joshi A.S, Dincer I, and Reddy B.V, "Comparative study of effect of cloudiness/haziness on the quality of solar radiation," *ASME- Journal of Solar Energy Engineering*; 2013

[7] Joshi A.S, Dincer I, and Reddy B.V, "Solar Exergy Maps for Performance Assessment of PV/T Systems," *International Journal of Exergy*; 2013

[8] Drachmann A.G, "Heron's Windmill," *Centaurus*; 1961; 7: 145–151

[9] Lohrmann D, "Von der östlichen zur west lichen Windmühle," *Archiv für Kulturgeschichte*; 1995; 10(f): 1–30

[10] Hassan A, Hill D, "Islamic Technology: An illustrated history," *Cambridge University Press* ; 1986; pg. 54

[11] Price J, "James Blyth – Britain's first modern wind power engineer," *Wind Engineering*; 2005; 29 (3): 191–200.

[12] Hurley B, "How Much Wind Energy is there? ," *Claverton Group*; 2012

[13] Global Wind Energy Council, "Global Wind Report Annual market update," 2012. www.gwec.net

[14] Wind Atlases of the World, http://www.windatlas.dk/World

[15] Turcotte D, Schubert G, "Geodynamics," *Cambridge University Press*; 2002; pp. 136–137

[16] GEA, "Geothermal Energy: International Market Update," Geothermal Energy *Association*; 2012; pg. 4–6

[17] Douglas C. A, Harrison, G. P., Chick, J. P., "Life cycle assessment of the Seagen marine current turbine," *Journal of Engineering for the Maritime Environment;* 2008; 91: 1-12

[18] Scheck J, "Wood-Fired Plants Generate Violations," *Wall Street Journal*; 2012

[19] Rowell R.M, Hokanson A.E, "Methanol from Wood: A Critical Assessment," *Academic Press*; 1979; NY

[20] European Environment Agency Scientific Committee, "Opinion of the EEA Scientific Committee on Greenhouse Gas Accounting in Relation to Bioenergy,"2011

[21] Torcellini P, Pless S, Deru M, Crawley D, "Zero Energy Buildings, a Critical Look at the Definition," *ACEEE*; 2006; Pacific Grove, California, USA.

[22] Energy Information Administration, "1999 Commercial Buildings Energy Consumption Survey," 2002; www.eai.doe.gov

[23] Crawley D, Torcellini P, "Understanding Zero-Energy Buildings," *ASHRAE Journal*; 2006; 48: 9- 62

[24] U.S Department of energy, *Building Energy Data Book*; 2005

[25] Energy Information Administration, *Annual Energy Outlook*; 2006; www.eai.doe.gov

[26] Li D, Yang L, Lam J, "Zero energy buildings and sustainable development implications - A review," *Energy*; 2013; 54:1-10

[27] International Energy Agency (IEA), *World Energy Outlook Paris*; 2010

[28] Ma L, Ellwood JM, Cullen JM, Li Z, "The Use of Energy in China: Tracing the Flow of Energy From Primary Source to Demand Drivers," *Energy*; 2012; 40: 174-88

[29] Chai Q, Zhang X, "Technologies and Policies for the Transition to a Sustainable Energy System in China," *Energy*; 2010; 35:3995-4002

[30] Ma L, Liu P, Fu F, Li Z, Ni W, "Integrated Energy Strategy for the Sustainable

Development of China," *Energy*; 2011; 36:1143-54

[31] Lam J, Hui S, "Sensitivity Analysis of Energy Performance of Office

Buildings," *Building Environment*; 1996; 31:27-39

[32] Masoso O, Grobler L, "A New and Innovative Look at Anti-Insulation

Behavior in Building Energy Consumption," *Energy and Buildings*; 2008; 40: 1889-1894

[33] Jentsch M, Bahaj A, James P, "Climate Change Future Proofing of Buildings - Generation and Assessment of Building Simulation Weather Files," *Energy Build*; 2008; 40: 2148-2168

[34] Artmann N, Manz P, "Heiselberg Climatic Potential for Passive Cooling of Buildings by Night-Time Ventilation in Europe," *Applied Energy*; 2007; 84: 187-201

[35] Muneer T, "Solar Radiation and Daylight Models for the Energy Efficient Design of Buildings," *Oxford: Architectural Press*; 1997

[36] Tian C, Chen T, Yang H, Chung T, "A Generalized Window Energy Rating System for Typical Office Buildings," *Solar Energy*; 2010; 84: 1232-1243

[37] Roussac A, Steinfeld J, Dear R, "A Preliminary Evaluation of Two Strategies for Raising Indoor Air Temperature Set points in Office Buildings," *Architecture Science Review*; 2011; 54: 148-56

[38] Sadineni S, Boehm R, "Measurements and Simulations for Peak Electrical load Reduction in Cooling Dominated Climate," *Energy*; 2012; 37: 689-697

[39] Lam J, Tsang C, Yang L, "Impacts of Lighting Density on Heating and Cooling

Loads in Different Climates in China," *Energy Conversion Management*; 2006; 47: 1942-1953

[40] Chung T, Burnett J, Wu M, "Office Lighting Retrofit Using Dimmable Electronic Ballast and Occupancy Controls," *HKIE Trans*; 2001; 8: 8-15

[41] Tiwari G, Mishra R, Solanki S, "Photovoltaic Modules and Their Applications, A Review on Thermal Modeling," *Applied Energy*; 2011; 88: 2287-2304

[42] Sharma R, Tiwari G, "Technical Performance Evaluation of Stand-Alone

Photovoltaic Array for Outdoor Field Conditions of New Delhi," *Applied Energy*; 2012; 92: 644-652

[43] Cheng T, Cheng C, Huang Z, Liao G, "Development of an Energy-Saving Module via Combination of Solar Cells and Thermoelectric Coolers for Green Building Applications," *Energy* ; 2011; 36: 133-140

[44] Celik A, "Optimization and Techno-Economic Analysis of Autonomous Photovoltaic-Wind Hybrid Energy Systems in Comparison to Single Photovoltaic and Wind Systems," *Energy Conversion Management*; 2002; 43: 2453-2468

[45] Nandi S, Ghosh H, "Prospect of Wind-PV-Battery Hybrid Power System as an Alternative to Grid Extension in Bangladesh," *Energy*; 2010; 35: 3040-3047

[46] Shimoda Y, Okamura T, Yamaguchi Y, Taniguchi A, Morikawa T, "City-Level Energy and CO_2 Reduction by Introducing New Residential Water Heaters," *Energy*; 2010; 35: 4880-4891

[47] Wang L, William J, Jones P, "Case study of zero energy house design in UK," *Energy and Buildings*; 2009; 41: 1215–1222

[48] Klein S, "TRNSYS Version.16," *Solar Energy Laboratory University of Wisconsin-Madison*; 2004

[49] Graça G, Augusto A, Lerer M, "Solar Powered Net Zero Energy Houses for Southern Europe: Feasibility study," *Solar Energy*; 2012; 86: 634-636

[50] Graça G, Lerer M, Paredes C, "WP 2, System and Component Characterization Report – Passive House," *Natural Works*; 2006; Portugal

[51] Christian J, Richards L, Childs P, Atchley J, Moon H, "Energy Efficiency, SIPS, Geothermal, and Solar PV Used in Near Zero-Energy House," *ASHRAE Transactions*; 2006; 112: 275

[52] Bejan A, Tsatsaronis G, Moran M, "Thermal Design and Optimization," *John Wiley and Sons*; 1996

[53] Censor Y, "Pareto Optimality in Multi-objective problems," *Applied Mathematical Optimization*; 1977; 4: 41–59

[54] Cunha D, Polak E, "Constrained Minimization under Vector-Valued Criteria in Finite Dimensional Spaces," *Journal of Mathematical Analysis and Applications*; 1967; 19: 103–124

[55] Kalyanmoy D, “Multi-Objective Optimization using Evolutionary Algorithms,” *John Wiley and Sons*; 2001

[56] Zadeh L, “Optimality and Nonscalar-Valued Performance Criteria,” *IEEE Transactions Automatic Control*; 1963; AC-8, No.1

[57] Matlab, “Mathematical Computing Software,” *The Math Works Inc. Natick Massachusetts U.S.A*; 1984-2013. http://www.mathworks.com

[58] Jung S, Kim T, Lee B, “Measurement of Sound Transmission Loss by Using Impedance Tube,” *Journal of the Korean Physical Society*; 2008; 53(2): 596-600

[59] Chung Y, Blaser A, ‘Transfer Function Method of Measuring in Duct Acoustics Properties,” *Journal of Acoustical Society of America*; 1980; 68(3)

[60] Carrier Corporation “Hourly Analysis Program, System Design Load Software,” Version: 4.2-a; 1999-2004

[61] ASHRAE “Handbook of Fundamentals, American Society of Heating, Refrigerating and Air-conditioning Engineers,” *Inc., Atlanta, GA*; 1993; Chapter 28

[62] Bereche R, Gonzales R, Nebra S, “Exergy calculation of lithium bromide–water solution and its application in the exergetic evaluation of absorption refrigeration systems LiBr-H2O,” *International Journal of Energy Research;* 2010

[63] Duffie J, Beckman W, “Solar engineering of thermal processes” John Wiley and Sons, Inc, Second Edition; 1991

[64] Hassoun A, Dincer I, “Development of power system designs for a net zero energy houses,” *Energy and Buildings*; 2014; 73; 120-129

Appendix A: Simulated Heat Load Calculations

Table A.1: Design parameters for calculating heat load

City Name	Beirut	
Location	Lebanon	
Latitude	33.9	Deg.
Longitude	-35.5	Deg.
Elevation	33.8	m
Summer Design Dry-Bulb	32.8	°C
Summer Coincident Wet-Bulb	25.6	°C
Summer Daily Range	8.3	°K
Winter Design Dry-Bulb	5.6	°C
Winter Design Wet-Bulb	1.8	°C
Atmospheric Clearness Number	1.00	
Average Ground Reflectance	0.20	
Soil Conductivity	1.385	W/(m-°K)
Local Time Zone (GMT +/- N hours)	-2.0	hours
Consider Daylight Savings Time	No	
Simulation Weather Data	N/A	
Current Data is	1993 ASHRAE Handbook	
Design Cooling Months	January to December	

Table A.2: Design day maximum solar heat gains

Month	**N**	**NNE**	**NE**	**ENE**	**E**	**ESE**	**SE**	**SSE**	**S**
January	71.1	71.1	82.8	307.8	546.7	692.1	789.7	798.1	784.0
February	83.6	83.6	208.9	429.9	644.0	761.9	783.7	743.8	709.9
March	97.4	101.5	346.8	568.1	696.6	759.9	718.9	628.1	577.4
April	110.9	246.6	450.3	629.7	713.5	688.2	603.6	467.6	393.0
May	120.1	344.5	528.6	653.1	695.6	633.6	504.1	338.4	260.1
June	151.3	378.5	545.8	658.6	680.2	600.5	458.4	285.2	213.3
July	122.7	340.8	519.5	648.1	681.1	612.0	491.3	327.0	251.5
August	116.1	241.6	446.6	612.1	686.1	663.4	581.5	450.2	378.9
September	101.1	103.4	312.8	536.7	671.8	718.2	695.5	613.0	564.0
October	86.5	86.5	179.4	438.0	613.3	729.2	759.2	723.3	693.2
November	72.4	72.4	81.6	309.9	526.2	696.3	766.6	779.7	775.2
December	65.7	65.7	65.7	243.3	497.6	661.0	773.5	800.1	799.4
Month	**SSW**	**SW**	**WSW**	**W**	**WNW**	**NW**	**NNW**	**HOR**	**Mult**
January	797.8	783.9	704.8	527.8	323.8	71.1	71.1	521.9	1.00
February	747.1	788.5	749.3	649.0	445.9	199.0	83.6	653.5	1.00
March	633.6	723.1	759.3	710.5	552.3	349.6	104.5	772.6	1.00
April	468.1	602.2	696.8	711.7	618.6	465.0	243.5	841.5	1.00
May	338.2	501.9	636.6	692.5	645.0	535.4	342.6	865.8	1.00
June	284.5	452.9	605.3	672.9	656.2	558.0	375.3	865.7	1.00
July	326.4	485.0	622.3	673.1	641.9	531.0	338.0	853.1	1.00
August	451.4	580.5	671.9	686.5	598.2	452.2	241.4	824.2	1.00
September	613.0	695.6	718.0	672.0	536.7	312.5	103.5	749.3	1.00
October	717.0	750.1	735.6	609.3	430.6	196.5	86.5	645.2	1.00
November	781.6	773.1	692.6	534.4	291.1	85.7	72.4	521.8	1.00
December	793.7	767.6	671.8	491.4	253.3	65.7	65.7	466.4	1.00

Table A.3: System cooling and heating design parameters

	COOLING			HEATING		
DB	32.5 °C			5.6 °C		
WB	25.5 °C			1.8 °C		
		Sensible	Latent		Sensible	Latent
Zone Loads	Details	(W)	(W)	Details	(W)	(W)
Window and Skylight Solar Loads	11 m²	926	-	11 m²	-	-
Wall Transmission	144 m²	168	-	144 m²	217	-
Roof Transmission	224 m²	42	-	224 m²	249	-
Window Transmission	9 m²	206	-	9 m²	440	-
Skylight Transmission	1 m²	31	-	1 m²	65	-
Door Loads	27 m²	336	-	27 m²	715	-
Floor Transmission	225 m²	0	-	225 m²	0	-
Partitions	0 m²	0	-	0 m²	0	-
Ceiling	0 m²	0	-	0 m²	0	-
Overhead Lighting	648 W	454	-	0	0	-
Task Lighting	0 W	0	-	0	0	-
Electric Equipment	675 W	675	-	0	0	-
People	6	431	360	0	0	0
Infiltration	-	0	0	-	0	0
Miscellaneous	-	500	400	-	0	0
Safety Factor	1% / 1%	38	8	1%	17	0
Total Zone Loads	-	3805	768	-	1703	0
Zone Conditioning	-	3330	768	-	1645	0
Plenum Wall Load	0%	0	-	0	0	-
Plenum Roof Load	70%	97	-	0	0	-
Plenum Lighting Load	30%	194	-	0	0	-
Return Fan Load	224 L/s	0	-	65 L/s	0	-
Ventilation Load	4 L/s	34	107	0 L/s	1	1
Supply Fan Load	224 L/s	4	-	3 L/s	-1	-
Hot Deck Supply Fan Load	0 L/s	0	-	62 L/s	-1	-

Duct Heat Gain / Loss	0%	0	-	0%	0	-
Total System Loads	-	3659	875	-	1644	1
Central Cooling Coil	-	3659	875	-	-28	0
Central Heating Coil	-	0	-	-	1671	-
Total Conditioning	-	3659	875	-	1644	0

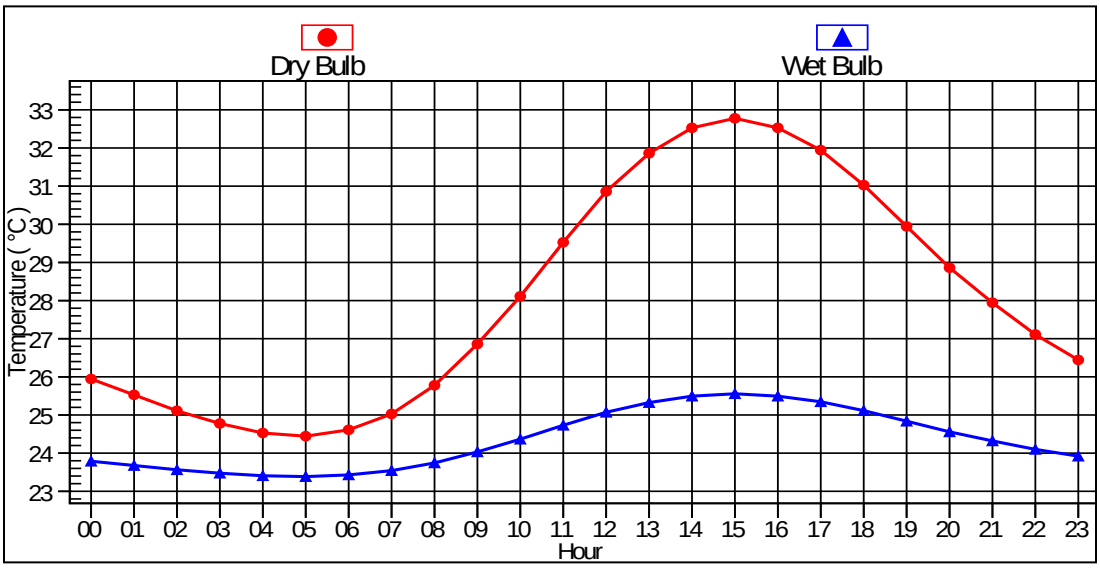

Figure A.1: July temperature profile

Table A.4: Sensible zone capacity and corresponding air flow

Space Name	Cooling	Time	Air	Heating	Floor	Flow/Area
	(kW)	Load	(L/s)	(kW)	(m²)	L/(s-m²)
House Near Tyre	3.8	July 1500	287	1.7	225.0	1.28

Table A.5: Space ventilation analysis

Space	Area	Maximum	Supply Air	Outdoor Air	Outdoor Air
	(m²)	Occupants	(L/s)	(% of supply)	(L/s)
House Near Tyre	225.0	6.0	286.9	2.0	5.7

Table A.6: Air system design load summary

	DESIGN COOLING			DESIGN HEATING		
DB	32.5 °C			5.6 °C		
WB	25.5 °C			1.8 °C		
		Sensible	Latent		Sensible	Latent
Structure	Area (m²)	(W)	(W)	Area (m²)	(W)	(W)
Window and Skylight Solar Loads	11	926	-	11	-	-
Wall Transmission	144	168	-	144	217	-
Roof Transmission	224 m²	42	-	224 m²	249	-
Window Transmission	9 m²	206	-	9 m²	440	-
Skylight Transmission	1 m²	31	-	1 m²	65	-
Door Loads	27 m²	336	-	27 m²	715	-
Floor Transmission	225 m²	0	-	225 m²	0	-
Partitions	0 m²	0	-	0 m²	0	-
Ceiling	0 m²	0	-	0 m²	0	-
Overhead Lighting	648 W	454	-	0	0	-
Task Lighting	0 W	0	-	0	0	-
Electric Equipment	675 W	675	-	0	0	-
People	6	431	360	0	0	0
Infiltration	-	0	0	-	0	0
Miscellaneous	-	500	400	-	0	0
Safety Factor	1% / 1%	38	8	1%	17	0
Total Zone Loads	-	3805	768	-	1703	0
Zone Conditioning	-	3330	768	-	1645	0
Plenum Wall Load	0%	0	-	0	0	-
Plenum Roof Load	70%	97	-	0	0	-
Plenum Lighting Load	30%	194	-	0	0	-
Return Fan Load	224 L/s	0	-	65 L/s	0	-
Ventilation Load	4 L/s	34	107	0 L/s	1	1
Supply Fan Load	224 L/s	4	-	3 L/s	-1	-
Hot Deck Supply Fan Load	0 L/s	0	-	62 L/s	-1	-

Space Fan Coil Fans	-	0	-	-	0	-
Duct Heat Gain / Loss	0%	0	-	0%	0	-
Total System Loads	-	3659	875	-	1644	1
Central Cooling Coil	-	3659	875	-	-28	0
Central Heating Coil	-	0	-	-	1671	-
Total Conditioning	-	3659	875	-	1644	0

Table A.7: Zone load

House near Tyre	Design Cooling			Design Heating		
Zone Loads	Details	Sensible (W)	Latent (W)	Details	Sensible (W)	Latent (W)
Window and Skylight Solar Loads	11 m²	959	-	11 m²	-	-
Wall Transmission	144 m²	161	-	144 m²	217	-
Roof Transmission	224 m²	36	-	224 m²	249	-
Window Transmission	9 m²	209	-	9 m²	440	-
Skylight Transmission	1 m²	31	-	1 m²	65	-
Door Loads	27 m²	340	-	27 m²	715	-
Floor Transmission	225 m²	0	-	225 m²	0	-
Partitions	0 m²	0	-	0 m²	0	-
Ceiling	0 m²	0	-	0 m²	0	-
Overhead Lighting	648 W	454	-	0	0	-
Task Lighting	0 W	0	-	0	0	-
Electric Equipment	675 W	675	-	0	0	-
People	6	431	360	0	0	0
Infiltration	-	0	0	-	0	0
Miscellaneous	-	500	400	-	0	0
Safety Factor	1% / 1%	38	8	1%	17	0
Total Zone Loads	-	3833	768	-	1703	0

Table A.8: Envelope loads for space

EXPOSURE	Area m²	U-Value W/(m²-°K)	Shade Coeff	Cooling Trans (W)	Cooling Solar (W)	Heating Trans (W)
North wall	34	0.097	-	26	-	51
Window 1	2	3.050	0.450	52	77	110
Door	9	1.703	-	113	-	238
East wall	43	0.097	-	48	-	65
Window 1	2	3.050	0.450	52	103	110
south wall	34	0.097	-	45	-	51
Window 1	2	3.050	0.450	52	93	110
Door	9	1.703	-	113	-	238
West wall	34	0.097	-	42	-	51
Window 1	2	3.050	0.450	52	447	110
Door	9	1.703	-	113	-	238
Roof	224	0.071	-	36	-	249
Skylight	1	3.019	0.456	31	240	65

Table A.9: Summer design data

Component	Location	Dry-bulb Temp (°C)	Specific Humidity (kg/kg)	Airflow (L/s)	CO2 Level (ppm)	Sensible Heat (W)	Latent Heat (W)
Ventilation Air	Inlet	32.5	0.01778	4	400	34	107
Vent - Return Mixing	Outlet	26.4	0.00981	224	3138	-	-
Central Cooling Coil	Outlet	12.8	0.00848	224	3138	3659	875
Supply Fan	Outlet	12.8	0.00848	224	3138	4	-
Cold Supply Duct	Outlet	12.8	0.00848	224	3138	0	-
Heating Supply Fan	Outlet	26.2	0.00965	0	3194	0	-
Central Heating Coil	Outlet	43.3	0.00965	0	3194	0	-
Hot Supply Duct	Outlet	43.3	0.00965	0	3194	0	-
Zone Air	-	25.1	0.00965	224	3194	3330	768
Return Plenum	Outlet	26.2	0.00965	224	3194	291	-

Table A.10: Winter design data

		Dry-Bulb	Specific Humidity	Airflow	CO2 Level	Sensible Heat	Latent Heat
Component	Location	(°C)	(kg/kg)	(L/s)	(ppm)	(W)	(W)
Ventilation Air	Inlet	5.6	0.00282	0	400	-1	-1
Vent - Return Mixing	Outlet	20.5	0.00779	3	792	-	-
Central Cooling Coil	Outlet	12.4	0.00779	3	792	28	0
Supply Fan	Outlet	12.8	0.00779	3	792	1	-
Cold Supply Duct	Outlet	12.8	0.00779	3	792	0	-
Heating Supply Fan	Outlet	20.8	0.00788	62	800	1	-
Central Heating Coil	Outlet	43.3	0.00788	62	800	1671	-
Hot Supply Duct	Outlet	43.3	0.00788	62	800	0	-
Zone Air	-	20.8	0.00788	65	800	-1645	0
Return Plenum	Outlet	20.8	0.00788	65	800	0	-

Table A.11: Roof details

Outside Surface Color	Light
Absorptivity	0.450
Overall U-Value	0.071 W/(m²-°K)

Table A.12: Roof layers details (inside to outside)

Layers	Thickness	Density	Specific Ht.	R-Value	Weight
	mm	kg/m³	kJ / (kg - °K)	(m²-°K)/W	kg/m²
Inside surface resistance	0.000	0.0	0.00	0.12064	0.0
203mm HW concrete	203.200	2242.6	0.84	0.11741	455.7
RSI-6.7 batt insulation	200.000	8.0	0.84	4.202	1.0
Asphalt roll	1.588	1121.3	1.51	0.02698	1.8
Acoustic insulation	58.420	0.0	0.00	6.63870	0.0
Asphalt sheathing	12.700	1121.3	1.47	0.25303	14.2
Outside surface resistance	0.000	0.0	0.00	0.05864	0.0
Totals	395.908	-		14.085	472.7

Table A.13: Window details

Detailed Input	Yes	
Height	1.52	m
Width	1.52	m
Frame Type	Aluminum with thermal breaks	
Internal Shade Type	Drapes - Semi-Open Weave - Light	
Overall U-Value	3.050	W/(m²-°K)
Overall Shade Coefficient	0.450	

Table A.14: Glass details (gap type 6mm air space)

Glazing	Glass Type	Transmissivity	Reflectivity	Absorptivity
Outer Glazing	6mm clear low-e	0.639	0.116	0.245
Glazing #2	6mm blue-green reflective	0.282	0.295	0.423
Glazing #3	not used	1.000	0.000	0.000

Table A.15: Door details

Gross Area	9.0 m²
Door U-Value	1.703 W/ (m²-°K)

Table A.16: Glass details

Glass Area	0.0 m²
Glass U-Value	3.293 W/ (m²-°K)
Glass Shade Coefficient	0.880
Glass Shaded All Day?	No

Table A.17: Overhang and fins details

Over hang		Projection from surface	700.0 mm
Over hang		Height above window	100.0 mm
Over hang		Ext. past RH side of window	100.0 mm
Over hang		Ext. past LH side of window	100.0 mm
Left Fin		Right Fin	
Projection from surface	500.0 mm	Projection from surface	700 mm
Height above window	100.0 mm	Height above window	100.0 mm
Dist. from edge of window	100.0 mm	Dist. from edge of window	100.0 mm

Table A.18: Wall details

Outside Surface Color	Light
Absorptivity	0.450
Overall U-Value	0.097 W/(m²-°K)

Table A.19: Wall layers details (inside to outside)

	Thickness	Density	Specific Ht.	R-Value	Weight
Layers	mm	kg/m³	kJ / (kg - °K)	(m²-°K)/W	kg/m²
Inside surface resistance	0.000	0.0	0.00	0.12064	0.0
plaster light weight aggregate	19.500	0.0	0.00	0.27200	0.0
13mm plywood	12.700	544.6	1.21	0.10952	6.9
expanded polystyrene rigid board	58.420	32.0	0.00	6.65357	1.9
R-24 Roxul Thermal Insulation	104.140	0.0	0.00	2.80000	0.0
102mm LW concrete block	101.600	608.7	0.84	0.26683	61.8
Outside surface resistance	0.000	0.0	0.00	0.05864	0.0
Totals	296.360	-		10.28120	70.6

Appendix B: A Matlab Code for Determining the Sound Pressure Level of the Acoustic Materials.

```
Clear all
Clc
Close all
%Finding the thickness of the thermal and acoustic Insulation that would satisfy the...
%requirements


% THERMAL CONDUCTIVITY
R_acoustic=zeros (1, 60);
LENGTH=zeros (1, 60);
RT=zeros (1, 60);
R_ins=zeros (1, 60);
T (2) =24; % Inside Temperature C
T (1) =32.8; % Outside Temperature C
Ri_air=0.12; % m2.C/W Resistance of inside air film
Ro_air=0.03; % m2.C/W Resistance of outside air film
R_light_weight_concrete_block=0.26683; % m2.C/W Resistance for 4" thickness
R_plaster=0.2722; %m2.C/W Resistance for 0.75" light weight Gypsum plaster.
R_plywood_sheating=0.111; % m2.C/W Resistance for1/2"
RTS=10; % Thermal resistance for above Wall composition set By Designer.
%ACOUSTIC INSULATION
R_acoustic=46; % Spl level to be attenuated.
Db=20; % SPL attenuated by 1" expanded Polystyrene.


For n=1:1:60
    LENGTH (n) =n/10;
    R_acoustic (n) = (LENGTH (n))*Db;
    If (R_acoustic - R_acoustic (n)) <=10^-6
        n;
        R_acoustic (n);
        LENGTH;
```

```
        Break
    End
End
R_expanded_polysterene_rigid_board=max  (LENGTH)*0.57728*5;  %units  are
in c.m2/w
Thickness_Acoustic_insulation=max (LENGTH); %Units IN Inch.
%R-1"=0.7 m2*K/W FOR R_24 ROXUL THERMAL INSULATION
For K=1:1:60
    R_ins(K)= 0.70*(1+K/10);


RT(K)=Ro_air+R_light_weight_concrete_block+R_plywood_sheating+R_ins(K)+
Ri_air+R_expanded_polysterene_rigid_board;
    If (RTS-RT (K)) <=10^-6
        K;
        Break


    End
End;
Thickness_Thermal_insulation=1+max (K)/10; % units are in inch.
% refcoeff_tf
% Plots reflection coefficient from a transfer function, after being
% exported as a .csv file.


a = 0.077/2; % Radius
f = 1:2600;


For n = 1: length (f)
    K (n) = 2*pi*f (n)/343;
    Ka (n) = k (n)*a;
    Rtheo (n) = 1 + 0.01336*ka (n) - 0.59079*ka (n) ^2 + 0.33576*ka (n)
^3 - 0.06432*ka (n) ^4;
End


Vmic1_WOOD=xlsread ('ACOUSTIC_PROJECT.xlsx', 10,'C24:C2023')/0.000254;
Vmic2_WOOD=xlsread ('ACOUSTIC_PROJECT.xlsx', 10,'B24:B2023')/0.000254;
DT=0.0002;
```

```
[Hest_WOOD, fest_WOOD] = tfestimate (Vmic2_WOOD, Vmic1_WOOD, [], [],
5199, 1/dt);
For n=1: length (Hest_WOOD)
    Hestmag_WOOD (n) = abs (Hest_WOOD (n));
    Hestphase_WOOD (n) = atan2 (imag (Hest_WOOD (n)), real (Hest_WOOD
(n)));
End


Vmic1_3=xlsread ('ACOUSTIC_PROJECT.xlsx', 8,'B24:B2023')/0.000254;
Vmic2_3=xlsread ('ACOUSTIC_PROJECT.xlsx', 8,'C24:C2023')/0.000254;
DT=0.0002;
[Hest_3, fest_3] = tfestimate (Vmic2_3, Vmic1_3, [], [], 5199, 1/dt);
For n=1: length (Hest_3)
    Hestmag_3 (n) = abs (Hest_3 (n));
    Hestphase_3 (n) = atan2 (imag (Hest_3 (n)), real (Hest_3 (n)));
End
Vmic1_1=xlsread ('ACOUSTIC_PROJECT.xlsx', 7,'B24:B2023')/0.000254;
Vmic2_1=xlsread ('ACOUSTIC_PROJECT.xlsx', 7,'C24:C2023')/0.000254;
DT=0.0002;
[Hest_1, fest_1] = tfestimate (Vmic2_1, Vmic1_1, [], [], 5199, 1/dt);
For n=1: length (Hest_1)
    Hestmag_1 (n) = abs (Hest_1 (n));
    Hestphase_1 (n) = atan2 (imag (Hest_1 (n)), real (Hest_1 (n)));
End
% calculate Reflection coefficient
c = 343; %speed of sound
L = 0.15; % Dimensions of impedance tube
s= 0.02;
f=1: length (fest_1);
For n= 1: length (fest_1)
    k = 2*pi*fest_1 (n)/c;
%     R(n)=(Hest(n)-imag(Hest(n)))/(real(Hest(n))-Hest(n));
     R_1 (n) = (Hest_1 (n)-exp (-i*k*s))/ ((exp (k*s) - Hest_1 (n))*exp
(i*k*2*L));
    Rexp_1 (n) = abs (R_1 (n));
    Rphase_1 (n) = atan2 (imag (R_1 (n)), real (R_1 (n)))*180/pi;
end
```

```
 c = 343; %speed of sound
L = 0.15; % Dimensions of impedance tube
s= 0.02;
f=1: length (fest_3);
For n= 1: length (fest_3)
    k = 2*pi*fest_3 (n)/c;
%     R(n)=(Hest(n)-imag(Hest(n)))/(real(Hest(n))-Hest(n));
     R_3 (n) = (Hest_3 (n)-exp (-i*k*s))/ ((exp (k*s) - Hest_3 (n))*exp
(i*k*2*L));
    Rexp_3 (n) = abs (R_3 (n));
    Rphase_3 (n) = atan2 (imag (R_3 (n)), real (R_3 (n)))*180/pi;
End
For n= 1: length (fest_WOOD)
    k = 2*pi*fest_WOOD (n)/c;
%     R(n)=(Hest(n)-imag(Hest(n)))/(real(Hest(n))-Hest(n));
     R_WOOD (n) = (Hest_WOOD (n)-exp (-i*k*s))/ ((exp (k*s) - Hest_WOOD
(n))*exp (i*k*2*L));
    Rexp_WOOD (n) = abs (R_WOOD (n));
    Rphase_WOOD  (n)  =  atan2  (imag  (R_WOOD  (n)),  real  (R_WOOD
(n)))*180/pi;
end
 % Plots the theoretical curve for the reflection coefficient of an
open-ended impedance tube.


% close all
% clear all
% clc


a = 0.077/2; % Radius
Ftheo = 1:2600;


For n = 1: length (ftheo)
    K (n) = 2*pi*ftheo (n)/343;
    Ka (n) = k (n)*a;
    Rtheo (n) = 1 + 0.01336*ka (n) - 0.59079*ka (n) ^2 + 0.33576*ka (n)
^3 - 0.06432*ka (n) ^4;
End
```

```
Figure ('name', 'Theoretical Reflection Coefficient','numbertitle','off')
Plot (ftheo, Rtheo)
Xlabel ('Frequency, (Hz)')
Ylabel ('Rtheo_0')
Axis ([0 2600 0 1.1])
%refcompare.m
% compares reflection coefficient of a measurement against the
% theoretical curve and then plots fig files as input.

% load theoref.mat



%% To plot from previous figures
[Figfile, figpath] = uigetfile ('.fig', 'Select the fig file');
Open (fullfile (figpath, figfile))

Line = findall (gcf,'type','line');
Fexp = get (line (2),'xdata');
Rmag = get (line (2),'ydata');
Close all
%% Plotting
Figtitle = inputdlg ('Figure title?', 'Title');

Figure ('name', figtitle {1},'numbertitle','off')

Hold on
Title ('Magnitude')
Xlabel ('Frequency (Hz)')
Ylabel ('|R|')
Plot (fexp, Rmag,'color','r')
Plot (ftheo, Rtheo,'linewidth', 2)
Axis ([0 2600 0 1.1])
Legend ('Experimental', 'Theoretical')
Grid on
```

```
% save figure
If exist ('tfpath')
    Cd (tfpath)
Elseif exist ('figpath')
    Cd (figpath)
End
Hgsave (gcf, [figtitle {1},'_theocompare'])
Saveas (gcf, [figtitle {1},'_theocompare'],'png')


plot(fest_1,Rexp_3,'DisplayName','Rexp_3','XDataSource','fest_1','YData
Source','Rexp_3');...
     hold
all;plot(fest_1,Rexp_1,'DisplayName','Rexp_1','XDataSource','fest_1','Y
DataSource','Rexp_1');...
     Hold off; figure (gcf);
 %plot      (fest_WOOD,      Rexp_WOOD,'DisplayName','Rexp_WOOD      vs.
fest_WOOD',’XDataSource’,
    % 'fest_WOOD','YDataSource','Rexp_WOOD'); figure (gcf)
```

Appendix C: Exergoeconomic Analysis and Optimization Code

```
%%OPTIMIZATION OF TOTAL SYSTEM COST $/HR Vs. GLOBAL SYSTEM EXERGETIC
%%EFFICIENCY.
% Using Multiobjective genetic algorithm
%%

clc;
clear;
%@gaplotrankhist @gaplotscorediversity @gaplotdistance @gaplotselection
options = gaoptimset;
options = gaoptimset (options,'PopulationSize', 120);
options = gaoptimset (options,'ParetoFraction', 0.65);
options = gaoptimset (options,'CrossoverFcn', {@crossoverintermediate
[] });
options = gaoptimset (options, 'Display', 'off');
options = gaoptimset (options,'PlotFcns', {     @gaplotpareto    });
[x,fval,exitflag,output,population,score] = ...
    gamultiobj (@PHD_PROPOSAL_SYSTEM1, 27, [], [], [], [],

[298,28,39,238.6,0.4,5.897,0.012,0.04,15,1.1,2.51,29,0.673,0.021,0.294,
91.82,0.04,7.2,0.66,64.85,9.4,6.66,12.63,30.72,62.31,5.83,0.7934],...

[307,33,47,280.4,0.7822,8.929,0.02888,0.06,20,3.4,4,38,0.935,0.029,0.37
,106.7,0.07,7.9,0.69,74.85,18.77,30.18,22.69,32.04,98.05,5.95,0.9182],o
ptions);
```

Appendix D: Acoustics Experimental Description

- Experimental set up

The experiment is conducted at the acoustics and noise control lab at the UOIT campus where SPL and reflection coefficients are measured for the following acoustical materials by two different techniques:

- Impedance tube experiment

A speaker is placed at the face of one end of a tube and is sealed properly by using two wooden flanges to insure that there is no leakage of transmitted sound, while at the other end the individually tested material, 1″ of rigid polystyrene foam and 2″ of Roxul fiberglass is fixed by two flanges to secure the test in place and to make sure that no noise is leaking. Two Pressure microphones are installed at the surface of the tube as shown in the following figures the experiment was conducted to calculate the reflection coefficients using: A 100x15 cm PVC pipe arranged as shown in Figure D.1.

In this study, procedure and evaluation of Impedance tube method will follow [46, 47]:

“In this method, a broadband stationary random acoustic wave in a tube is mathematically decomposed into its incident and reflected components using a simple transfer-function relation between the acoustic pressures at two locations on the tube wall. The wave decomposition leads to the determination of the complex reflection coefficient from which the complex acoustic impedance and the sound absorption coefficient of a material and the transmission loss of a silencer element can be determined.”

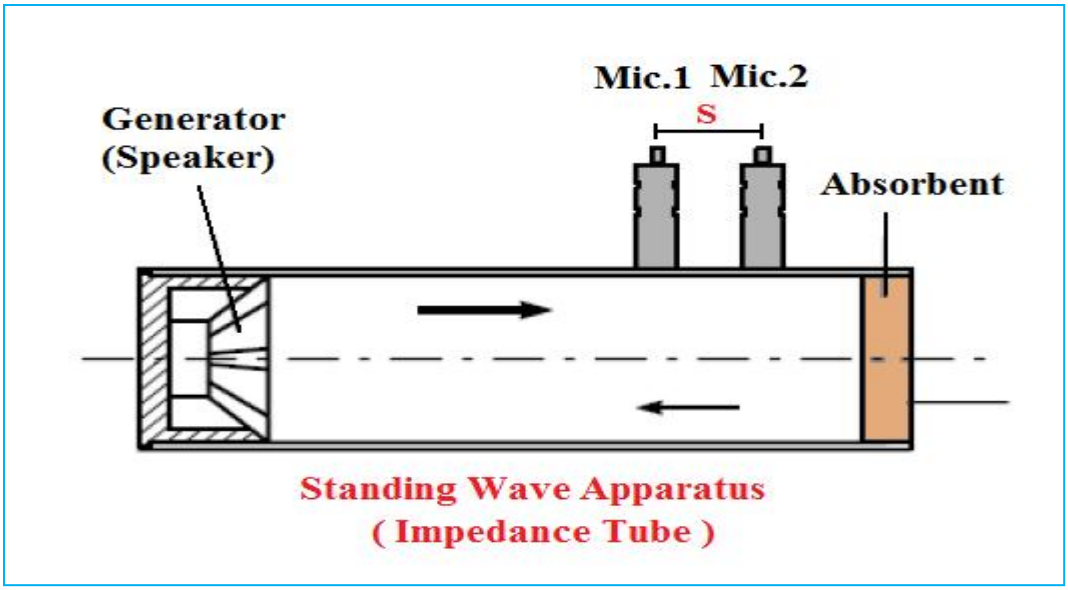

Figure D.1: Impedance tube.

Figure D.2: Speaker that generates the noise.

FigureD.2 shows the speaker attached to one end of the pipe through a flange combination and is properly sealed to prevent any noise leakage from openings. The

microphones are on the other side of the pipe where S = 2 cm. and L= 15 cm being the distance from the face of the acoustic material to the first microphone.

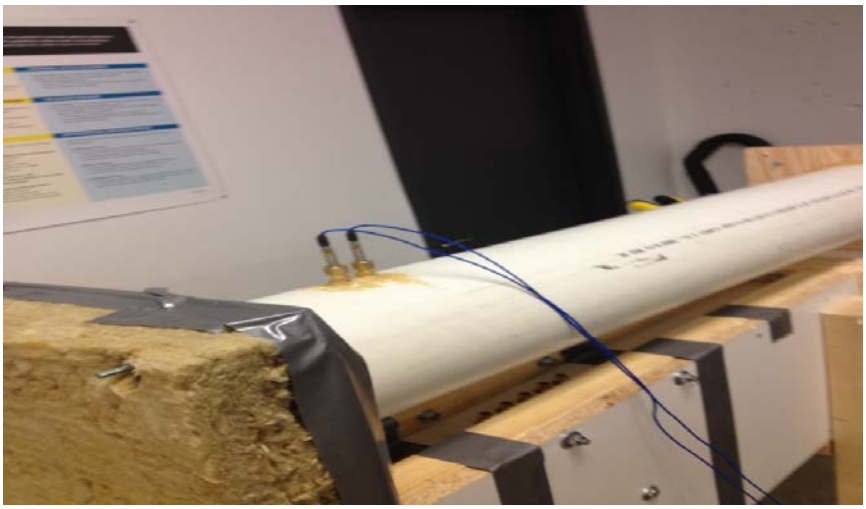

Figure D.3: Impedance tube with the two microphones inserted along with the 3 inch acoustical material installed and well sealed.

Figure D.3 shows the impedance tube with the specimen to be tested and the two microphones that carry the voltage signal back to the sensor signal conditioner shown in Figure D.4 which is connected to the analog output series instrument Figure D.5 and to the lab view software Figure D.6 to analyze the signal and perform the required tasks.

Figure D.4: Sensor signal conditioner.

Figure D.5: Analog output series instrument.

Figure D.6: Equipment to transfer signal from microphones into lab view software.

- Enclosure experiment

In this experiment an enclosure is made up of:

- 3 inch stone wool Roxul insulation material+ 1 inch rigid foam insulation made from Expanded Polystyrene (Figure D.7).
- 3 inch stone wool Roxul insulation material+ 2 inch rigid foam insulation made from Expanded Polystyrene (Figure D.8).

The enclosure is made up of the acoustic material as indicated in Figures D.7 and D.8.The enclosure is well sealed to avoid any sound leakage and a free field microphone is installed inside the enclosure while a generated noise is built on the outside using a speaker .The microphone signal is connected to the analog instrument and then transferred to the lab view software where the *FFT* algorithm produces *rms* voltage values that is recorded at different frequencies' and then transformed into pressure signal by multiplying with the voltage to pressure sensitivity factor of the microphone. After which the *SPL* is calculated and the attenuation by each material can be evaluated.

Figure D.7: 3″ Roxul stone wool fiberglass +1″ expanded rigid polystyrene insulation foam

Figure D.8: 3″ Roxul stone wool fiberglass +2″ expanded rigid polystyrene insulation foam